THE INFLUENCE OF CARBON-OXYGEN SURFACE GROUPS AND A WATER-MISCIBLE PRIMARY ALCOHOL ON THE VOLTAMMETRIC DETECTION OF BOVINE HEMOGLOBIN IN AQUEOUS ELECTROLYTE USING CARBON ELECTRODES

by

Justin L. Tom

Submitted in partial fulfilment of the requirements
for the degree of Doctor of Philosophy

at

Dalhousie University
Halifax, Nova Scotia
October 2017

Table of Contents

List of Tables

List of Figures

Abstract

This thesis focuses on the electrochemical reduction of bovine hemoglobin (BHb) using carbon electrode materials. Carbon materials are abundant and affordable, but have variable carbon-oxygen surface functional groups and varying ability to electrochemically detect BHb. To better understand the role of carbon-oxygen surface groups in the electrochemical behavior of BHb, surface groups were identified using attenuated total reflectance Fourier transform infrared spectroscopy, X-ray photoelectron spectroscopy, and temperature programmed desorption. The identified surface groups were then correlated with BHb electroactivity and key surface groups were further identified through selective carbon surface modifications. The results show that carbonyl, quinone, and ether surface groups inhibit BHb electroreduction on carbon.

BHb has a slow electron transfer with bare electrodes, showing minimal electrochemical response in aqueous electrolyte. Nafion-bound BHb on carbon surfaces exhibits enhanced response, but until this work, the effects of a water-miscible primary alcohol solvent present in Nafion have been ignored. The presence of an alcohol solvent in Nafion is shown in this thesis to further increase the electrochemical response of BHb. Furthermore, adding a water-miscible primary alcohol to a BHb-containing electrolyte results in an increased BHb response.

The mechanisms by which the alcohol increase BHb electroactivity were examined. The water-miscible primary alcohols modified both BHb and the glassy carbon electrode. Ultraviolet-visible absorption and fluorescence data provide evidence of BHb denaturation, likely opening the heme cavity and facilitating the electron transport. Adding alcohol to a BHb-containing electrolyte formed more electroactive BHb films. Additionally, the alcohols changed the carbon-oxygen surface groups on the carbon material, showing a complex relationship where some alcohols removed inhibiting carbon-oxygen surface groups to increase BHb activity, while other alcohols had the opposite effect.

The work presented in this thesis contributed new understandings regarding the electrochemistry of BHb on carbon electrode surfaces and helps avoid spurious conclusions for alcohol-containing BHb films. Understanding carbon-oxygen surface functional groups can be used to intelligently modify carbon electrodes for improving BHb detection. BHb detection was further improved by adding alcohol to the electrolyte, a simple and inexpensive method. The mechanisms by which alcohol influences BHb reactivity was elucidated.

List of Abbreviations and Symbols Used

1-PrOH	1-propanol
AFM	Atomic force microscopy
ATR-FTIR	Attenuated total reflectance Fourier transform infrared spectroscopy
BHb	Bovine hemoglobin
CV	Cyclic voltammogram
DPV	Differential pulse voltammogram
E	Potential
E_b	Binding energy
E_k	Kinetic energy
EtOH	Ethanol
GC	Glassy carbon
Hb	Hemoglobin
HHb	Human hemoglobin
i	Imaginary number
I	Current
IR	Infrared
k	Extinction coefficient
MeOH	Methanol
MSE	Mean squared error
n	Index of refraction
N	Complex index of refraction

Nf_{solid}	Solid Nafion 117
$Nf_{suspension}$	Nafion film created from a liquid suspension
PB	Phosphate buffer
PTFE	Polytetrafluoroethylene
SCE	Saturated calomel electrode
SEM	Scanning electron microscope
TGA	Thermal gravimetric analysis
TPD	Temperature programmed desorption
Trp	Tryptophan
Tyr	Tyrosine
UV/Vis	Ultraviolet-visible
XPS	X-ray photoelectron spectroscopy
β	Phase change
Δ	Phase difference ratio
λ	Wavelength
Φ	Work function
Ψ	Amplitude ratio

Acknowledgements

The first person I want to thank is my supportive supervisor, Dr. Heather Andreas. She has given me a lot of useful advice and freedom to explore my own research topic; I could not ask for a better supervisor. I have also met and worked with many caring people in her research group over the years: Crystal Weagle, Bethany Wilkes, Gillian Davies, Mallory Davis, Adrienne Allison, Felicia Licht, Philip Jakubec, Alex Hare, and Drs. Michelle MacDonald and Alicia Oickle, you have all been great to work with!

I would also like to acknowledge and thank my committee members Dr. Jan Rainey, Dr. Mark Stradiotto, and Dr. Peng Zhang for their feedback. Overall, my experience with the Department of Chemistry at Dalhousie University has been very positive over the years.

I am also very thankful for the expertise given from several people who made the tricky problems solvable. The very thin platinum wires were sealed in glass by Todd Carter to help create the microcavity electrodes and Daniel MacDougall from the biomedical engineering department made their very tricky depth measurements possible. I also want to thank Dr. Jeff Dahn for allowing me to use some of his instruments and Drs. David Hall and Robbie Sanderson for instructing me how to operate them. Also, a thank you to Dr. Jan Rainey for allowing me to use your AFM instrument and Dr. Roderick Chisholm for teaching me how to use it. Thank you Dr. Peng Zhang for allowing me to use your fluorometer. Andy George, the expert XPS technician, and Patricia Scallion, the expert SEM technician, thank you for making numerous procedures go smoothly. I also want to thank Dalhousie University, our chemistry department, NSERC, and the Nova Scotia Health Research Foundation for supporting my research.

I also cannot forget about thanking my mom who supported my decision to do a PhD by lending me a helping hand when there was not enough time in the day to do everything.

Chapter 1 Introduction

Electrochemical biosensors are an active area of research with applications in the fields of diagnostics, biotechnology, and environmental studies.[1–4] An electrochemical biosensor is a device that recognizes a biological event through the use of an electrode to convert the recognition into a readable electronic signal.[5] There is promising potential for electrochemical biosensors due to their speed, sensitivity and low-cost.[2,5] Electrochemical biosensors are becoming more portable and affordable as electronics become smaller and more common. A commercially successful example that show these qualities is the blood glucose monitor.[4–6] New research and development in electrochemical biosensors also contribute to the exciting research of developing lab-on-a-chip devices.[5]

Electrochemically sensing hemoglobin (Hb) may provide an alternative way to detect Hb, an important protein due to the role it plays in various diseases,[7–10] where Hb is currently measured by using the absorption of visible light.[7] The electrochemical activity of Hb is widely believed to be due to the oxidation and reduction of iron within the heme group.[11–14] Direct electron transfer between Hb and an electrode is generally considered to be difficult because the four redox active heme groups are buried in the interior hydrophobic regions of the protein.[15,16]

The low cost and abundance of carbon makes it a promising material for biosensor electrodes. A known issue when using carbon electrode materials is that its behavior may vary when electrochemically sensing Hb.[12,17–21] Hb has been shown to be electrochemically active on carbon black,[22] carbon nanotubes,[14,18,20,23,24] glassy carbon,[19]

and pyrolytic graphite;[21] but inactive on pyrolytic graphite,[17] and glassy carbon.[20] A disagreement exists whether carbon-oxygen surface functional groups improve[18,19] or inhibit[12] the electrochemical activity of Hb on carbon electrodes. There are suggestions that more C-O surface groups such as phenolic or alcoholic groups are responsible for favoring the electron transfer possibly due to changing polypeptide conformations.[19] However, more recent experimental evidence suggests less oxidized carbon surfaces have a larger electrochemical response to Hb.[12] Knowledge of the carbon-oxygen surface functional groups and their modification in the context of experimental evidence is key to fundamentally understand the electrochemical activity of Hb.

Whether Hb is immobilized on a carbon electrode or is present in the electrolyte is another possible variable. Opposing results for pyrolytic graphite have been reported where the immobilized Hb was electrochemically active,[21] while Hb dissolved in the electrolyte was inactive.[17] Nafion is a commercially available product convenient for creating thin films, which may be used to immobilize Hb onto the electrode surface.[14,22,23,25,26] An often overlooked problem is whether the solvent used to prepare the Nafion thin film has any effect during the immobilization procedure. Therefore, the solvent present in Nafion may interact with Hb and consequently affect the electrochemical detection of Hb. A fundamental study of the solvent effects in Nafion on Hb is necessary to provide a better understanding on its effects on the electrochemical detection of Hb.

The research presented in this thesis aimed to develop a better understanding of the variation in the electrochemical behavior of Hb on carbon electrode materials. The background information necessary to understand the techniques used in this thesis as well

as literature references leading up to the experiments are described in Chapter 2. Chapter 3 described the experimental methods and techniques used in this thesis.

Chapter 4 presents a thorough examination of the carbon-oxygen surface functional groups on five different carbon electrode materials. Carbon-oxygen surface functional groups were characterized using X-ray photoelectron spectroscopy (XPS), temperature programmed desorption (TPD), and attenuated total reflection Fourier transform infrared spectroscopy (ATR-FTIR). Chapter 4 also presents the electrochemical activity of Hb with respect to the presence and identity of the carbon-oxygen surface functional groups. The electrochemical activity of Hb was examined by the use of cyclic voltammetry and differential pulse voltammetry. After identifying the surface functional groups that impact the electrochemical activity of Hb, a carbon material was modified to enhance its electrochemical activity towards Hb.

Chapter 5 focuses on electrochemically examining Hb in an aqueous-alcohol electrolyte using a glassy carbon electrode or Hb immobilized on glassy carbon with a film of Nafion. The immobilization of Hb was studied electrochemically by using either a Nafion suspension to create a thin film or a solid piece of Nafion to hold Hb onto the electrode surface. The Nafion suspension contained an alcohol solvent while the solid piece of Nafion had no solvent. Differential pulse voltammetry was used to investigate whether the alcohol solvent present in a Nafion suspension had any consequence on the electrochemical detection of Hb by adding an alcoholic solvent to an electrolyte containing Hb and phosphate buffer.

Chapter 6 investigates evidence for changes to Hb or the glassy carbon electrode after exposure to the aqueous-alcohol electrolyte that may be responsible for affecting the

electrochemical activity of Hb. After exposing Hb to an aqueous-alcohol electrolyte, fluorescence and ultraviolet-visible spectroscopy provided evidence for changing the structure of Hb. Ultraviolet-visible spectroscopy is useful for tracking possible changes in the heme structure of Hb,[27–31] while fluorescence is useful for tracking changes in the environment near the fluorescing tryptophan residues.[32,33] Possible formation of a thicker protein film on the electrode surface after exposure to Hb in aqueous-alcohol electrolyte may be responsible for observing a different electrochemical response. The formation of a possibly thicker protein film on the electrode surface was attempted *ex situ* using atomic force microscopy and spectroscopic ellipsometry. Changes to the carbon-oxygen surface groups on the carbon electrode surface after being exposed to aqueous-alcohol electrolyte were studied using XPS. The overall conclusions as well as suggestions for future work are presented in Chapter 7.

Chapter 2 Background

2.1 Bovine Hemoglobin

Bovine hemoglobin (BHb), visualized in Figure 2.1, is a globular blood protein with a molecular weight of about 64,500 Da and a diameter of approximately 5.5 nm.[34,35] The dimensions of BHb are approximately 65 x 55 x 50 Å.[30,34,35] BHb consists of four subunits arranged as a tetramer: two alpha subunits and two beta subunits.[11,34,36,37] Each subunit consists of a polypeptide chain and a heme group (Figure 2.1c). Non-covalent interactions hold these four subunits together.[11]

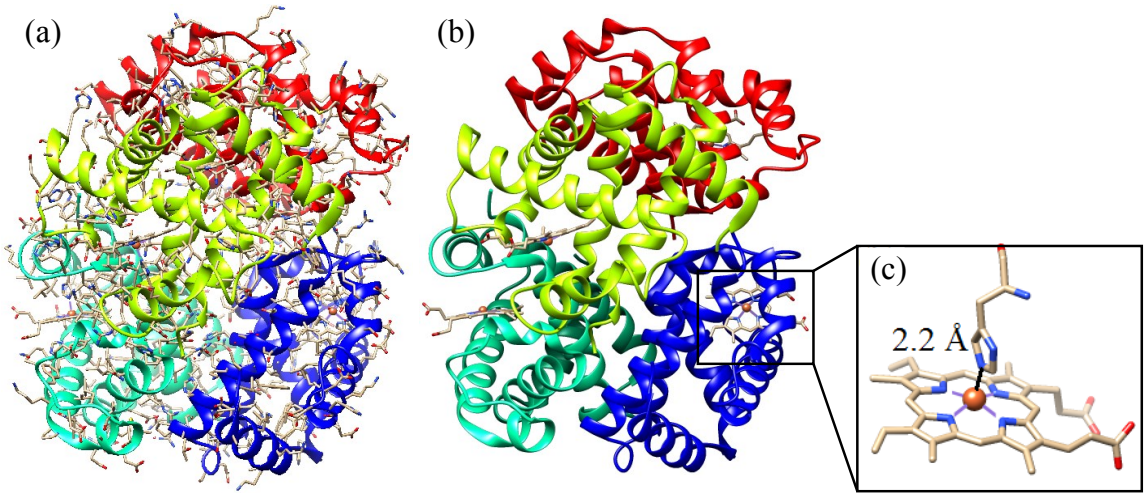

Figure 2.1 A crystal structure of BHb obtained from the Protein Databank (identifier 1HDA) illustrating its globular structure and the four subunits (a and b).[34,35] The amino acid residue side chains were removed to more clearly indicate the location of the heme structures in the protein (b). A close-up illustration of one of four heme structures in BHb showing the four bound nitrogen atoms (blue) in the porphyrin ring and one nitrogen atom from a histidine residue coordinated (black) to the Fe atom (red sphere) (c). All images were produced using the software Chimera.[34,35]

The polypeptide in an alpha subunit contains 141 amino acids and a beta subunit contains 145 amino acids.[34,35] There are 3 tyrosine (Tyr) residues and 1 tryptophan (Trp) residue in an alpha subunit and there are 2 Tyr residues and 2 Trp residues in a beta subunit.[34,35] Therefore, there are a total of 10 Tyr and 6 Trp residues in BHb that can potentially be probed by the use of fluorescence, as will be discussed later in Section 2.6.2. The locations of the Trp and Tyr residues are highlighted in Figure 2.2 with their estimated distances to the nearest heme group based on the crystal structure of BHb.

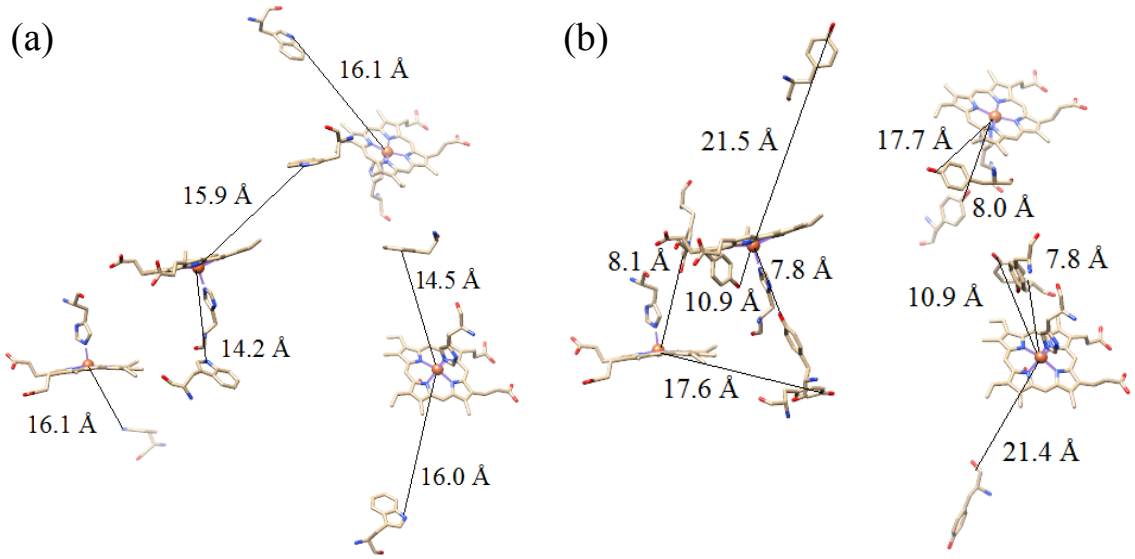

Figure 2.2 Illustration of Trp residues (a) and Tyr residues (b) with their approximate distances to the nearest heme group in BHb with the same positions as those shown in Figure 2.1. The remaining protein structures and amino acid residues were removed for clarity. These illustrations were produced using the software Chimera.[34,35]

Each heme group can be found buried within a hydrophobic cavity located near the surface of BHb.[11,30,34,35] The four nitrogen atoms from the heme group are bound to iron, as shown in Figures 2.1c and 2.2. Histidine from a polypeptide chain is bound axially to the iron, leaving the sixth position available for another ligand such as oxygen.[30] If the heme iron is in the ferrous (Fe^{2+}) state, it allows for reversible bonding

of oxygen to hemoglobin (Hb).[8] Ferric iron (Fe^{3+}) in Hb is called methemoglobin or ferrihemoglobin and cannot bind oxygen.[8–12] When ferrous Hb binds to oxygen, the ferrous Hb is oxidized to ferric Hb and the bound oxygen is reduced to superoxide.[38]

Changing the oxidation state of iron in Hb can potentially be used for diagnostic electrochemical biosensor applications. Hb is involved in some clinical conditions such as methemoglobinemia and anemia.[8–10] Methemoglobinemia is due to a large accumulation of methemoglobin (ferrihemoglobin) where Hb cannot bind to oxygen and anemia is a deficiency of Hb.[8–10] Both of these conditions are important to recognize and, thus, their detection is essential to minimize long-term damage.[8–10]

2.2 Electrochemically Sensing Hemoglobin

Currently, the most common approach to quantify Hb in blood is to make optical measurements using either laboratory instruments or commercially available point-of-care optical devices.[39–42] However, optical interferences, such as the presence of ambient light, are known to be potential causes of erroneous readings.[43] In these cases, an alternate route of detection such as the use of an electrochemical method may be more desirable.

Electrochemical biosensors have several advantages for use at a physician's office or at a patient's home.[4,5] In general, they have the advantages of rapid measurement, simplicity, sensitivity, low operating cost, low construction cost and the possibility of miniaturization.[4,5] A disadvantage of using electrochemical biosensors may be poor selectivity where interference may occur from electrochemical reagents other than the Hb analyte.[6]

Obtaining an electrochemical signal for Hb may also provide insight into its reaction mechanism with other proteins[11] or provide an alternative means for direct Hb detection, which is important due to possible cytotoxic effects from Hb[9] and the important role Hb plays in various diseases such as anemia.[7,8] However, direct electron transfer between Hb and an electrode surface is difficult due to large polypeptide chains obstructing access to the heme groups.[44] Each Hb contains a total of four iron ions, one iron from each heme group,[11,37] which are potentially redox-active by changing oxidation state between 2+ and 3+.[11]

Due to the difficulty of electrochemically accessing the iron in Hb, researchers have devised many creative ways to circumvent this problem; for example, by developing mediators to aid in the electron transfer,[11,15,45–49] incorporating Hb into a film on the electrode surface,[17,24,50–59] or by adsorbing Hb onto metal oxides attached to an electrode.[21,60–65] Although Hb attached to an electrode can be used for studying the catalytic reduction and detection of hydrogen peroxide,[14,20,22,23,44,55,56,63,64] examining the electrochemical activity directly from Hb, particularly with Hb in solution, is the focus of this thesis. Various strategies used to electrochemically sense Hb are discussed next.

2.2.1 Mediated Electron Transfer

Because of the difficulty in attaining an electron transfer between an electrode surface and Hb, mediators are sometimes employed to help transfer electrons between Hb and the electrode surface.[15,46–49] For example, ferricyanide can be used to oxidize Hb present in a blood sample as ferricyanide reduces to ferrocyanide and the ferrocyanide is then quantitatively oxidized using an electrode to regenerate ferricyanide.[45] Mediators

attached to the electrode surface have also been used to detect and quantify Hb, some of which are ferrocenecarboxylic acid,[15] Nile Blue,[46] and methylene blue.[47–49] The quantification of Hb using the mediated electron transfer strategy is possible within the μM[15,46,48] or nM concentration range.[49]

One of the issues with mediator-modified electrodes is leaching of the mediator into the electrolyte with repeated use.[48] Another issue is that these mediators may not be specific to Hb; thus interference from other redox active species in a sample is possible.[48] As a result, other strategies to electrochemically sense Hb have been attempted.

2.2.2 Hemoglobin on Modified Electrodes with Metal Oxides, Nanomaterials, or Layered Structures

Modifying the electrode surface to electrochemically examine Hb is a far more common strategy than using mediators.[11] Examples of different materials used to prepare the electrode surface sampled from the literature are listed in this section.

The immobilization of Hb onto electrode surfaces modified with a metal oxide has been shown to improve the electrochemistry of Hb.[21,60–65] For example, Hb adsorbed onto nanocrystalline SnO_2 films[62] on a conductive fluorine-doped tin oxide-coated glass was shown to be electrochemically active. Other examples include Hb adsorbed onto nickel oxide nanoparticles[63] or cobalt oxide nanoparticles[64] on a glassy carbon electrode, Fe_3O_4 nanoparticles with adsorbed Hb on pyrolytic graphite,[21] and Hb on Fe_3O_4-graphene composite materials.[65] In the examples provided previously, the number of layers were typically limited when investigating the electrochemical activity of Hb. In one study, Hb was shown to be more active when Fe_3O_4 nanoparticles were arranged in alternating layers with Hb on a pyrolytic graphite electrode.[21] Research has shown that up to six

stacks of Fe_3O_4/Hb bilayers were electrochemically active and has stated that additional bilayers resulted in no further increase in Hb activity.[21]

Hb adsorbed on carbon nanotubes, which are sometimes held together using a Nafion polymer,[14,23] is known to be electrochemically active.[18,24,66] The electrostatic adsorption of Hb onto the carbon nanotubes was believed to improve its electrochemical activity.[18] Later research showed that carbon nanotubes with metal oxide impurities have higher Hb electrochemical activity than purified carbon nanotubes where the metal oxide impurities help bind Hb to the carbon nanotubes.[23]

Hb is also known to be electroactive on electrodes modified with quantum dots. For example, Hb mixed with CdSe-ZnS quantum dots bound by Nafion on a glassy carbon electrode was reported to be electrochemically active.[67] Quantitative detection of Hb in the electrolyte is also possible using a glassy carbon modified with cadmium sulfide quantum dots.[68]

Gold nanoparticles may be used to enhance the electrochemistry of Hb. For example, Hb adsorbed onto graphene-gold nanoparticle composite materials[69] or carbon nanotubes modified with gold nanoparticles[70] were shown to exhibit higher Hb activity. The increased Hb activity may have been due to the significantly increased surface area available for trapping Hb.[69,70]

Changing the pore characteristics on the electrode surface may also allow more Hb to bind onto the electrode surface to help increase the electrochemical activity of Hb.[13,25,52] For example, increasing the pore size of heat-treated carbon nanofibers,[25] increasing the pore volume of mesoporous carbon,[13] or creating characteristic V-shaped

pores in polyaniline-mesocarbon composite materials[52] may have resulted in increased Hb binding to the electrode surface, resulting in increased Hb electrochemistry.

Adsorption onto clay materials is another strategy to achieve increased Hb electrochemistry. More specifically, Hb adsorbed onto either a montmorillonite clay attached to a glassy carbon electrode[71,72] or Bentonite clay on a pyrolytic graphite electrode were shown to be electrochemically active.[73,74] The clays were believed to have minimal electrostatic repulsion to Hb due to both the hydrophobic and hydrophilic interactions on the composite clay surface stabilizing the adsorbed Hb, resulting in more redox active Hb.[71,75]

Surfactants may also be used to modify the electrode surface. The formation of a surfactant bilayer structure may be a more favorable environment for the immobilization of Hb and perhaps help with the electron transfer between Hb and the electrode.[76] An example of this may be where acetylene black was mixed with a didodecyldimethylammonium bromide surfactant and Hb.[76] The use of this particular surfactant was believed to form an ordered surfactant bilayer structure to aid in immobilizing Hb on the electrode surface and facilitate the electron transfer process.[76]

Observation of the Hb electroactivity is known to be possible through the incorporation of Hb into a hydrogel. Some examples include mixing Hb with a sodium alginate hydrogel[77] or a konjak glucomannan hydrogel.[59] The increased electrochemical activity of Hb in a hydrogel was believed to be due to exposing the heme groups in Hb to a more hydrophobic environment in the hydrogel than in the aqueous electrolyte.[59]

Other film materials may be used to trap Hb onto a carbon electrode surface to increase Hb electroactivity, some of which are polytetrafluoroethylene,[56] gelatine,[55]

gluten,[57] and chitosan.[53,54,58] In some cases, the conductivity must be increased by including other components, such as adding graphene to a chitosan film.[53] To avoid conductivity issues, Hb may also be trapped in a conductive polymer, such as polypyrrole, which has been shown to exhibit Hb electrochemistry.[78]

The main disadvantage of modifying the electrode surface with a metal oxide, a nanomaterial, or a layered structure is the time consuming process required to prepare the electrode for the electrochemical examination of Hb. Similar to the mediated electron transfer strategy, μM to nM concentrations of Hb may be detected using electrodes modified with either a metal oxide or nanomaterial.[68,70] Many believe that Hb adsorbed on or incorporated into a layered electrode surface involves a one electron and one proton transfer from heme,[17,21,52,54–57] but are uncertain regarding how many hemes are redox active in Hb on the modified electrode surface. Therefore, the direct electrochemical examination of Hb may not be fully accessing all available hemes in Hb.

2.2.3 Denaturation of Hemoglobin

Another perhaps more direct approach to observe Hb electrochemistry is to denature the protein structure itself, thereby releasing the potentially redox-active heme groups. For instance, guanidine hydrochloride denaturant was added to the electrolyte in order to achieve Hb electroactivity in solution using a glassy carbon electrode, where no Hb electroactivity was observed without guanidine hydrochloride.[29] Common single-chain surfactants well-known to denature protein structures, such as sodium dodecyl sulfate, are known to increase the electroactivity of Hb.[79] Other methods of unfolding the

protein structure to increase Hb electroactivity include incubating adsorbed Hb in acidic electrolyte[80] and urea.[71]

Sometimes, exposing Hb to particular solvents may enhance the electrochemical activity of Hb. In one example, the electrochemical activity of Hb in a hydrogel was shown to increase in an electrolyte containing 50% ethanol and 50% phosphate buffer, which may be due to partial dehydration of the heme cavity in Hb.[59] In another example, clear Hb electroactivity was reported after incubating a pyrolytic graphite electrode in a mixture of Hb, dimethyl sulfoxide and water.[81] Although the authors of the publication did not give reasons why adding dimethyl sulfoxide increased the electrochemical activity of Hb, there is clear evidence elsewhere that dimethyl sulfoxide changes the secondary and tertiary Hb protein structure.[82] These changes to the protein structure are likely responsible for the increased electrochemical activity of Hb.

An additive that stabilizes the protein structure may have the opposite effect, where the electroactivity of Hb is expected to decrease. Glycerol is known to stabilize and prevent significant denaturation of protein structures.[83] When a pyrolytic graphite electrode modified with Hb and a phosphatidylglycerol choline surfactant revealed Hb electroactivity,[83] adding greater concentrations of glycerol to the electrolyte decreased the electrochemical activity of Hb as expected.[83]

The protein denaturation strategy has the obvious disadvantage of not being specific to Hb since other heme-containing proteins will also be affected. However, this strategy clearly shows that the protein structure of Hb is indeed inhibiting electrochemical access to the redox-active heme groups and is a progression towards attaining higher Hb electroactivity.

2.2.4 Electrochemistry of Hemoglobin on Silver Electrodes

Slow electron transfer of Hb on a metal electrode is believed to be due to the adsorption of Hb on the metallic surface, thus inducing changes to the protein conformation that may be restricting access to the electrochemically active hemes.[84] Hb electroactivity has been reported using a silver electrode in a buffered electrolyte containing Hb.[85,86] Other published works using a silver electrode modified with adsorbed iodide were shown to increase the electrochemistry of Hb.[87] Evidence has strongly suggested that the heme group is not responsible for the redox behavior of Hb seen on silver electrodes, but appears to be related to the formation of a complex between silver and the amino acids, promoted by the presence of chloride in aqueous electrolyte.[84] Therefore, the use of a silver electrode would be less selective than the modified electrodes described in previous sections since all proteins are composed of amino acids.

2.2.5 Electrochemistry of Hemoglobin on Carbon Electrodes

The advantages of using a carbon electrode are affordability and a wide usable potential range.[88–90] Despite these advantages, carbon can have complicated reactivity. Many of the reactions on carbon surfaces occur on the surface defects as well as on the edges of the graphene sheets in a carbon material.[88,89] Exposing the reactive surface defects along the edges of the graphene sheets to oxygen or moisture can result in carbon-oxygen surface functional groups.[88]

Although nitrogen, sulphur, oxygen, and halogen may be present on some carbon surfaces,[91] depending on the source of carbon, its history and the manufacturing process involved,[88–90] the most common carbon surface functionalities contain oxygen.[92] Some

of the oxygen-containing surface functionalities are phenols, carboxylic acids, lactones, carbonyls, and quinone groups.[88,93]

A common theory regarding the electrochemical reactivity between Hb and carbon electrodes is that the carbon-oxygen surface functional groups on the carbon electrode may play a role in the electroactivity of Hb.[18,19,22,23] Several studies from the literature reported electrochemical activity of Hb prepared on carbon black,[22] carbon nanotubes,[14,18,20,23,24] and pyrolytic graphite[17,21] electrodes. The presence of oxygen surface groups on carbon black[22] and carbon nanotubes[14] were believed to help with the electron transfer process of immobilized Hb. More specifically, the introduction of more COOH surface groups on carbon was believed to be associated with increased electrochemical activity of immobilized Hb due to favorable electrostatic interactions where the modified carbon was negatively charged and Hb was positively charged.[18,52]

Some of the discrepancies in the electrochemical activity of Hb on carbon surfaces found in the literature will be presented here. Conflicting results may be seen, where one study reported no direct electrochemistry between a Hb-incubated pyrolytic carbon electrode,[81] but another study also used a Hb-incubated pyrolytic carbon electrode and clearly observed Hb activity.[21] Electrochemical examination of Hb in a neutral pH buffer was shown to have no activity using a pyrolytic graphite electrode.[17] Other studies observed no electrochemical activity of Hb in a neutral pH electrolyte using glassy carbon[29] or Hb dried on glassy carbon,[14,20,63] yet glassy carbon has been reported to electrochemically reduce Hb in solution[12,19,26] and when Hb is held onto the glassy carbon surface using a Nafion polymer.[23] Phenol surface groups on a polished glassy carbon surface are known to exist and have been suggested to be involved in changing

the polypeptide conformation of Hb to favor the electron transfer process.[19] If the oxygen-containing surface functional groups are responsible for the Hb reactivity, it is unclear why no reactivity was seen in the other studies that used glassy carbon or pyrolytic graphite electrodes, which is a direct disagreement based on observed results.

More recent experimental evidence suggested an opposite interpretation, where Hb was observed to have greater electrochemical activity on less oxidized carbon materials,[12] which highlights the inconsistent assignment of carbon-oxygen surface groups being responsible for the electrochemistry of Hb. The inconsistency in the electrochemical activity of Hb could perhaps be explained by a detailed examination of the carbon-oxygen surface groups on different carbon materials, as will be undertaken in this thesis.

2.3 Overview of Relevant Electrochemical Techniques

2.3.1 Cyclic Voltammetry

Cyclic voltammetry is an electrochemical technique where an applied potential is varied while measuring the current response. The potential starts at E_1 and the potential changes at a linear rate towards E_2. Then, the applied potential reverses direction with the same linear rate from E_2 and returns to E_1. The linear rate at which the potential changes is also called the sweep rate. An illustration of the applied potentials during a cyclic voltammetry experiment is provided in Figure 2.3.

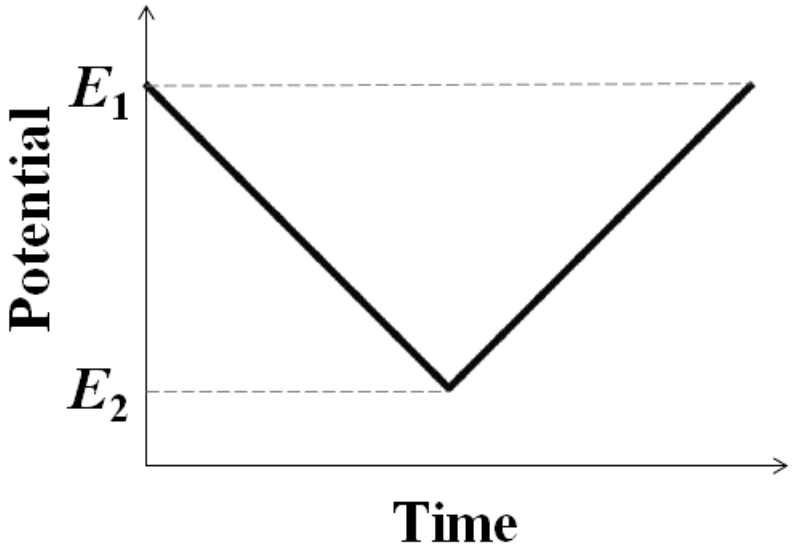

Figure 2.3 An illustration of the applied potential during a cyclic voltammetry experiment.

2.3.2 Differential Pulse Voltammetry

Differential pulse voltammetry is an electrochemical technique that changes the applied potential in a series of pulses. Figure 2.4 is a simplified diagram illustrating the differential pulse voltammetry technique. The adjustable parameters in this technique are the initial potential (E_i) held for a period of time (t_i), pulse width (P_w), pulse height (P_h), step height (S_h), and step time (S_t). The parameters S_h and S_t directly affect the sweep rate. During a pulse (illustrated in Figure 2.4), potential E_1 is held for a set time, followed by a sudden ($P_h + S_h$) change to potential E_2 held for an amount of time (P_w). The currents I_1 and I_2 are measured immediately before the end of each potential hold at E_1 and E_2 respectively. The difference of I_2 and I_1 is recorded as a point versus the applied potential E_1 in a differential pulse voltammogram (DPV). The next pulse starts at potential E_3, which is S_h above E_2. The process described is then repeated numerous times until the entire voltammogram is recorded.

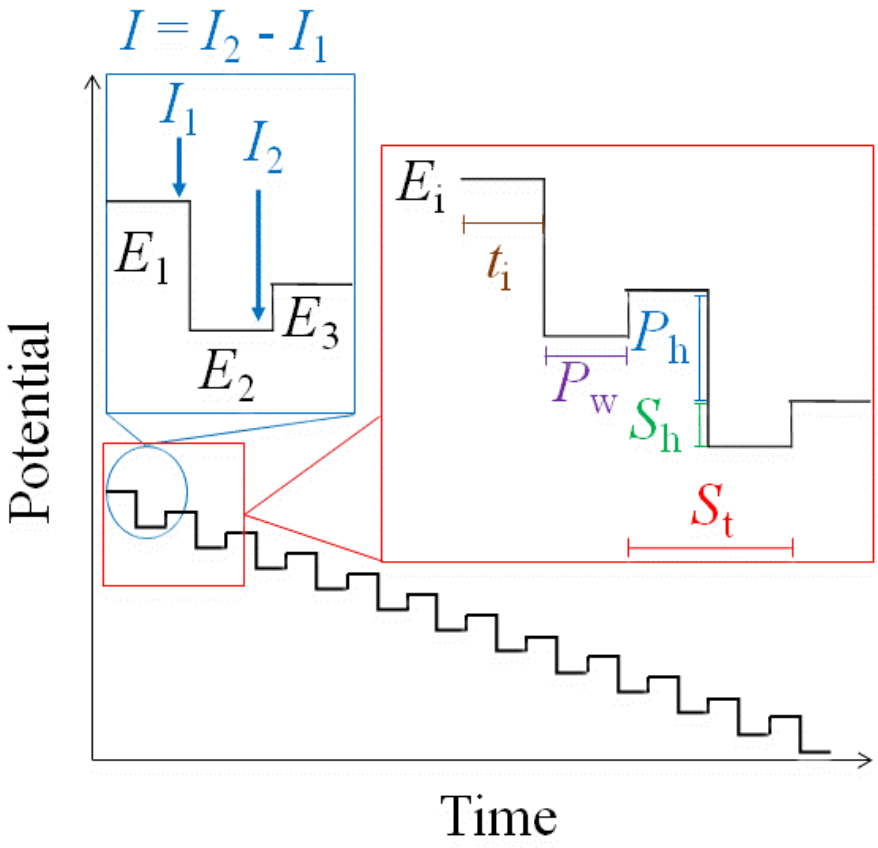

Figure 2.4 A simplified diagram illustrating how differential pulse voltammetry operates. Note that in a differential pulse voltammetry experiment, several more pulses are performed.

The measured current includes both the charging current and the analyte redox current. Charging currents are not a result of electron transfers like redox reactions. Instead, charging currents originate from changes in the double layer of charge, which exists at any material interface.[94,95] For simplicity, the double layer may be visualized as a layer of charge on the electrode surface and a layer of opposite charge from the electrolyte near the electrode surface. As a potential is applied to the electrode, the double layer of charge changes, meaning current flows (*i.e.* the charging current). Differential pulse voltammetry preferentially removes more charging current than the redox current when recording the measured currents, which relies on the fact that

charging currents are orders of magnitude faster than redox currents when an electric potential is applied.[96] As a result, the currents due to redox reactions are emphasized and the charging currents are suppressed in a DPV.[95]

2.4 Carbon Surface Oxide Characterization Techniques

Surface-sensitive examination of carbon electrode materials for carbon-oxygen groups is required to begin resolving the opposing interpretations presented previously in Section 2.2.5. Commonly employed techniques for examining carbon surface oxide groups are Boehm titrations,[97–108] temperature programmed desorption,[93,98,100–105,109,110] infrared spectroscopy,[93,100–106,110–112] and X-ray photoelectron spectroscopy.[93,98,102,104,106,109,113–124] The Boehm titration was not used in this thesis due to the large amount of carbon sample required.[125,126] The techniques used in this thesis are temperature programmed desorption, attenuated total reflectance Fourier transform infrared spectroscopy, and X-ray photoelectron spectroscopy. These techniques will be discussed next.

2.4.1 Temperature Programmed Desorption

Temperature programmed desorption (TPD) is a straightforward technique that uses heat to desorb the carbon-oxygen surface groups from the carbon surface while using the sample weight changes and evolved gas content to quantify the different carbon surface oxide groups. TPD continuously measures the weight of the sample as a function of temperature, while a mass spectrometer identifies the components of the evolved gases.[93,104,127] TPD requires the careful use of a programmable temperature-controlled

furnace that heats the sample at a constant rate under an inert atmosphere.[93,104,127] As the temperature increases, different carbon-oxygen surface functional groups on a carbon sample will desorb as CO or CO_2 gases.

Less stable surface groups, such as carboxylic acids, desorb at lower temperatures as CO_2 gas, and more stable surface groups, such as carbonyls, desorb at higher temperatures as CO gas. A list of known desorption temperatures for various carbon-oxygen surface functional groups identified by the use of TPD were well summarized by Figueiredo *et al.*[93] A simplified adaptation of the summary is presented in Table 2.1.

Table 2.1. A simplified table illustrating the identification of several different carbon-oxygen surface groups on carbon by the use of TPD adapted from the work of Figueiredo *et al.*[93]

Carbon-Oxygen Surface Group	Evolved Gas	Temperature Range / °C
Carboxylic acid	CO_2	100-400
Lactone	CO_2	350-600
Anhydride	$CO + CO_2$	350-600
Phenol	CO	600-700
Quinone	CO	700-980
Carbonyl	CO	700-1100
Ether	CO	700-1100

2.4.2 Attenuated Total Reflectance Fourier Transform Infrared Spectroscopy

Infrared (IR) spectroscopy can be useful to help confirm the presence of particular functional groups by examining the vibrations of atoms.[128,129] IR spectroscopy can be performed in either transmission or reflectance modes.[93,100–106,110–112] Due to the high absorbance of carbon, obtaining useful information by the use of transmission IR spectroscopy is typically very difficult and time consuming;[111,130] therefore reflectance spectroscopy in the form of attenuated total reflectance Fourier transform infrared

(ATR-FTIR) spectroscopy was used in this thesis. ATR-FTIR has the benefit of requiring very little sample preparation and can be a surface sensitive technique.[111,130]

ATR-FTIR is a modification of IR where the sample is in direct contact with an infrared-transparent crystal that has a higher index of refraction than the sample.[129] The infrared light passes through the crystal and reaches the interface. Total internal reflection occurs and creates an evanescent wave to probe the sample.[129,131] Some of the energy from the evanescent wave is absorbed by the sample and thus attenuates the infrared beam.[129,131] Then the reflected infrared beam returns to the detector. The intensity of the reflected infrared beam from the sample is then compared to the intensity of the reference infrared beam, which is then recorded. ATR-FTIR data is interpreted similarly as transmission IR data.[111,130] Figure 2.5 is a simplified illustration of how ATR-FTIR is used to probe a carbon sample.

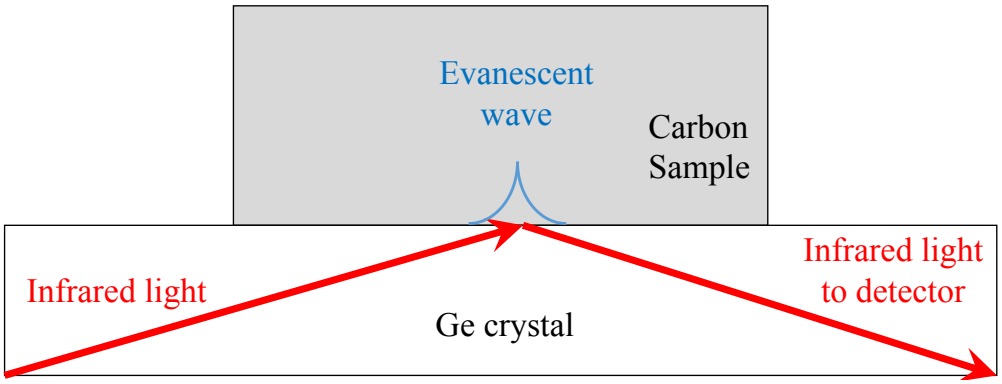

Figure 2.5 A diagram illustrating the evanescent wave probing a sample when internal reflection of infrared light occurs. This figure has been adapted from reference 129.

The sample cannot have an index of refraction similar or above that of the crystal used in ATR-FTIR, otherwise the infrared light will be lost since internal reflection will not occur.[129,131] Therefore, choosing an appropriate crystal for the sample to be examined is important. Diamond is typically used for ATR-FTIR analysis but Ge was used in this

work because Ge has a much larger index of refraction ($n \approx 4$ for Ge and $n \approx 2.4$ for diamond).[132] Some examples of using Ge crystal in ATR-FTIR for the examination of carbon samples can be found in the literature.[111,131]

2.4.3 X-ray Photoelectron Spectroscopy

X-ray photoelectron spectroscopy (XPS), also sometimes called electron spectroscopy for chemical analysis (ESCA),[133] is a surface-sensitive technique that uses X-ray radiation to probe a sample to obtain surface chemical information by measuring the kinetic energy and number of emitted photoelectrons. The sample is first placed under a high vacuum and then struck with X-rays.[133] The incoming X-rays may then interact with a core-level electron from the sample, resulting in the emission of a photoelectron near the sample's surface if the energy of the X-ray photon is larger than the electron binding energy.[133] Typically the emitted photoelectrons within the first ten nanometers from a sample surface are detected since their inelastic mean free path are on the order of a few nanometers.[133] Therefore, only the emitted photoelectrons near the surface of the sample are detected; this is why XPS is a surface-sensitive technique.

In XPS, the kinetic energy of the emitted photoelectrons (E_k) from a sample is measured. E_k cannot be used to uniquely identify the element, but the binding energy (E_b) can.[133] By applying the conservation of energy, the total energy of the known incident X-ray source hv, is equal to the sum of the kinetic energy E_k, binding energy E_b, and the work function Φ.[133] The X-ray energy source used in XPS is typically either Al Kα (1486.6 eV) or Mg Kα (1253.6 eV).[133] The work function Φ is the energy needed to

remove an excited electron from a sample into vacuum.[133] The experimentally useful relationship that relates to E_b may be more conveniently expressed as Equation 1:

$$E_b = h\nu - E_k - \Phi \quad (1).$$

E_b values will depend on the chemical environment of the atom emitting the photoelectrons;[133] an electron near an atom's nucleus will have a larger E_b than an electron farther away from the nucleus. Neighboring atoms bound to the atom emitting the photoelectron also influence the E_b of the photoelectron due to a different electron distribution. A more electronegative neighboring atom attracts the negative charge of electrons, thus, a partial positive charge remains on the atom being probed, resulting in increased E_b required to emit a photoelectron. Therefore, E_b shifts can give information about the chemical environment of the atom, such as the oxidation state and possibly the identity of bound neighbor atoms. For example, in a C_{1s} XPS spectrum, a peak from C=O is expected to appear at a higher E_b than C-O, which is expected to be higher than that of C=C.[133]

XPS data are typically displayed as a graph of the counts of photoelectrons per second as a function of E_b. Identification of the neighboring atoms and their quantification is possible by fitting peaks to the XPS spectrum.[133] The number of photoelectrons emitted from the sample depends on the surface concentration.[133] Calculation of the integrated area under the fitted peak in the XPS spectrum, after consideration of the background and sensitivity factors related to instrument parameters, can be used to estimate the surface concentration of elements within particular chemical environments on the sample.[133]

2.5 Measuring the Thickness of Thin Protein Films

It is proposed in this thesis that thin films of Hb may form on an electrode surface upon exposure to a solution of Hb. Thickness measurements of the Hb protein film were attempted using spectroscopic ellipsometry and atomic force microscopy; these techniques will be described next.

2.5.1 Spectroscopic Ellipsometry

Spectroscopic ellipsometry is a non-destructive technique that tracks how polarized light changes when interacting with the sample.[134,135] Changes in the light's polarization are sensitive to the thickness and optical constants, *n* and *k*, of a thin film sample deposited on the surface of a substrate.[134,135] The optical constant *n* represents the refractive index and *k* represents the attenuation of light, which is also sometimes called the extinction coefficient[136] where transparent materials would have an extinction coefficient of zero. Therefore, *n* and *k* form a set of optical constants defined for a particular wavelength of light.[136]

Spectroscopic ellipsometry is sensitive to the sample film thickness.[134–136] Reflected light from the film surface and reflected light from the bottom of the film will separate more with increasing sample film thickness, causing a phase delay, which can be related to the film thickness and the optical constants.[134–136]

There are two measured values in spectroscopic ellipsometry, the amplitude ratio Ψ and phase difference ratio Δ, which describe the changes in polarization when the incident polarized light interacts with the sample film, as noted in Equation 2.[136] The incident light contains parallel (*p*) and perpendicular (*s*) components, relative to the plane

of incidence.[134–136] The sample surface interacts with the *p* and *s* components of the incident light differently, which causes a change in the polarization of the reflected light. R_p and R_s are reflection coefficients for the *p* and *s* components of the polarized light and *i* is the imaginary number.[135]

$$\tan(\Psi)e^{i\Delta} = \frac{R_p}{R_s} \tag{2}$$

The measured Ψ and Δ values by themselves are generally not useful. Finding the film thickness requires the use of Ψ and Δ values in a model to describe the interactions between the polarized light and the film. Different optical models have been proposed for different materials,[135] which will be discussed in more detail in Chapter 6.

Multiple wavelengths (λ) are used in order to find a unique answer to the film thickness.[136] The equation directly relevant to calculating the film thickness *d* is shown in Equation 3 below:

$$d = \frac{\beta\lambda}{2\pi N_{\text{film}} \cos(\Theta_{\text{film}})} \tag{3}$$

$$N = n + ik \tag{4}$$

where β is the phase change from the top of the film to the bottom of the film, *N* is the complex number defined in Equation 4, and Θ_{film} is the angle of the refracted light in the film. In the case of a transparent film, *N* is simply the refractive index of the film, *n*. The measured data are used together with fitting software and Equations 2-4 to solve for the film thickness.[136,137] A complete mathematical treatment is beyond the scope of this thesis, but can be found in references 136, 138, and 139.

Fitting errors must be accounted for when fitting data to a model in order to obtain the film thickness and are estimated using the mean squared error (MSE) defined in Equation 5 by the CompleteEASE fitting software:[138]

$$\mathrm{MSE} = 1000 \times \sqrt{\frac{1}{3L - M}\sum_{x=1}^{L}\left(\left(S_{1(m,x)} - S_{1(e,x)}\right)^2 + \left(S_{2(m,x)} - S_{2(e,x)}\right)^2 + \left(S_{3(m,x)} - S_{3(e,x)}\right)^2\right)} \quad (5)$$

$$S_1 = \cos(2\Psi) \quad (6)$$

$$S_2 = \cos(2\Psi)\cos(\Delta) \quad (7)$$

$$S_3 = \sin(2\Psi)\sin(\Delta) \quad (8)$$

where L in Equation 5 denotes the number of different wavelengths used to obtain the data, x is a counter variable to keep track of the added errors for each recorded wavelength, M is the number of fitted parameters selected in the optical model, subscripts m and e indicate whether the parameter was found from the model or experimental data respectively, and S is defined by Equations 6-8.[138] A scaling factor of 1000 is included in the definition of MSE in Equation 5 to account for typical instrumental errors such that an ideal fit yields a MSE approximately 1.[138] The fitting errors are typically larger than the instrumental errors.[138] Methods that can help reduce the fitting errors will put more confidence into the calculated film thicknesses.

The Kramers-Kronig relations are a set of mathematical relations that serves two purposes. First, the Kramers-Kronig relations ensure that the values obtained in spectroscopic ellipsometry are physically reasonable by being able to derive the imaginary component from the real component of the refractive index, and vice versa, because the index of refraction can be defined as a complex function (Equation 4).[138,139] Second, the mathematical relations impose mathematical restraints such that the total

number of fitting parameters is reduced, which help decrease the fitting errors involved in calculating the film thickness.

Spectroscopic ellipsometry may be useful for calculating the sample film thickness, but is highly dependent on the optical model used to fit the measured data. Ideally, other techniques should be used to help complement the calculated film thickness, such as the use of atomic force microscopy.

2.5.2 Atomic Force Microscopy

Atomic force microscopy (AFM) is a useful technique to obtain surface information and morphology on an angstrom scale or better.[140,141] Figure 2.6 is a simplified illustration of the key components used in AFM. AFM relies on using a tip attached to a cantilever spring to mechanically probe the surface of a sample.[140,141] As the tip scans the sample surface, a height difference map is generated by plotting the amount of laser deflection from the cantilever, which is detected by a photodiode.[140] AFM tips can have radii as small as 30 nm or as large as 2 µm, but sharp AFM tips are required to obtain high resolution images.[140] Commercially available AFM tips are typically made of silicon or silicon nitride.[140] As the AFM tip probes the sample surface, usually the AFM images are collected line by line while recording the variation in the sample's height.[141]

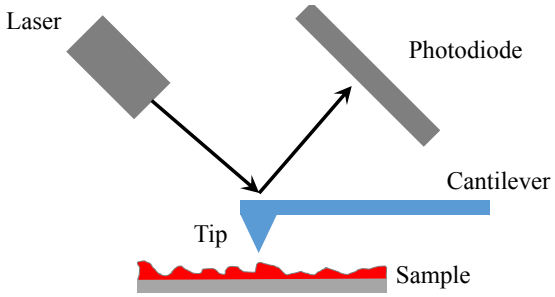

Figure 2.6 A simplified illustration of an AFM instrument.

Contact and intermittent contact modes are the two commonly used modes in AFM to collect surface sample images. In contact mode, the tip attached to the cantilever is pressed against the sample surface with a particular force and the cantilever is bent slightly. The force between the tip and the sample surface is dependent on the separation distance, and the composition of the tip and the sample.[140] Force measurements may also be useful to understand how different materials may adhere to the sample.[140] These force measurements can be made during contact mode by the application of Hooke's Law (Equation 9):

$$F = -\boldsymbol{k}x \tag{9}$$

where F is the force, $\boldsymbol{k}$ is the known spring constant of the cantilever, and x is the deflection in the cantilever. The issue with contact mode is that the tip may drag across the sample surface during the scan, which may result in damaging the sample surface and the tip. One workaround to this issue is to oscillate the cantilever.[142] In intermittent contact mode, the cantilever oscillates such that the AFM tip makes contact with the sample surface for brief periods of time, therefore avoiding the issue of having the AFM tip drag across the surface.

2.6 Characterizing Hemoglobin in Solution

2.6.1 Ultraviolet-Visible Spectroscopy

Ultraviolet-visible (UV/Vis) spectroscopy is a technique that examines the absorption of light in the ultraviolet and visible regions of the electromagnetic spectrum. UV/Vis spectroscopy can be used to obtain information regarding certain structural features of Hb, which are well-known in the literature.[19,27–30] In particular, the Soret

absorption peak arising from the porphyrin structure of heme in Hb is the most intense absorption peak, and is generally found between 405-430 nm in Hb.[30,143] The position of the Soret peak is sensitive to changes in the heme structure of Hb, including changes to the axial ligand bound to the iron.[30] A red-shifted Soret peak is likely due to more interactions between the Fe and an axial ligand within a heme group, and a blue-shifted Soret peak is likely due to fewer interactions.[143] For example, oxyhemoglobin, where oxygen is bound to iron, is known to have its Soret peak at 415 nm,[30] and ferrihemoglobin, where the iron has an oxidation state of 3+ with no oxygen bound, has a Soret peak at 405 nm.[27,28,30]

2.6.2 Fluorescence

Fluorescence is a widely used technique, especially in biochemical research, due to its high sensitivity and non-destructive nature.[32] Fluorescence is a spectroscopic technique where a molecule is excited by absorbing incident light, loses some energy, and then relaxes to ground state while emitting light of a longer wavelength than the incident light.[144] Phenylalanine (Phe), tyrosine (Tyr), and tryptophan (Trp) are amino acids that are known to fluoresce with emission maxima near 282 nm, 303 nm, and 348 nm respectively in water.[32,145] Excitation maxima are also known for Phe, Tyr, and Trp, which are near 258 nm, 275 nm, and 280 nm respectively in water.[145] Of these three amino acids, Trp is generally the dominant source of fluorescence.[32] The positions of the Trp residues in BHb were shown previously in Figure 2.2a in Section 2.1. The fluorescence of a Trp residue in a protein is sensitive to its microenvironment. For

example, exposing Trp to a more polar environment is expected to have its fluorescence shifted towards a longer wavelength.[29,32]

In addition to the shift in the Trp emission peak, its emission intensity may also change in Hb due to the well-known Förster resonance energy transfer.[33,146,147] An energy transfer from the excited Trp residues to the heme lowers the Trp fluorescence emission.[146,148] The Trp emission intensity is known to increase immensely after removal of the heme group in Hb.[146] The energy transfer is known to be possible up to a distance of 10 nm and the distance from the excited Trp residues to the heme group is proportional to the fluorescence;[32] thus, large increases in Trp emission intensity in Hb may also indicate increasing distance between the heme and Trp residues.

Chapter 3 Experimental Methods

3.1 Electrochemical Experiments

All electrochemical measurements were made using a Bio-Logic VMP3 multipotentiostat connected to a three-electrode system consisting of a platinum mesh counter electrode, a reference electrode, and a working electrode. Either a Hg/Hg_2SO_4 (saturated K_2SO_4) (measured as 0.692 V versus the standard hydrogen electrode) or a Ag/AgCl (1 M KCl) (measured as 0.221 V versus the standard hydrogen electrode) was used as the reference electrode in this thesis. All electrochemical results in this thesis are reported against the Hg/Hg_2SO_4 (saturated K_2SO_4) reference electrode for consistency, with the exception of the pencil working electrodes that are reported against the Ag/AgCl (1 M KCl). The pencil electrode experiments were attempts to reproduce Majidi's electrochemical results of hemoglobin on pencil electrodes;[149] the Ag/AgCl reference electrode was used in this thesis because it contains chloride like the saturated calomel reference electrode used in Majidi's work. For all other experiments, the Hg/Hg_2SO_4 reference electrode was used to avoid possible chloride contamination in the electrolyte since chloride has a well-known allosteric effect on hemoglobin,[34,150] meaning that chloride affects the ability of hemoglobin to bind oxygen,[34] which may influence the electrochemistry of hemoglobin.[36,151] All electrochemical data were recorded in an all-glass one compartment electrochemical cell using EC-Lab software.

Unless otherwise described, the electrolyte used for the electrochemical experiments was 0.1 M phosphate buffer (PB) with a pH of 7.08, measured using a SympHony posiIo pH electrode and meter (VWR International). The 0.1 M PB consisted

of K_2HPO_4 (≥98%, ACS Reagent, Sigma Aldrich) and KH_2PO_4 (≥99.0%, Sigma Life Science) in a 64.5% to 35.5% mole ratio dissolved in 18.2 MΩ·cm deionized Millipore water.

Deionized Millipore water with a resistivity of 18.2 MΩ·cm was used for washing and making all solutions, unless otherwise noted. Before and after every electrochemical experiment, all electrochemical cells and platinum mesh counter electrodes were carefully wiped with a Kimwipe to remove any excess hemoglobin, washed using distilled water, followed by a five minute submersion in 1 M NaOH (>97.0%, ACP, S-3700) to remove residual hemoglobin and, thereafter, washed several times using Millipore water.

3.1.1 Cyclic Voltammetry & Differential Pulse Voltammetry

In this thesis, cyclic voltammetry or differential pulse voltammetry was used to study the electrochemical behavior of hemoglobin. Cyclic voltammetry was conducted between 300 and -900 mV (versus the Hg/Hg_2SO_4) for all carbon electrodes, except for the pencil working electrodes, with a sweep rate of 20 mV s^{-1}. The pencil working electrodes were scanned using the same rate between -0.45 and 0.15 V versus the Ag/AgCl, which is equivalent to -0.92 to -0.32 V versus the Hg/Hg_2SO_4. Differential pulse voltammetry was also conducted between 300 and -900 mV with the same sweep rate. In differential pulse voltammetry, the initial potential was held for 2 seconds, all subsequent steps had a pulse height of 50 mV, pulse width of 250 ms, step height of -25 mV, and a step time of 1250 ms. Only the Spectracarb 2225 carbon fabric, Black Pearls 2000, and heat-treated Black Pearls 2000 carbon samples used a step time of 25 s

and an effective sweep rate of -1 mV s^{-1}, because of the high surface area of these samples and slow charging response. At least three replicates were performed for each sample to ensure reproducible results.

3.1.2 Different Carbon Materials as a Working Electrode

Several types of pencils, four different carbon powders, a carbon cloth, and three different types of working electrode sample holders were used in this thesis. Detailed descriptions of the working electrodes and the electrochemical cell will be given in the following subsections.

3.1.2.1 Pencil Working Electrodes

Majidi *et al.* successfully used a pencil working electrode to examine the electrochemical activity of hemoglobin, so several pencil electrodes were tested in this thesis with the goal of reproducing their results.[149] The brands and types of pencils tested as working electrodes in this thesis research were: Derwent Graphic (7B, 9B, 2.5 mm diameter, England), DeSerres (B, H, 2 mm diameter), Rotring (505210N, 2 mm diameter) and Staedtler (2B, 3B, 5B, 8B, F, 3H, 4H, 5H, 6H, 2 mm diameter, Mars Lumograph, Germany). All pencil working electrodes, except Rotring 505210N, were prepared by scraping the wooden casing away on both ends of the pencil, exposing a few centimeters of the pencil lead, ensuring that none of the wooden casing was near the electrolyte. The Rotring pencil had no wooden casing and was used as is. One end of the pencil was polished flat and smooth on filter paper (Whatman). The pencil lead was then wrapped tightly in Parafilm, leaving the flat polished end exposed to the electrolyte. The other unpolished end of the pencil was used to make an electrical connection to the

multipotentiostat. After each experiment, the end of the pencil lead electrode was sliced off and the newly exposed electrode was polished smooth on filter paper.

Human hemoglobin (HHb, Sigma Life Science, lyophilized powder, from human blood, H7379) was made with a concentration of 10 g L^{-1} by dissolution in 0.1 M PB. In the pencil-modified experiments, human hemoglobin was immobilized on a pencil electrode by drying 10 µL of the 10 g L^{-1} HHb on the electrode surface overnight in a refrigerator at *ca.* 4 °C.

A glass beaker cell with approximately 15 mL of 0.1 M PB electrolyte was used with the pencil as the working electrode. The PB electrolyte used for only these pencil experiments was made from $NaHPO_4$ (>99.0%, Sigma, S0751) and NaH_2PO_4 (>99.0%, Sigma, S0876) with a final pH of 7.00 to resemble the conditions used in Majidi's work.[149] A homemade Ag/AgCl (1 M KCl) (measured as 0.221 V versus the standard hydrogen electrode) with a glass frit was the reference electrode and a platinum mesh was used as the counter electrode. KCl (ACS reagent grade, Fisher Scientific) was used for the filling solution in the reference electrode.

3.1.2.2 Carbon Powder Working Electrodes

Powdered carbon is a common form of carbon materials. The carbon powders used in this thesis were: Black Pearls 2000 carbon black (Cabot, lot-935812), Vulcan XC-72 carbon black (Cabot, lot-1105528), graphite (>99.99%, Sigma-Aldrich, Batch # 15618DD, -325 mesh), and glassy carbon (99.95%, Aldrich Chemistry, 42297KJ, spherical powder, 2-12 microns). For most experiments, these carbon powders were used as-received and inserted in a microcavity electrode as described in Section 3.1.2.2.1 to study the electrochemistry of hemoglobin. The carbon-oxygen surface functionalities

were modified on the Black Pearls 2000 and Vulcan XC-72 carbon powders to alter their electrochemical activity with hemoglobin; the modifications will be described in detail in Section 3.1.3.

3.1.2.2.1 Microcavity Electrode

Carbon powders are usually mixed with a binder to prepare a paste that is made into an electrode. However, the effect of the binder on the carbon-oxygen surface groups and electrochemical activity of hemoglobin is unknown. To avoid the use of binders, a microcavity electrode was used. The construction of a microcavity electrode is well-known and has been described in several literature reports.[152–157] The microcavity electrode constructed in this thesis consisted of a thin platinum wire current collector (250 μm diameter) sealed in glass by Mr. Todd Carter (Scientific Glass Blower, Department of Chemistry, Dalhousie University). The glass-sealed end of the platinum was polished smooth with 600 grit SiC paper (Gatorgrit), followed by 3 μm diamond then 1 μm diamond polishes on nylon pads (BASi PK-4 MF-2060 polishing kit) with water rinses and 2-minute ultrasonication steps (Branson 1510 Ultrasonic Cleaner) between each polishing step to remove residual polish. The polishing steps were required to ensure the platinum was flat such that subsequent etching times were more reproducible. The other end of the platinum wire was used to make an electrical connection to the potentiostat.

The microcavity in the glass-sealed platinum holds the powdered carbon sample. Figure 3.1 shows a schematic of the microcavity. To create the microcavity, the smooth glass-sealed end of the platinum was submerged first in 3 mL of 37 % hydrochloric acid (99.99%, Sigma Aldrich), and heated to approximately 80 °C in a hot water bath. Then

1 mL of 70 % nitric acid (99.999%, Sigma Aldrich) was added drop by drop to create aqua regia with a volume ratio of 3:1. The etching in hot aqua regia proceeded for three hours. The microcavity electrode was then rinsed with Millipore water and ultrasonicated for 5 minutes. The etching process was repeated once more using another batch of hot fresh aqua regia. Figure 3.1 below is a close-up schematic view of the tip of the microcavity electrode.

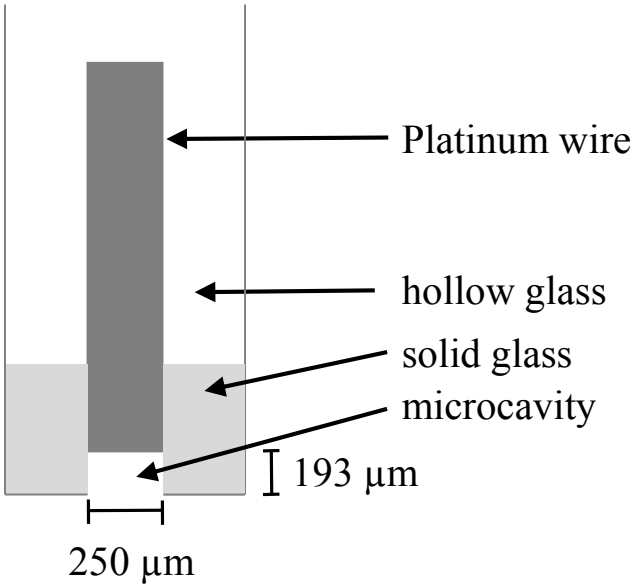

Figure 3.1 A close-up schematic view of a platinum microcavity electrode.

Operable microcavity dimensions were previously studied in detail by Cachet-Vivier *et al.*[156] The dimensions of an operable microcavity must have a depth-to-diameter ratio between 0.4 and 1.[156] If the ratio falls below the specified range, then the powder will easily fall out of the microcavity, and if the ratio is above the specified range, then there will be difficulty in obtaining a good electrical connection between the powder and the platinum wire current collector.[156] The depth of the microcavity was measured as 193 μm using an optical coherence tomography instrument constructed and operated by PhD candidate, Daniel MacDougall, (Adamson research

group, Department of Biomedical Engineering, Dalhousie University).[158] Thus, the depth-to-diameter ratio is approximately 0.77, which satisfies the operable ratio range specified by Cachet-Vivier *et al.*[156]

A powdered carbon sample was loaded into the microcavity by pressing the microcavity electrode onto a small amount of the sample powder spread on a clean microscope glass slide (Corning Incorporated, 2947-75x25, 75x25x1 mm, 0215 glass). The microcavity electrode was used to investigate the electrochemistry of the four carbon powders in 0.2 g L^{-1} bovine hemoglobin (BHb, Sigma Life Science, lyophilized powder, from bovine blood) with 0.1 M PB. A one-compartment glass cell containing 5 mL of electrolyte was used with the microcavity electrode.

Microcavity electrodes were conveniently reused to study the electrochemistry of different powders. Literature reports recommend the use of an ultrasonic bath to remove a powder from the microcavity.[155,157] The microcavity electrode used in this thesis was emptied by vertically suspending the electrode in an ultrasonic bath (Branson 1510 Ultrasonic Cleaner) filled with distilled water during a three minute ultrasonication process. To ensure cleanliness, cyclic voltammetry was conducted between -0.750 V and 1.300 V with a sweep rate of 1 V s^{-1} in 1 M sulfuric acid (98%, Caledon) for 100 cycles and then -0.670 V to 0.930 V, also with a sweep rate of 1 V s^{-1} in 1 M sulfuric acid, until a characteristic platinum CV was evident. Then the electrode was rinsed and was tested for cleanliness by the use of either a cyclic voltammetry or differential pulse voltammetry scan in 0.1 M PB immediately prior to experiments.

3.1.2.3 Carbon Fabric as a Working Electrode

The carbon fabric electrode material Spectracarb 2225 (Engineered Fibers Technology, Spectracarb Activated Carbon Fabric Type 2225-900) was used to study the electrochemistry of 0.2 g L^{-1} bovine hemoglobin (BHb) dissolved in 0.1 M PB in a one-compartment electrochemical glass cell containing 25 mL of electrolyte. A Swagelok setup, visually outlined in Figure 3.2, was used to hold approximately 10 mg of the Spectracarb 2225 fabric. The sticky carbon, consisting of approximately 50% melted beeswax and 50% graphite powder, acted as a current collector and prevented exposing of the nickel wire to the electrolyte. When fully assembled, the resistance between the Spectracarb 2225 fabric and the nickel wire was no greater than 15 Ω.

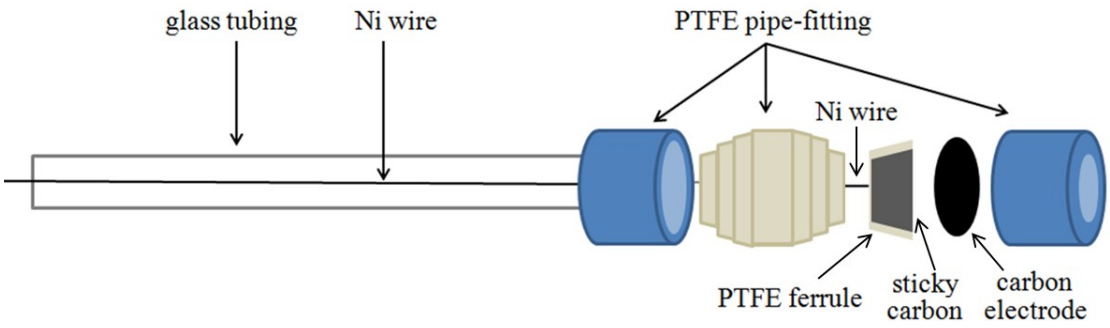

Figure 3.2 A diagram reproduced and modified from reference 159 outlining the Swagelok setup used for the electrochemical examination of Spectracarb 2225 carbon fabric.

3.1.3 Modification of Carbon-Oxygen Surface Groups

3.1.3.1 Removal of Black Pearls 2000 Surface Functionalities by the use of Heat Treatment

Black Pearls 2000 carbon black was modified by the use of a heat treatment to remove all COOR and phenolic surface groups.[93] A porcelain container (Fisherbrand porcelain combustion boat, 97 x 16 x 10 mm) borrowed from Dr. Timothy Hatchard

(research associate, Obrovac research group, Department of Chemistry, Dalhousie University) was cleaned by the use of ultrasonication in distilled water for 15 minutes. Further cleaning was performed by the use of heating in a tube furnace at a rate of 5 °C min^{-1} from room temperature to 1000 °C and the high temperature was held for several hours with flowing air. Andrew George (technician, Department of Physics, Dalhousie University) operated the tube furnace. The clean, dry porcelain container was then filled with Black Pearls 2000 carbon black powder and inserted into a tube furnace under Ar atmosphere at room temperature. The Ar flow rate was approximately 100 mL min^{-1}. The heating rate was 5 °C min^{-1} from room temperature to 1000 °C and the furnace was held at that temperature for two hours to remove all COOR and phenolic surface functional groups.[93] Then the sample was cooled in Ar atmosphere at an approximate rate of 10 °C min^{-1} to room temperature before removing the sample from the tube furnace. The heat-treated Black Pearls 2000 sample was then used for electrochemical testing to examine the electrochemical activity of hemoglobin.

3.1.3.2 Modification of Surface Functionalities of Vulcan XC-72 by the use of Electroreduction

Modification of Vulcan XC-72 was performed first by placing 4 mg of this carbon black in a glass vial containing 4 mL of 18.2 MΩ·cm water in an ultrasonication bath (Branson 1510 Ultrasonic Cleaner) two times, 5 minutes each, to create a suspension. 10 μL of the suspension was air-dried at room temperature onto thoroughly cleaned and polished glassy carbon electrodes (BASi-MF2012 and CHI 104, 3.0 mm diameter, mirror-like finish). The glassy carbon electrodes were previously cleaned using 3 and 1 μm diamond polishes (BASi PK-4 MF-2060 polishing kit) on nylon pads until a mirror-

like finish was achieved, with copious amounts of Millipore water for rinsing before and after each polishing step. The air-dried ultrasonicated Vulcan XC-72 was further processed by the use of an electrochemical reduction process similar to that used by Guo *et al*., which is known to preferentially reduce C=O surface groups.[160] The electrochemical reduction process involved applying a potential of -1.95 V versus Hg/Hg_2SO_4 for 15 minutes in a magnetically stirred 10 mM phosphate electrolyte (pH 5.03) purged with N_2 gas (Praxair).

The influence of removing C=O surface groups on the electrochemical activity of BHb was conducted using ultrasonicated Vulcan XC-72 before and after the electrochemical reduction process. These experiments were conducted in a one-compartment all-glass electrochemical cell with 5 mL of 0.1 M PB with a range of different BHb concentrations: 0.2, 0.1, 0.05, 0.01, 0.005, and 0.001 g L^{-1}.

3.1.3.3 Modification of Surface Functionalities of Carbon Fabric by the use of Electroreduction

A Spectracarb 2225 carbon fabric held in a Swagelok setup (described in Section 3.1.2.3) was electrochemically reduced to preferentially reduce C=O surface groups. The reduction procedure was the same as that described previously in Section 3.1.3.2.

3.1.4 Electrochemical Activity of Nafion-immobilized Bovine Hemoglobin on a Glassy Carbon Electrode

Immobilizing hemoglobin on an electrode surface using a polymer, such as Nafion,[23,25] is one strategy that may enhance its electrochemical activity.[11] 10 µL of 1 g L^{-1} BHb was air-dried on a glassy carbon electrode (CHI 104, 3.0 mm diameter), followed by a film of Nafion. Two forms of Nafion were used in this thesis; one was a

solid piece of Nafion, and another was a thin film formed from a liquid suspension, which will be described later in this section. The solid piece of Nafion (Nafion 117, Aldrich Chemical Company Inc., 0.007 inch thick) was washed and stored in Millipore water for approximately a week and pressed dry with a Kimwipe immediately before use.

A different cell configuration was required when using a solid piece of Nafion 117 polymer to hold BHb onto the glassy carbon surface because the Nafion did not stay attached to the glassy carbon electrode. Instead, a polytetrafluoroethylene (PTFE) Swagelok pipe fitting was used as an electrochemical cell. A 4.5 mm x 4.5 mm solid Nafion 117 film was pressed flat over the glassy carbon (3.0 mm glassy carbon inner diameter, 6.35 mm total diameter including the inert Kel-F polychlorotrifluoroethylene sealant) with or without the air-dried BHb film. The modified working electrode was inserted through a 6.35 mm diameter hole in the bottom of the Swagelok PTFE hollow screw. The screw was then held inside the Swagelok pipe fitting where a part of the pipe fitting was pressed against the edges of the solid Nafion 117 film on the working electrode. The Nafion film was held firmly in place by the finger-tight pressure of the screw applied to the Swagelok pipe fitting, and by the weight of both the electrolyte and Swagelok setup. The Swagelok cell was filled with 2 mL of 0.1 M PB (pH 7.08) electrolyte through the wider opening of the Swagelok pipe fitting. Leaks around the Nafion film were tested electrochemically by adding 0.2 g L^{-1} BHb in PB to the cell. The Hg/Hg_2SO_4 reference and Pt mesh counter electrodes were placed in the wider opening of the Swagelok pipe fitting. A detailed diagram of the modified Swagelok setup is shown in Figure 3.3 and a photograph of the setup can be seen in Figure 3.4.

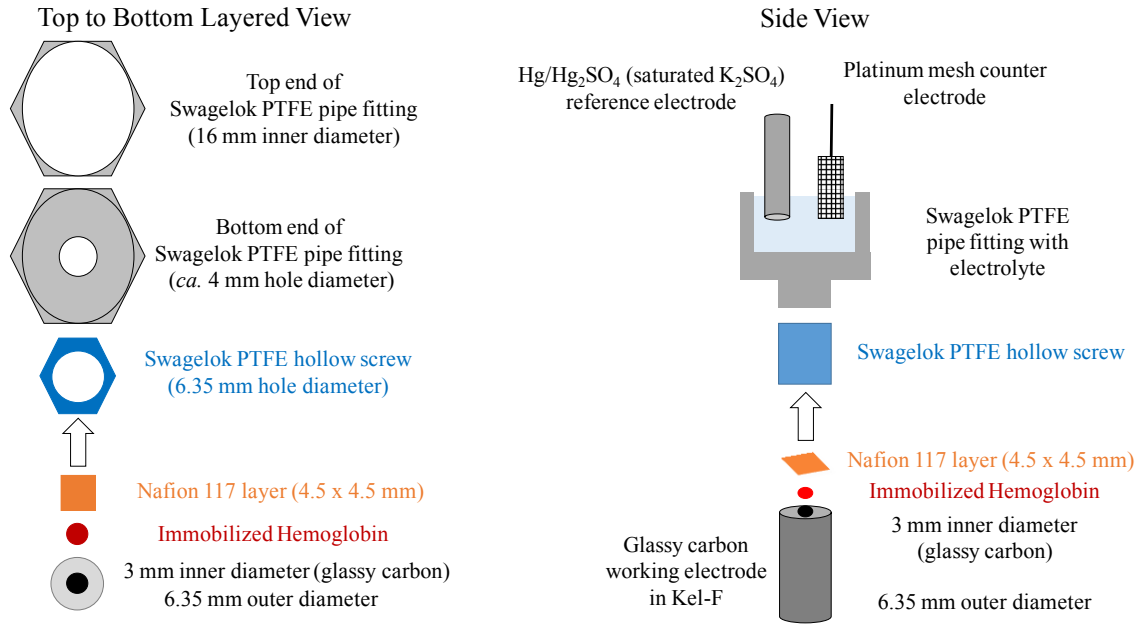

Figure 3.3 A top to bottom layered view and a side view of the Swagelok setup used as an electrochemical cell for studying the effects of solid Nafion on the electrochemical activity of BHb on a glassy carbon electrode.

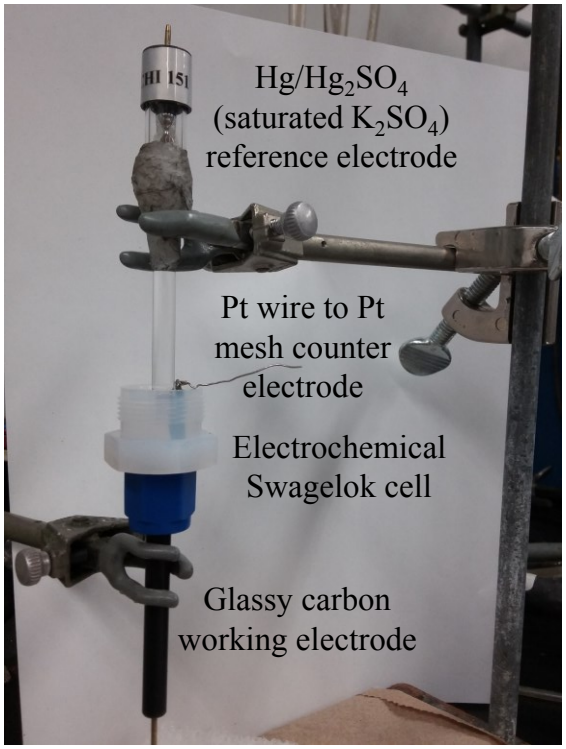

Figure 3.4 A photograph of the Swagelok cell for studying the electrochemical activity of solid Nafion-immobilized BHb on a glassy carbon electrode.

A thin film of Nafion prepared from a liquid suspension was another form of Nafion used to immobilize BHb on a glassy carbon electrode. After having 10 μL of 1 g L^{-1} BHb air-dried on a clean glassy carbon electrode, 10 μL of a liquid Nafion suspension (5.0-5.4% Nafion content by weight in *ca.* 45 ± 3 % water and 48 ± 3% 1-propanol, Ion Power Inc., DuPont DE521) was placed on top and air-dried to form a thin layer of Nafion. The modified electrode was electrochemically tested in a one-compartment glass cell containing 5 mL of 0.1 M PB (pH 7.08). As a control experiment, 10 μL of the Nafion liquid suspension was used create a thin film of Nafion on the glassy carbon working electrode, and then air-dried without BHb for electrochemical testing. For comparison purposes, BHb was air-dried on the glassy carbon working electrode without any Nafion for electrochemical testing.

The glassy carbon working electrode was cleaned and polished prior to electrochemical testing. The electrode was first cleaned by peeling away the Nafion film, and excess BHb was wiped away using a Kimwipe. Then the electrode was washed with Millipore water before and after being submersed in 1 M NaOH for *ca.* 5 minutes. The glassy carbon electrode was then polished as described previously in Section 3.1.3.2.

3.1.5 Effects of Aqueous-alcohol Electrolyte on the Electrochemical Reduction of Bovine Hemoglobin using a Glassy Carbon Electrode

A concern when performing electrochemical testing using Nafion-immobilized BHb are the possible differences in the prepared Nafion films on a glassy carbon electrode (CHI 104, 3.0 mm diameter). One of the main differences is the presence of 1-propanol in the liquid Nafion suspension,[161] which is not present in the solid piece of Nafion 117. Prior to electrochemical testing, liquid suspensions of Nafion may

sometimes be mixed with methanol[14,22,25] or ethanol.[23,162] To test whether the presence of 1-propanol in the currently used liquid Nafion suspension, or methanol or ethanol found in other Nafion preparations, have an effect on the electrochemical activity of BHb, an alcohol was added to the electrolyte.

To test the impact of alcohols on the electrochemical activity of BHb, a total of 10 mL electrolyte was used, which consisted of 0.1 M PB (pH 7.08), with or without 0.2 g L^{-1} BHb, and one of the following water-miscible primary alcohols: methanol (99.9%, Fisher Scientific), ethanol (100%, anhydrous), or 1-propanol (99.5%, Caledon Laboratory Chemicals). The alcohol content was varied in the electrolyte in increments of 10%, up to 60% by volume.

Exposing a polished glassy carbon electrode to methanol may also have an effect on the electrochemical activity of BHb. Therefore, a polished glassy carbon electrode was submersed in methanol for 30 minutes, and then rinsed with Millipore water before electrochemical testing in 0.2 g L^{-1} BHb with 0.1 M PB.

The glassy carbon working electrode was cleaned by following several steps. First, the electrode was wiped with a Kimwipe to remove any excess BHb from prior experiments. The glassy carbon was then rinsed with Millipore water before and after submersion in 1 M NaOH for *ca.* 5 minutes to remove any remaining BHb. The electrode was then finally polished using an identical procedure previously described in Section 3.1.3.2.

3.1.5.1 Influence of Oxygen in Phosphate Buffer Electrolyte during Electrochemical Experiments

To determine whether the increased reduction currents in the DPVs of BHb-free aqueous-alcohol electrolyte seen in Chapter 5 were due to more dissolved oxygen, DPVs of PB saturated with different gases were recorded. 10 mL of PB electrolyte was left standing in ambient air, saturated with nitrogen (>99.995%, Praxair), or saturated with oxygen (>99.5%, Praxair). The PB electrolyte was purged with either nitrogen or oxygen gas for approximately one hour prior to the electrochemical experiments and the gas continued to flow through the electrolyte during the experiments. A glassy carbon electrode (CHI 104, 3.0 mm diameter) was polished using the procedure described previously in Section 3.1.3.2 prior to use for the electrochemical experiments.

3.1.6 Electrochemical Activity of Bovine Hemoglobin Films Formed on a Glassy Carbon Electrode

BHb is known to adsorb directly onto carbon materials[163] and may be electrochemically active. The addition of an alcohol to the BHb-containing electrolyte during the adsorption process may change the electrochemical activity of BHb. The BHb-adsorption procedure used in this thesis research is described here.

BHb was adsorbed onto polished glassy carbon electrodes (CHI 104, 3.0 mm diameter). Prior to the adsorption procedure, the glassy carbon electrodes were polished and cleaned identically to the procedure described previously in Section 3.1.5. A glassy carbon electrode was first submerged in 0.1 M PB (pH 7.08), without any alcohol or with one of the following water-miscible primary alcohols: methanol (MeOH), ethanol

(EtOH), or 1-propanol (1-PrOH). Then BHb dissolved in 0.1 M PB was added to the mixture by using a pipette, attaining a final concentration of 0.2 g L^{-1} in the aqueous-alcohol mixture with a final alcohol content of either 0%, 30%, or 60% by volume. Glassy carbon was incubated in the mixture for 30 minutes, followed by a 10 minute submersion in Millipore water and a final rinse with Millipore water to remove any excess BHb before electrochemical testing.

3.2 Characterization of Carbon-Oxygen Surface Functional Groups

As discussed in Section 2.2.5, carbon surface oxides may affect the electrochemical activity of BHb; thus, surface-sensitive examination of carbon electrode materials for carbon-oxygen groups is required. The techniques used for this purpose were XPS, ATR-FTIR, and TPD.

3.2.1 X-ray Photoelectron Spectroscopy (XPS)

XPS data were collected for carbon samples by Andrew George (technician, Department of Physics, Dalhousie University) using a Thermo VG Scientific Multilab ESCA 2000 spectrometer with a Mg Kα X-ray source (1253.6 eV, 0.6 mm diameter spot size) and a CLAM4 MCD electron energy analyzer with a pass energy of 30 eV. The spectra of the carbon samples were collected at room temperature and a pressure of 1×10^{-9} Torr. The data were then analyzed using CasaXPS version 2.3.17PR1.1 software. The counts per second were normalized relative to the graphitic peak for all spectra. A Shirley background and Gaussian-Lorentzian functions were used when fitting XPS data. Only the XPS spectra for Vulcan XC-72 on glassy carbon plates and

Spectracarb 2225 required shifting relative to a graphitic peak position of 284.3 eV.[116–119] The binding energy shift was likely due to electrostatic charging during photoemission where the sample was becoming more positive, thus resulting in a shift of the XPS spectrum towards higher binding energy. Fitted C_{1s} XPS peaks were positioned based on known literature values: C=C at 284.3 eV,[116–119] C-O at 285.5 eV,[118–122] C=O from 286.8 to 287.1 eV,[98,102,106,117,118,121] COOR at 288.8 eV,[98,102,106,117,118,123] π-π* shakeup from 290.3 to 290.4 eV,[106,116,123,124] and plasmon processes at 292.6 eV.[106,124] Fitted O_{1s} XPS peaks, although less well-established than C_{1s} XPS peaks, were also positioned based on known literature values: C=O from 531 to 532 eV and C-O from 533 to 534 eV.[93,117,164,165] Monte Carlo simulations were performed using the CasaXPS software to provide one standard deviation error estimates based on a normal distribution to determine whether the surface concentration percentages calculated from fitted peaks of different carbon samples were considered significant.

3.2.1.1 Preparation of Carbon Samples for XPS

The carbon powders examined by the use of XPS were the same as those described previously in Section 3.1.2.2: graphite, glassy carbon, Vulcan XC-72, and Black Pearls 2000. Additionally, ultrasonicated and ultrasonicated/reduced samples of Vulcan XC-72 on clean glassy carbon plates (SPI Supplies) were tested by the use of XPS. The preparations of the ultrasonicated and ultrasonicated/reduced Vulcan XC-72 samples were described previously in Section 3.1.3.2. The carbon samples were stored in a desiccator for approximately a day until XPS analysis.

The glassy carbon plates were cleaned prior to use for XPS. The cleaning procedure began with an identical polishing step previously described in detail in Section

3.1.3.2 for the glassy carbon electrode. Additionally, the glassy carbon plates were ultrasonicated in Millipore water for 15 minutes to remove residual diamond polish.

Glassy carbon plates were also examined by the use of XPS to study the effects of aqueous-alcohol exposure. The clean glassy carbon plates were then submersed in aqueous-alcohol PB electrolyte for 30 minutes. The alcohol content in the electrolyte was one of 0% alcohol, 30% MeOH, 40% MeOH, 60% MeOH, 40% EtOH, 50% EtOH, 60% EtOH, 30% 1-PrOH, 50% 1-PrOH, or 60% 1-PrOH. After the removal from the aqueous-alcohol electrolyte, the glassy carbon plates were submersed in Millipore water for 10 minutes and then rinsed to avoid the crystallization of phosphates from the PB. The treated glassy carbon plate samples were kept dry in a desiccator until XPS analysis.

3.2.2 Attenuated Total Reflectance Fourier Transform Infrared Spectroscopy (ATR-FTIR)

ATR-FTIR spectra were recorded using an Agilent Technologies Cary 630 FTIR spectrometer fitted with an ATR accessory in single-bounce mode operating at a 45° angle. For each sample, 256 scans were collected over 600 to 4000 cm^{-1} with 4 cm^{-1} resolution using a Ge crystal. Scans of air were used for background subtraction immediately before scanning the sample, and further background subtraction of the measurements was performed by fitting a 3rd degree polynomial using the least-squares method.

3.2.3 Temperature Programmed Desorption (TPD)

TPD was conducted on a TA Instruments SDT Q600 system connected to a TA Instruments Discovery quadrupole mass spectrometer. The instrument and furnace were purged with Ar gas at a rate of 400 mL min^{-1} and then the flow was adjusted to 100 mL

min^{-1} for the measurement. Each carbon sample (*ca.* 2 mg) was held in an alumina crucible, equilibrated at 25 °C where the temperature was held at 25 °C until the sample weight was stable, and held at that temperature for a further 5 minutes to ensure stable measurements. The temperature was programmed to change at a linear rate of 5 °C min^{-1} from 25 to 1000 °C. Each carbon sample was tested three times to ensure reproducibility. The derivative of each thermal gravimetric analysis (TGA) plot was also used to emphasize small weight changes, in addition to TGA plots. The desorbed CO and CO_2 gases were sampled through a 300 °C heated capillary leading to the quadrupole mass spectrometer. The internal pressure of the mass spectrometer was 27 Torr. The dual Faraday detector collected data up to 50 *m/z* with particular attention on *m/z* of 28 (CO) and 44 (CO_2). All TPD data were processed using TA Universal Analysis version 4.5A software.

To calculate the amount of carbon surface oxides desorbed from the carbon surface, the intensity versus temperature plots from the mass spectrometer data were integrated while assuming a linear background. The resulting number was then divided by the heating rate, the charge of an electron (1.6×10^{-19} C), the mass of the carbon sample, and Avogadro's number. The final result was then expressed in comparable units of μmoles of carbon surface functionalities per g of carbon sample.

3.3 Scanning Electron Microscopy

Scanning electron microscope (SEM) images were collected for carbon samples by Patricia Scallion (technician, Department of Engineering, Dalhousie University) using a Hitachi S-4700 FEG scanning electron microscope to examine possible changes to the

carbon surface after treatments to modify its carbon-oxygen surface groups. An accelerating voltage of 5000 V was used for imaging the Black Pearls 2000 carbon before and after heat treatment. The Black Pearls 2000 carbon samples were mounted on carbon tape (Ted Pella Inc., PELCO Tabs, 12 mm outer diameter, 16084-1). A lower accelerating voltage of 2000 V was used for the Vulcan XC-72 powder as-received, after ultrasonication and after ultrasonication/electrochemical reduction. The ultrasonicated Vulcan XC-72 suspensions were air-dried on identical glassy carbon plates (SPI Supplies) for approximately 20 hours and then thoroughly washed with Millipore water and stored in desiccant before SEM measurements. The Vulcan XC-72 powder as-received was mounted on copper tape (3M) for SEM imaging. The ultrasonicated and ultrasonicated/reduced forms of Vulcan XC-72 on the glassy carbon plates were also mounted on copper tape for SEM imaging.

3.4 Hemoglobin Film Thickness Measurement

3.4.1 Atomic Force Microscopy (AFM)

An atomic force microscope was used to collect images of a clean polished glassy carbon plate and BHb-adsorbed glassy carbon plate using a JPK Nanowizard II Ultra instrument (Rainey lab, Department of Biochemistry & Molecular Biology, Dalhousie University). A silicon tip (NanoWorld, NCST-20, Pointprobe®, 2.8 μm thick, 150 μm in length, 27 μm in width, resonance frequency of 160 kHz, force constant 7.4 N m^{-1}), operating with a drive frequency of 163 kHz was used under intermittent contact mode to record images of the glassy carbon plate samples with and without adsorbed BHb. Contact mode was used to scratch the surface of the BHb-adsorbed glassy carbon plate.

The glassy carbon plate was cleaned using the procedure described previously in Section 3.2.1.1. A BHb-adsorbed glassy carbon sample was created by submersing a clean glassy carbon plate in 0.2 g L^{-1} BHb with 0.1 M PB for approximately 30 minutes, followed by submersion in Millipore water for 10 minutes and then rinsed with Millipore water to remove excess BHb. The BHb-adsorbed glassy carbon plate was then dried in air for approximately a day before imaging.

3.4.2 Spectroscopic Ellipsometry

Spectroscopic ellipsometry data were collected for BHb-adsorbed glassy carbon samples by Dr. Robbie Sanderson (laboratory manager, Dahn research group, Department of Physics, Dalhousie University) using a M-2000F J.A. Woollam spectroscopic ellipsometer in reflectance mode with a 65° angle of incidence relative to the vertical normal for all measurements. To ensure reproducibility, scans were performed on nine different areas of each sample. The wavelengths scanned were from 210 nm to 1000 nm. CompleteEASE version 4.24 software was used for all ellipsometry data processing. A detailed discussion regarding which models were used to calculate the hemoglobin film thickness on glassy carbon is presented in Section 6.3.3.1.

All samples were prepared on glassy carbon plates (SPI Supplies, 2.5 mm thick). The glassy carbon plates were cleaned by wiping with Kimwipe, extensive washing in distilled water, followed by a 10 minute soak in 1 M NaOH, and this procedure was repeated two more times. Then the plates were ultrasonicated in Millipore water for 10 minutes. The plates were then polished to a mirror-like finish using 1 micron diamond

polish, and ultrasonicated in Millipore water for 10 minutes followed by a final rinse with Millipore water to remove residual diamond polish.

On the day of spectroscopic ellipsometry measurements, BHb was adsorbed onto clean glassy carbon plates using the procedure previously described in detail in Section 3.1.6. The total concentration of BHb was 0.2 g L^{-1} in all the aqueous-alcohol mixtures. The total alcohol (MeOH, EtOH, or 1-PrOH) content in a given mixture was 0%, 30%, or 60%, by volume. The total volume for each mixture was 10 mL. After the glassy carbon plates were incubated in the mixture for 30 minutes, the glassy carbon plates were removed and submersed in a clean glass beaker of Millipore water for 10 minutes and then rinsed with Millipore water to remove any phosphates that may crystallize on the surface of the glassy carbon plates. The samples were then air-dried for approximately one hour prior to taking spectroscopic ellipsometry measurements.

3.4.2.1 Examining Hemoglobin-adsorbed Glass by the use of UV/Vis Spectroscopy

A Cary 5000 Ultraviolet-Visible (UV/Vis) spectrophotometer (Varian, Inc.) was used to examine BHb adsorbed on glass microscope slides (Corning Incorporated, 2947-75x25, 75x25x1 mm, 0215 glass) in double beam split mode. Background measurements were recorded on clean glass microscope slides, which were cleaned thoroughly using Millipore water, 1 M NaOH rinses, and copious amounts of Millipore water. Seven clean glass microscope slides were incubated in different aqueous-alcohol electrolytes with 0.2 g L^{-1} BHb for 30 minutes, identical to the BHb incubation procedure used on glassy carbon previously described in Section 3.1.6. Additionally, 1 mL of 0.2 g L^{-1} BHb in PB was air-dried on a 55 x 25 mm area of a clean glass microscope slide. The wavelength range was 200-800 nm and measurements were taken at a rate of

600 nm min^{-1}. Varian UV Scan (Cary WinUV) software was used for data collection from the instrument.

3.4.2.2 Examining Hemoglobin-adsorbed Glass by the use of Fluorescence

A Cary Eclipse instrument was used for fluorescence measurements (Zhang research group, Department of Chemistry, Dalhousie University). The excitation wavelength was 280 nm and the emission wavelengths were from 290 - 420 nm with a measurement rate of 120 nm min^{-1} and excitation and emission slits of 5 nm. Background measurements were recorded on clean glass microscope slides. The seven BHb-adsorbed glass microscope slides incubated in aqueous-alcohol electrolyte with BHb and one air-dried BHb sample on a glass slide were all prepared using the same procedure previously described in Section 3.4.2.1. The prepared glass microscope slides were then placed at a 30° angle from the incident light to increase the distribution of the incident light over a greater sample area and thus decrease sensitivity to the exact sample placement.[166]

3.5 Characterization of Bovine Hemoglobin in Aqueous-alcohol Electrolyte

3.5.1 UV/Vis Spectroscopy

A Cary 5000 Ultraviolet-Visible (UV/Vis) spectrophotometer (Varian, Inc.) was used with 1 cm path length quartz cuvettes in double beam split mode, with 0.1 M PB in the reference cuvette. Samples of aqueous-alcohol electrolyte containing alcohol (MeOH, EtOH, or 1-PrOH) content ranging from 0 to 60% in 10% increments by volume in PB without BHb were recorded as background scans. Preparation of the samples

containing 0.2 g L^{-1} BHb in an aqueous-alcohol electrolyte with different alcohol content was described previously in Section 3.1.5. These samples were measured using the wavelength range of 200-800 nm at a rate of 600 nm min^{-1}. Varian UV Scan (Cary WinUV) software was used for all data collection from the instrument.

3.5.2 Fluorescence

A Cary Eclipse instrument with a 10 mm quartz cuvette was used for fluorescence measurements (Zhang research group, Department of Chemistry, Dalhousie University). The excitation wavelength was 280 nm and the excitation and emission slits were 5 nm. The emission wavelengths were recorded from 290 - 420 nm with a measurement rate of 120 nm min^{-1}. Samples of 0.2 g L^{-1} BHb in an aqueous-alcohol electrolyte with varying alcohol content (0 to 60% by volume in 10% increments, MeOH, EtOH, or 1-PrOH) described previously in Section 3.1.5 were examined by the use of fluorescence. Background measurements were recorded for identical samples without BHb. The aqueous-alcohol mixtures prepared without BHb were identical to those previously described in Section 3.1.5.

Chapter 4 The Influence of Carbon-Oxygen Surface Functional Groups on the Electrochemical Detection of Bovine Hemoglobin

Much of the work presented in this chapter was published in "*The influence of carbon-oxygen surface functional groups of carbon electrodes on the electrochemical reduction of hemoglobin*", Justin Tom and Heather A. Andreas, *Carbon* **2017**, *112*, 230-237. JT was responsible for most of the data collection, all the analysis, and preparation of the manuscript.

Data on the characterization of carbon-oxygen surface functional groups on Spectracarb 2225 were previously published in "*Carbon oxidation and its influence on self-discharge in aqueous electrochemical capacitors*", Alicia M. Oickle, Justin Tom, and Heather A. Andreas, *Carbon* **2016**, *110*, 232-242. JT was responsible for most of the XPS, TPD, and ATR-FTIR data collection and the data analysis from TPD and ATR-FTIR experiments of Spectracarb 2225 presented in Sections 4.8.2 and 4.8.3. XPS data analyzed by HAA are presented in Section 4.8.4.

The entirety of Sections 4.2, 4.3, 4.8.1, 4.8.5, and the DPV results presented in Section 4.9 with their corresponding analyses are new to this chapter, and have not been previously presented in the manuscripts listed above. The TPD error analyses and O_{1s} XPS spectra for four carbon powders are presented in this chapter, and were not present in either publication.

Andrew George (Technician, Department of Physics, Dalhousie University) operated the XPS instrument, and Patricia Scallion (Technician, Department of Engineering, Dalhousie University) operated the SEM instrument.

4.1 Introduction

The abundance of carbon, its low cost and wide potential range are some of the reasons why carbon is a commonly used electrode material.[89,167,168] For instance, a pencil electrode is a readily affordable carbon electrode that can be used to electrochemically detect hemoglobin (Hb) for potential diagnosis of clinical diseases such as anemia.[149] As outlined previously in Section 2.2.5, the electrochemical activity of Hb on various carbon materials is inconsistent, which may be due to differences in carbon surface

oxides.[18,19,22,23] Some groups reported enhanced Hb electroactivity with an increase in carbon surface oxides,[18,52] while others observed enhanced activity when the surface oxides were removed.[12] A careful examination of the carbon-oxygen surface functional groups present on carbon electrode materials is necessary, and is the focus of this chapter. Knowledge of the link between Hb electroactivity and carbon surface oxides will provide better fundamental understanding of the various Hb electrochemical activities on carbon seen in the literature. Identification of a particular carbon-oxygen surface functionality that enhances or inhibits Hb electroactivity may allow for a more thoughtful and focused surface modification to either increase or remove the relevant functionality.

In this chapter, cyclic voltammetry and differential pulse voltammetry were used to evaluate the electrochemical activity of Hb on various carbon electrode materials. TPD, XPS, and ATR-FTIR were used to examine the presence of carbon-oxygen surface functional groups. Upon identification of possible inhibiting carbon-oxygen surface functionalities, these groups were removed from a carbon material, causing a significant increase in Hb activity, confirming the role of carbon-oxygen surface functionalities in inhibiting the Hb electroactivity.

The data presented in this chapter are split into several sections. Section 4.2 presents the electrochemical activity of Hb on a pencil electrode, including experimental results that are inconsistent with the literature data. Section 4.3 discusses why the platinum microcavity electrode, is an appropriate setup to examine the electrochemistry of BHb when filled with different carbon electrode materials. Section 4.4 examines and compares the electrochemical behavior of BHb in solution using four different carbon electrode materials. Section 4.5 is a discussion of the structural differences in the carbon

materials used. Section 4.6 then examines the surface functionalities of the four different carbon powders using TPD, ATR-FTIR, and XPS. Results from each technique are examined in detail and then combined to yield a more complete idea of the carbon-oxygen surface functional groups present on the carbon powders and the relationship of these surface functional groups to the electrochemical activity of BHb. The remaining sections in this chapter are results and discussions of carbon modifications to control particular carbon-oxygen surface functional groups (Sections 4.7-4.8) and an evaluation of the carbon modifications to electrochemically detect a range of BHb concentrations (Section 4.9).

4.2 Hemoglobin on a Pencil Electrode

This thesis work was originally initiated because of a literature report that showed excellent electrochemical activity from human hemoglobin (HHb) on a simple pencil electrode.[149] Figure 4.1 shows a typical result from attempts to reproduce the reported literature result when using the exact same pencil type (505210N) from the same supplier (Rotring). The Ag/AgCl (1 M KCl) reference electrode is expected to be -0.022 V versus the saturated calomel electrode, abbreviated as SCE, implying that the results shown in Figure 4.1a are shifted by +0.022 V relative to the literature results shown in Figure 4.1b. Since the potential shift is small, the CVs can still be easily compared, and the HHb redox peaks were expected at approximately -0.24 V (reduction) and -0.20 V (oxidation) versus Ag/AgCl (1 M KCl), as indicated by the red arrows in Figure 4.1a. A broad reduction peak was observed near -0.35 V versus Ag/AgCl (1 M KCl), suggesting that

the HHb reduction reaction is slow. The expected HHb redox peaks were not observed and the reported literature result was not reproducible using this pencil electrode.

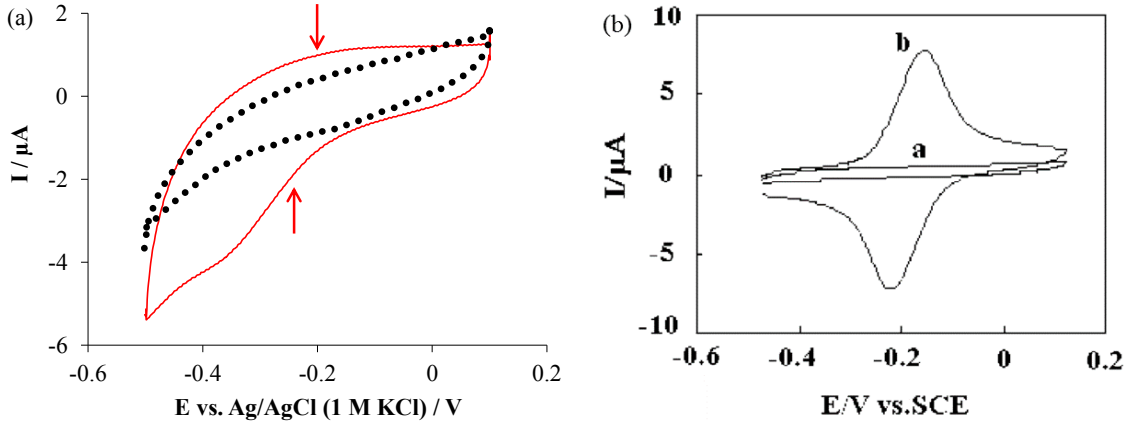

Figure 4.1 (a) CVs of Rotring 505210N pencil before (black dotted curve) and after modification with HHb (solid red curve) with red arrows indicating the location of the expected hemoglobin redox peaks. (b) Published literature CVs of a similar Rotring 505210N pencil before (cycle **a**) and after HHb immobilization (cycle **b**) from Majidi *et al. Electroanalysis* **2011**, *23*, 1984–1990, reproduced with permission for comparison purposes.

Several different brands of pencil electrodes (Derwent Graphic, DeSerres, Staedtler) of different pencil hardness (9B, 7B, 8B, 5B, 3B, 2B, B, HB, H, 3H, 4H, 5H, 6H) as described in Section 3.1.2.1, have also been attempted and each resulted in no HHb electroactivity. The type of graphite and binders and possibly other impurities present in pencils are not strictly controlled;[169] thus, the interactions between them and HHb would result in too many unknown variables. Therefore, the focus of the research was shifted to more controlled and known types of carbon.

4.3 Platinum Microcavity Electrode

A microcavity electrode is a convenient, reusable setup for studying the electrochemistry of different powders with reproducible results.[152,153,156] A diagram of

the microcavity electrode was provided previously as Figure 3.1 in Section 3.1.2.2.1 (page 36). A particularly important advantage of using the microcavity electrode for this work is that no binder is required to hold the carbon powder together, avoiding the additional interactions originating from the binder.[152,153] Avoiding the effects from a binder is imperative because its specific effects on Hb and carbon-oxygen surface functional groups is not known.

Before examining the electrochemistry of BHb using the microcavity electrode filled with a carbon powder, the electrochemical behavior of BHb must first be examined with the platinum microcavity electrode itself. Establishing the electrochemistry of BHb on platinum is important because the platinum is in direct contact with both the carbon powder and the electrolyte. Although the focus of this thesis is on the examination of the electrochemistry between BHb and carbon, there is the possibility of an interfering signal if BHb reacts on the platinum microcavity electrode. This section is a short investigation of the electrochemistry of platinum with and without the presence of BHb in the electrolyte before proceeding to study the electrochemical activity between BHb and carbon in the later sections.

Cyclic voltammetry and differential pulse voltammetry techniques were used to investigate the electrochemical behavior of BHb on the platinum microcavity electrode. The potential range of +0.3 to -0.9 V is the same as that used for studying BHb on the carbon powders. As shown in Figure 4.2, representative voltammograms for platinum in the presence of BHb did not reveal any new peaks when compared to the voltammograms in BHb-free electrolyte, suggesting that BHb is not redox-active on platinum within the potential range used. The decreases in current within the hydrogen underpotential (-0.9

to -0.7 V) and platinum oxide reduction (-0.3 to -0.1 V) regions of Figure 4.2 in the presence of 0.2 g L^{-1} BHb are consistent with literature results and are attributed to a smaller electroactive surface area as a result of protein adsorption on platinum.[16,170] Additionally, the CV shows a very slight increase in the anodic current at potentials more positive than *ca.* +0.1 V (Figure 4.2a). A similar observation has been noted in literature reports using a platinum electrode and has been associated with the oxidation of various amino acids.[171,172] Since this thesis is not concerned with the oxidation of amino acids on platinum, potentials more positive than +0.1 V were not examined further.

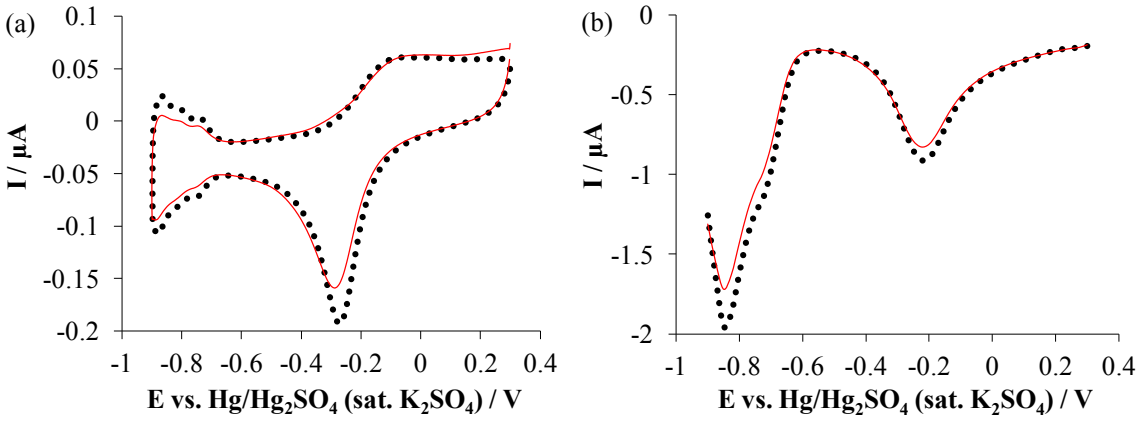

Figure 4.2 Representative cyclic voltammograms (a) and differential pulse voltammograms (b) of a clean microcavity electrode exposing only platinum to the 0.1 M PB (pH 7.08) electrolyte without (dotted black curves) and with 0.2 g L^{-1} BHb (solid red curves).

The lack of a new observable peak for BHb reaction on the platinum microcavity electrode is ideal for this research. If and when a peak arises from using a carbon powder inserted in the microcavity electrode in a BHb-containing electrolyte, then the peak can be attributed solely to the electrochemical activity of BHb on carbon.

4.4 Electrochemical Detection of BHb using Carbon

The electrochemical activity of BHb on carbon was examined by the use of cyclic voltammetry and differential pulse voltammetry using a microcavity platinum electrode filled with a carbon powder. The CVs of graphite and glassy carbon (Figure 4.3a and c, respectively) in BHb-containing electrolyte show a broad cathodic peak centered at approximately -0.69 V, matching literature values for Hb reduction.[12,19,68] The broad cathodic peak in Figure 4.3a is similar to that seen previously in Figure 4.1a, confirming that graphite was a major component in the Rotring 505210N pencil. More distinct cathodic peaks were observed at -0.575 V in the graphite and glassy carbon DPVs (Figure 4.3b and d respectively). The shift in the cathodic peak location in DPV when compared to the CV is consistent with data published by Toh *et al*.[12] A DPV is similar to taking a derivative of a linear sweep voltammogram where the peak potential in a DPV would be at an inflection point in the linear sweep voltammogram, resulting in a peak at an earlier potential in the DPV than in the CV. Therefore, the cathodic peak shift observed when comparing DPVs to CVs (Figure 4.3) is not specifically due to BHb, but rather fundamentally due to the technique itself.

BHb is obviously electrochemically active on the graphite and glassy carbon powders, but inactive on Vulcan XC-72 and Black Pearls 2000 powders (Figure 4.3e-h). While the CVs of Vulcan XC-72 and Black Pearls 2000 showed a small cathodic peak (Figure 4.3e and g), the DPVs showed very little or no reduction at the BHb potential (Figure 4.3f and h), suggesting that the cathodic CV peak was not due to BHb reduction on these carbons. Further experiments were performed where BHb-free PB electrolyte was injected into the cell and then re-examined by the use of cyclic voltammetry. An

increase in cathodic current was observed at *ca.* -0.7 V on both Vulcan XC-72 and Black Pearls 2000 (Figure 4.4a and b), suggesting that the CV peak in Figure 4.3e and g were not associated with BHb but are likely due to the reduction of O_2, which is introduced to the electrolyte during the injection.

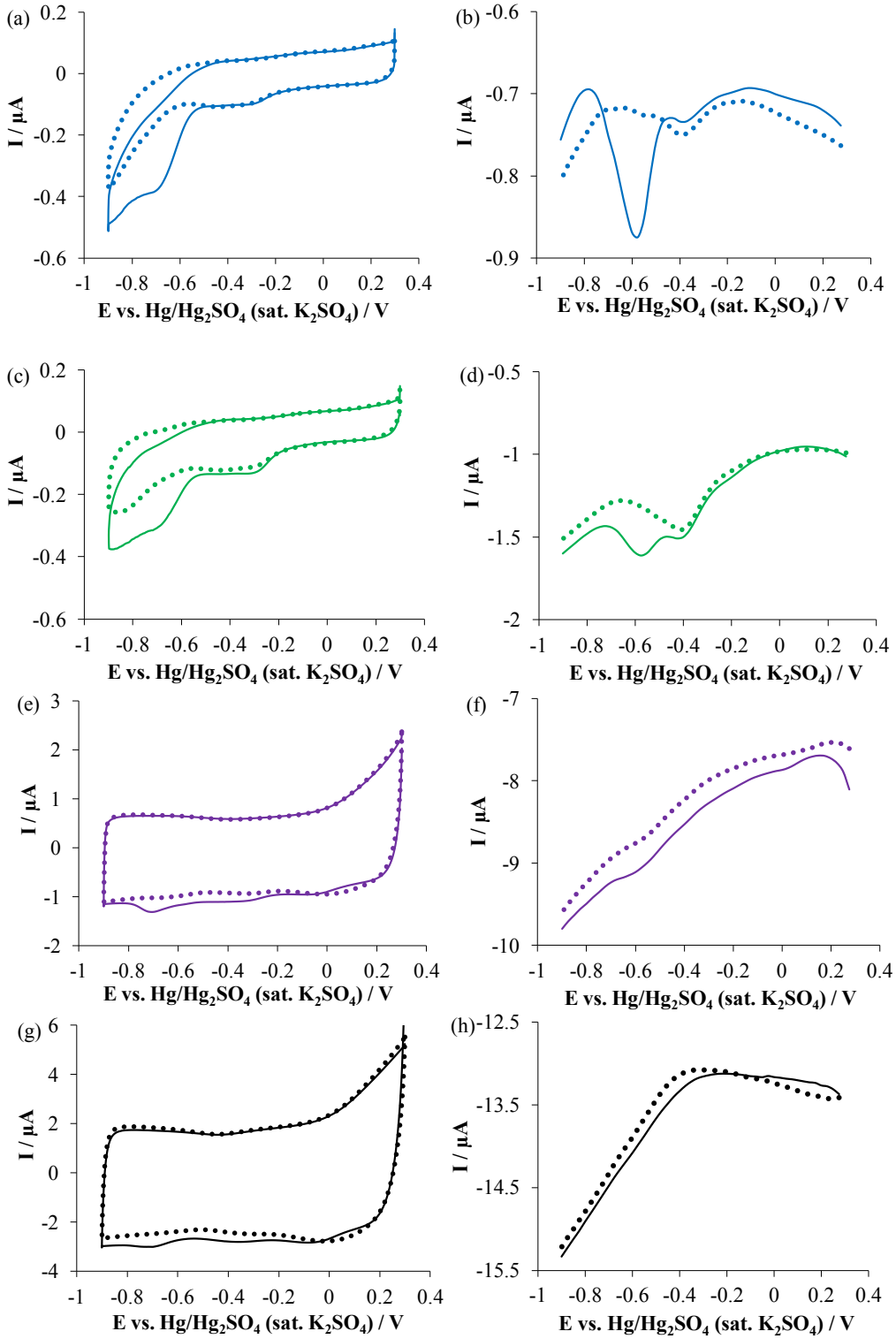

Figure 4.3 CVs (left column: a, c, e, g) and DPVs (right column: b, d, f, h) of graphite (a and b), glassy carbon (c and d), Vulcan XC-72 (e and f) and Black Pearls 2000 (g and h) in 0.1 M PB without (dotted curves) and with (solid curves) 0.2 g L^{-1} BHb.

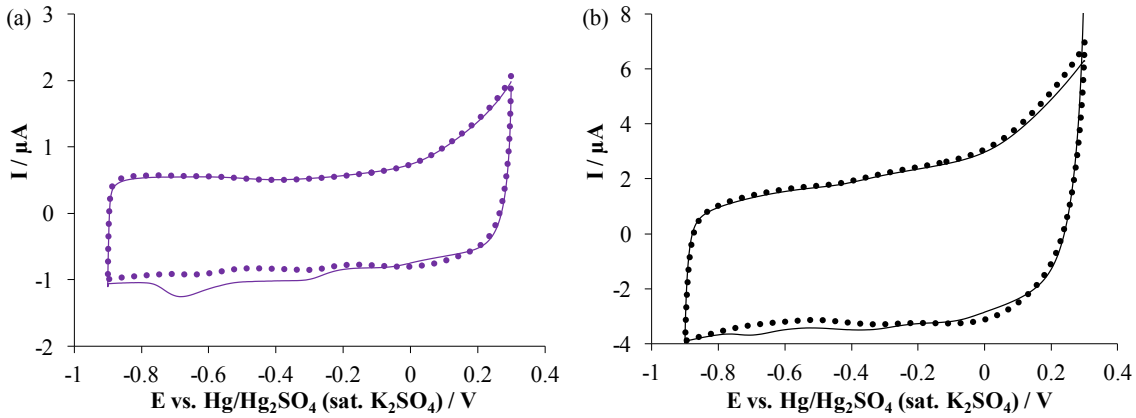

Figure 4.4 CVs of Vulcan XC-72 (a) and Black Pearls 2000 (b) in 0.1 M PB before (dotted curves) and after (solid curves) injection of BHb-free PB into the electrochemical cell.

These data (Figures 4.3 and 4.4) indicate that BHb is electrochemically active on graphite and glassy carbon materials, but inactive on the Vulcan XC-72 and Black Pearls 2000 carbon blacks. The voltammograms indicate that the BHb electrochemical activity decreases in the order of graphite, glassy carbon, Vulcan XC-72 and Black Pearls 2000. The data demonstrate that different carbon materials have different electrochemical behavior with BHb under identical conditions, supporting the observations seen in the literature. To develop an effective electrochemical biosensor for BHb, a careful choice of carbon electrode material is essential, and a fundamental understanding of the different carbon-oxygen surface groups present may be required for the development of the appropriate biosensor electrode materials.

4.5 Consideration of Structural Differences in Carbon Electrode Materials on the Electrochemical Activity of BHb

The difference in the electrochemical activity of BHb on the different carbon materials cannot simply be explained by their structural differences. BHb electroactivity

does not scale with the surface area because, based on literature findings, the surface area of the carbon materials used here increases in the order of glassy carbon (1 m^2 g^{-1})[173] < graphite (3 m^2 g^{-1})[173] < Vulcan XC-72 (205 m^2 g^{-1})[118] < Black Pearls 2000 (1500 m^2 g^{-1}),[173,174] whereas BHb electroactivity increases in the order of Black Pearls 2000 < Vulcan XC-72 < glassy carbon < graphite.

Micropores, with diameters < 2 nm,[175] may prevent the relatively large BHb protein, which has a diameter of 5.5 nm,[176] from accessing some of the surface. Glassy carbon and graphite powders have a very low degree of microporous structure; while 50% of Vulcan XC-72's surface area is in micropores[175] and Black Pearls 2000 has 61% microporous area.[174] Accounting for the micropores, then approximately 102 m^2 g^{-1} and 585 m^2 g^{-1} of the surface area would be available for Vulcan XC-72 and Black Pearls 2000 to be electrochemically active towards BHb; these adjusted areas are still orders of magnitude larger than the surface areas of glassy carbon (1 m^2 g^{-1})[173] and graphite (3 m^2 g^{-1})[173]. Because of the large overall surface area for Vulcan XC-72 and Black Pearls 2000, significant BHb electrochemical activity on the remaining accessible surface is still expected, even if the surface area associated with microporosity was eliminated.

The degree of disorder or, conversely, graphitization has also been considered. The degree of disorder of all the carbon materials used in this research is well-studied in the literature. A carbon's degree of disorder may be estimated by examining the ratio of the intensities from the D (representing structural disorder) and G (representing graphitic structure) bands measured by Raman spectroscopy.[177–179] Graphite is known to have a low degree of disorder (high graphitization)[177,180,181] and exhibits good Hb electrochemical activity. In contrast, glassy carbon, which is also BHb-active, has a

higher degree of disorder (lower graphitization)[177,181,182] with a disorder-to-graphitization ratio > 1.[177] Vulcan XC-72 and Black Pearls 2000 have intermediate disorder with a disorder-to-graphitization ratios of 1.04[162] and 0.94[174] respectively, but exhibit little to no BHb electrochemical activity. Since the electrochemical detection of BHb was clearly more pronounced on both highly disordered glassy carbon and highly graphitized graphite powders, but not on either intermediate-disordered carbon blacks, then the degree of disorder cannot be the most influential factor in electrochemically reducing BHb. Thus, another difference must account for the different electrochemical activity of BHb on these different carbon materials.

4.6 Carbon-Oxygen Surface Functionality Characterization of Carbon Powder Electrode Materials

Other research groups have suggested that carbon-oxygen surface functional groups may influence the electrochemical reduction of Hb.[12,18,19] The presence of carbon-oxygen surface functional groups may be the key to explain the inconsistencies seen in the published data for Hb electrochemistry on carbon. These surface groups are clearly important, but the electrochemical activity of Hb is inconsistently attributed to whether more[18,52] or fewer[12] carbon-oxygen surface groups exist. Therefore, this section details the identification of which carbon-oxygen surface functional groups are present on the carbon powder materials and relates the results to the observed BHb electrochemistry shown in Section 4.4.

Prior to examining the carbon-oxygen surface functional groups, other elements may be present on the carbon surface as impurities that should be investigated, which

may cause spurious Hb electrochemical activity. Impurities on the surface of the four carbon powders examined in this chapter were investigated by the use of XPS. XPS results showed that only carbon and oxygen were detected on the surface of all four carbon powders studied (Figure 4.5). The XPS detection limit is typically 0.1 atomic %, suggesting no significant surface contaminants on the carbon powders.

The C_{1s} XPS spectra in Figure 4.6 qualitatively suggest that Black Pearls 2000 has the highest degree of oxidation of the four carbon powders studied, as shown by higher intensities in binding energies between 285 and 289 eV. Oxygen is more electronegative than carbon; thus, carbon bonded to oxygen shifts the carbon binding energies to higher values. The degree of surface oxidation can be calculated from the XPS data by taking the ratio of the integrated oxygen and carbon peaks. The data in Figure 4.5 show that Black Pearls 2000 (5.0% ± 0.4% O), Vulcan XC-72 (4.7% ± 0.4% O), and glassy carbon (4.4% ± 0.5% O) had similar degrees of surface oxidation, with graphite having the lowest degree of surface oxidation (1.1% O). Graphite and glassy carbon both have high BHb electrochemical activity (Figure 4.3a-d, Section 4.4) but have very different degrees of surface oxidation (1.1% O and 4.4% O respectively). BHb was electrochemically active on glassy carbon (Figure 4.3c and d, Section 4.4), but exhibited little to no activity on Vulcan XC-72 and Black Pearls 2000 (Figure 4.3e-h, Section 4.4), suggesting that the overall degree of carbon surface oxidation is not predictive of the electrochemical activity of BHb. Therefore, the specific carbon-oxygen bonding environment (*i.e.* carbon-oxygen functional groups) on the carbon surface must be a more important factor for the electrochemical reduction of BHb.

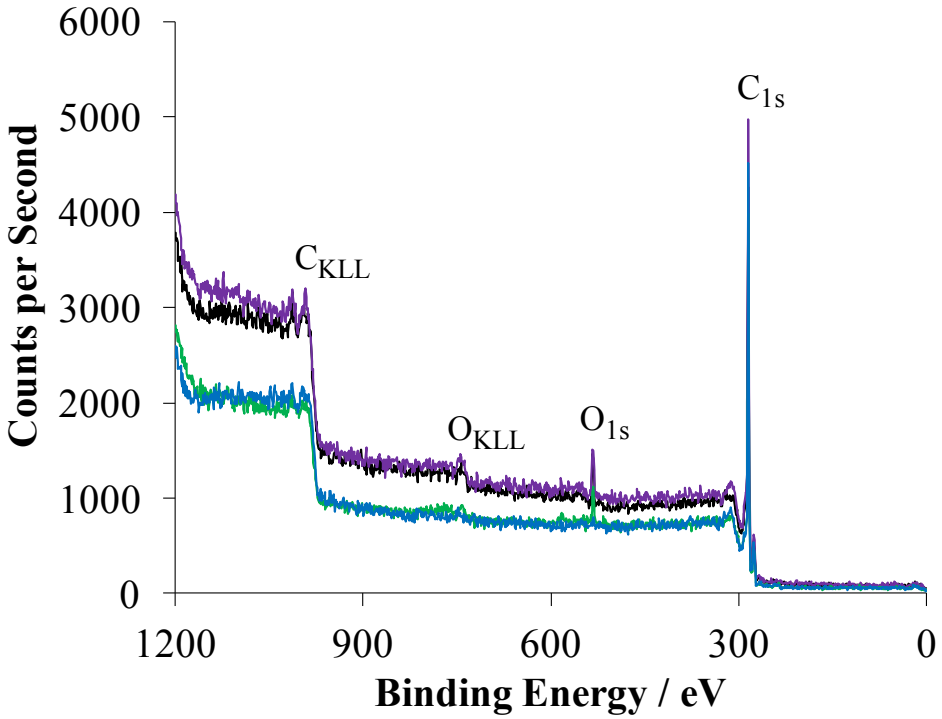

Figure 4.5 XPS spectra showing that only carbon and oxygen were detected on the four carbon powders used in this thesis: Black Pearls 2000 (black), Vulcan XC-72 (purple), glassy carbon (green), and graphite (blue).

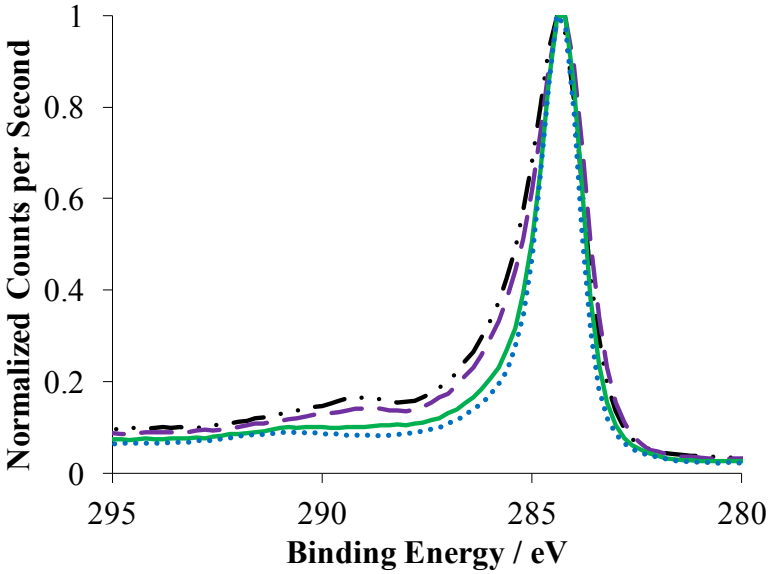

Figure 4.6 Normalized C_{1s} XPS spectra of four carbon powders studied in this chapter: Black Pearls 2000 (black dot-dot-dash curve), Vulcan XC-72 (purple dashed curve), glassy carbon (green solid curve), and graphite (blue dotted curve).

A combination of XPS, TPD and ATR-FTIR were used to identify the specific carbon-oxygen surface functionalities on the as-received carbon powders. Results from each technique will be discussed separately in detail and then combined with the other techniques as this chapter progresses.

4.6.1 Carbon-Oxygen Surface Functional Groups Identified by the use of TPD

As described previously in Section 2.4.1, TPD is a combination of thermal gravimetric analysis (TGA), where the sample weight is measured continuously as the temperature is changed, and a mass spectrometer detector that may yield quantitative information on carbon-oxygen surface functional groups. A typical TGA plot is presented in Figure 4.7a, but due to relatively small weight losses, its derivative is also shown in Figure 4.7b to more clearly indicate the weight loss of possible surface functional groups present on the carbon powders. This section refers to the peaks seen in the derivative TGA plots.

The small peak (Figure 4.7b) centered near 350-360 °C suggests the presence of either a carboxylic anhydride or a carboxylic acid surface functional group.[93] However, this could not be confirmed due to the absence of a CO_2 signal (Figure 4.7c) at these temperatures from the mass spectrometer detector, likely due to very low sample weight loss. Since this peak is present in all of the carbon powders, the surface functionality corresponding to this peak is likely not a significant factor in the different BHb electrochemical activities. The peak centered near 590 °C for Black Pearls 2000, coupled with the small increase in CO_2 detection, (Figure 4.7b and c) at that temperature suggests the presence of a lactone group.[93,118,183,184] The amount of surface lactones on Black

Pearls 2000 obtained by integratiing mass spectrometry data (see Table 4.1) is 26 μmol g^{-1}, which agrees with the literature value of 24 ± 7 μmol g^{-1} obtained by the use of Boehm titration for this carbon.[125] No surface lactones were present on graphite, glassy carbon, or Vulcan XC-72 based on the integrated mass spectrometry data presented in Table 4.1.

The increase in CO_2 detection at temperatures above 600 °C for all carbons (Figure 4.7c and Table 4.1) cannot be assigned to a particular carbon-oxygen surface functional group and could be due to the occurrence of a secondary reaction.[93,185] For example, a Boudouard reaction could take place where $CO_{(g)}$ is released as the result of a decomposed surface oxide, and reacts with a surface oxide on carbon to form $CO_{2(g)}$ and a free carbon surface site.[93,123,186] Therefore, the $CO_{2(g)}$ trend (Figure 4.7c and Table 4.1) suggests that Black Pearls 2000, which has the largest amount of evolved $CO_{2(g)}$, may have formed the largest amount of $CO_{(g)}$ and graphite may have formed the least. In consideration of the estimated errors from the standard deviation of three replicate trials (Table 4.1), Vulcan XC-72 and glassy carbon evolved similar amounts of $CO_{2(g)}$, suggesting that they may have also evolved similar amounts of $CO_{(g)}$. These two carbons in particular had different BHb electroactivity, suggesting again that the carbon-oxygen bonding environment on the carbon surfaces is more important than the amount of surface oxygen. Since the $CO_{(g)}$ release relates to phenol, ether, carbonyl, and quinone surface decomposition, the $CO_{2(g)}$ trend implies the amounts of these groups may be the greatest on Black Pearls 2000 and the least on graphite powders.

To separate phenols from ethers, carbonyls, and quinones, the temperature range of the weight loss can be used. A surface phenol is expected to decompose as $CO_{(g)}$

within a temperature range of 600 to 700 °C.[93,186] Sample weight loss from 600 to 700 °C (Figure 4.7b) coupled with the $CO_{2(g)}$ release (Figure 4.7c), due to the possible Boudouard reaction, suggests that surface phenols may be present on both Vulcan XC-72 and Black Pearls 2000 carbon powders, but cannot be confirmed due to a lack of expected $CO_{(g)}$ release (Figure 4.7d). The lack of weight loss (Figure 4.7b), $CO_{2(g)}$ evolution (Figure 4.7c), and $CO_{(g)}$ evolution (Figure 4.7d) between 600 and 700 °C observed on the glassy carbon and graphite powders indicate no surface phenols.

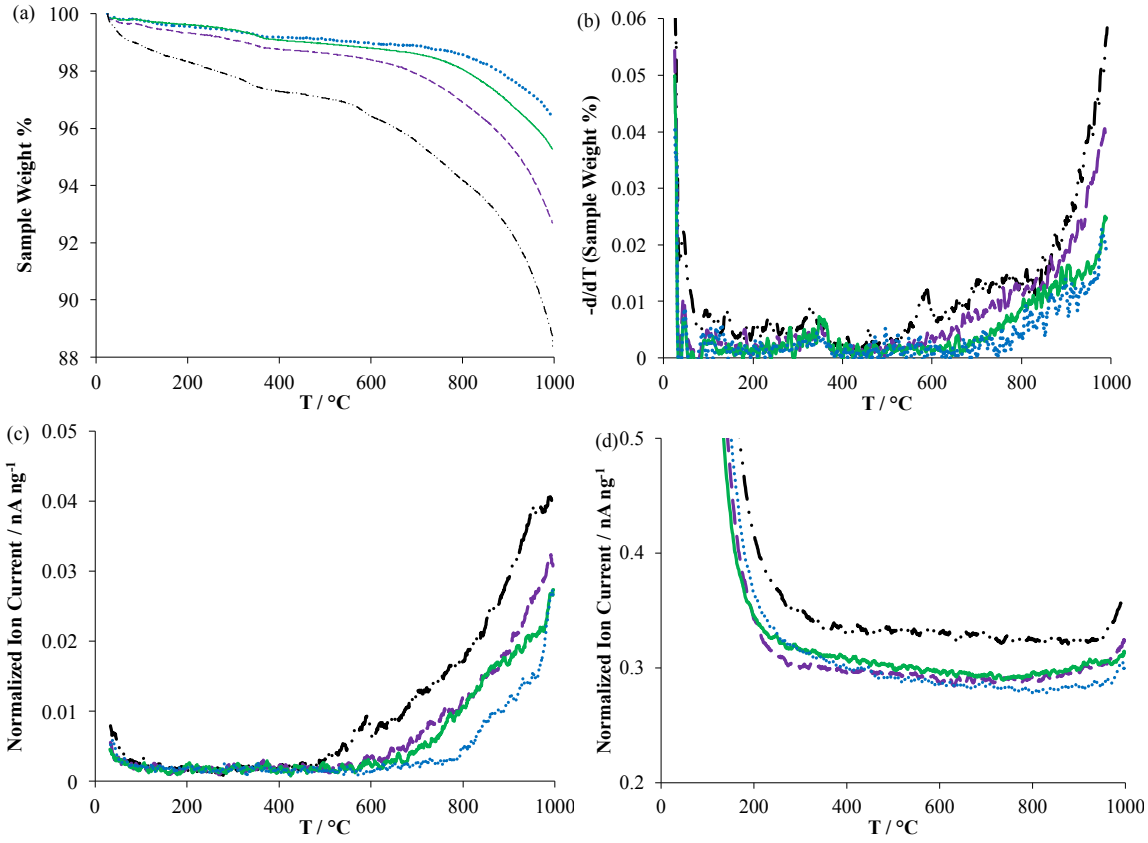

Figure 4.7 A TGA plot of the sample weight with respect to temperature (a) and its derivative (b) with mass spectrometer detector responses for *m/z* 44 (CO_2) (c) and *m/z* 28 (CO) (d). All data shown here are an average of three replicates for Black Pearls 2000 (black dot-dot-dashed curve), Vulcan XC-72 (purple dashed curve), glassy carbon (green solid curve) and graphite (blue dotted curve).

A broad derivative TGA peak near 750 °C (Figure 4.7b) indicates the presence of a possible ether surface functional group[93] on Vulcan XC-72, Black Pearls 2000, and glassy carbon powders. The most evident difference in the TGA data of the as-received carbon powders are at temperatures greater than *ca.* 800 °C (Figure 4.7a and b) with simultaneous CO release (Figure 4.7d), suggesting the presence of either a C=O or quinone surface group.[93,110,118,183,184] TPD data (Table 4.1) suggests the amount of carbonyl or quinone surface groups increase in the following order: graphite < glassy carbon < Vulcan XC-72 ≈ Black Pearls 2000.

Table 4.1 Quantification of carbon surface oxides from integrating TPD mass spectrometry data. The reported results are an average of three replicates with one standard deviation.

	Amount of functionality from TPD Gas Release μmol g^{-1} sample		
	CO	CO_2 500 – 600 °C	CO_2 600 – 1000 °C
Black Pearls 2000	297 ± 6	26 ± 7	158 ± 2
Vulcan XC-72	294 ± 3	Negligible	146 ± 2
Glassy Carbon	246 ± 7	Negligible	144 ± 5
Graphite	166 ± 25	Negligible	51 ± 17

CO_2 evolution at temperatures above those for lactones (600 °C) could not be reliably assigned to a known carbon-oxygen surface functional group. To account for CO_2 evolution at these higher temperatures, a Boudouard reaction was assumed to occur, which implies that two CO from carbon surface oxides are required to form one $CO_{2(g)}$.[93] Based on the total evolved CO and CO_2 gases from the TPD data summarized in Table 4.1 and assuming the Boudouard reaction occurred above 600 °C, the amount of carbon surface oxide increases in the order of: graphite (268 ± 42 μmol g^{-1}) < glassy carbon

(534 ± 12 μmol g^{-1}) < Vulcan XC-72 (586 ± 5 μmol g^{-1}) < Black Pearls 2000 (639 ± 10 μmol g^{-1}).

These results may appear to contradict the similar degree of surface oxidation of glassy carbon, Vulcan XC-72, and Black Pearls 2000 carbon powders determined by the use of XPS, but in fact reveal additional information regarding the location of the carbon surface oxides. XPS is known to probe up to 10 nm from the sample surface,[133] suggesting that pores deeper than 10 nm from the surface are not probed for carbon-oxygen surface groups. On the other hand, TPD does not have a similar constraint as long as $CO_{(g)}$ and $CO_{2(g)}$ are evolved, implying that carbon surface oxides likely exist in pores deeper than 10 nm on the Vulcan XC-72 and Black Pearls 2000 powders.

Various carbon-oxygen surface functional groups were identified using TPD. Carboxylic acid or anhydride surface groups may be present on the four carbon powders tested, but could not be confirmed due to a lack of detected $CO_{2(g)}$. The identification of surface phenols on Vulcan XC-72 and Black Pearls 2000 by the use of TPD were also inconclusive due to a lack of detected $CO_{(g)}$. Based on TPD, greater amounts of surface ether, quinone, and carbonyl groups may be present on Vulcan XC-72 and Black Pearls 2000 when compared to either glassy carbon or graphite powders. Additionally, surface lactones were found only on Black Pearls 2000 and not on the other carbon materials. The effects of these surface oxides on BHb electroactivity will be discussed later in Section 4.6.4. TPD analysis for carbon is typically complemented using other characterization techniques, such as ATR-FTIR and XPS to help confirm the different carbon surface oxides. The results from these complementary techniques will be discussed in the next two subsections.

4.6.2 Carbon-Oxygen Surface Functional Groups Identified by the use of ATR-FTIR

As discussed previously in the background chapter, ATR-FTIR is a surface sensitive technique used in this thesis to help identify the different carbon-oxygen functional groups on the carbon surfaces in conjunction with TPD and XPS. Unlike TPD and XPS, only qualitative comparisons of the different carbon powders are possible by the use of ATR-FTIR because the sample powder's particle size and packing characteristics are well-known to change the reflectance in the ATR-FTIR spectra.[130,131] The results are shown in Figure 4.8, following its interpretation.

The presence of a very broad peak ranging from 3250 and 3400 cm^{-1} for all carbon powders suggests an O-H group,[128,186] which may be due to either a phenol group, a carboxylic acid group, or adsorbed water on the carbon surface from the air. Carboxylic acid surface groups are possible on all the powders, but only Black Pearls 2000 and Vulcan XC-72 may possibly have phenolic surface groups as suggested by the use of TPD results discussed previously in Section 4.6.1. The peak at 2350 cm^{-1} is most likely due to the presence of adsorbed CO_2 present on all the carbon powders.[187] The peak near 2000 cm^{-1} present on Black Pearls 2000, Vulcan XC-72, and glassy carbon could be a C=O group belonging to an ester.[111] Another peak near 1850 cm^{-1} also present on Black Pearls 2000, Vulcan XC-72, and glassy carbon, may be interpreted as a C=O group belonging to an anhydride.[93,128] A weak peak located at 1700 cm^{-1} could suggest that carbonyl groups[93,128,188] are present on both Black Pearls 2000 and Vulcan XC-72, but absent on graphite and glassy carbon powders. Another peak at 1550 cm^{-1} suggests

the presence of quinone groups,[93,102,128,188] again on both Black Pearls 2000 and Vulcan XC-72 powders, but not on glassy carbon nor graphite.

Peaks located within the range of 1000-1300 cm^{-1} indicate C-O surface groups,[93,102,188] which may be interpreted as either a phenol or ether group on the carbon powders. However, on these glassy carbon and graphite powders, phenol groups were not in evidence in the TPD data in Section 4.6.1. Therefore, the corresponding C-O peaks from the ATR-FTIR spectra of glassy carbon and graphite were assigned to ether surface groups. For the Vulcan XC-72 and Black Pearls 2000 carbon blacks, the C-O peaks may be assigned as ether and phenol surface groups[93,128] since both of these groups may exist as discussed in Section 4.6.1. A more detailed consideration and discussion of the possible surface phenols and its influence on the electrochemistry of BHb will continue in Section 4.7.

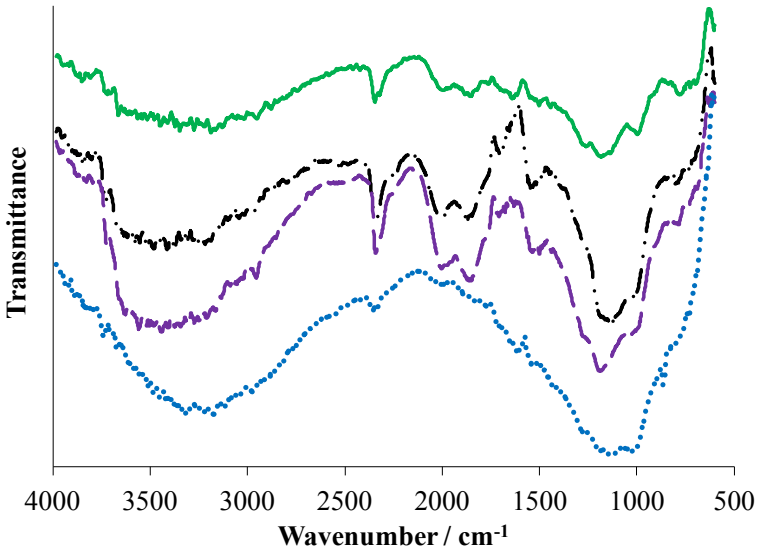

Figure 4.8 ATR-FTIR spectra of four carbon powders studied in this thesis: glassy carbon (green solid curve), Black Pearls 2000 (black dot-dot-dash curve), Vulcan XC-72 (purple dashed curve), and graphite (blue dotted curve). The transmittance of the carbon spectra were shifted for clarity.

In summary, the ATR-FTIR spectra suggest that ester or anhydride surface groups may be present on the glassy carbon, Vulcan XC-72, and Black Pearls 2000 powders. The ATR-FTIR spectra also suggest that Black Pearls 2000 and Vulcan XC-72 powders may have carbonyl and quinone surface groups, agreeing with TPD (Section 4.6.1) and XPS (Section 4.6.3) results. Additionally, ATR-FTIR data suggest that glassy carbon and graphite powders may not have quinone or carbonyl surface groups due to the absence of corresponding ATR-FTIR peaks (Figure 4.8).

4.6.3 Carbon-Oxygen Surface Functional Groups Identified by the use of XPS

XPS may be used to identify and quantify different carbon-oxygen surface functional groups due to their different chemical environments. The O_{1s} and C_{1s} XPS spectra of the four carbon powders were fitted to quantify these different chemical environments. The carbon-oxygen surface groups previously identified by the use of TPD and ATR-FTIR were used as a guide to assign different carbon-oxygen surface groups during peak fitting.

O_{1s} XPS spectra for Black Pearls 2000, Vulcan XC-72, glassy carbon, and graphite powders are presented in Figure 4.9a-d. The O_{1s} XPS fitted peak binding energies ranging from 531 to 532 eV have been assigned as C=O and 533 to 534 eV have been assigned to C-O based on previous literature reports.[93,117,164,165] The broadness of the fitted peaks in the O_{1s} XPS spectra were also matched to literature reports by constraining the full width at half maximum between 1.5 and 2.2 eV.[93,165] A tabulated summary of the fitted results is shown in Table 4.2.

After fitting the C=O and C-O surface groups to the O_{1s} XPS spectra of the carbon samples tested, only Black Pearls 2000 could be reliably resolved (Figure 4.9). For the Vulcan XC-72 and glassy carbon powders, the estimated errors in the C=O and C-O relative surface concentrations were so large that these surface groups could not be reliably compared between different carbon samples (Table 4.2). The apparent shift towards lower peak binding energy for the fitted C=O and C-O peaks in the glassy carbon powder sample (Figure 4.9c) may be due to the presence of more thermally stable C=O and C-O surface groups.[164] The fitted peak shifts in the glassy carbon powder sample are unlikely due to X-ray damage given its common use in X-ray techniques or surface charging given its conductivity. The graphite sample examined had a noisy O_{1s} XPS spectrum (Figure 4.9d), likely due to the low abundance of surface oxygen (1.1% O, Section 4.6), meaning this spectrum could not be fitted reliably. The fitted peaks for O_{1s} XPS spectra of the three carbon powders were not well-resolved and have significant peak overlap, resulting in uncertain and unreliable data interpretation. Black Pearls 2000 was the only carbon sample that had reliable O_{1s} XPS fittings, showing that there are more C-O surface groups than C=O carbon powder, which is consistent with the weight losses in the temperature ranges corresponding to surface ethers and phenols seen from the TPD data (Section 4.6.1).

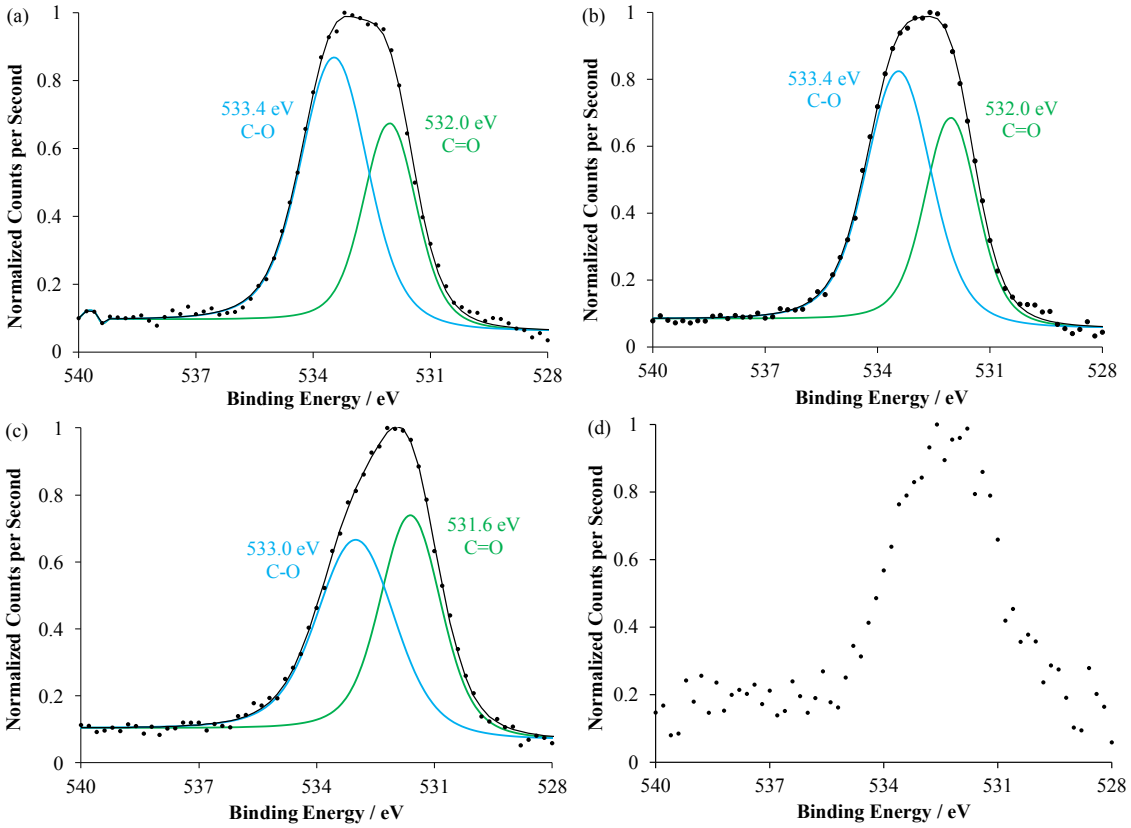

Figure 4.9 Fitted O_{1s} XPS data for as-received Black Pearls 2000 (a), Vulcan XC-72 (b), glassy carbon (c), and graphite (d) carbon powders. The dotted points represent the original O_{1s} XPS spectra. The solid colored fitted peaks represent the C-O and C=O bonding environments. The solid black curve represents the sum of the fitted peaks.

Table 4.2 A tabulated summary of C-O and C=O surface groups for each as-received carbon powder based on fitted O_{1s} XPS spectra. Each entry listed in the table contains the relative percent surface concentration based on integration under the fitted peak, the full width at half maximum, and the center position of the fitted peak. Errors in the relative percent surface concentration were estimated using one standard deviation calculated from Monte Carlo simulations assuming a normal distribution.

	C-O	C=O
Black Pearls 2000	66 ± 8% 2.08 eV 533.4 eV	34 ± 8% 1.57 eV 532.0 eV
Vulcan XC-72	60 ± 10% 2.06 eV 533.4 eV	40 ± 10% 1.67 eV 532.0 eV
Glassy Carbon	53 ± 17% 2.20 eV 533.0 eV	47 ± 17% 1.87 eV 531.6 eV
Graphite	No reliable fit	

Interpretation of C_{1s} XPS spectra is more reliable and well-established than O_{1s} interpretation. Figure 4.10 is a visual representation of all the peaks used to fit the C_{1s} XPS spectra and Table 4.3 presents the numerical parameters used to fit each peak as well as their resulting relative surface concentrations for Black Pearls 2000, Vulcan XC-72, glassy carbon, and graphite carbon powders. Although not a carbon-oxygen surface functional group, the π-π* shakeup is also presented; the π-π* shakeup originates from the aromaticity of the sp^2 carbons. Quantitative comparisons of the π-π* shakeup surface concentrations cannot be made reliably between samples due to high estimated errors (*ca.* ±3 %).

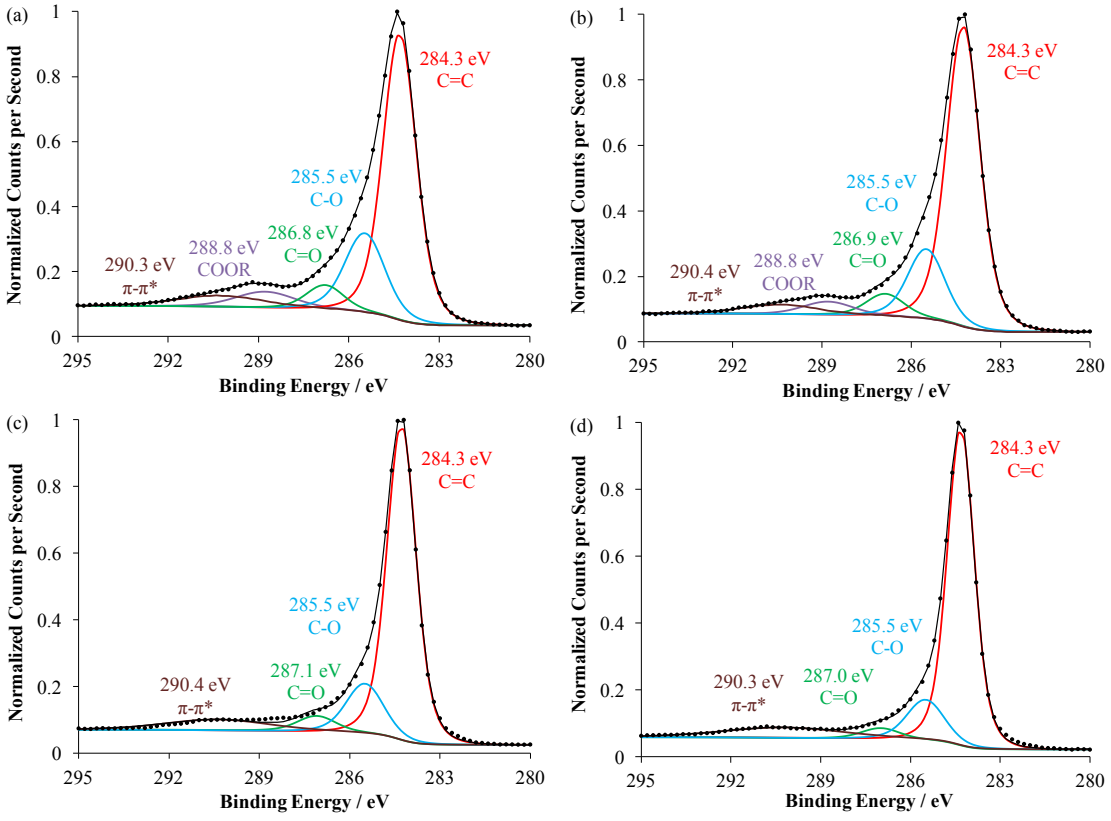

Figure 4.10 Fitted C_{1s} XPS data for as-received Black Pearls 2000 (a), Vulcan XC-72 (b), glassy carbon (c), and graphite (d) carbon powders. Dotted black curves represent the original C_{1s} XPS spectra. Each solid colored fitted peak represents a certain surface group. The black solid curve represents the sum of the fitted peaks.

The carbon-oxygen surface groups identified and quantified by the use of C_{1s} XPS for each carbon powder sample are summarized in Table 4.3. The fitted peak centered at 285.5 eV suggests C-O surface functional groups, which can be interpreted as an ether or phenol.[106,120,121] An increase in the C-O surface concentrations (graphite < glassy carbon < Vulcan XC-72 < Black Pearls 2000) agrees with the TPD evidence presented previously in Section 4.6.1. A fitted XPS C_{1s} peak centered between 287.1 eV and 286.8 eV, suggests the presence of a carbonyl group on all four carbon powders,[98,102,106,117,118,121] with the same trend of increasing surface carbonyl groups as TPD (Section 4.6.1), which was graphite < glassy carbon < Vulcan XC-72 ≈ Black Pearls 2000. The fitted peak centered at 288.8 eV (Table 4.3 and Figure 4.10) suggested the presence of COOR surface groups,[98,102,106,117,118] which are interpreted as either a lactone, carboxylic acid, or anhydride. The COOR surface group assignment on the Vulcan XC-72 and Black Pearls 2000 was consistent with ATR-FTIR results, as was the lack of COOR groups suggested by the use of C_{1s} XPS on graphite. COOR surface groups were expected on the glassy carbon powder by the use of ATR-FTIR, but the quantity of COOR was negligible on the glassy carbon powder after fitting the C_{1s} XPS spectrum, likely due to the fitted π-π^* shakeup peak overlapping the fitted COOR peak.

Table 4.3 A tabulated summary of different surface groups represented by the corresponding fitted peak in the C_{1s} XPS spectra for each as-received carbon powder. Each entry listed in the table contains the relative percent surface concentration based on integration under the fitted peak, the full width at half maximum, and the center position of the fitted peak.

	C=C	C-O	C=O	COOR	π-π* shakeup
Black Pearls 2000	61.4% 1.31 eV 284.3 eV	20.3% 1.57 eV 285.5 eV	5.8% 1.47 eV 286.8 eV	6.1% 2.31 eV 288.8 eV	6.4% 3.5 eV 290.3 eV
Vulcan XC-72	67.7% 1.33 eV 284.3 eV	17.3% 1.47 eV 285.5 eV	5.6% 1.50 eV 286.9 eV	4.5% 1.99 eV 288.8 eV	4.9% 3.03 eV 290.4 eV
Glassy Carbon	72.0% 1.14 eV 284.3 eV	14.6% 1.47 eV 285.5 eV	4.6% 1.50 eV 287.1 eV	Negligible	8.8% 4.10 eV 290.4 eV
Graphite	73.2% 1.07 eV 284.3 eV	12.8% 1.47 eV 285.5 eV	3.4% 1.50 eV 287.0 eV	Negligible	10.6% 4.78 eV 290.3 eV

4.6.4 Discussion of BHb Electroactivity in regards to Identified Carbon-Oxygen Surface Functional Groups

Interpretation of all of the TPD, ATR-FTIR, XPS, and electrochemical data suggests that sufficient quinone, carbonyl, phenol, lactone, and ether surface groups may be inhibiting the electrochemical activity of BHb on carbon (Table 4.4). The presence of more C=O carbonyl and quinone surface groups found on the Vulcan XC-72 and Black Pearls 2000 powders strongly suggest that these surface groups likely inhibit BHb electroactivity since BHb was inactive on these two powders. Possible carboxylic acid and anhydride surface groups on all four of the carbon powders tested are unlikely to influence the BHb electroactivity on these carbon powders since BHb was active on glassy carbon and graphite, and inactive on Vulcan XC-72 and Black Pearls 2000, but cannot be ruled out. Surface lactones identified on the Black Pearls 2000 powder may be involved in inhibiting the electrochemical reduction of BHb because surface lactones

were not found on the other carbon materials. The identification of surface phenols on Vulcan XC-72 and Black Pearls 2000 was inconclusive; thus, the effect of surface phenols on the electrochemistry of BHb is inconclusive. Ether surface groups are present on all carbon materials, but their exact quantities were uncertain. In order to unambiguously confirm which carbon oxide surface group had a greater impact on the electrochemistry of BHb, carbon modification by removing particular carbon-oxygen surface groups is necessary, which will be described next.

Table 4.4 A summary of possible carbon surface oxides identified using TPD, ATR-FTIR, and XPS.

	Carbon-Oxygen Surface Groups					
	COOH or Anhydride	Lactone	Phenol	Ether	Carbonyl & Quinone	BHb Electroactivity
Black Pearls 2000	Present	Present	Possible	Present	Present	no
Vulcan XC-72	Present	None	Possible	Present	Present	no
Glassy Carbon	Possible	None	None	Present	Some Present	yes
Graphite	Possible	None	None	Present	Little Present	yes

4.7 Modification of Black Pearls 2000 by the use of a Heat Treatment

Knowledge of the carbon-oxygen surface functional groups from the previous sections may be used to modify a carbon material to improve BHb electrochemical reduction. In the previous sections, several different carbon-oxygen surface groups were identified as possibly being responsible for inhibiting BHb electroactivity. If the removal of some of these carbon-oxygen surface functional groups improves the electrochemical activity of BHb, then the removed surface groups can be directly linked to inhibition of

the electrochemical reduction of BHb. Black Pearls 2000 was chosen for modification since it had the highest degree of surface oxidation of the four carbon powders tested and showed no BHb electroactivity. In this section, selective removal of surface lactones, carboxylic acids, anhydrides, and phenols was performed by the use of a heat treatment of the Black Pearls 2000 carbon black at 1000 °C for 2 hours. According to Figueiredo *et al.*, this temperature is well-known to be sufficient for the complete removal of these groups, but is insufficient for the complete removal of carbonyl, quinone, or ether groups,[93] which may also inhibit BHb electrochemical reduction. The heat treatment will distinguish whether the COOR (*i.e.* lactones, carboxylic acids, and anhydrides), and phenolic surface groups are more important in the electrochemical reduction of BHb than the carbonyl, quinone, and ether surface groups.

Careful observation of TGA data are required to monitor the complete removal of the COOR and phenolic surface groups. TGA was recorded during the entire heating and cooling processes under an Ar atmosphere (Figure 4.11). The process of heating to 1000 °C was expected to have similar results to those presented in Figure 4.7a. Holding the temperature at 1000 °C ensures the complete removal of all phenolic and COOR surface groups, while only partially removing ethers, carbonyls, and quinones.[93] The cooling process was recorded to ensure the surface carboxylic acids, anhydrides, lactones, and phenols were completely removed from the carbon surface. Some sample weight decrease continued during the cooling process from 1000 to 800 °C (Figure 4.11a), due to incomplete removal of ethers, carbonyls, and quinones.[93] No significant sample weight changes were observed when cooling to temperatures below 800 °C (Figure 4.11a and b),

suggesting the complete removal of all COOR and phenolic surface groups on this carbon after the heating procedure.[93]

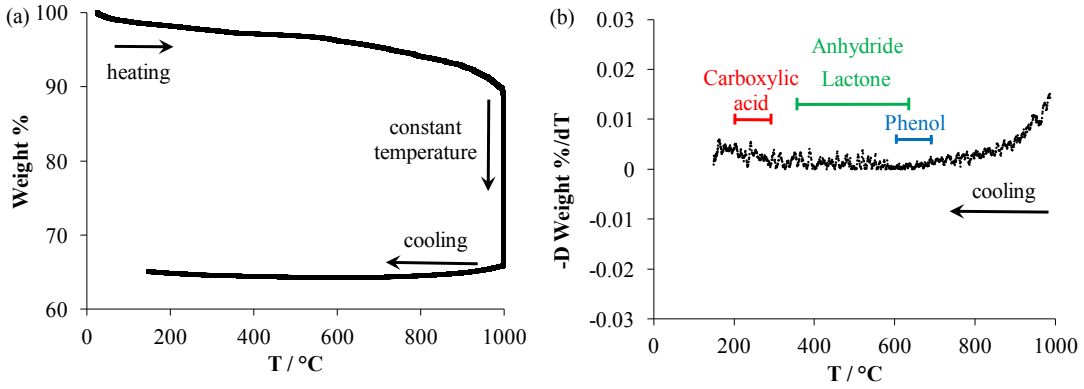

Figure 4.11 A representative TGA of the Black Pearls 2000 heated from room temperature to 1000 °C with a 2 hour temperature hold and the cooling process under Ar atmosphere (a) and the derivative TGA (b) of the cooling process to emphasize no weight losses at temperatures below 800 °C. Temperature ranges for the expected weight losses corresponding to surface carboxylic acid (red), anhydride (green), lactone (green), and phenol (blue) surface groups are labeled in panel (b).

DPVs of the as-received Black Pearls 2000 are reproduced in Figure 4.12a for ease of comparison with the heat-modified Black Pearls 2000 in Figure 4.12b. The heat-treated Black Pearls 2000 showed no significant enhancement in the electrochemical activity of BHb (Figure 4.12b), indicating that carboxylic acid, anhydride, lactone, and phenol surface groups have a negligible impact on the electrochemical reduction of BHb.

The heat treatment used was not expected to significantly change the carbon surface morphology. Heating the Black Pearls 2000 powder at a similar temperature of 950 °C under an inert Ar atmosphere does not significantly change the carbon surface area.[189] Heat-treated Black Pearls 2000 did not show a different surface morphology of Black Pearls 2000 as suggested by the use of scanning electron micrographs presented in Figure 4.13.

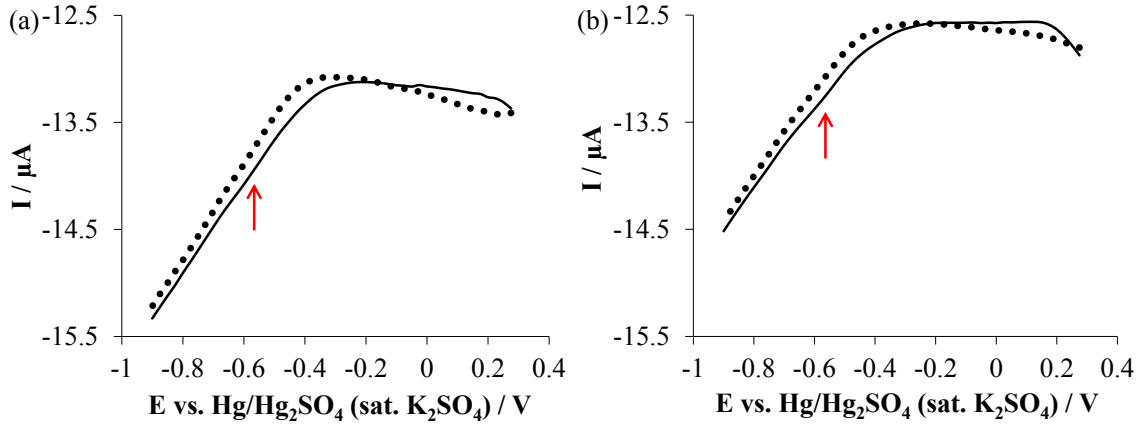

Figure 4.12 DPV of as-received Black Pearls 2000 (a) was reproduced for convenience. A representative DPV of heat-treated Black Pearls 2000 lacking carboxylic acid, anhydride, lactone, and phenol surface groups (b). The electrolyte was 0.1 M PB without (dotted curve) and with (solid curve) 0.2 g L^{-1} BHb. Red arrows indicate the location of the expected BHb reduction peak.

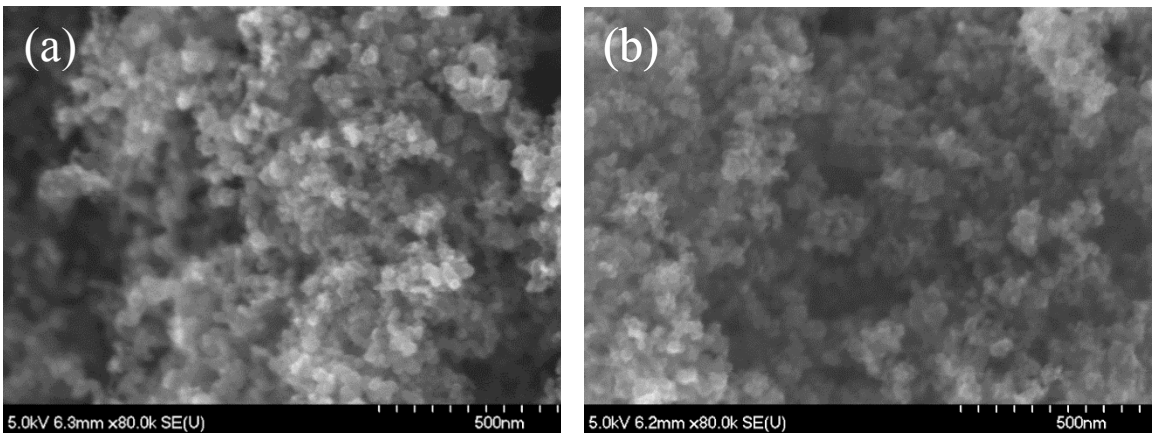

Figure 4.13 Scanning electron micrographs of as-received Black Pearls 2000 carbon black powder (a) and after heat treatment under Ar atmosphere for 2 hours at 1000 °C (b).

4.8 Modification of Carbon by the use of Carbonyl C=O Removal

To examine whether carbonyl surface groups inhibit the electrochemical activity of BHb, a procedure known to remove C=O surface groups from a carbon surface was used and the BHb electrochemical activity was examined after the removal of C=O surface groups. The known C=O removal procedure was a simple electrochemical

reduction process in aqueous phosphate solution, and the authors of this procedure showed C=O removal using infrared spectroscopy.[160]

Several difficulties were encountered when performing the electrochemical reduction process. The platinum microcavity electrode loaded with carbon powder failed due to excessive evolution of hydrogen and subsequent loss of the carbon powder. Therefore, a different electrode setup that does not require the platinum microcavity electrode was necessary. Two different electrode setups were tested. One electrode setup was a carbon fabric held in a Swagelok setup (Section 3.1.2.3), and another setup used an aqueous carbon suspension prepared on a glassy carbon electrode (Section 3.1.3.2).

4.8.1 Electrochemistry of BHb on Spectracarb 2225

Spectracarb 2225 is a binderless woven carbon electrode material known to have a very high surface area of *ca.* 2100 m^2 g^{-1}.[173] Examination of Spectracarb's electrochemistry with BHb and identification of its carbon-oxygen surface functionalities is necessary before attempting electrochemical reduction modification. The electrochemical activity of BHb on Spectracarb 2225 was examined by the use of differential pulse voltammetry. The DPVs from Figure 4.14 clearly indicate no BHb electroactivity; therefore, examination of the carbon-oxygen surface functionalities on Spectracarb 2225 is the next logical step to determine whether its surface groups are responsible for the lack of BHb activity.

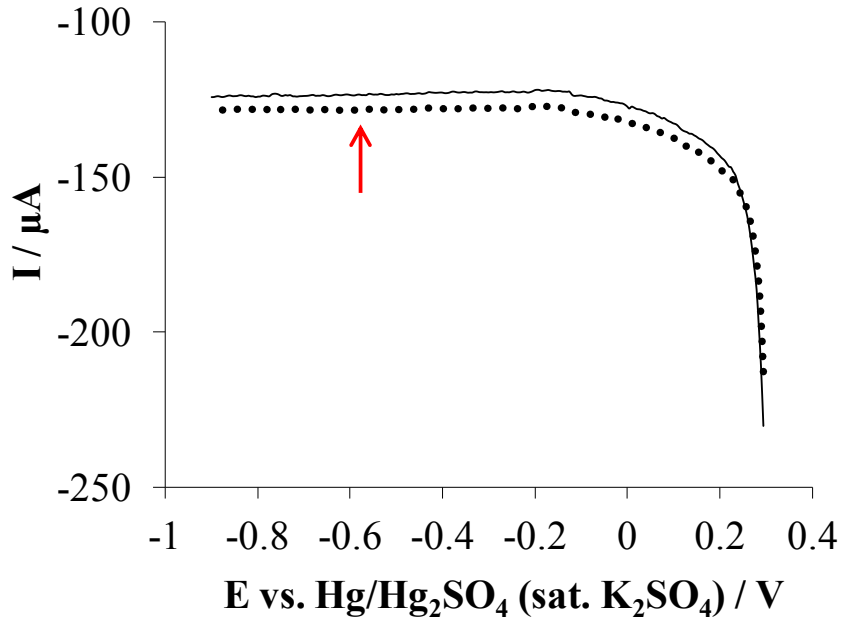

Figure 4.14 Representative DPVs of Spectracarb 2225 in 0.1 M PB (pH 7.08) without (dotted black curve) and with (solid black curve) 0.2 g L^{-1} BHb present in the electrolyte. A red arrow indicates where the BHb reduction peak is expected to appear on a carbon surface.

4.8.2 Characterizing Carbon-Oxygen Surface Functionalities on Spectracarb 2225 by the use of Temperature Programmed Desorption

To examine the carbon-oxygen surface functionalities on Spectracarb 2225, TPD was employed. The TGA plot (Figure 4.15a) shows the most sample weight loss in comparison to all the carbons tested previously (Figure 4.7a), suggesting a greater concentration of carbon-oxygen surface functional groups. The TGA plot and its derivative (Figure 4.15a and b) show that the majority of the Spectracarb 2225 weight loss occurred at temperatures higher than approximately 600 °C. Integration of the mass spectrometer signal for CO_2 from 500 to 600 °C reveals a negligibly small amount of surface lactones,[93] approximately 7 ± 6 µmole of lactone per gram of carbon. At temperatures of 600 °C and above, a release of CO_2 was observed with a peak at 920 °C (Figure 4.15c). As described previously in Section 4.6.1, no particular carbon-oxygen

surface functional group could be assigned but the release of $CO_{2(g)}$ could be from the released $CO_{(g)}$ reacting with a carbon surface oxide due to a possible Boudouard reaction. From 600 to 1000 °C, 440 ± 20 μmole of $CO_{2(g)}$ per gram of carbon was evolved, suggesting that 880 ± 40 μmole of carbon surface oxide per gram of carbon may be present on the Spectracarb 2225 if the Boudouard reaction occurred, which is significantly more than the evolved $CO_{2(g)}$ of all the carbons examined previously in Section 4.6.1. At temperatures of 800 °C and above, the release of $CO_{(g)}$ was averaged to be 450 ± 30 μmole of surface groups per gram of carbon, suggesting larger collective amounts of ether, carbonyl, and quinone surface groups than those present on the carbon powders. In consideration of the BHb electrochemical activity, the greater surface concentrations of these groups are likely responsible for the inactivity of BHb on Spectracarb 2225.

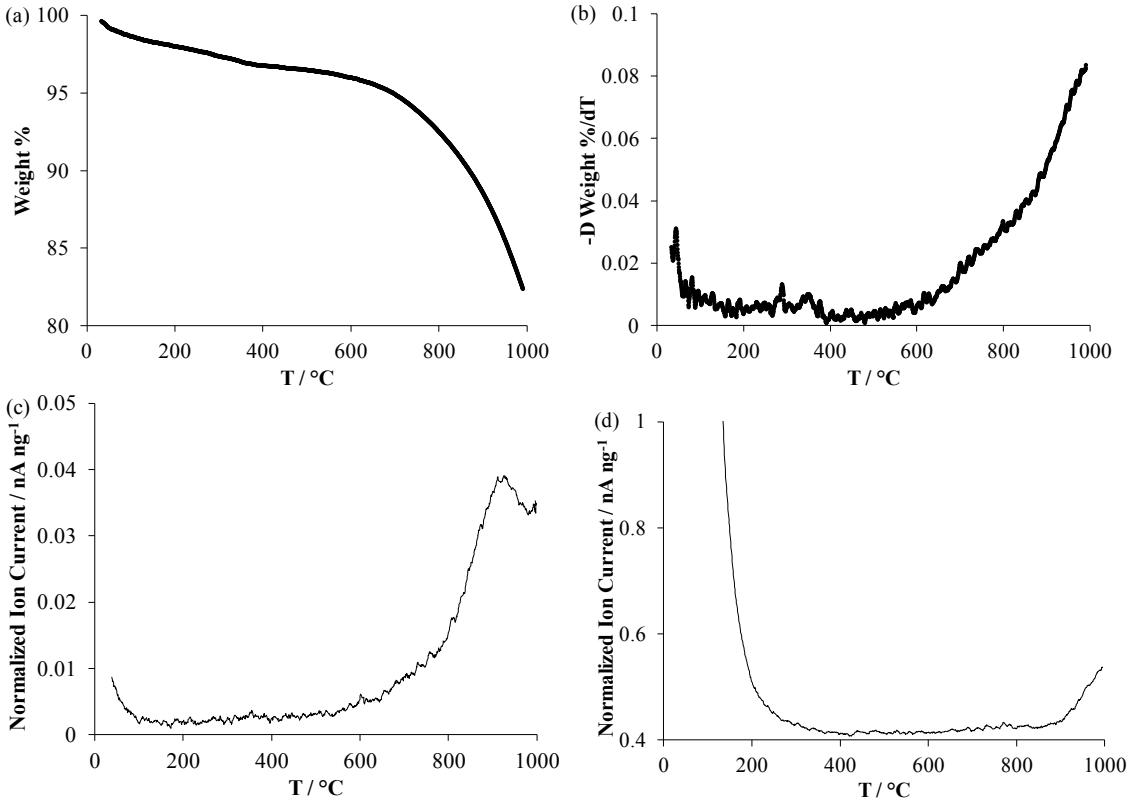

Figure 4.15 TGA (a) and derivative TGA plots (b) of Spectracarb 2225. The mass spectrometer detector response to *m/z* 44 (CO_2) (c) and *m/z* 28 (CO) (d) are also shown. All of the TPD data shown here are an average of three replicate trials.

4.8.3 Characterizing Carbon-Oxygen Surface Functionalities on Spectracarb 2225 by the use of ATR-FTIR

Spectracarb 2225 was also characterized using ATR-FTIR (Figure 4.16). A distinct peak at 1550 cm^{-1} suggests the presence of quinone surface groups on Spectracarb 2225,[93,102,128,188] agreeing with the findings from TPD (Section 4.8.2). The ATR-FTIR spectrum also revealed the presence of C-O, where its corresponding peak is centered at 1040 cm^{-1}.[93,102,188] Since there is a lack of O-H stretching peaks at wavenumbers higher than 3000 cm^{-1}, the results suggest that there may be a lack of phenols and carboxylic acids, implying that the C-O groups should be assigned to ether groups, agreeing with the TPD data in Section 4.8.2. Other features of the ATR-FTIR

spectrum could not be reliably distinguished from the baseline. The ATR-FTIR results here coupled with the lack of BHb activity on Spectracarb 2225 shown in Section 4.8.1 strongly suggest that the presence of surface quinones and ethers on the Spectracarb 2225 carbon surface may be inhibiting the electrochemical reduction of BHb.

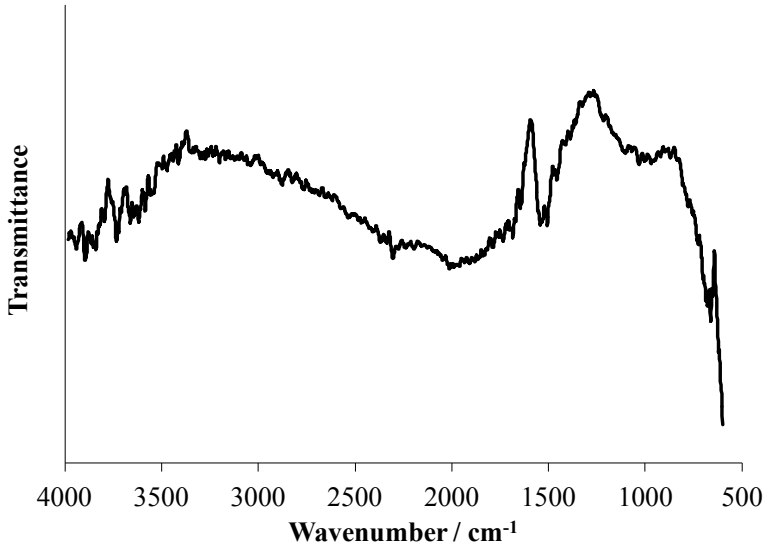

Figure 4.16 ATR-FTIR spectrum of Spectracarb 2225.

4.8.4 Characterizing Carbon-Oxygen Surface Functionalities on Spectracarb 2225 by the use of XPS

The XPS spectrum of Spectracarb 2225 in Figure 4.17a showed only the presence of C_{1s} (284 eV) and O_{1s} (532 eV). Known C_{KLL} and O_{KLL} peaks due to Auger electrons located at 991[190,191] and 746 eV,[190,192] respectively, were seen (Figure 4.17), similar to those also observed previously (Figure 4.5, Section 4.6). A 4.0% degree of surface oxidation was calculated for Spectracarb 2225 based on integration of the area under C_{1s} and O_{1s} peaks, which is similar to that of the glassy carbon powder (4.4 ± 0.5%) described previously in Section 4.6. The results here reinforce that the degree of surface

oxidation determined by the use of XPS is not the most important factor in determining the ability of a carbon to electrochemically reduce BHb because BHb was electrochemically active on the glassy carbon powder, but not on the Spectracarb 2225. However, TPD data suggested that significantly more carbon-oxygen surface groups were present on Spectracarb 2225 than on the glassy carbon powder, which appears to contradict the XPS data. The apparent contradiction may be resolved by considering the structure of the Spectracarb 2225 material, the limitation of XPS, and the operation of TPD.

Spectracarb 2225 carbon fabric is a woven material known to have an open pore structure, as stated in its product description. As explained previously in Section 4.6.1, XPS can probe approximately the first 10 nm from the sample surface.[133] If the pores in Spectracarb 2225 are deeper than 10 nm from the sample surface, then XPS cannot be used to analyze the possible carbon-oxygen surface groups in those pores. However, TPD may be used to investigate the carbon surface oxides in these deep pores as long as $CO_{(g)}$ and $CO_{2(g)}$ are released and detected as a function of temperature. Therefore, the observed increase in carbon surface oxides on the Spectracarb 2225 by the use of TPD over XPS is certainly plausible.

The fitted peaks representing different surface groups in the C_{1s} XPS spectrum are presented visually in Figure 4.17b and the relative surface concentrations of different carbon surface groups are presented numerically in Table 4.5. The surface amount of C-O ether on Hb-inactive Spectracarb 2225 (15.0%) is similar to that of the Hb-active glassy carbon powder (14.6%, Section 4.6.3), suggesting that perhaps up to 15% ether surface groups is not sufficient to affect the electrochemical reduction of BHb and that

the C=O carbonyl groups are likely more influential in inhibiting BHb activity. The surface amounts of carbonyl C=O on Spectracarb 2225 (7.3%) are very high, even higher than the previously characterized carbon powders where the highest amount was 5.8% on Black Pearls 2000 (Section 4.6.3). The increased surface amounts of C=O quantified by the use of C_{1s} XPS are consistent with the TPD results. Both Spectracarb 2225 and Black Pearls 2000 were BHb-inactive, suggesting that the carbonyl C=O surface groups are influential in inhibiting BHb electrochemistry.

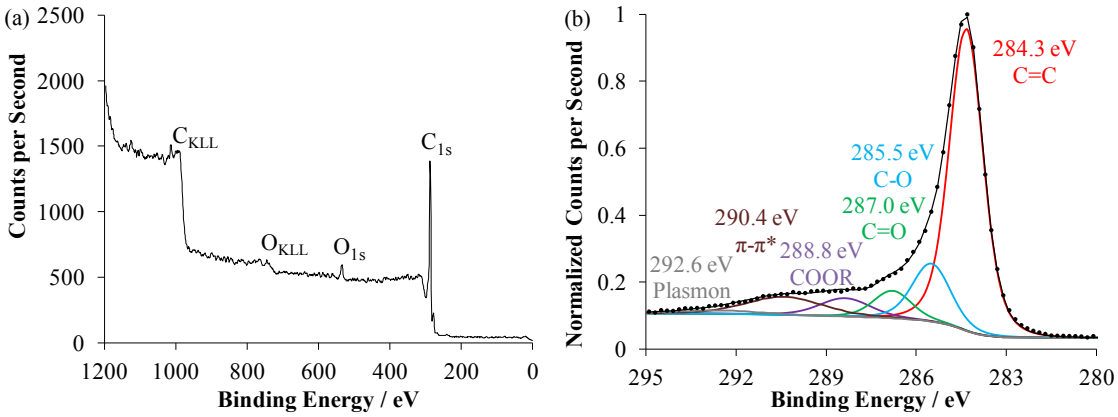

Figure 4.17 XPS spectra examining other possible elements (a) and a fitted C_{1s} XPS spectrum of Spectracarb 2225 (b). The dotted black curve represents the original C_{1s} XPS spectrum, each solid colored fitted peak represents a certain surface group, and the black solid curve represents the sum of the fitted peaks (b).

Table 4.5 A summary of tabulated C_{1s} XPS results from peak fitting Spectracarb 2225. The listed values are the relative surface concentration, full width at half maximum, and the center of the fitted peak position for each fitted peak representing a different surface group.

	C=C	C-O	C=O	COOR	π-π* shakeup	Plasmon
Spectracarb 2225	62.8 % 1.31 eV 284.3 eV	15.0% 1.50 eV 285.5 eV	7.3% 1.50 eV 287.0 eV	5.3% 2.00 eV 288.8 eV	7.5% 3.00 eV 290.4 eV	2.1% 3.20 eV 292.6 eV

4.8.5 Electrochemical Reduction of Spectracarb 2225

The electrochemical reduction modification of Spectracarb 2225 to remove carbonyl surface groups (Section 3.1.3.3) failed. Hydrogen gas was generated on the Spectracarb 2225 surface during the electroreduction procedure, likely becoming trapped within the pores of the carbon material, preventing the removal of carbonyl surface groups. As hydrogen gas continued to evolve during the electrochemical reduction modification, the buildup of pressure deep within the pores of the Spectracarb 2225 may have expanded the pores, eventually damaging the carbon surface. The attempted electrochemical reduction treatment resulted in visibly damaging the Spectracarb 2225 material.

Although the electrochemical reduction modification of Spectracarb 2225 was unsuccessful, important information regarding the electrochemistry of BHb on this carbon was gained. Spectracarb 2225 contains carbon surface oxide groups consisting of mainly ethers, carbonyls, and quinones. More carbonyl and quinone groups were seen on Spectracarb 2225 than those seen previously for carbon powders. Since the amount of ether groups is less on the Spectracarb 2225 than those on the BHb-inactive carbon powders (Section 4.6) and BHb was not electrochemically active on Spectracarb 2225, then it may be hypothesized that the carbonyl and quinone surface groups are more important than surface ethers in inhibiting the electrochemistry of BHb.

4.8.6 Electrochemical Reduction Modification of a Vulcan XC-72 Aqueous Suspension

To electroreduce a carbon powder, the carbon material may be attached to a glassy carbon electrode following Guo's method.[160] Ultrasonication was used to create

an aqueous suspension of the carbon material for casting onto glassy carbon. Creation of the carbon suspension posed problems due to carbon aggregation in the suspension and on the glassy carbon, but a concentration of 1 g L^{-1} yielded a stable aqueous suspension and an even film upon drying. A suspension of the Vulcan XC-72 powder, formed through ultrasonication in Millipore water, was then cast onto a glassy carbon electrode for the electrochemical reduction modification procedure (Section 3.1.3.2).

The CVs and DPVs of the bare glassy carbon, ultrasonicated (before reduction) Vulcan XC-72, and the ultrasonicated/reduced Vulcan XC-72 are shown in Figure 4.18a and b. The current on the glassy carbon electrode in both BHb-free and BHb-containing electrolyte was approximately an order of magnitude smaller than that observed on the ultrasonicated Vulcan XC-72, meaning that the BHb response on glassy carbon can be ignored when considering the Vulcan XC-72 experiments. Nevertheless, the glassy carbon electrode, before and after the electrochemical reduction modification, was evaluated since its contribution to BHb electrochemistry is not known. Ultrasonication of the glassy carbon was not attempted since ultrasonication has been shown to damage the surface of the glassy carbon.[193] No increase in the BHb cathodic current near -0.7 V (Figure 4.18c and d) was observed after electroreduction of the glassy carbon electrode. The results suggest that the majority of the increased cathodic current previously seen in Figure 4.18a and b is indeed due to Vulcan XC-72 and the modifications of that material.

Experiments were not performed on as-received Vulcan XC-72 because this carbon did not remain attached to the glassy carbon electrode upon insertion into the electrolyte. Nevertheless, previous data on the as-received Vulcan XC-72 using a microcavity electrode showed that BHb was barely electroactive on this carbon (Figure

4.18e and f, reproduced from Figure 4.3e and f in Section 4.4). Ultrasonication of Vulcan XC-72 in water was required to create a slurry to affix the carbon onto the glassy carbon electrode. After the carbonyl surface groups were removed by the use of electroreduction[160] of the ultrasonicated Vulcan XC-72 carbon, a clear increase in the BHb electroactivity was observed (Figure 4.18a and b).

It is difficult to directly compare the electroactivity of the unmodified Vulcan XC-72 with the modified carbon (Figure 4.18) because different electrode setups (microcavity electrode versus films on glassy carbon) use different amounts of carbon powder, resulting in different surface areas and currents. To facilitate comparison, the current was normalized to the double-layer current (*i.e.* the current at a potential where no redox reaction takes place) to account for the different electrode surface areas; -0.3 V was chosen for this potential. It is obvious in the resulting normalized voltammograms (Figure 4.19a and b) that there is a difference in the voltammograms recorded in the absence of BHb. The cathodic currents recorded in BHb-free electrolytes were higher for the ultrasonicated/reduced Vulcan XC-72 in the CVs near the BHb peak reduction potential (*ca.* -0.64 V, Figure 4.19a), but were lower in the DPVs (*ca.* -0.575 V, Figure 4.19b). These results suggest a fast reduction reaction on the carbon surface, likely originating from the ultrasonication process changing the carbon powder and the carbon surface groups.[194]

Further data processing is required to account for the changing carbon response in BHb-free electrolytes. The normalized reduction currents at the peak BHb reduction potential in BHb-free electrolytes (Figure 4.19) were used as background current. The results of the normalized and background-subtracted peak BHb reduction current (Figure

4.20) clearly showed that the electrochemical reduction of BHb increased in the order of as-received Vulcan XC-72 < ultrasonicated Vulcan XC-72 < ultrasonicated/reduced Vulcan XC-72. The difference in BHb enhancement in the CVs and DPVs is likely due to the ultrasonication process changing the carbon material and carbon surface groups[194] as discussed previously. Since the electroreduction modification procedure removes surface carbonyl groups and an increase in BHb electroactivity was observed, these results confirm that the carbonyls on the electrode surface inhibit BHb electroactivity.

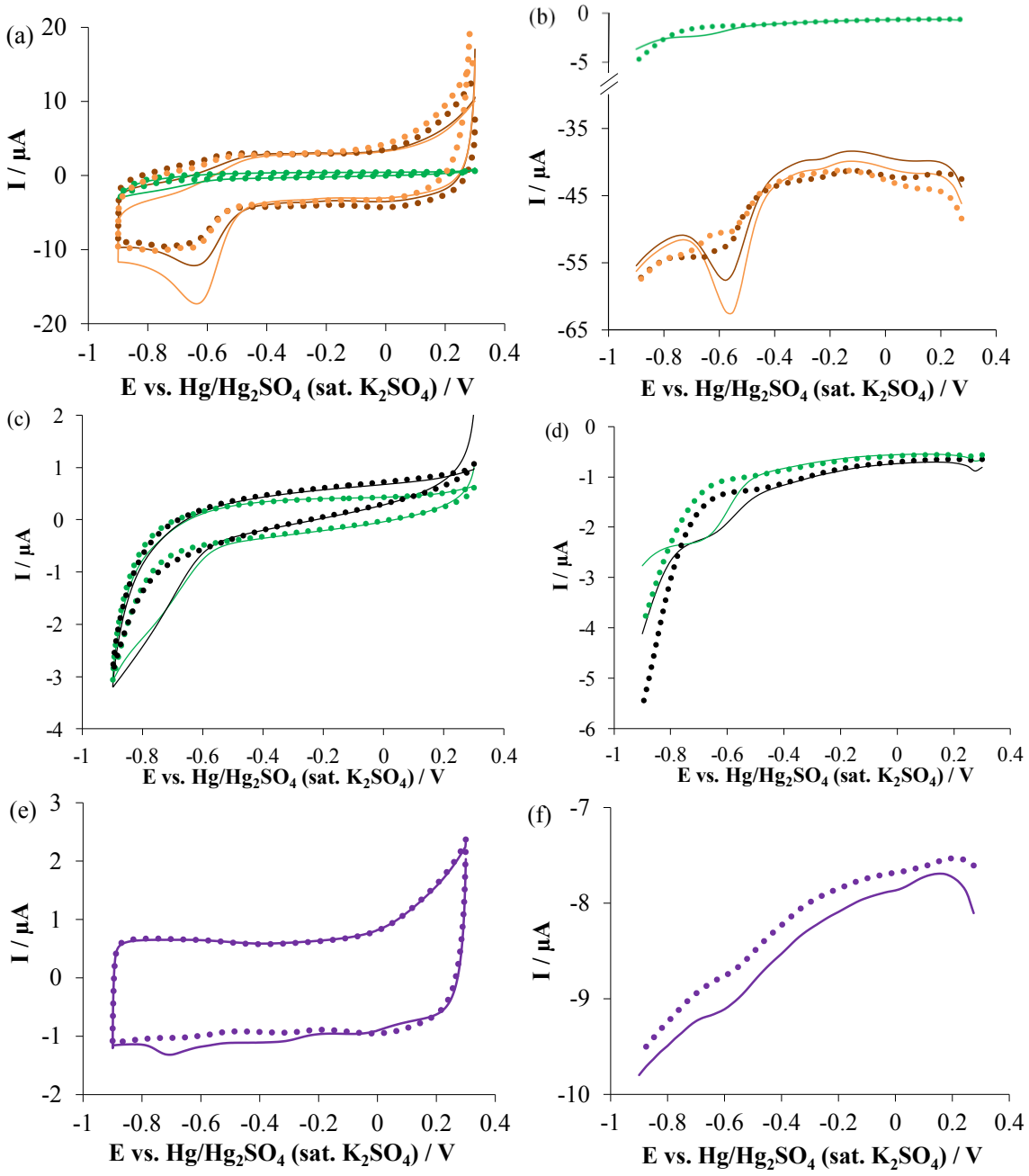

Figure 4.18 Representative CVs (a,c,e) and DPVs (b,d,f) of glassy carbon before (a-d, green curves) and after electroreduction modification (c-d, black curves), ultrasonicated Vulcan XC-72 on glassy carbon (a-b, brown curves), ultrasonicated/reduced Vulcan XC-72 on glassy carbon (a-b, orange curve), and as-received Vulcan XC-72 powder (e-f, purple curves, reproduced from Figure 4.3e and f for ease of comparison) in 0.1 M PB (dotted curves) containing 0.2 g L^{-1} BHb (solid curves).

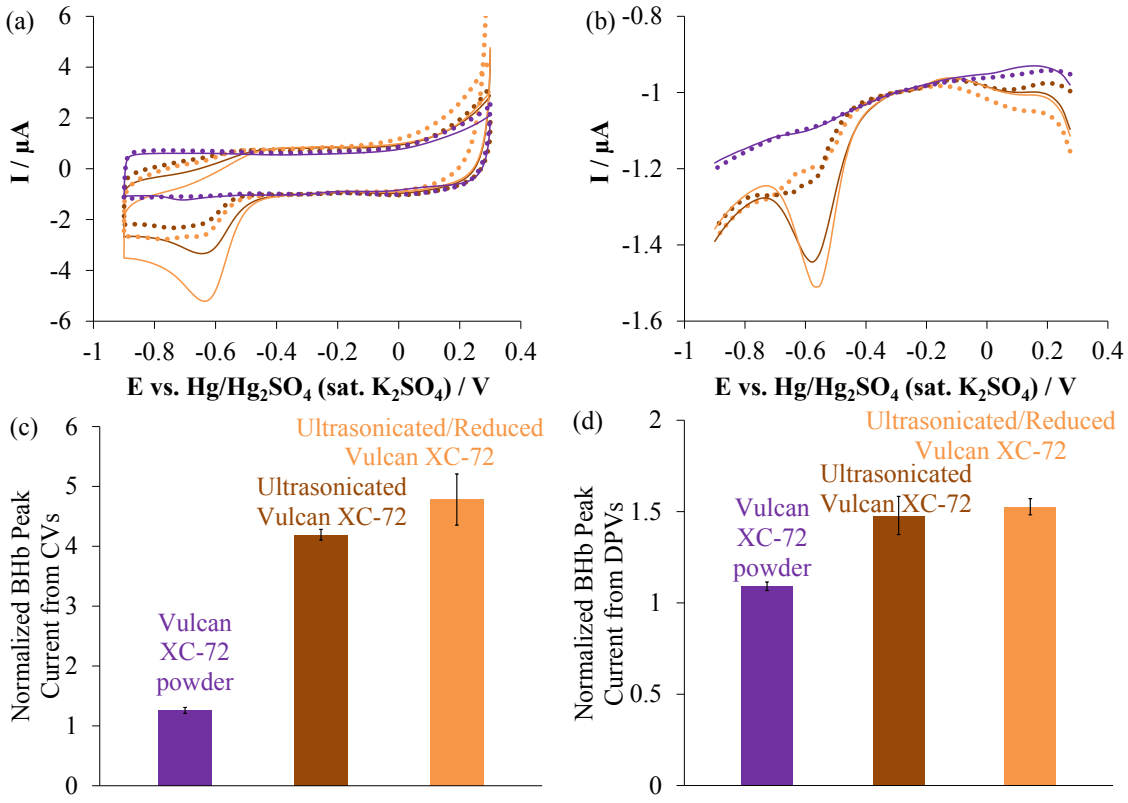

Figure 4.19 CVs (a) and DPVs (b) normalized to the double-layer current at -0.3 V. The normalized BHb peak currents for each Vulcan XC-72 processing stage from the CVs (c) and DPVs (d) are shown with error bars indicating one standard deviation from three replicates.

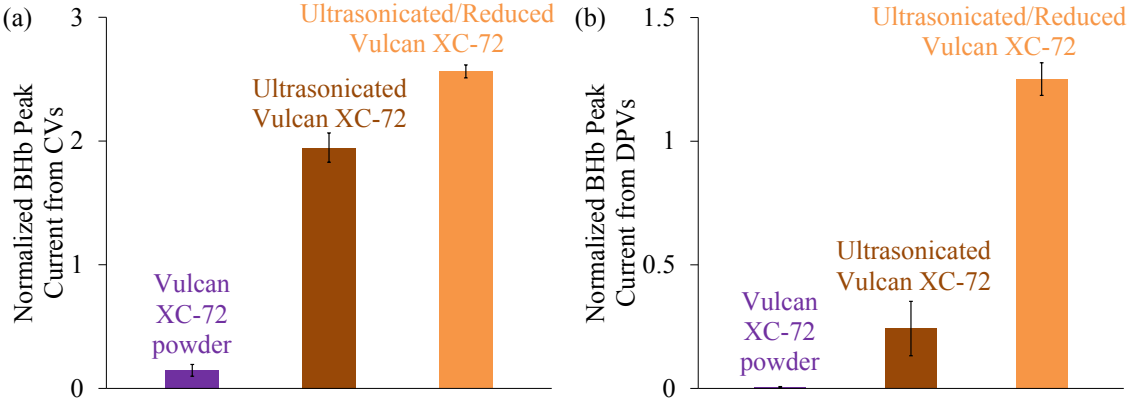

Figure 4.20 Normalized and background-subtracted average electrochemical BHb reduction current from CV (a) and DPV data (b) using at least three replicate trials for each of as-received (purple), ultrasonicated (brown), and ultrasonicated/reduced (orange) forms of Vulcan XC-72.

4.8.7 Surface Characterization of Ultrasonicated/Reduced Vulcan XC-72

Scanning electron micrographs of the Vulcan XC-72 show that the surface morphology did not significantly change during the ultrasonication or reduction processing procedures (Figure 4.21). This suggests that the improvement in the electrochemical reduction of BHb is not because of the change in the electrode surface morphology, but must instead be a result of a change in surface chemistry. Therefore, the carbon surface functional groups were examined by the use of XPS.

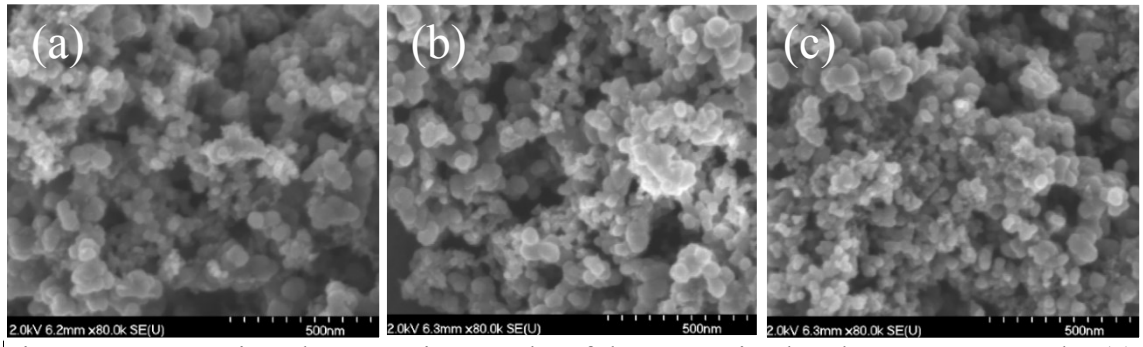

Figure 4.21 Scanning electron micrographs of the as-received Vulcan XC-72 powder (a), after ultrasonication in water (b), and after an electrochemical reduction treatment of the ultrasonicated carbon (c).

To help explain the differences in the electrochemistry of BHb on the as-received Vulcan XC-72, its ultrasonicated form, and its ultrasonicated/reduced form, C_{1s} XPS was used to quantify the amounts of carbon surface functionalities with particular focus on the C=O carbonyl and C-O ether groups. The fitted peaks are shown in Figure 4.22 and the complete fitting details with the relative surface concentrations are presented in Table 4.6.

The fitted C_{1s} XPS data for as-received Vulcan XC-72 and ultrasonicated Vulcan XC-72 (Table 4.6) show a decrease in C-O (17.3 → 13.5%), and COOR (4.5 → 3.5%) groups after ultrasonication. The increase in C=O (5.6 → 6.5%) is not significant when

considering the one standard deviation errors estimated by the use of Monte Carlo simulations. As noted previously in Section 4.7, the presence of COOR surface groups (*i.e.* carboxylic acids, anhydrides, lactones) do not affect the electrochemistry of BHb on carbon. The enhanced BHb electrochemical activity is likely due to the significant removal of the C-O ether groups, consistent with the C_{1s} XPS results described previously (Section 4.6.3).

The C_{1s} XPS for the ultrasonicated/reduced Vulcan XC-72 sample showed a surprising new peak at a higher binding energy of 292.6 eV, which was not previously seen on the ultrasonicated Vulcan XC-72 nor on the as-received Vulcan XC-72. The peak positioned at 292.6 eV was assigned to a plasmon process.[106,124] Surface plasmons are sensitive to surface modifications.[195] Changes to the intensity of the dipole moments on the surface are expected to change their interaction with surface plasmons.[195,196] The appearance of this peak is likely due to the removal of carbonyl surface groups, in turn changing the intensity of the dipole moments on the carbon surface since fewer electronegative oxygen are present.

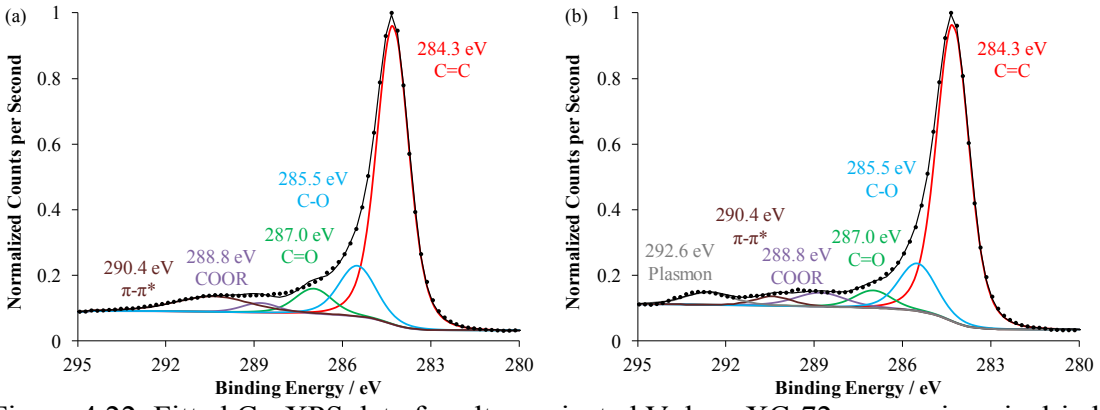

Figure 4.22 Fitted C_{1s} XPS data for ultrasonicated Vulcan XC-72 suspension air-dried on a glassy carbon plate (a), and electrochemically reduced ultrasonicated Vulcan XC-72 suspension on a glassy carbon plate (b). The dotted black curve represents the measured XPS data and the solid black curve represents the summation of all the fitted peaks.

Table 4.6 Summary of results after fitting the C_{1s} XPS spectra for as-received, ultrasonicated, and ultrasonicated/reduced forms of Vulcan XC-72. Each entry listed in the table contains the relative percent surface concentration based on integration under the fitted peak, the full width at half maximum, and the center position of the fitted peak. Monte Carlo simulations were employed to estimate one standard deviation errors when calculating the relative percent surface concentrations of C-O, C=O and COOR groups.

	C=C	C-O	C=O	COOR	π-π* shakeup	Plasmon
Vulcan XC-72	67.7 ± 2% 1.33 eV 284.3 eV	17.3 ± 1% 1.47 eV 285.5 eV	5.6 ± 0.9% 1.50 eV 286.9 eV	4.5 ± 0.5% 1.99 eV 288.8 eV	4.9 ± 2% 3.03 eV 290.4 eV	Negligible
Ultrasonicated Vulcan XC-72	68.6 ± 2% 1.29 eV 284.3 eV	13.5 ± 1% 1.50 eV 285.5 eV	6.5 ± 0.7% 1.50 eV 287.0 eV	3.5 ± 0.5% 2.00 eV 288.8	7.9 ± 2% 3.00 eV 290.4 eV	Negligible
Ultrasonicated and Reduced Vulcan XC-72	70.6 ± 3% 1.31 eV 284.3 eV	13.0 ± 1% 1.50 eV 285.5 eV	4.7 ± 0.9% 1.50 eV 287.0 eV	3.8 ± 1% 2.00 eV 288.8 eV	4.7 ± 2% 3.00 eV 290.4 eV	3.2 ± 1% 1.637 292.6 eV

Electrochemical reduction of the ultrasonicated Vulcan XC-72 did not significantly change the COOR and C-O surface groups (Table 4.6). The electrochemical reduction process preferentially removed the C=O surface groups, resulting in a decrease from 6.5% to 4.7% (Table 4.6), agreeing with the significant decrease in C=O signal from the infrared spectroscopic results of Guo *et al.*[160] The removal of C=O resulted in an additional increase in BHb electrochemical activity (Figures 4.18 and 4.20), consistent with the relationship between C=O and BHb activity shown in Sections 4.8.1-4.8.4 and 4.6.4.

The two-step carbon modification confirms that surface ethers, decreased by the use of ultrasonication, and carbonyls, decreased by the use of electrochemical reduction, inhibit BHb electrochemical activity on carbon materials. These carbon modifications provide a relatively simple method for converting an electrochemically-inactive-BHb carbon material into a much more active material.

4.9 Effectiveness of Detecting Different BHb Concentrations

Due to the successful improvement in BHb detection using the ultrasonicated/reduced Vulcan XC-72, various BHb concentrations, ranging from 0.001 to 0.2 g L^{-1}, were examined. CVs and DPVs without BHb were used for background subtraction to account for small variations in the background currents, likely due to slight differences in the formation of the Vulcan XC-72 films on the glassy carbon electrode. The BHb concentration range used in this research is similar to the concentrations used by Toh *et al*.[12] No BHb activity was observed when 0.001 g L^{-1} BHb was used (Figure 4.23), whereas this was the lowest concentration where BHb activity was observed by Toh *et al*.[12] A response was evident when at least 0.005 g L^{-1} BHb was used; however, there was no significant difference between the response of the ultrasonicated Vulcan XC-72 and ultrasonicated/reduced Vulcan XC-72, due to the small current (Figure 4.23a).

For all BHb concentrations above 0.005 g L^{-1}, the ultrasonicated/reduced Vulcan XC-72 showed an increased response over the ultrasonicated Vulcan XC-72 in the CVs (Figure 4.23a), whereas the increased response was seen at 0.1 g L^{-1} BHb and above in the DPVs (Figure 4.23b). For high concentrations of BHb (*i.e.* 0.1 g L^{-1} BHb and above), the BHb reduction current was likely limited by the number of available reactive carbon surface sites. Increased BHb reduction current was expected on the ultrasonicated/reduced Vulcan XC-72 since more reactive carbon surface sites would be available to react with BHb after removing the inhibiting carbonyl surface groups and the expected increase in current was observed. At lower BHb concentrations (*i.e.* 0.01 to 0.05 g L^{-1} BHb), the BHb reduction current is limited by the diffusion of BHb to the carbon surface, resulting in similar BHb peak currents on both the ultrasonicated and

ultrasonicated/reduced carbons. The similar BHb peak currents were observed in the DPVs (Figure 4.23b), but clear differences were seen in the CVs (Figure 4.23a). The difference between CVs and DPVs likely arises from the experimental procedure because DPVs preferentially remove fast processes when periodically recording currents, whereas CVs continuously record the currents. A larger BHb peak reduction current was observed on the ultrasonicated/reduced Vulcan XC-72 than on the ultrasonicated Vulcan XC-72 in the CVs, implying that a fast reaction occurred, such as the reduction of adsorbed BHb. The differential pulse technique preferentially remove faster processes (*i.e.* the reaction of adsorbed BHb) than slower processes (*i.e.* diffusion of BHb), likely resulting in the observed similar BHb peak reduction currents on both modified carbons for the BHb concentrations of 0.01 to 0.05 g L^{-1} in the DPVs.

In the above analysis, in order to explain the higher CV current for the reduced versus ultrasonicated/reduced carbon, it must be assumed that more BHb is adsorbed on the ultrasonicated/reduced Vulcan XC-72. This assumption is consistent with literature showing that additional Hb adsorbs onto hydrophobic surfaces relative to hydrophilic surfaces.[197] The ultrasonicated/reduced carbon likely has a more hydrophobic surface than the ultrasonicated carbon due to the selective reduction of surface carbonyl groups. As a result, greater amounts of BHb preferentially adsorbed onto the more hydrophobic ultrasonicated/reduced Vulcan XC-72 carbon surface, resulting in greater BHb electroactivity and agreeing with the CVs (Figure 4.23a).

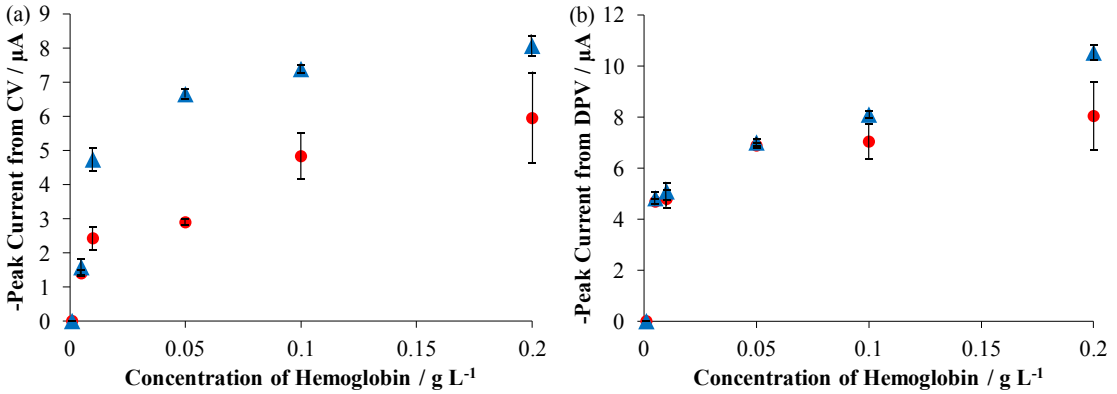

Figure 4.23 Plots of background-subtracted peak currents from CVs (a) and DPVs (b) of ultrasonicated Vulcan XC-72 on glassy carbon (red dots) and ultrasonicated/reduced Vulcan XC-72 on glassy carbon (blue triangles) in 0.1 M PB (pH 7.08) containing a concentration range of BHb: 0.001, 0.005, 0.01, 0.05, 0.1, and 0.2 g L^{-1}. An average of three replicate trials with one standard deviation for each concentration is shown in this plot.

While comparing the DPVs in different BHb concentrations, the peak BHb reduction potential was observed to shift 50 mV negative, from -0.575 V (0.1 g L^{-1} BHb) to -0.625 V (0.005 g L^{-1} BHb) as shown in Figure 4.24, but no peak shift was seen in the CVs due to broad reduction peaks (not shown). The tetrameric form of Hb exists in equilibrium with its dissociated dimeric form,[198,199] and significant dissociation occurs at concentrations less than a few µM of Hb,[11,198,200] (*i.e.* below 0.2 g L^{-1} BHb). The negative potential shift due to the dimers is consistent with published results showing that smaller heme-containing proteins, such as myoglobin, had more negatively shifted heme redox peaks than Hb on carbon.[201]

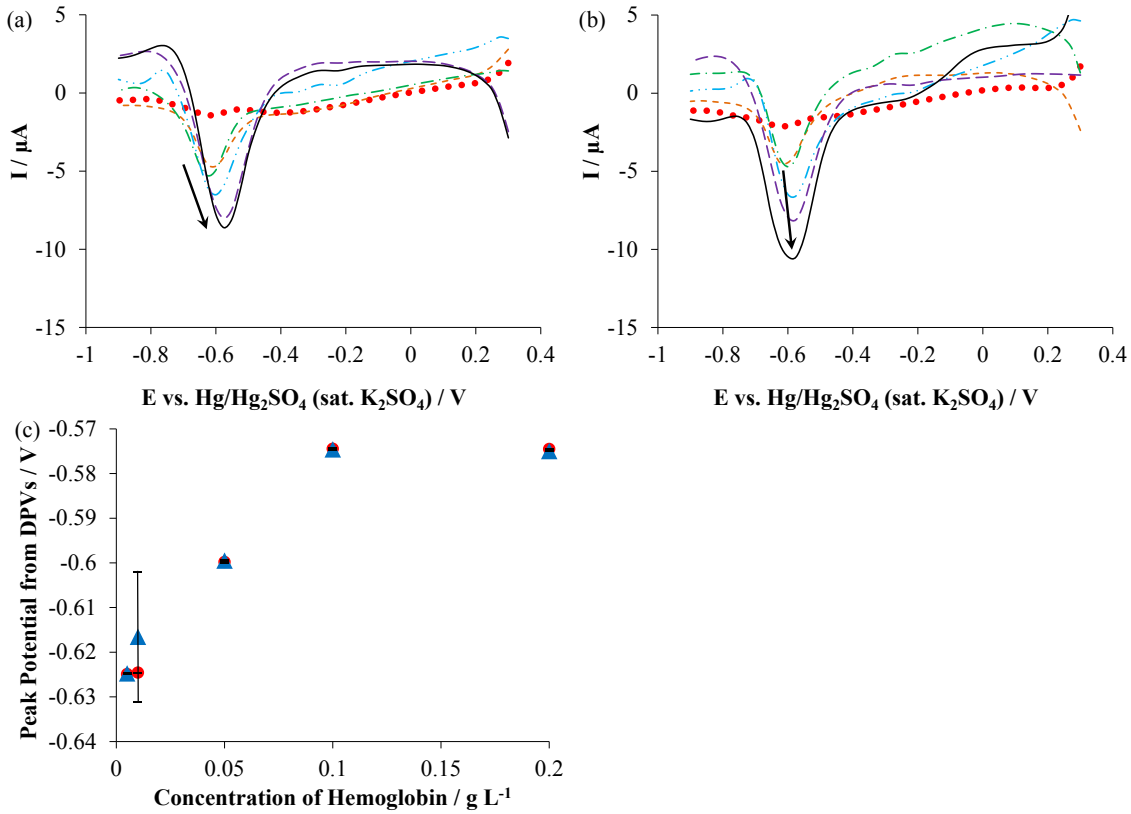

Figure 4.24 Background subtracted DPVs of the ultrasonicated (a) and ultrasonicated/reduced (b) Vulcan XC-72 in 0.1 M PB (pH 7.08) with the following concentrations of BHb: 0.001 (dotted red), 0.005 (dashed orange), 0.01 (dot-dashed green), 0.05 (dot-dot-dashed blue), 0.1 (dashed purple), and 0.2 g L^{-1} (solid black). Plots of peak BHb reduction potentials from DPVs (c) of ultrasonicated Vulcan XC-72 (red dots) and ultrasonicated/reduced Vulcan XC-72 on glassy carbon (blue triangles); a peak was lacking for electrolyte containing 0.001 g L^{-1} BHb; thus not shown. An average of three replicate trials with one standard deviation for each concentration is shown (c).

BHb responded differently to the ultrasonicated and ultrasonicated/reduced Vulcan XC-72 carbon materials. Either of these two modified carbons can be used to detect BHb concentrations as low as 0.005 g L^{-1}. The BHb responses were higher on the ultrasonicated/reduced Vulcan XC-72 than on the ultrasonicated Vulcan XC-72 for BHb concentrations greater than 0.005 g L^{-1} in the CVs and above 0.05 g L^{-1} in the DPVs where additional BHb adsorbed on the more hydrophobic surface may have reacted faster than BHb diffusing to the carbon surface. These experiments confirmed that C-O and

C=O surface groups inhibited BHb reduction, since their removal resulted in converting an inactive carbon into a more active carbon electrode material.

4.10 Conclusions

As shown in this chapter, the C-O ether, C=O carbonyl, and quinone surface functional groups are responsible for inhibiting the electrochemical reduction of BHb in a neutral pH PB electrolyte on carbon electrodes. A Spectracarb 2225 carbon fabric and four different carbon powder electrode materials: glassy carbon, graphite, Vulcan XC-72 and Black Pearls 2000 were examined in this chapter. TPD, XPS and ATR-FTIR were used to identify the carbon-oxygen surface functionalities and cyclic voltammetry and differential pulse voltammetry monitored the electrochemical activity of BHb. XPS showed that the overall degree of surface oxidation has no relationship with BHb electroactivity. Additionally, the presence of small amounts of COOR and phenol surface groups does not affect the electrochemistry of BHb, and selective removal of these groups by heat treatment resulted in no change in the electrochemical reduction of BHb. The data from TPD, ATR-FTIR, and XPS were consistent in suggesting that the increased presence of C=O or C-O surface functional groups inhibit the electrochemical activity of BHb. Ultrasonication of the Vulcan XC-72 removed C-O ether surface functionalities and resulted in a significant increase in the carbon's electrochemical activity with BHb. Further processing of the ultrasonicated Vulcan XC-72 by performing an electrochemical reduction treatment selectively removed C=O surface groups and further improved its electrochemical activity with BHb. Therefore, to enhance the electrochemical activity of BHb for biosensor applications, the C-O ether and C=O

surface functionalities should be removed on carbon electrode surfaces, but the exact mechanism for the inhibition is not yet known.

The C=O and C-O on the carbon surface may be hydrogen-bonding with the polar amino acid residues in BHb, possibly changing the protein conformation and partially closing the heme pocket, thus making the reduction more difficult. Alternately, the C=O or C-O surface groups may be causing the BHb to adsorb on the carbon surface in a different orientation such that the hydrophobic region, containing the electrochemically active heme group, is further from the electrode surface, as illustrated in Figure 4.25, thus inhibiting the ability for electron transfer. Future work is proposed (Chapter 7) to address the mechanism by which carbon surface groups affect BHb electroactivity.

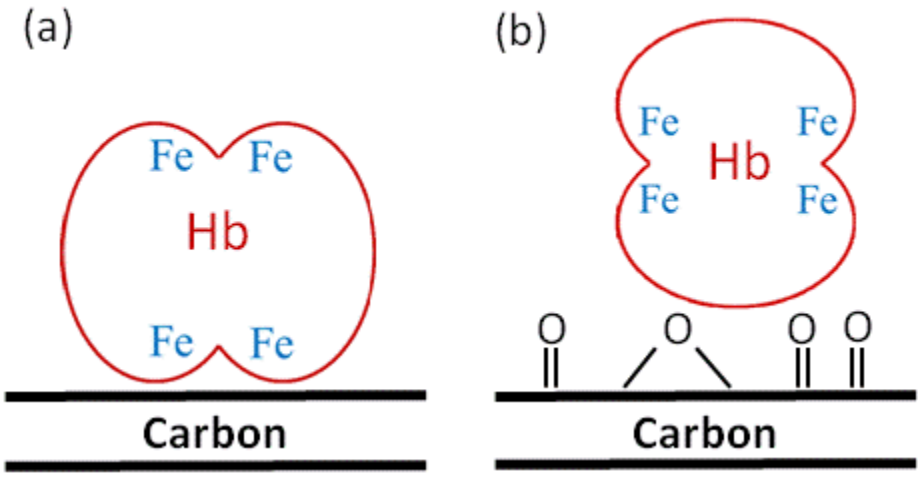

Figure 4.25 An illustration of a carbon surface without carbon surface oxides (a) and with carbon-oxygen surface groups interacting with Hb.

The ultrasonicated/reduced Vulcan XC-72 was evaluated for the detection of BHb from a concentration range of 0.001 g L^{-1} to 0.2 g L^{-1}, with 0.005 g L^{-1} of BHb found to be the lowest detectable concentration. The ultrasonicated/reduced Vulcan XC-72 improved the peak BHb reduction current over the ultrasonicated Vulcan XC-72 for BHb

concentrations above 0.005 g L^{-1} in the CVs and above 0.05 g L^{-1} in the DPVs. The voltammograms showed that the BHb peak reduction potential shifted negatively with decreasing BHb concentrations, which was likely due to the dissociation of BHb.

Chapter 5 Enhanced Electrochemical Detection of Bovine Hemoglobin using a Glassy Carbon Electrode by Adding an Alcohol

The work presented in this chapter was submitted as "*Enhanced Hemoglobin Electroactivity on Glassy Carbon due to a Water-miscible Primary Alcohol in an Electrolyte or as a Binder Solvent*", Justin Tom, Philip J. Jakubec, and Heather A. Andreas, to Sensors and Actuators B in 2017. JT was responsible for the majority of the data collection, analysis, and manuscript preparation. CV data were not presented in the paper but are presented in this chapter. PJJ contributed additional data on the detection limit and sensitivity of hemoglobin in methanol-containing electrolyte and wrote its associated section in the manuscript; this section is not necessary to understand the work presented in this thesis and is not shown.

5.1 Introduction

The electrochemical activity of hemoglobin (Hb) is believed to be related to the redox reaction of the iron within the heme prosthetic group.[11–14] However, the four heme groups in Hb are located in relatively deep hydrophobic regions of the protein and the direct electron transport between these hemes and an electrode surface is difficult.[15,16,22] Thus, while Hb can be detected in solution, as shown in Chapter 4, it is more common to use an electrochemical mediator[11,48,202] or to immobilize Hb directly on the electrode surface to observe electrochemical activity.[11,13,23,53,66,70,72,203]

An important factor that separates research showing carbons which exhibit Hb electrochemical activity from those that do not is whether a binder is used to hold the materials on the electrode. Often, the binder is Nafion,[14,22,23,25,26] which is commonly prepared from its liquid form, usually mixed with a water-miscible primary alcohol such as methanol,[14,22,25] or ethanol,[23,162] and then cast and dried to form a thin film. The effect of an alcoholic solvent used in preparation of Nafion thin films to immobilize Hb is often

overlooked. Alcohol has been shown to cause Hb denaturation,[204] aggregation,[205] and conformational changes.[205] Whether these changes caused by an alcohol solvent in Nafion also change the electrochemistry of Hb is unclear. Non-alcoholic solvent effects on Hb have been seen with dimethyl sulfoxide, which improved the electrochemical activity of Hb,[81] while glycerol decreased its electrochemical activity.[83] However, the impact of a water-miscible primary alcohol on Hb electrochemical activity on unmodified carbon has not been studied. Knowledge of the potential impact of the alcohol used in Nafion film formation is vital in order to understand whether Nafion itself impacts the electrochemical activity of Hb on carbon electrodes, and, specifically, whether a water-miscible primary alcohol such as methanol, ethanol, or 1-propanol may impact experiments where electrochemical activity of Hb is observed. This chapter examines and discusses the impact of these alcohols on the electrochemical activity between a glassy carbon electrode and BHb.

5.2 Differences in BHb Electrochemistry by Nafion Preparation

Immobilization of Hb is a commonly used technique to study its electrochemical activity.[11,13,23,53,66,70,72,203] The purpose of the electrochemical experiments presented in this section is to determine whether the electrochemical activity of BHb is different upon immobilization with and without alcohol exposure from a Nafion film. Two differently prepared Nafion layers were used to immobilize BHb on a glassy carbon electrode. One Nafion layer was a solid Nafion film without any solvent (Nf_{solid}) and the other was created by using a drop cast method from a liquid Nafion suspension ($Nf_{suspension}$). BHb was immobilized by using 10 μL of 1 g L^{-1} BHb and either 10 μL of the liquid Nafion

suspension to form a thin film or a solid piece of Nafion to hold BHb in place on the electrode surface (Section 3.1.4).

The CVs and DPVs of BHb immobilized on the glassy carbon electrode surface by using Nafion are shown in Figure 5.1. The CV and DPV results for BHb on glassy carbon without Nafion were also plotted for comparison purposes. The electrochemical activity of BHb increased when either Nf_{solid} or $Nf_{suspension}$ was used to immobilize BHb on glassy carbon; this was expected, since BHb not bound by a layer of Nafion (GC/BHb) was visibly dissolving in the electrolyte. From the CVs (Figure 5.1a) and DPVs (Figure 5.1b), it is clear that the magnitude of the BHb-reduction currents are very different for BHb bound to the glassy carbon by the use of a Nafion suspension ($GC/BHb/Nf_{suspension}$) and BHb bound by using solid Nafion ($GC/BHb/Nf_{solid}$). Indeed, the BHb-reduction current from $GC/BHb/Nf_{suspension}$ was almost an order of magnitude larger than that of $GC/BHb/Nf_{solid}$, which may be evidence for the 1-propanol solvent present in the liquid Nafion suspension[161] improving the electrochemical activity of BHb. Other different mechanisms are also possible, such as the $Nf_{suspension}$ creating a more intimate contact between the BHb layer and glassy carbon, facilitating the electron transfer. However, these results, coupled with the knowledge that alcohols may cause Hb to denature,[204] aggregate,[205] or change its conformation,[205] which may then impact the electrochemical activity of BHb, were intriguing enough to warrant further studies as shown later in this thesis.

The peak potentials for BHb-reduction in the DPVs (Figure 5.1b) for $GC/BHb/Nf_{solid}$ and $GC/BHb/Nf_{suspension}$ were clearly different. From Figure 5.1b, the negative peak potential shift from -0.55 V for $GC/BHb/Nf_{solid}$ to -0.625 V for

GC/BHb/$Nf_{suspension}$ could be due to BHb interacting with the 1-propanol solvent from the liquid Nafion suspension. As a result of the interaction, BHb may be forming a thicker film[81] on the glassy carbon electrode or BHb is denaturing by unfolding its protein structure.[80] These possibilities will be explored further in Chapter 6. A less intimate contact between BHb and the glassy carbon may be expected when using a solid piece of Nafion compared to Nafion created from a liquid suspension. The less intimate contact may result in a more difficult electron transfer, thus a more negative reduction potential was expected when solid Nafion was used versus the Nafion suspension. However, the data in Figure 5.1 are opposite to this expectation, suggesting that the Nafion suspension is likely modifying the BHb, either through denaturation or unfolding. The electrochemical impact of the alcohol solvent on BHb-reduction will be presented later in Section 5.4.

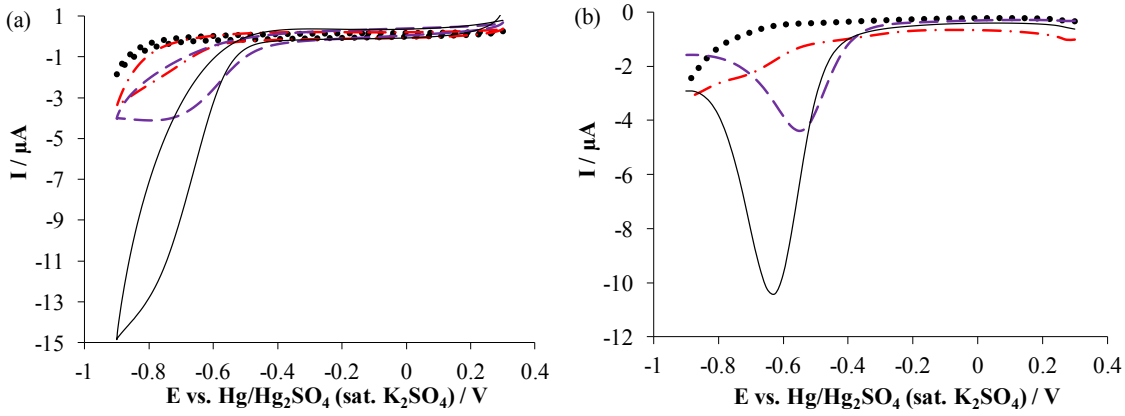

Figure 5.1 Representative CVs (a) and DPVs (b) of glassy carbon (dotted black curve), GC/BHb (dot-dashed red curve), GC/BHb/Nf_{solid} (dashed purple curve), and GC/BHb/$Nf_{suspension}$ (solid black curve) in 0.1 M PB pH 7.08.

5.3 Nafion on Glassy Carbon as a Barrier to BHb

A lack of BHb movement through the Nafion layer ensures that the Nafion film acts as a barrier to BHb. Therefore, Nafion holds BHb in place if BHb is immobilized on the electrode surface. The purpose of the electrochemical experiments in this section is to determine whether BHb passes through the Nafion layer. If BHb from the electrolyte cannot reach the glassy carbon electrode through the Nafion layer, then no electrochemical reduction is expected from BHb. These experiments distinguish whether the decreased electrochemical activity of GC/BHb/Nf_{solid} compared to GC/BHb/$Nf_{suspension}$ seen previously (Figure 5.1) is due to the loss of BHb immobilized by using a solid piece of Nafion on the electrode surface.

In this section, a glassy carbon electrode was modified with a layer of Nafion and then tested in a BHb-containing PB electrolyte. Two types of Nafion were used: a liquid suspension ($Nf_{suspension}$) and a solid film (Nf_{solid}). $Nf_{suspension}$ was formed by drop casting a Nafion suspension directly on the glassy carbon electrode followed by air-drying. Nf_{solid} was held in place on the electrode surface using a modified Swagelok setup described previously in Section 3.1.4. The interaction between the glassy carbon and solution-based BHb was then examined electrochemically.

Nafion films were hypothesized to block BHb access to the electrode surface and prevent BHb electrochemistry. This hypothesis was confirmed in the CV (Figure 5.2a and c) and DPV (Figure 5.2b and d) results obtained using either Nf_{solid} (Figure 5.2a and b) or $Nf_{suspension}$ (Figure 5.2c and d) where no change in the voltammograms were observed with or without BHb in the electrolyte. According to the results from Chapter 4 and published literature sources, a Hb-reduction peak was expected between the potential

ranges of -0.575 to -0.7 V on a carbon electrode,[12,26,206] which was clearly absent in Figure 5.2a-d.

The voltammograms of $Nf_{suspension}$ (Figure 5.2c and d) on glassy carbon show a higher background than for Nf_{solid} (Figure 5.2a and b), despite using the same glassy carbon electrode between replicate trials. The increased background may be a result of exposing the glassy carbon electrode surface to the 1-propanol solvent present in $Nf_{suspension}$,[161] resulting in changes to the carbon-oxygen surface groups on the glassy carbon surface, which will be discussed in greater detail in Section 6.2. These results are the first evidence that the 1-propanol may also change the carbon electrode during exposure to the liquid Nafion suspension.

The CVs of Nf_{solid} on glassy carbon (Figure 5.2a) show greater diagonal tilting than the CVs of $Nf_{suspension}$ on glassy carbon (Figure 5.2c), likely due to increased electrical resistance. The increase in electric resistance in Figure 5.2a could be due to Nf_{solid} being a thicker Nafion film than $Nf_{suspension}$ on the glassy carbon electrode. An increase in resistance results in a greater drop in the applied potential through the film, resulting in a lower effective potential on the electrode surface. Thus, the peak BHb-reduction potential for Nf_{solid}-immobilized BHb would be expected to appear at a more negative potential. Contrary to the expectation, a positive peak potential shift was seen in Figure 5.1b, suggesting that another variable such as the presence of the 1-propanol solvent in $Nf_{suspension}$ may be a more influential factor on the peak position.

The increased cathodic background current seen at potentials more negative than -0.75 V is most likely due to the electrochemical reduction of oxygen.[12] Similar results published by Toh *et al.* on the electrochemical reduction of oxygen were also observed

on glassy carbon after purging their PB electrolyte of oxygen using nitrogen.[12] The greater oxygen reduction currents from the $Nf_{suspension}$-modified glassy carbon electrode are possible since oxygen may be trapped between the glassy carbon surface and Nafion layer during the Nafion film formation.

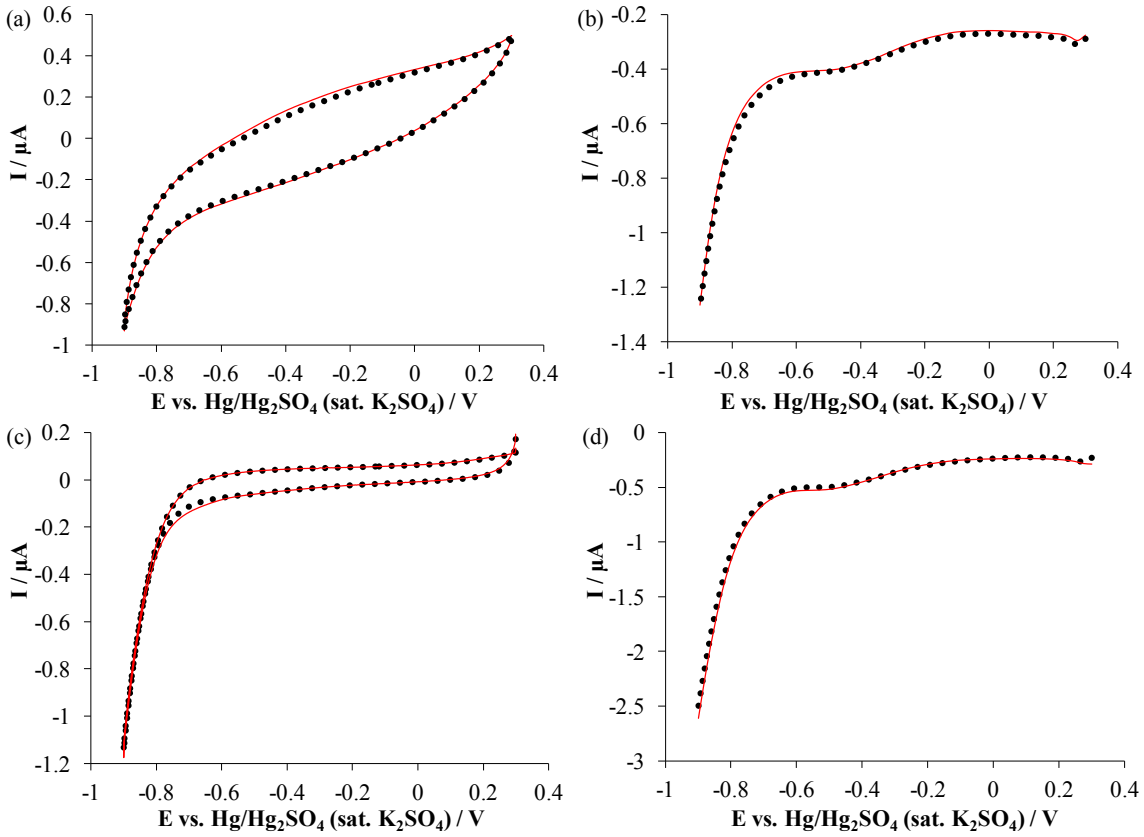

Figure 5.2 CVs (a and c) and DPVs (b and d) of a glassy carbon modified with either a layer of solid Nafion (a and b) or an air-dried Nafion suspension thin film (c and d) in 0.1 M PB without BHb (dotted black curves) and with 0.2 g L^{-1} BHb (solid red curves).

The CV and DPV results in this section imply that BHb from the electrolyte cannot pass through a Nafion layer to be electrochemically reduced on the glassy carbon electrode. The results suggest that Nafion will hold the immobilized BHb on glassy carbon for electrochemical studies since Nafion is acting as a barrier to BHb. Since BHb cannot penetrate the Nafion layer, then no loss of BHb would be expected if BHb was

immobilized using Nafion on the glassy carbon electrode. Thus, the lower BHb-reduction current observed when using Nf_{solid} compared to $Nf_{suspension}$ cannot be due to loss of BHb through the Nafion layer (Figure 5.1). A negative peak potential shift for Nf_{solid}-immobilized BHb was expected due to increased electrical resistance indicated by the slanted shape in its CV (Figure 5.2a), but a positive shift was observed. The negative peak shift for $Nf_{suspension}$-immobilized BHb suggests that the liquid Nafion suspension was affecting the electrochemical reduction of BHb where a thicker film incorporating BHb may be forming[81] or BHb may be unfolding,[80] possibly from exposure to the 1-propanol solvent present in $Nf_{suspension}$. The results of this section emphasize the potential importance of the 1-propanol solvent in $Nf_{suspension}$ affecting the electrochemical reduction of BHb.

5.4 Impact of Methanol, Ethanol, and 1-Propanol on the Electrochemical Reduction of Bovine Hemoglobin

The 1-propanol solvent present in $Nf_{suspension}$ but not in Nf_{solid} may be related to the increased BHb-reduction current and negative BHb peak potential shift seen previously in Section 5.2. As mentioned in previous sections, Nafion can be suspended as a liquid using a water-miscible primary alcoholic solvent such as methanol (MeOH),[14,22,25] ethanol (EtOH),[23,162] or 1-propanol (1-PrOH).[161] Therefore, this section explores the possibility that the addition of an alcohol to a PB electrolyte containing BHb may be increasing the electrochemical activity of BHb.

Changes to the reduction potential may indicate changes in the protein folding of a heme-containing protein, or exposing the redox-active heme group to a solvent, as

suggested from the results of theoretical calculations.[207] Therefore, following the BHb-reduction peak may be useful because a negative peak potential shift could suggest a formation of a film containing BHb on the electrode surface,[81] possibly indicating changes in the protein conformation on the electrode surface or that the protein is unfolding.[80] In Section 5.2, the BHb-reduction peak was more clearly defined in the DPVs than in the CVs. Therefore, differential pulse voltammetry was employed instead of cyclic voltammetry to investigate the electrochemical behavior of BHb in aqueous-alcohol electrolyte.

Small BHb peak potential shifts were seen in the DPVs shown in Figure 5.3a-c. Initially, a positive BHb peak potential shift was observed when the BHb-containing electrolyte contained at least 20% MeOH (Figure 5.3a), 30% EtOH (Figure 5.3b), or 10% 1-PrOH (Figure 5.3c). However, alcoholic content higher than 20% MeOH, 40% EtOH, or 30% 1-PrOH shifted the BHb peak negative. Changing the solvent polarity may denature a heme-containing protein and possibly expose the redox-active heme group to the solvent, which may be partly responsible for shifting the reduction peak potential.[207] Changes to the peak potential of the heme group have also been suggested to be dependent on the folded state of the protein[207] as this may also change the structure surrounding the heme cavity. Possible changes in the interactions between the heme-bound iron and the protein may change how the heme-bound iron is able to accept an electron. The use of UV/Vis and fluorescence techniques may provide some evidence for change in the heme group or exposure of the protein to the solvent, which will be presented and discussed in Section 6.4. Other mechanisms are also possible, some of which will be discussed in Chapter 6.

At any concentration of alcohol tested in this section in the BHb-containing electrolyte, the electrolyte appeared slightly cloudy, indicating some agglomeration/precipitation. Alcohol is well-known to denature BHb,[208–210] which is likely responsible for some loss in BHb solubility. When the electrolyte contained both alcohol and BHb, some precipitate may have also formed on the electrode surface. Increasing the alcohol content in the electrolyte may have precipitated more BHb onto the glassy carbon such that a thicker BHb film may have formed, suggesting changes in BHb conformation on the glassy carbon. The negative BHb-reduction peak shift observed in the DPVs of electrolytes with higher alcohol content (> 20% MeOH, > 40% EtOH, > 30% 1-PrOH, Figure 5.3a-c) may also be evidence for incorporating more BHb in a particular conformation into a film on the electrode surface.[81] Evidence for a BHb film existing on the glassy carbon electrode surface will be presented and discussed later in Chapter 6.

Increasing the MeOH concentration increased the BHb-reduction current (Figure 5.3a). The BHb-reduction current exhibited a small increase with increasing MeOH content up to 30% MeOH. Large increases in BHb-reduction current were observed at higher MeOH content in the electrolyte. Several different mechanisms may be responsible for the increases in BHb-reduction, such as a thicker film formation containing BHb in a particular conformation, increased protein denaturation, or changes in the heme environment. The possible mechanisms responsible for increasing the BHb-reduction will be discussed later in Chapter 6.

Changes in BHb-reduction current were observed in aqueous-alcohol electrolytes containing BHb with EtOH (Figure 5.3b) or 1-PrOH (Figure 5.3c). Adding either EtOH

or 1-PrOH to BHb-containing electrolyte initially resulted in a larger increase in BHb-reduction than that seen for MeOH (Figure 5.3a-c), which may be partly due to EtOH and 1-PrOH being less polar than MeOH. However, BHb-reduction starts to plateau when EtOH reaches 50%. For 1-PrOH, the BHb-reduction is maximal at 50% but falls at higher concentrations. Again, possible mechanisms responsible for the changes in BHb-reduction at these higher alcohol concentrations will be discussed later in Chapter 6.

As the alcohol content in the BHb-containing electrolyte increased, the cathodic peak shape changed (Figure 5.3a-c) meaning that the peak current may not give an accurate representation of the amount of reduced BHb. To obtain a more accurate measure of the amount of BHb reaction, the amount of BHb-reduction charge was used instead of the peak current. The BHb reduction charge was calculated by removing the current contributions from a background DPV of PB without BHb or alcohol, integrating the area under the BHb-reduction peak, and dividing by the scan rate of 0.020 V s^{-1}. The calculated results summarized in Figure 5.3d reveal that the maximal amount of charge transferred between the glassy carbon electrode and BHb occurred when 60% MeOH was present in the BHb-containing electrolyte. A trend is clearly visible where more alcohol in the electrolyte generally led to more charge transfer between the electrode surface and BHb with two exceptions. The exceptions were observed in the DPVs of BHb-containing electrolyte with 60% EtOH or 60% 1-PrOH, where the amount of BHb-reduction either did not change significantly or it decreased (Figures 5.3d), suggesting that more than one mechanism may be at play between BHb, the glassy carbon, and the alcohol (Chapter 6). The data indicate that exposing BHb to MeOH, EtOH, or 1-PrOH in the electrolyte generally increase the electrochemical reduction of BHb. The electrochemical data

suggest that the alcohol in the Nafion suspension may enhance the electrochemical reduction of BHb.

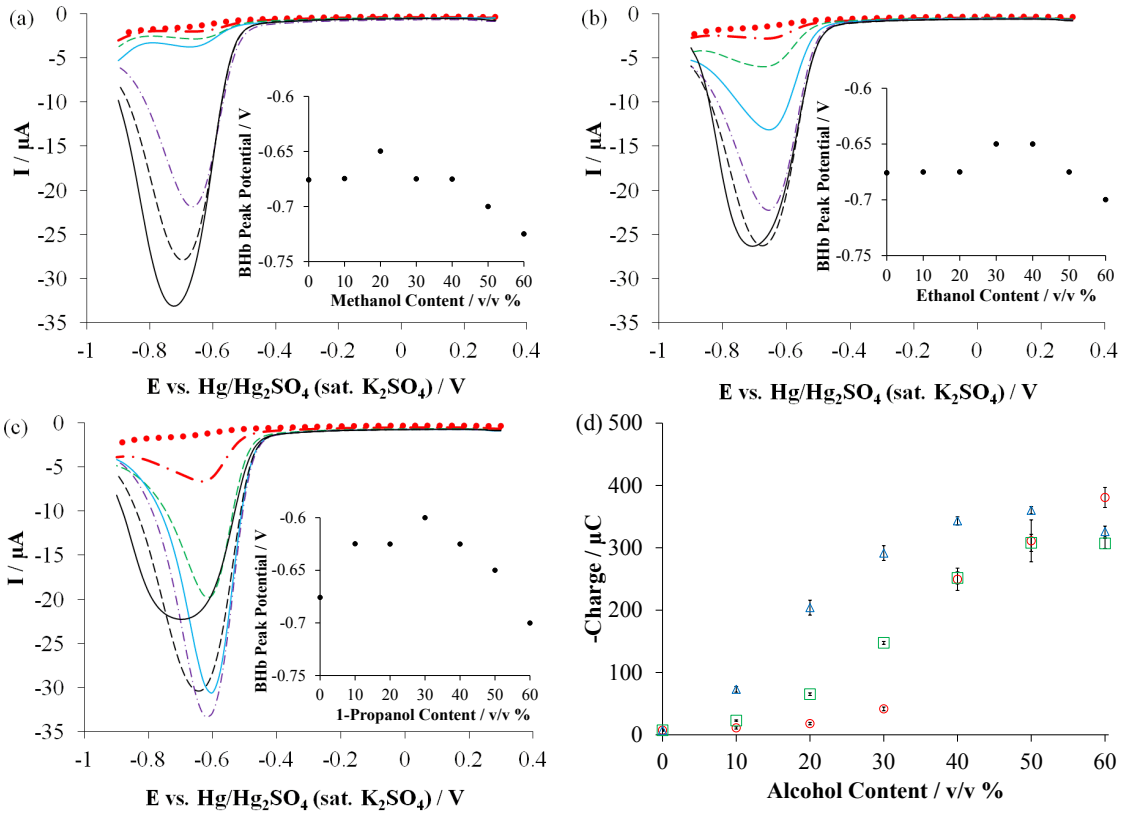

Figure 5.3 Representative DPVs of 0.2 g L^{-1} BHb in 0.1 M PB with MeOH (a), EtOH (b), or 1-PrOH (c) at a concentration of 0% (dotted red curve), 10% (dot-dashed red curve), 20% (dashed green curve), 30% (blue solid curve), 40% (purple dot-dashed curve), 50% (dashed black curve), or 60% (solid black curve). Insets (a-c) show the BHb peak potential for each corresponding alcohol. (d) Background-subtracted charge for MeOH (red circles), EtOH (green squares), or 1-PrOH (blue triangles). The error bars indicate one standard deviation from three replicate trials.

To investigate whether the alcohol itself contributes to the electrochemical reduction current seen in Figure 5.3, DPVs of aqueous-alcohol electrolyte without BHb were examined. An increase in cathodic current starting at potentials more negative than *ca.* -0.75 V was observed (Figure 5.4a-c), which was more negative than the peak potential of BHb seen previously. Data from Figure 5.4d suggests that the increased cathodic current may be due to the reduction of oxygen since the current decreased under

nitrogen atmosphere and increased under oxygen atmosphere. Published DPV data by Toh *et al.* showed that the oxygen reduction occurred at potentials more negative than the reduction of Hb despite having their PB electrolyte purged of oxygen using nitrogen.[12] While their electrochemical data were collected in mildly acidic electrolyte,[12] and a neutral pH electrolyte was used in this thesis research, the difference in electrolyte pH was not expected to significantly alter the reduction potential of oxygen[211] or Hb[26] when using a bare glassy carbon electrode. As the amount of MeOH or EtOH increased from 0 to 60%, a larger cathodic current was observed, implying the reduction of more oxygen. Oxygen reduction is reasonable, considering that a mixture of water and a water-miscible primary alcohol are known to have a higher oxygen solubility with increasing alcohol content.[212–214] Whether the reduction of more dissolved oxygen overlaps with the reduction of BHb will be considered later in this section.

Similar to MeOH and EtOH, 1-PrOH exhibited an increase in reduction, but unlike MeOH and EtOH, 1-PrOH exhibited a maximum at 30% followed by a current decrease at higher concentrations (Figure 5.4c). The specific reason for the maxima and current decrease may be due to the adsorption of impurities present in 1-PrOH. Another similar alcohol, 2-propanol, is known to affect the electrochemistry of a polished glassy carbon electrode after exposure, likely due to the adsorption of oxygen-containing impurities from 2-propanol.[215] When greater than 30% 1-PrOH was present in the electrolyte, more carbon-oxygen impurities from 1-PrOH may also be adsorbing onto the glassy carbon electrode such that the electrochemical reduction of oxygen may be increasingly unfavorable. XPS evidence for increasing carbon-oxygen surface groups on glassy carbon upon 1-PrOH exposure is presented and discussed in Section 6.2.

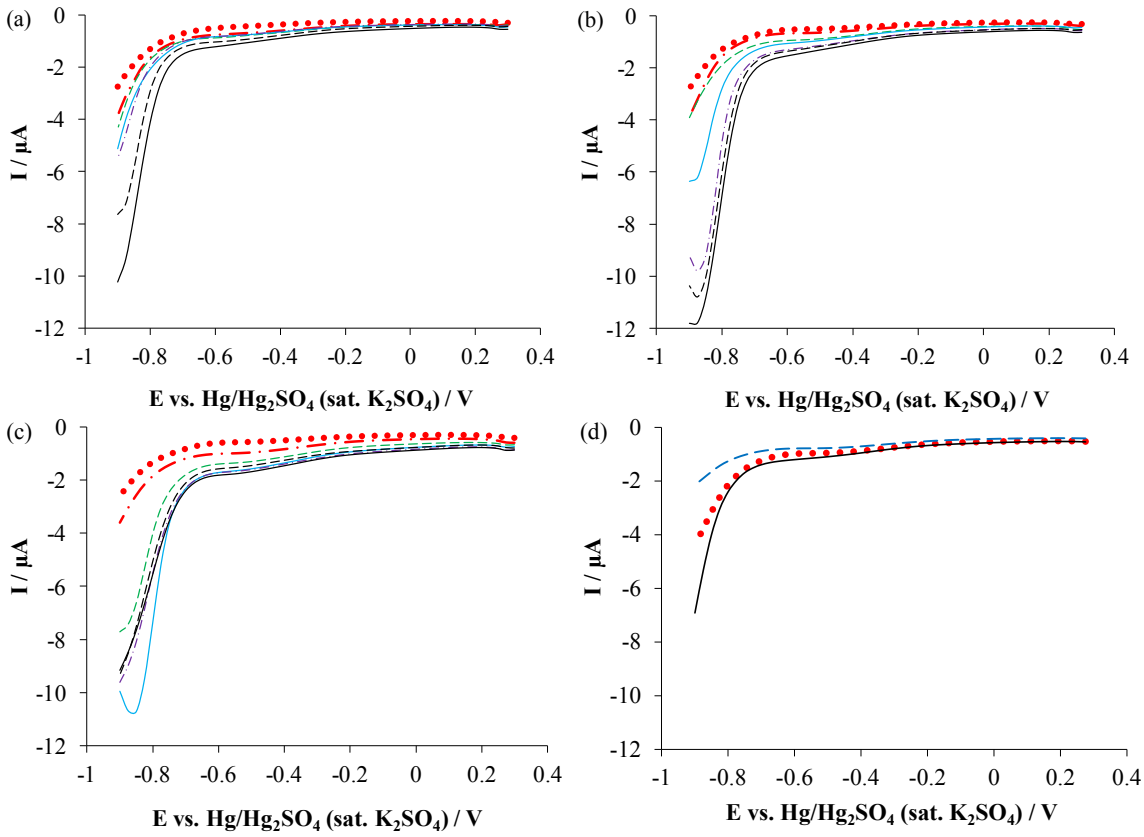

Figure 5.4 DPVs of a glassy carbon electrode in 0.1 M PB with 0% (dotted red curve), 10% (dot-dashed red curve), 20% (dashed green curve), 30% (blue solid curve), 40% (purple dot-dashed curve), 50% (dashed black curve), or 60% (solid black curve) of MeOH (a), EtOH (b), or 1-PrOH (c). DPVs of a glassy carbon electrode in 0.1 M PB left standing in air (dotted red curve), after one hour in nitrogen (dashed blue curve), or after one hour in oxygen (solid black curve) (d).

A change to the carbon surface or the carbon-oxygen surface groups may also contribute to the change in BHb-reduction as the carbon electrode is exposed to an alcohol. One literature report used XPS to show that a carbon-composite material washed with MeOH had less oxygen on its surface than the as-received carbon-composite material.[216] The reported results suggest that exposing carbon to MeOH may change the amount of carbon-oxygen surface functional groups. The removal of specific oxygen-containing carbon surface functional groups (*i.e.* carbonyls and ethers) is important in improving the electron transfer between Hb and the electrode,[206] as shown in Chapter 4.

XPS evidence for changing the carbon-oxygen surface groups on glassy carbon upon exposure to aqueous-MeOH are presented in Section 6.2. Thus, water-miscible primary alcohols may be changing the glassy carbon itself, adding another possible mechanism of reactivity and further complicating the use of an alcohol as a Nafion solvent.

To examine if exposing glassy carbon to MeOH changes the carbon-oxygen surface groups and BHb-reduction, the polished glassy carbon electrode was incubated in MeOH, rinsed, and then examined in a MeOH-free electrolyte. After MeOH incubation pretreatment, CVs and DPVs of the carbon electrode in BHb-free electrolyte showed an increase in reduction current between -0.8 and -0.9 V (Figure 5.5a and b). This increase cannot solely be due to an increase in dissolved oxygen, as per the data in Figure 5.4, since the electrolyte here did not contain any alcohol nor additional oxygen gas. The change must therefore come from a MeOH-induced modification of the carbon itself since MeOH is known to lower the surface oxygen content on carbon composite surfaces[216] and an increase in the electrochemical reduction was observed on the MeOH-modified glassy carbon, likely involving changes in the carbon-oxygen surface groups.

When the MeOH-modified glassy carbon electrode was tested in a BHb-containing electrolyte, there was an increase in BHb-reduction current versus the BHb-reduction on an unmodified glassy carbon (Figure 5.5a and b). These results suggest that the MeOH-modified glassy carbon is responsible for the increased electrochemical activity of BHb. Indeed, the measured BHb reduction current for the MeOH-modified electrode was larger than the current calculated when combining currents from the glassy carbon with the increases due to MeOH-functionalization and BHb-reaction (insets in Figure 5.6a and b), suggesting that the difference in the electrochemical reduction of BHb

may originate from the change in carbon-oxygen surface groups. XPS evidence for changes in the carbon surface oxide groups will be presented in Section 6.2.

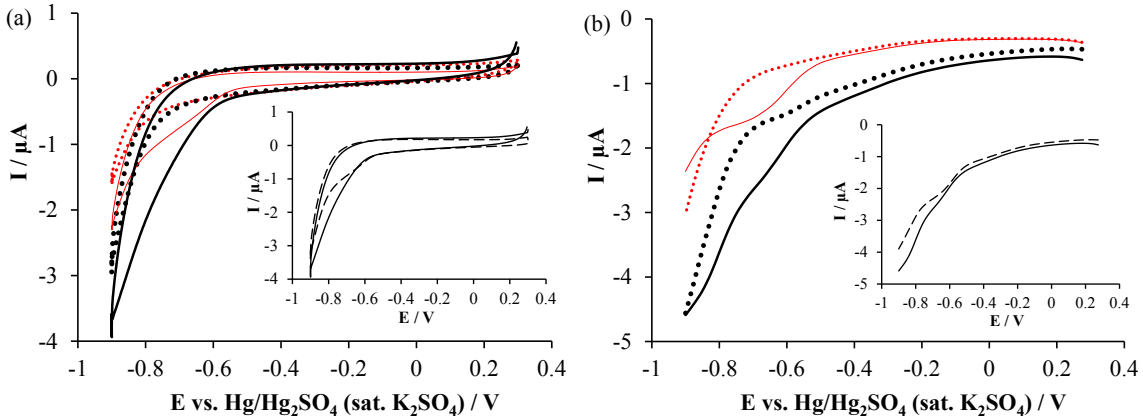

Figure 5.5 CVs (a) and DPVs (b) of a glassy carbon electrode pretreated with MeOH in 0.1 M PB (black thick-dotted curve) + 0.2 g L^{-1} BHb (black solid curve) and glassy carbon with no MeOH pretreatment in 0.1 M PB (red thin-dotted curve) + 0.2 g L^{-1} BHb (red solid curve). Insets show the linear combination of MeOH-pretreated glassy carbon + glassy carbon in 0.2 g L^{-1} BHb with the glassy carbon background removed (black dashed curve) and is compared to the MeOH-pretreated glassy carbon electrode in 0.2 g L^{-1} BHb (black solid curve).

Using DPVs of glassy carbon in aqueous-alcohol electrolyte (Figure 5.4) as a background, one can eliminate the effects of oxygen from the BHb studies (Figure 5.3). The calculated results (Figure 5.6a-c) show overcompensation for the electrochemical reduction of oxygen, indicated by positive current, when 50% EtOH, 60% EtOH, or > 20% 1-PrOH was present in the electrolyte, suggesting that there may be less dissolved oxygen in the electrolyte when BHb is present in highly alcoholic electrolytes; *i.e.* the expected increase in oxygen solubility by adding more alcohol[212–214] may no longer be true. It is unclear exactly why there may be less dissolved oxygen in the electrolyte, but it is possible that some dissolved oxygen is consumed directly as BHb denatures, or indirectly as BHb reacts with EtOH or 1-PrOH. The other possibility may be that BHb,

like an alcohol, is also changing the carbon-oxygen surface groups on the glassy carbon itself.

After excluding the oxygen effects in the DPVs by background subtraction, the resulting BHb-reduction shown in Figure 5.6a-d appear to have similar trends in peak potential and BHb-reduction with increasing alcohol content to those seen previously in Figure 5.3a-d. Therefore, the reduction current possibly due to increased dissolved oxygen in the electrolyte does not appear to influence the reduction of BHb (Figures 5.3d and 5.6d). However, the alcohols are likely changing the carbon-oxygen surface groups, which may also be changing the electrochemical reduction of BHb. Evidence for changes in the carbon-oxygen surface groups on glassy carbon after being exposed to aqueous-alcohol electrolyte will be presented and discussed later in Section 6.2.

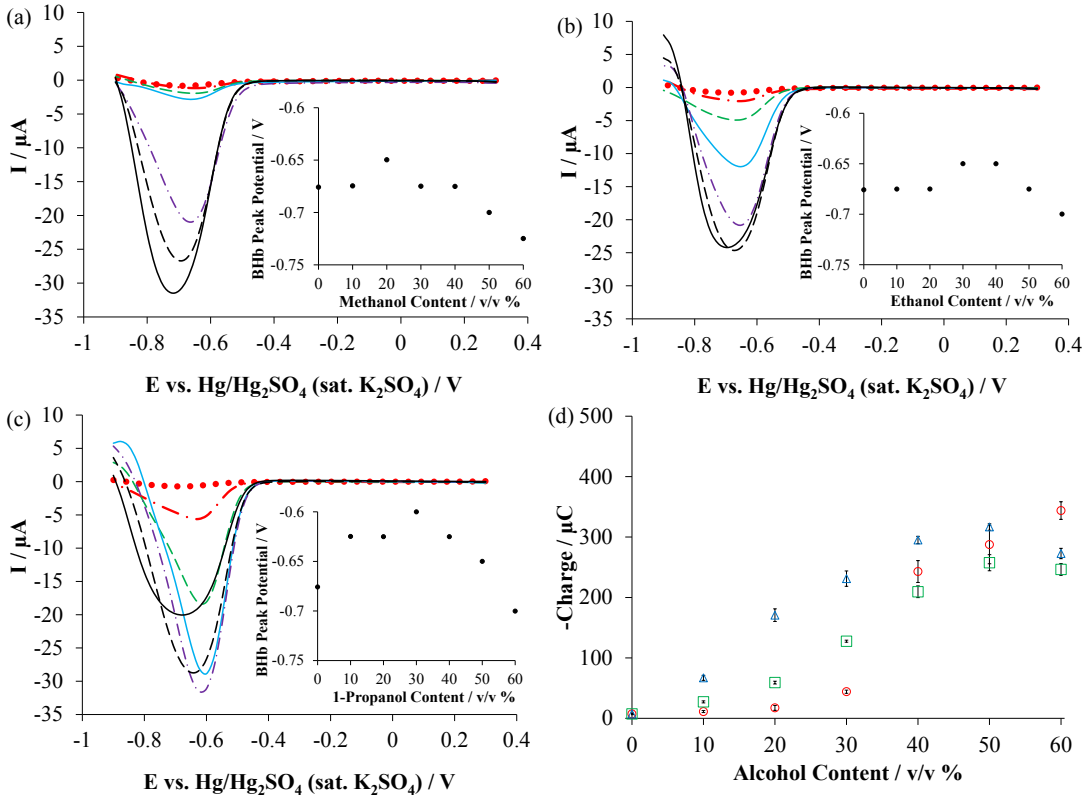

Figure 5.6 DPVs of Figure 5.3 after using Figure 5.4 for background subtraction to account for oxygen reduction. The electrolyte contained 0.2 g L^{-1} BHb in 0.1 M PB with one of: MeOH (a), EtOH (b), or 1-PrOH (c) at a concentration of 0% (dotted red curve), 10% (dot-dashed red curve), 20% (dashed green curve), 30% (blue solid curve), 40% (purple dot-dashed curve), 50% (dashed black curve), or 60% (solid black curve). Insets (a-c) show the BHb peak potential. The background-subtracted charge for MeOH (red circles), EtOH (green squares), and 1-PrOH (blue triangles) are shown with error bars indicating one standard deviation from three replicates (d).

In this section, an increase in alcohol content in BHb-containing electrolyte was observed to increase the electrochemical reduction of BHb with the exception of 50 to 60% EtOH resulting in no significant change in BHb-reduction and 50 to 60% 1-PrOH resulting in a decrease in BHb-reduction. Adding 60% MeOH in the electrolyte resulted in the largest increase in BHb-reduction. Lower amounts of 1-PrOH added to the BHb-containing electrolyte increased BHb-reduction more than adding similarly lower amounts of EtOH or MeOH. The addition of a water-miscible primary alcohol to the

electrolyte may have increased the reduction of dissolved oxygen and/or carbon-oxygen surface groups, but this reduction does not appear to overlap with the reduction of BHb. The possible change in carbon-oxygen groups upon exposing the glassy carbon to a water-miscible primary alcohol may also affect the reduction of BHb. Overall, the data presented in this section showed that the addition of a water-miscible primary alcohol to the BHb-containing electrolyte appears to increase the electrochemical reduction of BHb, suggesting that the alcohol present in a Nafion suspension also affects BHb-reduction. The data also suggest that if a binder containing an alcoholic solvent must be used, use of a low MeOH content is preferable due to the least impact on BHb-reduction, while EtOH or 1-PrOH should be avoided.

5.5 Nafion-immobilized BHb and Alcohol-exposed BHb have Additive Enhancements to the Electrochemical Reduction of BHb

Another way to provide further evidence that the alcohol solvent in the Nafion boosts the electrochemical reduction of BHb is to consider the individual contributions of each component to the electrochemical reduction of BHb. Previously it was shown (Figure 5.1b) that the GC/BHb/$Nf_{suspension}$ conditions produced a larger BHb-reduction current than GC/BHb/Nf_{solid}. This large BHb-reduction current may have arisen from: (1) the reduction of BHb immobilized on carbon, (2) an enhancement in BHb-reduction due to 1-PrOH modifying the BHb, (3) a BHb-enhancement from 1-PrOH modifying the carbon, and/or (4) extra reactivity of carbon-oxygen surface groups and/or dissolved oxygen due to 1-PrOH modifying the carbon. The relative contributions of each factor are estimated using the experiments described in Sections 5.2 and 5.4 and combined; this

combination is then compared to the measured result from GC/BHb/$Nf_{suspension}$. If the 1-PrOH solvent is modifying the BHb and carbon surface, as expected, the calculated DPV considering these four contributions should appear similar to the DPV for GC/BHb/$Nf_{suspension}$.

The reduction of the immobilized BHb (contribution 1) is represented by the use of DPV of GC/BHb/Nf_{solid} (Figure 5.1b, Section 5.2), denoted as $I_{GC/BHb(s)/Nf(s)}$ in Relation 5.1. The reduction current contribution from 1-PrOH affecting the BHb-reduction (contributions 2 and 3) and oxygen/carbon-oxygen surface group reduction (contribution 4) is accounted for using the DPV data of the glassy carbon electrode in an electrolyte containing 1-PrOH, BHb, and PB (Figure 5.3c, Section 5.4), represented by $I_{GC\ in\ BHb\ \&\ 10\%\ 1\text{-}PrOH(aq)}$. It should be noted however, that these 1-PrOH data include a component of BHb in solution, which does not apply when considering GC/BHb/$Nf_{suspension}$. Thus, this contribution must be removed by subtracting the current contributions of glassy carbon in BHb-containing electrolyte (Figure 5.3, Section 5.4), represented as $I_{GC\ in\ BHb(aq)}$. The different current contributions from the DPVs used for the calculation are shown collectively in Figure 5.7a for ease of comparison. Relation 5.1 outlines the calculations using the currents (I) from the various DPVs

$$I_{GC/BHb(s)/Nf(s)} + I_{GC\ in\ BHb\ \&\ 10\%\ 1\text{-}PrOH(aq)} - I_{GC\ in\ BHb(aq)} \approx I_{GC/BHb(s)/Nf(suspension)} \qquad (5.1).$$

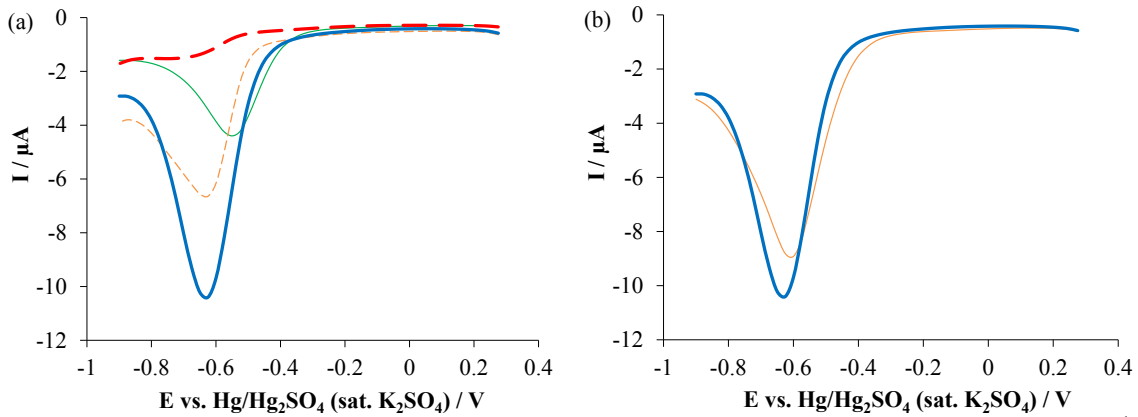

Figure 5.7 For comparison purposes, the individual DPVs of: glassy carbon in 0.2 g L^{-1} BHb (thick red dashed curve, from Figure 5.3, Section 5.4), GC/BHb/Nf_{solid} (thin green solid curve, from Figure 5.1b, Section 5.2), glassy carbon in 0.2 g L^{-1} BHb with 10% 1-PrOH (thin orange dashed curve, from Figure 5.5, Section 5.4), and GC/BHb/$Nf_{suspension}$ (thick blue solid curve, from Figure 5.1b, Section 5.2) were recreated (a). The calculated results using Relation 5.1 are shown as the thin orange curve (left side of Relation 5.1) and solid thick blue curve (right side of Relation 5.1).

The results of using Relation 5.1 show that the left-hand-side of Relation 5.1 is similar to the right-hand-side of Relation 5.1 with some extra current arising near the BHb peak maximum when a Nafion suspension was used (Figure 5.7b). A smaller current contribution and a positive BHb-peak potential shift were observed on the calculated DPV composed of other DPVs by using the left-hand-side of Relation 5.1. These differences likely stemmed from the less intimate contact between the immobilized BHb and the glassy carbon for the GC/BHb/Nf_{solid} in contrast to GC/BHb/$Nf_{suspension}$. The calculated result of Relation 5.1 cannot distinguish the solvent effects of 1-PrOH on glassy carbon and on BHb, but it suggests that the 1-PrOH solvent present in $Nf_{suspension}$ increases the electrochemical reduction of BHb, separate from the enhancement due to Nafion-immobilized BHb.

5.6 Conclusions

The results, data, and interpretations presented in this chapter show that the presence of an alcohol solvent in a Nafion suspension impacts BHb electrochemistry when this Nafion is used to immobilize BHb into a film. For the first time, the 1-PrOH solvent present in a liquid Nafion suspension during the preparation of immobilizing BHb on glassy carbon was shown to have an additional enhancement to the electrochemical reduction of BHb when compared to Nafion-immobilized BHb without any 1-PrOH. The electrochemical research was extended to include water-miscible primary alcohols of different concentrations in a PB electrolyte containing BHb where the addition of any one of MeOH, EtOH, or 1-PrOH was observed to increase the BHb-reduction current. The addition of 1-PrOH had a larger effect on the electrochemical reduction of BHb than MeOH or EtOH. A water-miscible primary alcohol should be avoided as a binder solvent when immobilizing Hb films. If an alcoholic solvent must be used, then low MeOH concentrations is strongly preferred over either EtOH or 1-PrOH. These electrochemical results suggest that caution should be used when preparing Nafion films from a liquid Nafion suspension containing a water-miscible primary alcoholic solvent.

The non-linear relationship between BHb-reduction and the alcohol concentration suggests that multiple mechanisms are likely involved in the enhancement of BHb-reduction. Some of the mechanisms contributing to the increased BHb-reduction may be due to denaturation of BHb as the alcohol content increased, formation of a thicker film incorporating BHb suggested by a negative BHb-reduction peak potential shift, or a change in carbon-oxygen surface groups. The increased BHb-response from the MeOH-modified glassy carbon and decreased background reduction current for high

concentrations of 1-PrOH in the electrolyte suggests that carbon-oxygen surface groups may be changing, which may be partly responsible for the increased BHb-reduction.

Chapter 6 Mechanisms for the Improved Electrochemical Response of Bovine Hemoglobin in Aqueous-alcohol Electrolyte

A manuscript is in preparation for submission based on the work presented in this chapter. JT is responsible for the majority of the data collection, all the analysis, and manuscript preparation. CV data presented in Section 6.3.1 and AFM data presented in Section 6.3.2 are unlikely to be present in the manuscript but are presented in this chapter.

Andrew George (Technician, Department of Physics, Dalhousie University) operated the XPS instrument, and Dr. Robbie Sanderson (Lab Manager, Department of Physics and Atmospheric Sciences, Dalhousie University) operated the spectroscopic ellipsometer.

6.1 Introduction

In Chapter 5, a significant increase in BHb electrochemical signal was observed when the BHb and/or glassy carbon electrode was exposed to an aqueous-alcohol electrolyte. This chapter examines some of the origins of the increased BHb electrochemical signal. Exposing glassy carbon to aqueous-alcohol may have changed the carbon-oxygen surface groups on glassy carbon to favor the electrochemical activity of BHb, as suggested in Chapter 5; XPS was used to test this theory (Section 6.2). Film formation and denaturation of BHb on glassy carbon were also considered as possibilities for enhancing the electrochemical detection of BHb. The presence of a BHb film was investigated electrochemically (Section 6.3.1). Exposing BHb to aqueous-alcohol may have produced thicker protein films as the alcohol content increased; hence, the thickness of the deposited films was examined further by the use of atomic force microscopy (Section 6.3.2) and spectroscopic ellipsometry (Section 6.3.3). Finally, a closer examination of how BHb may have denatured in the aqueous-alcohol electrolyte is then

presented using UV/Vis absorption and fluorescence spectroscopy (Section 6.4). These mechanistic considerations provide greater fundamental understanding of how BHb electroactivity may have increased after alcohol exposure.

6.2 Changes in Carbon-Oxygen Surface Groups after Alcoholic Exposure as a Possible Source of Increased BHb Electroactivity

Previously in Chapter 4, the removal of surface ethers and carbonyls on carbon electrodes were shown to increase the electrochemical activity of BHb. Exposing a carbon material to methanol is known to decrease the amount of surface oxygen,[216] which is likely to also change the amount of carbon-oxygen surface groups. Therefore, carbon-oxygen groups on glassy carbon were examined by the use of XPS after incubation in aqueous-alcohol electrolyte to examine whether alcohol exposure is removing the inhibiting ether or carbonyl surface groups, resulting in the improved electrochemical reduction of BHb seen upon exposure to one of MeOH, EtOH, or 1-PrOH (Chapter 5).

The C_{1s} XPS spectra for glassy carbon incubated in various concentrations of MeOH, EtOH, and 1-PrOH with PB are shown in Figure 6.1, with the fitting results for the C-O (*i.e.* phenols and ethers) and C=O (*i.e.* carbonyls and quinones) surface groups given in Table 6.1. Focusing on the C-O and C=O surface groups known to inhibit BHb electroactivity, the data in Table 6.1 show how difficult it is to draw a relationship between carbon-oxygen surface groups and BHb-electroactivity because C-O increases while the C=O decreases for certain alcohol concentrations (0 – 30% MeOH and 0 – 40% EtOH, Figure 6.2, recreated from Figure 5.3d for the reader's convenience). Thus, the expected BHb activity improvements from removing C=O surface groups would be offset

by the increased C-O surface groups. However, it is interesting to note that while the BHb response increases very little through the 0 – 30% MeOH concentration range, the 0 – 40% EtOH range evidences a large increase in BHb electroactivity, suggesting that another mechanism must dominate in these EtOH concentrations. Similarly, there are alcohol ranges (*e.g.* 0 – 30% 1-PrOH) where the increase in C-O and C=O would be expected to lead to a decrease in BHb electroactivity, yet an increase is seen. Again, this indicates that another mechanism dominates, possibly film formation or BHb denaturation (discussed in Sections 6.3 and 6.4 respectively). Nevertheless, there are ranges of these data which evidence the expected correlation between surface groups and BHb electroactivity. For instance, above 50% EtOH or 1-PrOH, a significant increase in C=O (EtOH) or C-O (1-PrOH) surface groups are seen and the BHb activity plateaus (EtOH) or decreases (1-PrOH), consistent with these surface groups inhibiting BHb electroactivity. Additionally, increasing MeOH above 30% resulted in significant decreases in C-O and C=O surface groups (Table 6.1) that likely contributed to the large increase in BHb-reduction seen for these MeOH concentrations, consistent with an increased BHb response due to the carbon surface modification (Chapter 4). Indeed, as will be shown later in Section 6.5, the 60% MeOH-containing electrolyte resulted in the highest BHb activity of the three aliphatic alcohols tested (Figure 6.2), due to the carbon surface modification working in conjunction with film formation and protein denaturation.

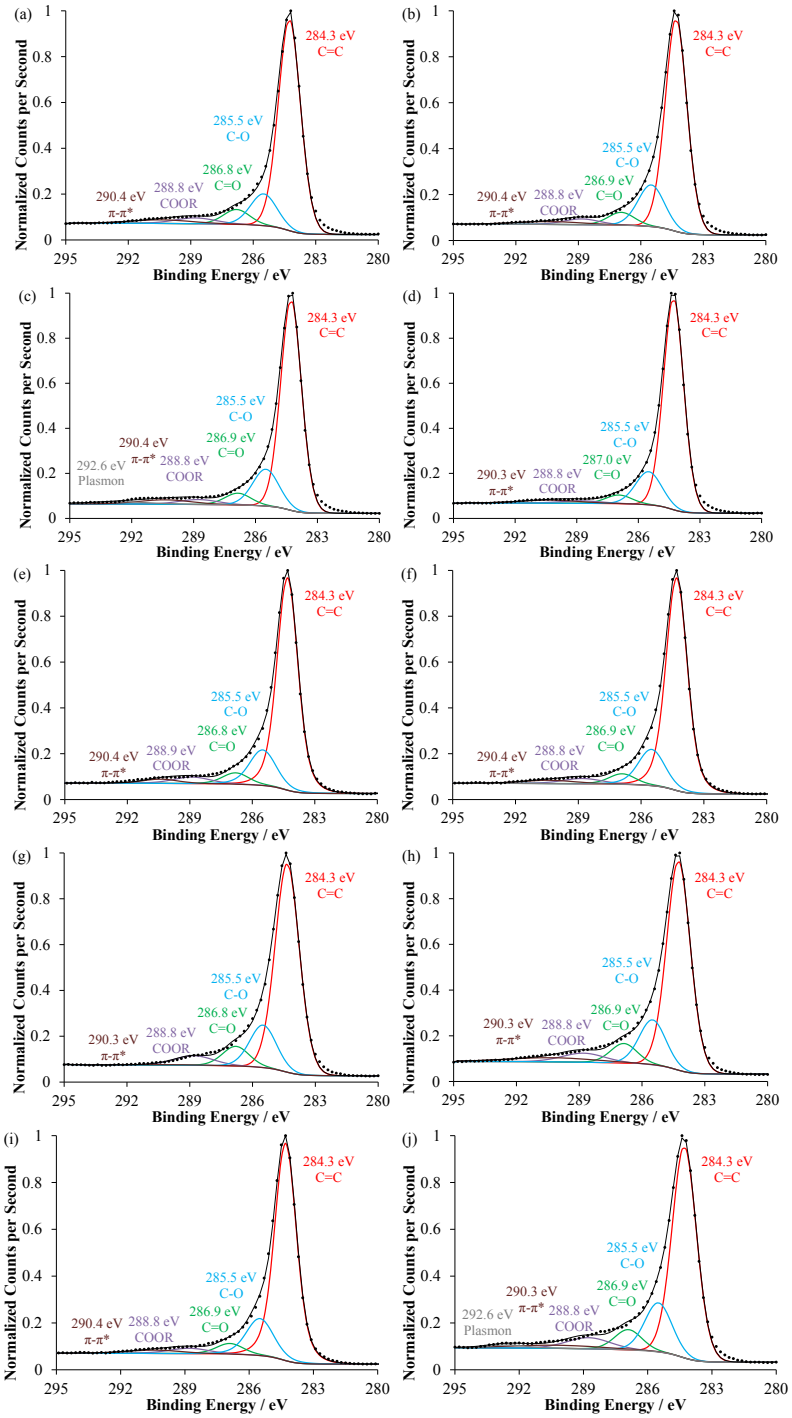

Figure 6.1 Fitted C_{1s} XPS spectra of polished glassy carbon exposed to no alcohol (a), 30% MeOH (b), 40% MeOH (c), 60% MeOH (d), 40% EtOH (e), 50% EtOH (f), 60% EtOH (g), 30% 1-PrOH (h), 50% 1-PrOH (i), or 60% 1-PrOH (j) aqueous-alcohol electrolyte. The experimental data are represented by the dotted black curves and the sum of the fitted curves are represented by the solid black curve.

Table 6.1 A summary of fitted peaks representing different surface groups from C_{1s} XPS data for each alcohol treatment used on glassy carbon. Each entry listed in the table contains the relative surface composition based on integration under the fitted peak, the full width at half maximum, and the center position of the fitted peak. The associated fitting errors for the carbon surface oxides were estimated using one standard deviation assuming a normal distribution from Monte Carlo simulations.

Polished Glassy Carbon Exposed to	C=C	C-O	C=O	COOR	π-π* shakeup	Plasmon
no alcohol	73.5 ± 0.6% 1.26 eV 284.3 eV	13.2 ± 0.5% 1.50 eV 285.5 eV	6.2 ± 0.3% 1.50 eV 286.8 eV	3.7 ± 0.3% 2.30 eV 288.8 eV	3.4 ± 0.4% 3.47 eV 290.4 eV	Negligible
30% MeOH + PB	71.6 ± 0.8% 1.23 eV 284.3 eV	17.1 ± 0.6% 1.50 eV 285.5 eV	5.3 ± 0.3% 1.50 eV 286.9 eV	3.1 ± 0.3% 2.00 eV 288.8 eV	2.9 ± 0.9% 3.83 eV 290.4 eV	Negligible
40% MeOH + PB	70.5 ± 1% 1.18 eV 284.3 eV	15.6 ± 0.3% 1.50 eV 285.5 eV	5.0 ± 0.3% 1.50 eV 286.9 eV	3.1 ± 0.5% 2.25 eV 288.8 eV	3.7 ± 0.7% 3.00 eV 290.4 eV	2.1 ± 0.8% 3.48 eV 292.6 eV
60% MeOH + PB	75.8 ± 0.6% 1.16 eV 284.3 eV	15.3 ± 0.3% 1.50 eV 285.5 eV	4.0 ± 0.2% 1.50 eV 287.0 eV	1.8 ± 0.6% 2.40 eV 288.8 eV	3.1 ± 0.7% 3.37 eV 290.3 eV	Negligible
40% EtOH + PB	73.1 ± 2% 1.18 eV 284.3 eV	15.5 ± 0.8% 1.50 eV 285.5 eV	5.0 ± 0.6% 1.50 eV 286.8 eV	4.0 ± 0.8% 2.10 eV 288.9 eV	2.4 ± 0.9% 2.00 eV 290.4 eV	Negligible
50% EtOH + PB	73.6 ± 2% 1.20 eV 284.3 eV	15.7 ± 0.8% 1.50 eV 285.5 eV	4.6 ± 0.6% 1.50 eV 286.9 eV	3.4 ± 0.7% 2.20 eV 288.8 eV	2.7 ± 2% 3.00 eV 290.4 eV	Negligible
60% EtOH + PB	71.0 ± 0.8% 1.36 eV 284.3 eV	16.0 ± 0.5% 1.50 eV 285.5 eV	7.4 ± 0.3% 1.50 eV 286.8 eV	5.2 ± 0.4% 2.21 eV 288.8 eV	0.4 ± 0.8% 5.00 eV 290.3 eV	Negligible
30% 1-PrOH + PB	66.9 ± 0.7% 1.34 eV 284.3 eV	16.1 ± 0.4% 1.50 eV 285.5 eV	7.0 ± 0.3% 1.50 eV 286.9 eV	5.2 ± 0.6% 2.40 eV 288.8 eV	4.8 ± 1% 4.87 eV 290.3 eV	Negligible
50% 1-PrOH + PB	69.1 ± 0.7% 1.25 eV 284.3 eV	15.9 ± 0.3% 1.50 eV 285.5 eV	6.5 ± 0.4% 1.50 eV 286.9 eV	4.1 ± 0.5% 2.30 eV 288.8 eV	4.4 ± 1% 4.00 eV 290.4 eV	Negligible
60% 1-PrOH + PB	65.1 ± 0.8% 1.34 eV 284.3 eV	16.9 ± 0.6% 1.50 eV 285.5 eV	7.0 ± 0.3% 1.50 eV 286.9 eV	6.1 ± 1% 2.40 eV 288.8 eV	3.5 ± 1% 5.00 eV 290.3 eV	1.4 ± 0.6% 2.07 eV 292.6 eV

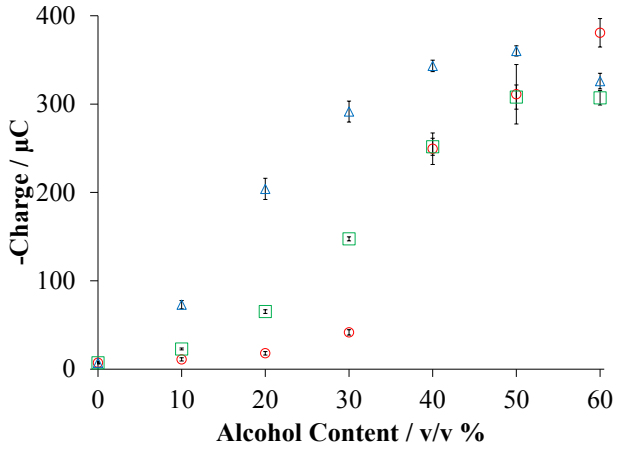

Figure 6.2 Recreated from Figure 5.3d showing background-subtracted BHb charge for various concentrations of MeOH (red circles), EtOH (green squares), or 1-PrOH (blue triangles) in 0.2 g L^{-1} BHb with PB. The error bars indicate one standard deviation from three replicate trials.

6.3 BHb Film Formation on Carbon as a Possible Mechanism for the Improved BHb Electroactivity

The electrochemical data presented in Sections 5.2 and 5.4 suggested that a BHb film might have formed on the glassy carbon electrode upon exposure to BHb in aqueous-alcohol electrolyte. For instance, there was a distinct shift in the BHb reduction peak potential towards more negative values, consistent with the potential shift of Hb films seen in the literature.[81] A film of BHb or a change in BHb film thickness may indicate protein denaturation, facilitating the electron transfer process and may be partly responsible for the observed higher currents. The presence of a BHb film was tested electrochemically after incubating glassy carbon in aqueous-alcohol with BHb (Section 6.3.1). The thickness of the BHb films on glassy carbon were measured by using atomic force microscopy (Section 6.3.2) and spectroscopic ellipsometry (Section 6.3.3).

6.3.1 BHb Film Formation on Glassy Carbon

The purpose of the electrochemical experiments in this section is to test whether an electrochemically active BHb film forms on an incubated glassy carbon electrode. In this section, the incubated glassy carbon electrode was created by submerging the glassy carbon electrode in an aqueous-alcohol electrolyte containing BHb, similar to the conditions previously used in Chapter 5, and then washed with water to remove any excess alcohol or BHb. The modified glassy carbon with a possible BHb film was then transferred into an electrochemical cell filled with an alcohol- and BHb-free PB electrolyte for electrochemical testing.

The glassy carbon incubated in BHb without alcohol had a small electrochemical response (Figure 6.3a and b), suggesting that BHb adsorbed as a film, even in the absence of alcohol. Positively shifted reduction peaks were observed on glassy carbon incubated in BHb with 1-PrOH when compared to similar incubations with EtOH or MeOH (Figure 6.3c-h), suggesting a more facile electron transfer, which may originate from more favorable BHb adsorption orientations on the carbon surface, for example if BHb adsorbed with its heme groups closer to the electrode surface. Larger BHb-reduction peaks were observed after incubating glassy carbon in electrolytes containing BHb and the less polar 1-PrOH than either EtOH or MeOH, suggesting that BHb with a particular conformation or more BHb may have adsorbed on glassy carbon, resulting in a thicker BHb film or a larger surface coverage.

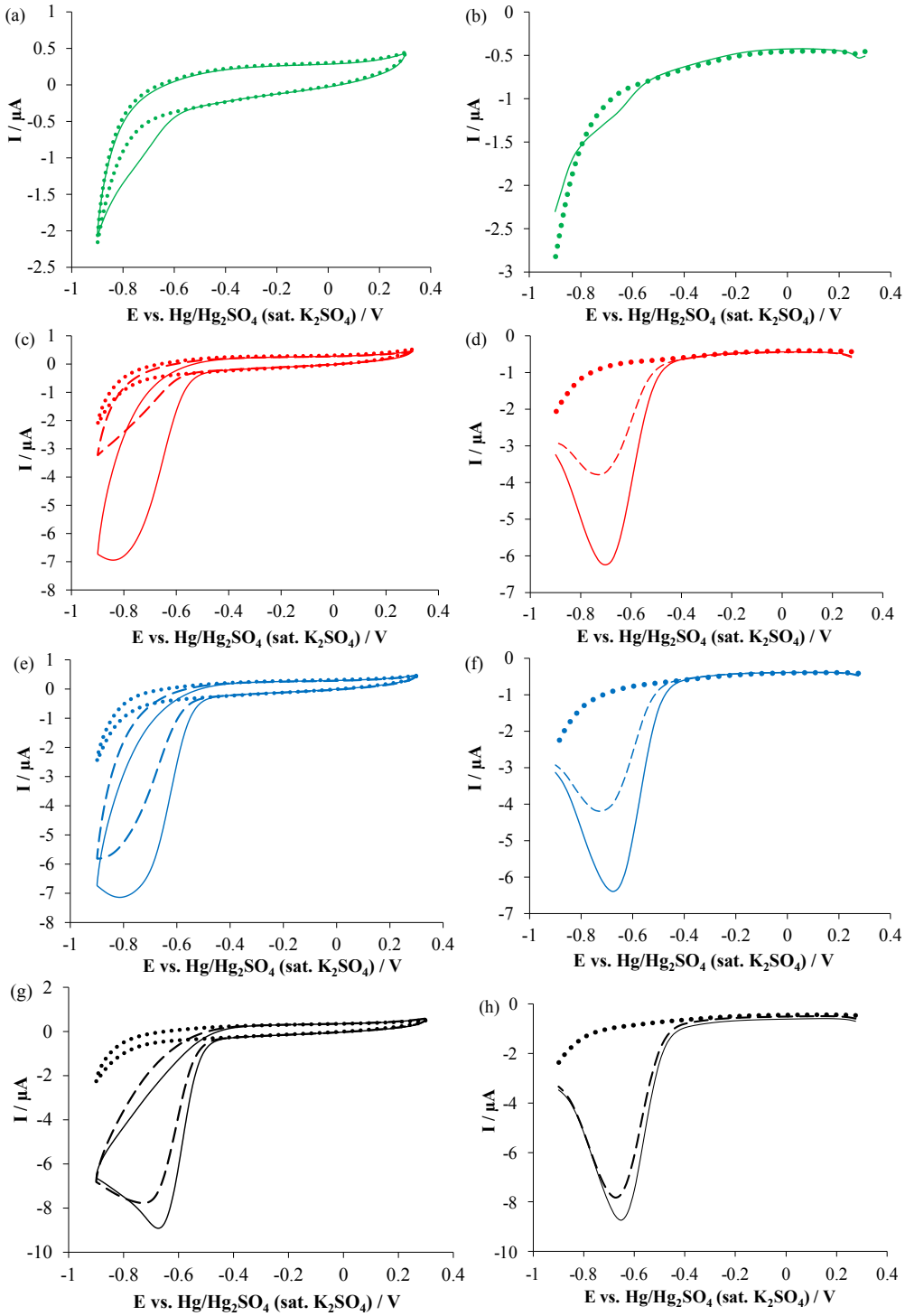

Figure 6.3 Representative CVs (a, c, e, g) and DPVs (b, d, f, h) of glassy carbon in 0.1 M PB (pH 7.08) (dotted curves) after incubation in 0.2 g L^{-1} BHb in PB with: no alcohol (a, b), MeOH (c, d), EtOH (e, f), or 1-PrOH (g, h). 30% and 60% alcoholic electrolyte content used during incubation are represented by dashed and solid curves respectively (c-h).

6.3.2 Film Thickness Estimates from the use of Atomic Force Microscopy

A thickness measurement of BHb films adhered to a polished glassy carbon plate was made by the use of atomic force microscopy (AFM). The procedure for adsorbing BHb onto glassy carbon was described previously in Section 3.4.1. A BHb-adsorbed region was created by submerging part of a glassy carbon plate into the incubating solution containing BHb, while the remaining glassy carbon sample surface remained clean. The measurement of the BHb film thickness was attempted by determining a height difference between regions on glassy carbon without and with adsorbed BHb. The surface of a clean, polished glassy carbon plate is shown in Figure 6.4a and with adsorbed BHb in one region of the glassy carbon shown in Figure 6.4b. The interface between the bare and BHb-adsorbed carbon surface was difficult to image, but in this image, the bare glassy carbon was expected to be at the bottom of Figure 6.4b. The BHb-adsorbed surface appeared more rough than the clean, polished glassy carbon surface, possibly due to localized accumulation of BHb. A height difference of *ca.* 5.5 nm, the diameter of BHb, was expected in Figure 6.4b as the AFM tip moved across a possible boundary between the BHb-adsorbed region and the clean glassy carbon surface. However, the boundary was not observed by using AFM likely because the height differences gradually changed, making a direct height difference measurement impossible to determine the adsorbed BHb thickness. Therefore, no BHb film thickness was obtained.

In an attempt to controllably remove some of the adsorbed BHb and form a bare space to enable a height difference measurement, the surface of the adsorbed BHb on glassy carbon was scratched using the AFM tip. The AFM tip was replaced between

scratching and measurement to prevent possible changes to the tip caused by using the scratching procedure, which may affect the measurements. After scratching the sample surface in the shape of a square, a decrease in height was expected, but a clear *ca.* 1.5 nm height increase was observed (Figure 6.4c). As a comparison, a clean piece of glassy carbon was also scratched using the AFM tip, resulting in no height difference (not shown). The results suggest that the adsorbed BHb on glassy carbon may have been partially lifted off from the glassy carbon surface due to dragging of the AFM tip, possibly creating a gap between the glassy carbon and BHb when scratched. Since a thickness measurement was inconclusive by the use of AFM for BHb adsorbed onto glassy carbon, this technique was not attempted for glassy carbon samples incubated in aqueous-alcohol with BHb.

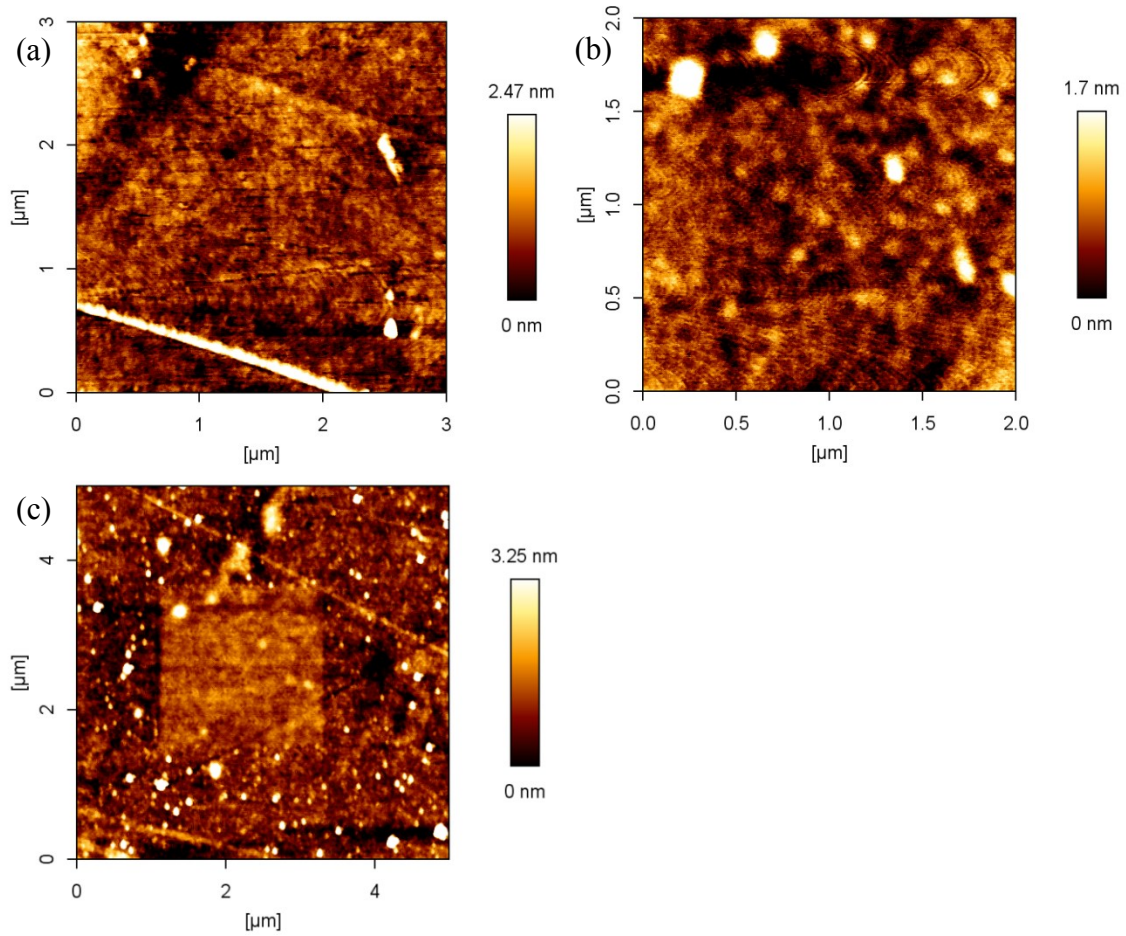

Figure 6.4 Atomic force micrographs recorded using intermittent contact mode by raster scanning the samples of a polished glassy carbon surface (a), with adsorbed BHb (b), and after scratching the surface of the BHb film (c).

6.3.3 Film Thickness Estimates from the use of Spectroscopic Ellipsometry

To determine whether a BHb film forms a thicker film in the presence of alcohol, spectroscopic ellipsometry was employed to estimate the film thickness. However, in spectroscopic ellipsometry, a model is required to obtain physically relevant parameters such as the film thickness.

6.3.3.1 Spectroscopic Ellipsometry Model Considerations

As discussed previously in Section 2.5.1, the use of measured spectroscopic ellipsometry data to estimate a film thickness requires a model that properly and physically describes the system in order to extract meaningful parameters. The essential information required are: the type of material being measured, whether the materials are transparent, how many layers of different materials are expected, and what models are currently known to describe those materials.

In this study, a two-layer model was used, illustrated in Figure 6.5, since the samples measured were thin films of BHb (top layer) on polished glassy carbon (bottom layer). A different model for each layer was used, since each layer interacts with the incoming light differently.

Figure 6.5 A diagram illustrating a two-layer model used for spectroscopic ellipsometry to determine the thickness of the BHb layer.

In some literature studies, spectroscopic ellipsometry has been used to measure protein film thicknesses on amorphous carbon materials using a Tauc-Lorentz model for the carbon.[217,218] However, the Tauc-Lorentz model is typically used for modelling amorphous semiconductors and insulators,[219] which is not appropriate in this research because glassy carbon is neither a semiconductor nor an insulator. More recent studies have suggested the use of a B-spline model for amorphous carbon, which makes no assumptions regarding the interactions between the material being modeled and light.[220] A B-spline model has also been used successfully to describe amorphous carbon from

spectroscopic ellipsometry data.[220] Thus, the glassy carbon substrate was represented by a B-spline model in this work.

The Cauchy model is one of the more commonly used spectroscopic ellipsometry models for determining thicknesses of adsorbed proteins.[135,136] This model is mathematically simple and assumes that the material being modeled is optically transparent.[135] Although there are limited reports of modeling Hb using spectroscopic ellipsometry,[221–223] some published works modeled the Hb film assuming the film is transparent, but it was unclear if a Cauchy model was used.[221,223] Others have assumed a particular index of refraction when calculating the adsorbed Hb film thickness.[222,224] Since the assumption of a transparent protein film appears to be widespread, the Cauchy model was used to describe the BHb layer in this thesis.

To test whether a thin layer of BHb was transparent, BHb was adsorbed onto glass slides in PB with and without alcohol by using the same incubation procedure for adsorbing BHb onto glassy carbon for electrochemical testing (Sections 3.1.6, 3.4.2.1, and 3.4.2.2). The absorbance of the BHb-adsorbed glass slides were measured by the use of UV/Vis spectroscopy. The well-known, strongly-absorbing Soret peak from BHb is expected near 412 nm for a thick dry Hb film cast on glass,[73,74] which was confirmed at 413 nm (Figure 6.6a). Figure 6.6b-d shows the absence of the Soret peak on the glass slides coated by using the incubation procedure, suggesting either no BHb was present on the glass slides or the adsorbed BHb was transparent. Rubbing a Kimwipe on the glass slides exposed to BHb with 30 or 60% alcohol resulted in smudging, implying that there was a thin film of BHb on the glass since rubbing a Kimwipe on glass without BHb and

alcohol exposure did not result in smudging. These observations and results suggest that the thin BHb films on glass are transparent.

Fluorescence measurements were also attempted to further test for BHb transparency since fluorescence was expected to be more sensitive than absorbance measurements.[144] The fluorescing Tyr and Trp amino acid residues in proteins were expected to peak between 300 and 400 nm.[32,225,226] An example of a thick fluorescing dry film of BHb cast on glass is shown in Figure 6.6e. Although the absence of fluorescence peaks (Figure 6.6f-h) for the incubated BHb-adsorbed glass slides may be due to a lack of sufficient material for fluorescence, quenching of fluorescence, or the film is transparent, but when combined with the UV/Vis absorption results, these suggest that the thin BHb layer is transparent and the Cauchy model is valid.

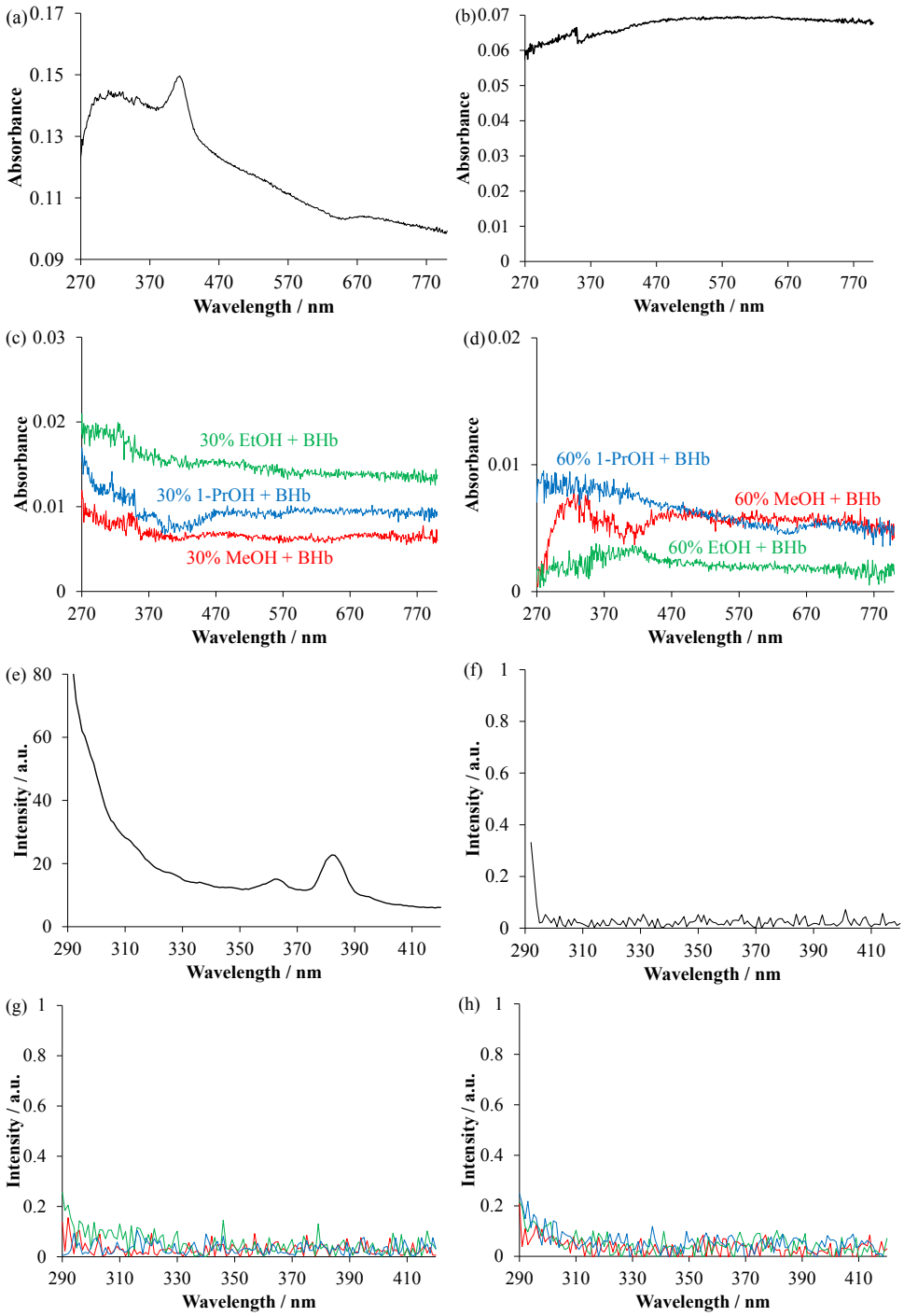

Figure 6.6 Background subtracted UV/Vis (a-d) and fluorescence (e-h) spectra of a thick BHb film cast onto a glass slide (a,e) or BHb-adsorbed glass slides after incubation in 0.2 g L^{-1} BHb dissolved in 0.1 M PB (b,f) with 30% (c,g) or 60% (d,h) MeOH (red), EtOH (green), or 1-PrOH (blue).

6.3.3.2 Protein Film Thickness from the use of Spectroscopic Ellipsometry

With a proper model for the adsorbed BHb layer on glassy carbon samples, the thickness of the BHb layer on glassy carbon can be estimated. As shown in Section 2.5.1, the film thickness is related to the optical constants; however, the optical constants for glassy carbon were not available in the CompleteEase software database. Regardless, spectroscopic ellipsometry measurements of clean glassy carbon without BHb were fitted with the B-spline model described in Section 6.3.3.1 to obtain the optical constants for bare glassy carbon. Fitting the optical constants with Kramers-Kronig compliance, which are mathematical relations to connect the real and imaginary components of a complex function, is essential to ensure the quantities obtained are physically reasonable; for example, the optical constant *k* cannot be negative because *k* represents the attenuation of light.[136] Kramers-Kronig compliance also helps to reduce fitting errors due to the additional mathematical constraints. Once the bare glassy carbon data were fitted and the optical constants (*n* and *k*) were calculated, the same optical constants were used for all future modeling since glassy carbon was used as the substrate throughout all spectroscopic ellipsometry measurements of adsorbed BHb films.

The results of fitting the optical constants, *n* and *k*, for a clean polished glassy carbon are shown in Figure 6.7. The fitted *n* and *k* values are slightly different in magnitude but similar in the overall shape when compared to the *n* and *k* values published by Williams and Arakawa.[227] The differences in magnitude may be due to differences in the source of glassy carbon considering that the literature results published by Williams and Arakawa examined glassy carbon made by the Plessey Company[227] and the glassy carbon used in this research originated from SPI Supplies. Glassy carbon is

typically made from a controlled pyrolysis involving a polymeric material[228] and the variation in the polymer used for pyrolysis to create glassy carbon could be responsible for the slightly differing optical constants. The introduction of different elements from the polymer used to create glassy carbon, such as chlorine atoms from poly(vinylidene chloride)[228,229] or nitrogen atoms from poly(acrylonitrile)[228,229] would be expected to change the optical constants. Therefore, the optical constants should be different depending on the polymer precursor used to create glassy carbon since the optical constants are intrinsic to the material being examined and are dependent on the oscillation of electrons in the material.[136]

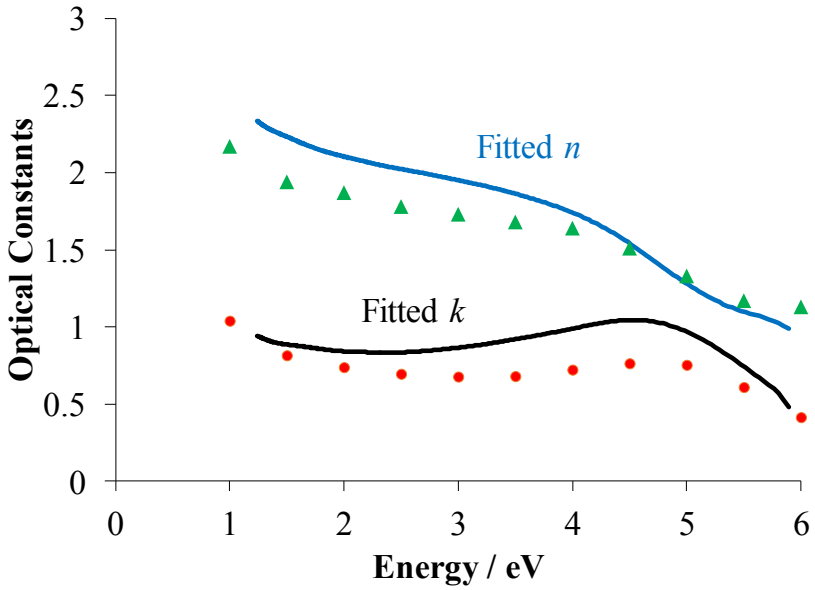

Figure 6.7 Fitted optical constants *n* (blue solid curve) and *k* (black solid curve) of polished glassy carbon from spectroscopic ellipsometry are used for calculating BHb film thicknesses. For comparison purposes, *k* (red dots) and *n* (green triangles) values of polished glassy carbon were plotted from published data by Williams and Arakawa.[227]

As stated previously, measured ellipsometry data without a model is generally not useful, since many of the plots for the different glassy carbon samples with adsorbed BHb appear similar, as seen in Figure 6.8. Nevertheless, some information can be

derived from these data. Upon closer inspection, a very broad shoulder visible between 250 to 400 nm (Figure 6.8b-h denoted with a * symbol), and a sharp peak visible in Figure 6.8g near 220 nm for the measured Ψ values (also denoted with a * symbol) suggests the presence of a thin film;[138] these features were absent in the bare glassy carbon sample data (Figure 6.8a). The peaks and shoulders are due to the interference between the light reflecting from the surface of the film and the reflected light from the bottom of the film; thus, the peak and shoulder seen in Figure 6.8g suggests a thicker film on glassy carbon incubated in 30% 1-PrOH with PB and BHb when compared to the other samples due to more interference.[138]

Spectroscopic ellipsometry data were obtained without incident for all samples except for the film formed when glassy carbon was incubated in 60% MeOH with PB and BHb. For this sample, only one measurement was possible from repeated trials and realignments, because very little to no reflection was detected, resulting in noisy data for the one successful attempt (Figure 6.8d). The difficulty may have stemmed from diffuse reflection due to a rough surface scattering light away from the detector. A complementary technique to obtain the protein film thickness such as X-ray reflectivity would be ideal.[230] Quantifying the BHb film thickness by using UV/Vis absorption or fluorescence was not possible since the BHb films were transparent as shown previously in Section 6.3.3.1. Despite the difficulties in measuring the protein film formed from the incubation solution containing 60% MeOH, the spectroscopic ellipsometry data obtained were fitted using the same model and procedure as the other samples to estimate the film thickness, but the results for glassy carbon prepared by incubation in 60% MeOH with PB and BHb should be interpreted cautiously due to noisy data.

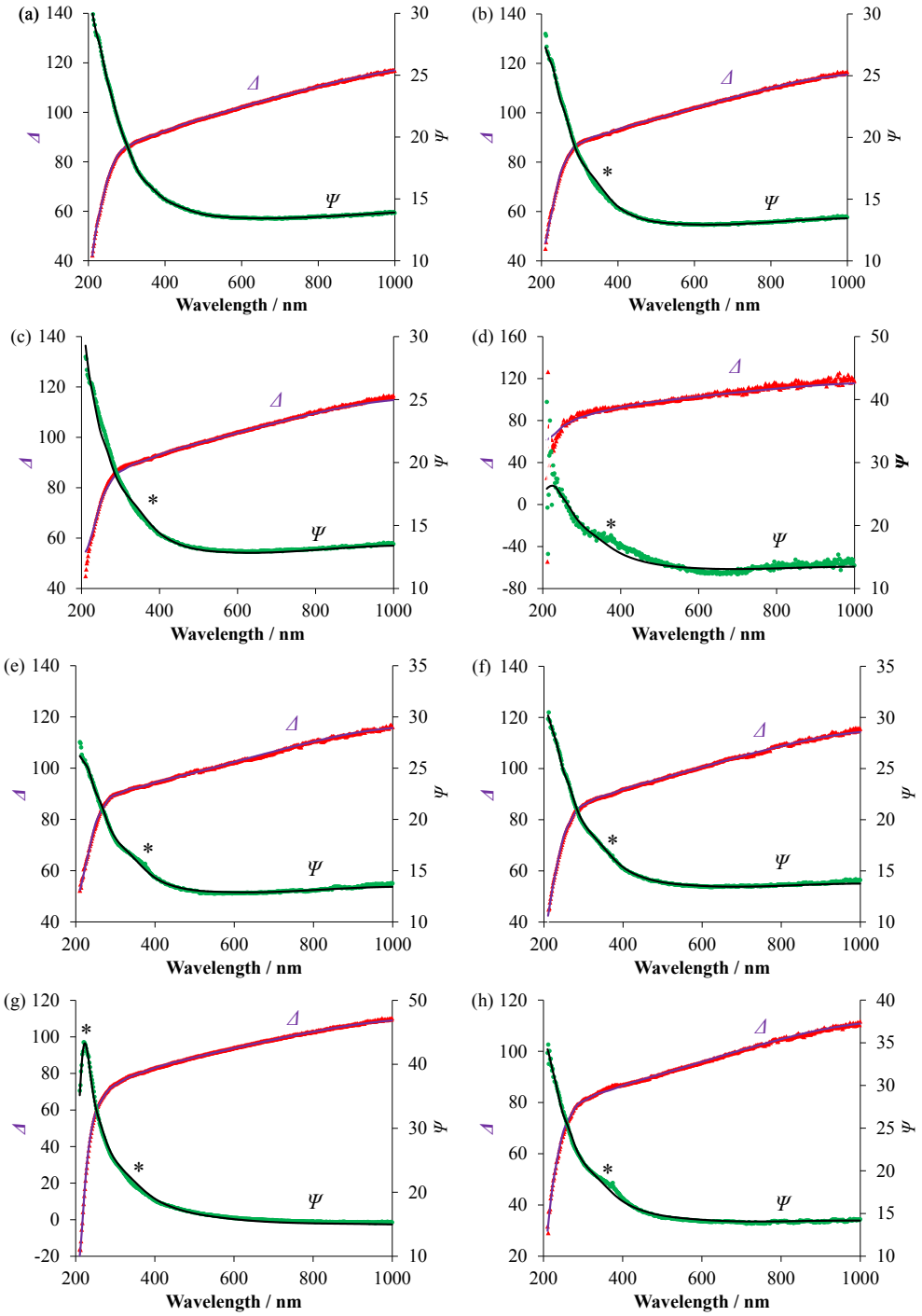

Figure 6.8 Representative spectroscopic ellipsometry plots of measured Δ (red triangles) and Ψ (green dots) values with the fitted Δ (purple curve) and Ψ (black curve) values for polished glassy carbon (a) exposed to 0.2 g L^{-1} BHb in 0.1 M PB (b) containing: 30% MeOH (c), 60% MeOH (d), 30% EtOH (e), 60% EtOH (f), 30% 1-PrOH (g), or 60% 1-PrOH (h). The symbol * emphasizes the location of a very broad shoulder or peak in the graphs.

Another important consideration is the error involved in the fitting process. A common method to quantify how well the theoretical Δ and Ψ values generated from the optical model fit the spectroscopic ellipsometry data is to calculate the mean squared error (MSE), defined in Section 2.5.1. The CompleteEASE processing software used the 2-layer optical model detailed in Section 6.3.3.1 to fit the measured data and calculate possible film thicknesses until the lowest possible MSE was obtained. As a guideline for most applications, models with well-fitted systems should have MSE less than 20.[138]

Protein film thicknesses from each sample in Figure 6.8 are tabulated in Table 6.2. The BHb thickness of 49 Å adsorbed onto glassy carbon without any alcohol exposure is larger than a previous literature value of 40 Å on a gold substrate,[223] but is similar to one of the known dimensions of Hb, which is 50 x 55 x 65 Å.[34,35] A layer of BHb may be thinner on gold, possibly because of partial denaturation involving the strong binding between Au and sulfur-containing amino acid residues[231,232] in BHb, such as methionine and cysteine.[34]

The data tabulated in Table 6.2 suggest that the thicknesses of all the adsorbed BHb films formed on glassy carbon after incubation in aqueous-alcohol solutions with BHb were larger than those formed without an alcohol, except for 30% EtOH which appeared similar in thickness. The increased BHb film thickness may be due to more alcohol-denatured BHb depositing on the glassy carbon surface. Increasing the amount of 1-PrOH from 30% to 60% resulted in a thinner film. Contaminants from 2-propanol can adsorb onto carbon[215] and similarly 60% 1-PrOH may have sufficient contaminants to compete with BHb adsorption. Other possibilities involving changes in the BHb structure such that it no longer retains its globular shape upon exposure to the alcohol and

packs into a more spatially efficient film during adsorption are also likely. The implications of film thickness on the electrochemical activity of BHb will be discussed next.

Table 6.2 A summary of the BHb film thickness and estimated number of BHb layers on glassy carbon obtained using spectroscopic ellipsometry and a Cauchy and B-spline two-layer model. Errors in the thickness were estimated based on a 90% confidence interval.

Glassy carbon incubated in	MSE	Thickness / Å	Estimated Number of BHb Layers
BHb + no alcohol	4	49.3 ± 0.3	1
BHb + 30% MeOH	9	63 ± 2	1.3
BHb + 60% MeOH	52	80 ± 20	1.6
BHb + 30% EtOH	4	48 ± 2	1
BHb + 60% EtOH	6	66.4 ± 0.9	1.3
BHb + 30% 1-PrOH	7	170.3 ± 0.7	3.5
BHb + 60% 1-PrOH	6	101.1 ± 0.5	2

The BHb charge, obtained from the background-subtracted DPV BHb-reduction peaks of glassy carbon incubated in alcohol- and BHb-containing PB (Figure 6.3), was plotted as a function of the film thickness in Figure 6.9a. When the MeOH content increased from 0% to 30% to 60% during incubation, the electrochemical activity of BHb increased with the film thickness. The estimated number of BHb layers appear to increase up to 1.6 layers of BHb upon exposure to 60% MeOH, suggesting that a thicker protein film could result in a more electrochemically active film. The increase in BHb-reduction and protein film thickness may be a result of MeOH denaturing BHb. Evidence for MeOH denaturing BHb is discussed later in this chapter.

The addition of 30% EtOH to the electrolyte containing BHb and PB during incubation increased the electrochemical activity of BHb but resulted in a similar film thickness as an alcohol-free incubation. These results could suggest that EtOH denatured

BHb and caused more heme groups to be electrochemically active while not sufficiently unraveling the protein structure to affect the estimated film thickness. Alternatively, partial dehydration of the heme cavity may result in weakening hydrogen bonds in the heme cavity allowing the heme cavity to be more easily reorganized, facilitating the electron transfer.[59,233] Another possibility may be that the orientation of adsorbed BHb on the carbon surface changed such that the heme groups may be aligned closer to the carbon surface resulting in more BHb-reduction. Further work would be required to analyze the orientation of the redox-active heme groups in the protein film by using other techniques, such as angle-resolved XPS to probe the film at different depths. The addition of 60% EtOH to the incubation mixture led to an increase in both the electrochemical reduction of BHb and the film thickness slightly beyond a monolayer, suggesting that the thicker film is an important consideration, similar to the MeOH-incubated films.

Adding 1-PrOH during the incubation stage resulted in thicker and more electrochemically active BHb films. In particular, 30% 1-PrOH resulted in the thickest BHb film and a very high electrochemical activity, supporting the conclusion that more electroactive BHb adsorbed on the surface. When incubated in 60% 1-PrOH, BHb electroactivity again increased, but the film thickness was smaller (Table 6.2). These results suggest that for high 1-PrOH content, the protein film may be more dense (more electroactive Hb per unit film volume) or that the additional 1-PrOH resulted in increased denaturation, causing more electroactivity per Hb molecule, though less BHb adsorbed (thinner films), possibly due to competitive adsorption by other solution species, such as contaminants from the 1-PrOH alcohol. As suggested previously for EtOH, the

orientation of the heme groups within the film may also be changing towards the carbon surface, which are expected to be more active than hemes oriented away from the carbon surface.

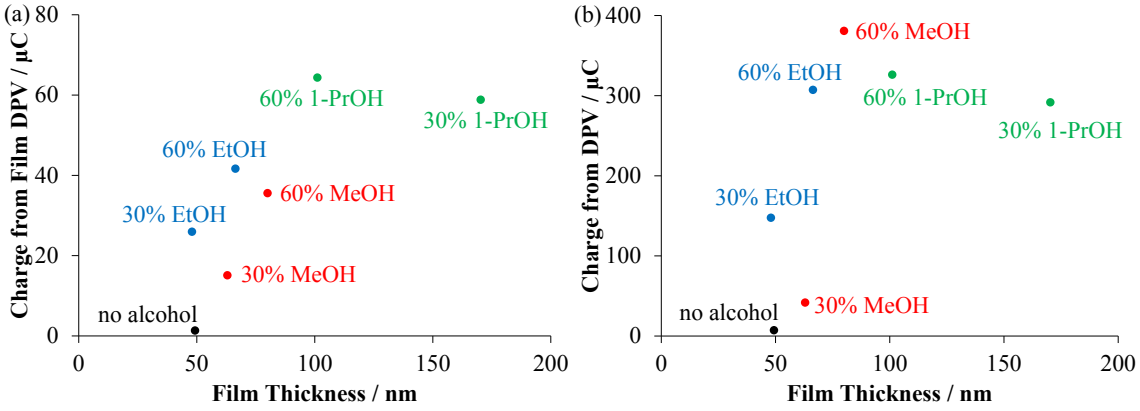

Figure 6.9 A representative plot of BHb charge calculated from background-subtracted DPVs of glassy carbon with an electrochemically active film of BHb formed from incubation in aqueous-alcohol with BHb (a) or glassy carbon in aqueous-alcohol electrolyte with BHb previously seen in Figure 5.3 (b) as a function of film thickness on glassy carbon.

The adsorbed BHb films created during incubation may provide some understanding of possible film formation resulting in enhanced BHb-electrochemistry in BHb-containing aqueous-alcohol electrolytes. Large increases in the electrochemical reduction of BHb observed previously in aqueous-alcohol electrolyte (Figure 5.3, Chapter 5) may in part be connected to the film thicknesses. BHb-reduction in aqueous-alcohol electrolyte (Figure 6.9b) showed much larger DPV charges versus films formed by incubation (Figure 6.9a) but the trends relating charge to film thickness were similar, suggesting that adsorbed BHb films contribute only part of the BHb activity, implying that other mechanisms are also contributing. For example, maximum BHb-reduction was achieved in electrolyte containing 60% MeOH, PB, and BHb, likely in part due to decreased inhibitory surface C=O groups on the glassy carbon surface (Section 6.2),

whereas film formation from an incubation in 60% MeOH, PB, and BHb did not result in the most electrochemically active film.

In summary, these data suggest that increasingly thick BHb films led to higher BHb electrochemical responses, but the correlation is not perfect. As an example, films formed by incubation with EtOH were thinner but more active than those formed in MeOH-containing incubation solutions. The difference in activity may in part be due to increased protein denaturation by EtOH, a change in heme group orientation favoring greater accessibility, partial dehydration in the heme cavity, or other mechanisms. High concentrations of 1-PrOH in the incubation solution also resulted in thinner but more electroactive films, possibly due to competitive adsorption of contaminants from 1-PrOH with BHb, the formation of a denser protein film through denaturation, or orienting the hemes on the carbon surface to favor the reduction of BHb. Since denaturation of BHb may be an important consideration, the evidence for BHb denaturation by using an alcohol is presented next.

6.4 Structural BHb Changes as a Possible Mechanism for its Increased Electrochemical Activity

As mentioned in Section 2.1, the redox-active heme groups are buried within the hydrophobic regions of BHb, which are difficult to access electrochemically. Therefore, alcohol-induced changes to the BHb conformation[205,208] may lead to increased BHb-reduction, such as those seen in Chapter 5. In Section 6.3, the formation of a BHb film contributed to some of the observed BHb electroactivity, but in most cases, a significant amount of BHb-reduction remains unaccounted for because the BHb-reduction charge in

aqueous-alcohol electrolyte was much larger than those of the films formed by incubation (Figure 6.9). Changes in the BHb protein structure may be responsible for the unaccounted increase in BHb-reduction. UV/Vis absorption and fluorescence spectroscopy were used to indicate possible changes in the protein structure of BHb (illustrated in Figure 6.10) as a possible mechanism for the increased electrochemical reduction of BHb in aqueous-alcohol electrolyte.

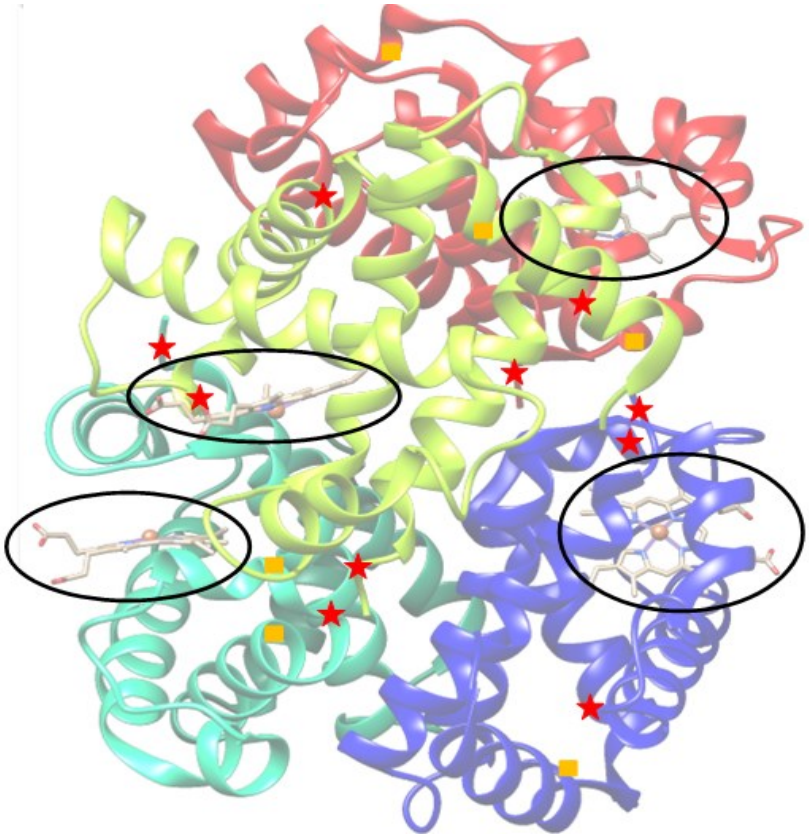

Figure 6.10 A diagram illustrating different parts of BHb being probed. The heme groups (within the circled regions) were examined using UV/Vis absorption, the tyrosine residues (red stars ★) were probed by using UV absorption, and the tryptophan residues (orange squares ■) were examined using fluorescence. Chimera was used in the construction of this figure.[34,35]

6.4.1 Probing BHb for Structural Changes near Heme and Tyrosine Residues in Aqueous-alcohol Electrolyte by the use of UV/Vis Absorption Spectroscopy

UV/Vis absorption spectroscopy may be used to identify changes in the environment near the redox-active heme groups of Hb in solution.[143] The Soret peak is the most sensitive absorption peak and is generally found between 405-430 nm for Hb.[30,143] The position of the Soret peak is sensitive to changes in the heme structure, as systematically studied by Wang and Brinigar, who examined optical spectra of Hb and heme complexes with different ligands.[143] A shift in the Soret peak towards a longer wavelength was shown to be due to stronger interactions between the Fe and an axial ligand within a heme group, while shifts towards shorter wavelengths were associated with greater steric hindrance and decreased interactions between Fe and the axial ligand.[143] The increase in steric hindrance is likely from conformational changes in the peptide chain connected to the axial histidine ligand bound to iron as BHb denatures. Changes in the Soret peak position may indicate a change in the heme structure or the protein structure near the heme[143,208] since a histidine residue connects a peptide chain axially to the heme (illustrated in Figure 6.11). MeOH, EtOH, and 1-PrOH are all known to change the conformation of Hb in solution,[205] with Hb suggested to have specific binding sites for MeOH and EtOH involving steric interactions.[234]

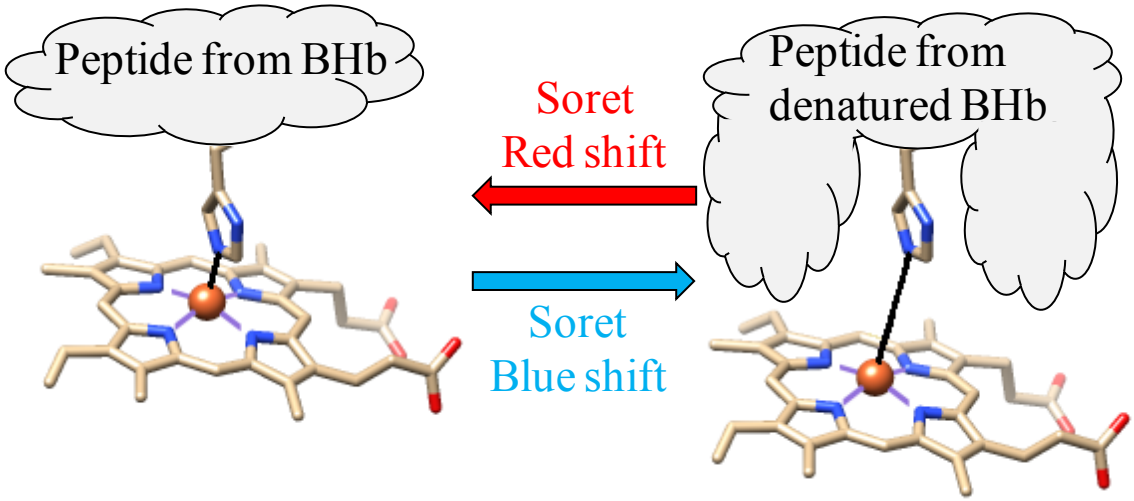

Figure 6.11 Illustration of weaker heme Fe-histidine interactions with increased steric hindrance in a heme group of BHb resulting from sufficient alcohol exposure. Blue portions of the illustration represent nitrogen and the red sphere represents iron. The software Chimera aided in the preparation of this illustration.[35]

UV/Vis absorption data (Figure 6.12a-d) show a small blue-shift in the Soret peak when adding small amounts of alcohol (up to 30% MeOH or 10% EtOH) to the electrolyte, evidencing decreased Fe-histidine bonding interactions in the heme with increased steric hindrance.[143] The addition of more alcohol (40-50% MeOH, or 20% EtOH) to the electrolyte was observed to slightly red-shift the Soret peak, suggesting slightly tighter heme environments, similar to that of unmodified BHb. Further addition of EtOH (30-40%) or 1-PrOH (10-20%) clearly shifted the Soret peak towards longer wavelengths with the most red-shifted peak observed in 40% EtOH and 20% 1-PrOH. The red-shifted Soret peaks indicate a protein conformation with greater bonding interactions between Fe and the histidine ligand in the heme group of Hb.[143] As the alcohol content increased further (60% MeOH, > 40% EtOH, > 20% 1-PrOH), the Soret peak clearly blue-shifted, showing a decrease in the Fe-histidine ligand bonding interaction and an increase in steric hindrance[143] likely originating from conformational changes due to protein denaturation induced by the alcohol. These results suggest that

BHb in 1-PrOH is changing the heme environment similar to those in EtOH and MeOH. However, less 1-PrOH was required to achieve the changes, likely due to 1-PrOH being a less polar alcohol than EtOH and MeOH, implying that 1-PrOH denatures BHb more than EtOH and MeOH. The possible implications of these heme changes to the electrochemistry of BHb will be discussed later in Section 6.5.

The strong absorption peak between 210 and 220 nm in Figure 6.12a-c is most likely due to the peptide bonds.[235] However, interpretation of the peptide bond absorption here is unreliable due to the absorption cutoff by the aliphatic alcohols near 210 nm[132] and is more appropriately examined by the use of another technique such as circular dichroism.[235] Circular dichroism studies of BHb in aqueous-alcohol solutions already showed that the addition of more alcohol decreased the alpha helix content in BHb, suggesting that BHb likely exhibited a less folded protein structure.[205]

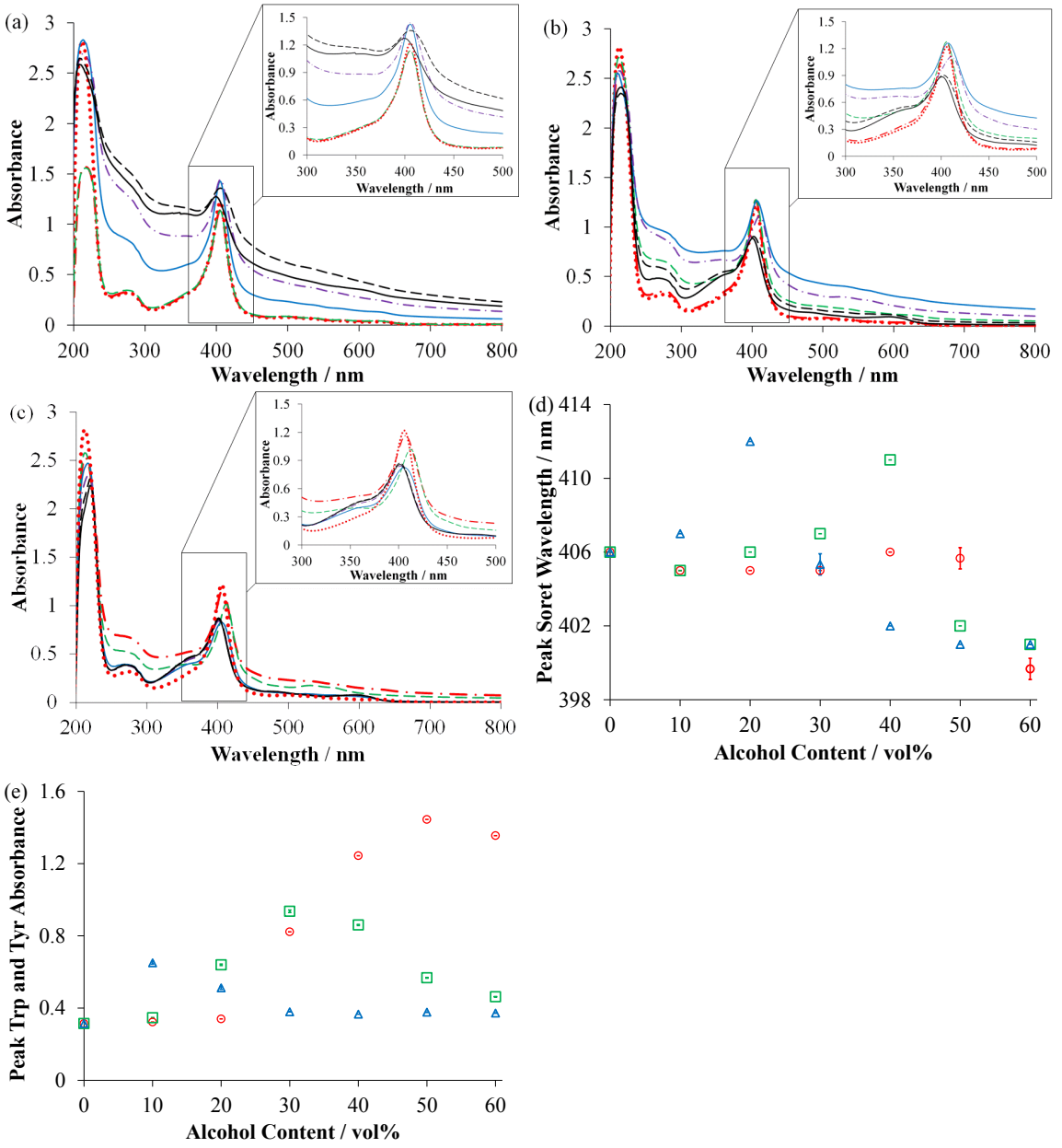

Figure 6.12 Background subtracted UV/Vis spectra of 0.2 g L^{-1} BHb in 0.1 M PB (pH 7.08) with 0% (dotted red curve), 10% (dot-dashed red curve), 20% (dashed green curve), 30% (blue solid curve), 40% (purple dot-dashed curve), 50% (dashed black curve), or 60% (solid black curve) concentrations by volume of either MeOH (a), EtOH (b), or 1-PrOH (c). The peak Soret wavelength (d) or peak tyrosine and tryptophan absorbance at 280 nm (e) as a function of alcohol content were plotted for MeOH (red circles), EtOH (green squares), and 1-PrOH (blue triangles) with error bars indicating one standard deviation from three replicates.

Near 280 nm is the absorption peak for tryptophan (Trp) and tyrosine (Tyr)[32,236] in Figure 6.12a-c. Denaturation of a protein structure where the Trp and Tyr residues are moving into a less polar environment, such as being buried in a more hydrophobic region of the protein, is expected to increase their absorption.[236] Although Trp residues have a higher absorption than Tyr residues, Tyr residues are known to be much more sensitive to changes in polarity of their environment than Trp residues in globular proteins, resulting in larger absorption changes near 280 nm;[236] thus, changes in absorption at this wavelength were mainly attributed to Tyr. An increase in the absorbance near 280 nm is clearly seen when 30-50% MeOH, 20-30% EtOH, or 10% 1-PrOH was present in the BHb-containing electrolyte when compared to the alcohol-free electrolyte (Figure 6.12e). These results suggest that the environment near the Tyr residues is becoming less polar, meaning that the Tyr residues are likely moving into more hydrophobic regions of BHb. The absorption peak began to decrease when exposed to > 50% MeOH, > 30% EtOH, or > 10% 1-PrOH (Figure 6.12e), suggesting that the polarity of the Tyr environments increased,[236] which may be interpreted as increased solvent exposure relative to their previously hydrophobic surroundings and the protein is unraveling, while also likely opening the heme cavities. These results also imply that 1-PrOH denatures BHb more than EtOH, which in turn denatures more than MeOH, agreeing with the previous Soret peak results.

Changes in the Soret absorption peak wavelength revealed information regarding changes to the heme environment, while changes in the absorption intensity at 280 nm revealed changes to the environment around the Tyr residues. In all of the alcohols tested (1-PrOH, EtOH, MeOH), the heme Fe-histidine interaction changed significantly

(60% MeOH, 40% EtOH, 20% 1-PrOH) at an alcohol concentration just above that of where the polarity of the Tyr residues decreased the most (in electrolytes containing 50% MeOH, 30% EtOH, or 10% 1-PrOH). The changing polar environments in the Tyr residues is likely due to the Tyr residues moving inward toward the hydrophobic protein core as the Fe-histidine interaction tightened (40% EtOH or 20% 1-PrOH). In the case of MeOH, the heme Fe-histidine interaction loosened (60% MeOH), but for EtOH (40%) and 1-PrOH (20%), the Fe-histidine interaction tightened first, followed by loosening when more EtOH or 1-PrOH was added to the electrolyte. After adding sufficient alcohol, the Tyr residues experienced an increase in polarity, likely due to increased solvent exposure as the Fe-histidine interaction loosens, indicating protein unfolding.

Three important points may summarize these UV/Vis absorption results. The first point is that the alcohols used in this research decrease the polar environment near the Tyr residues in BHb, followed by changes to the heme environment with an increase in the polar environment of the Tyr residues, which is consistent with increased solvent exposure. The second point is that 1-PrOH denatures BHb more than EtOH, which in turn also denatures more than MeOH since 1-PrOH required the least amount of alcohol to both weaken the heme Fe-histidine interaction in BHb, as indicated by changes in the Soret absorption peak wavelength, and more easily expose the Tyr residues to the solvent. The third point is that the exact effects of EtOH and 1-PrOH on BHb were different from that of MeOH, since no large increase in heme Fe-histidine interaction was observed (*i.e.* insignificant Soret redshift) for any MeOH concentration tested, implying that the change in protein conformation involved in the 1-PrOH and EtOH-induced BHb changes were different from those of MeOH. These changes in the environments of the

Tyr residues and heme groups are consistent with unraveling of the BHb structure upon alcohol exposure where the Fe-histidine interaction is changing and the Tyr residues are experiencing different polarities in their environment. Changes in absorption in other regions of the UV/Vis spectrum were either too weak to be discerned as a peak or did not yield useful diagnostic information pertaining to changes in BHb structure here in this work. A detailed examination of Trp fluorescence may be useful to see further changes in the BHb structure upon alcohol exposure, which is discussed next in Section 6.4.2.

6.4.2 Examining BHb for Structural Protein Changes in Aqueous-alcohol Electrolyte by the use of Fluorescence

Fluorescence is useful for obtaining information regarding changes to the surroundings of fluorescing amino acid residues such as Trp and Tyr.[7,32] Amongst the fluorescing amino acids, Trp has the highest quantum yield.[7,32] The Trp fluorescence peak typically shifts towards longer wavelengths as the polarity of the Trp environment increases since an excited Trp has a larger dipole moment and interacts more strongly with its environment.[7,32] In the case of Trp buried in a hydrophobic region of a protein, a redshifted emission peak coupled with a decrease in fluorescence intensity corresponds to Trp exposed to a more polar environment where solvent reaching the Trp residue may disperse more energy from the excited fluorescing Trp.[32] Conversely, as the polarity of the Trp environment decreases, the Trp fluorescence peak would shift towards a shorter wavelength with a corresponding increase in fluorescence intensity.[32]

Other factors can affect Trp fluorescence such as an energy transfer.[33,146,147] Hb is known to have low fluorescence intensity when exciting Trp residues due to Förster resonance energy transfer.[33,146,147] Förster resonance energy transfer can occur when the

energy of an excited chromophore (*i.e.* Trp) is transferred to another chromophore within 10 nm (*i.e.* heme group),[32] resulting in a lower fluorescence intensity.[33,146,147] There are a total of six Trp residues in BHb, each of which are approximately 1.4 to 1.6 nm from the nearest heme group.[34,35,237] The efficiency of the energy transfer is inversely proportional to the sixth power of the distance between the two chromophores.[32] As a consequence, conformational changes resulting in increased Trp-heme distance will decrease the energy transfer efficiency and increase the fluorescence intensity. The quantum efficiency of Trp fluorescence is known to increase by about 40% if all heme groups are removed from Hb with no shift in the peak emission wavelength,[33,238] and therefore no shift in the emission peak wavelength is expected from the Förster resonance energy transfer mechanism.

Changes in the Trp fluorescence of BHb in solution could qualitatively indicate solvent exposure of the buried Trp residues and/or increased Trp-heme distances, indicating exposure of the buried components in BHb, likely including the heme groups. Exposing the heme groups may be partly responsible for the enhanced BHb-reduction in aqueous-alcohol electrolyte seen previously in Chapter 5, which will be discussed later in Section 6.4.3.

The fluorescence data of BHb in aqueous-alcohol electrolyte in Figure 6.13a-c show the intensity of the emission peaks decreasing for 0 to 40% MeOH content, but increasing for higher MeOH concentrations and for all concentrations of EtOH and 1-PrOH up to 60%. The increased fluorescence intensity can be explained by the decrease in Förster resonance energy transfer where the Trp-heme distances are likely increasing, indicating BHb denaturation. Adding a less polar alcohol to the electrolyte

increases the Trp-heme distance since the largest increase in fluorescence intensity was observed using 1-PrOH and the least using MeOH, which is consistent with the fact that 1-PrOH denatures BHb more than either EtOH or MeOH.[205] Therefore, changes in the fluorescence intensity of BHb show protein denaturation. However, the resonance energy transfer mechanism cannot be used to explain a decrease in fluorescence intensity from 0 to 40% MeOH because that would imply the Trp-heme distance are decreasing, which is a very unlikely scenario. Exposing the Trp residues to the more polar solvent relative to the hydrophobic protein core could result in decreased fluorescence intensity, but the decreased intensity is usually coupled with a red-shifted Trp emission peak, which was not observed from 0 to 40% MeOH (Figure 6.13a and d) and makes the solvent exposure mechanism unlikely based on the results. Based on the data in Figure 6.13, no other mechanism can be reasonably proposed for the decrease in intensity for electrolytes containing 0 to 40% MeOH, but other fluorescence quenching mechanisms are possible, perhaps involving the peptide bond.[239,240]

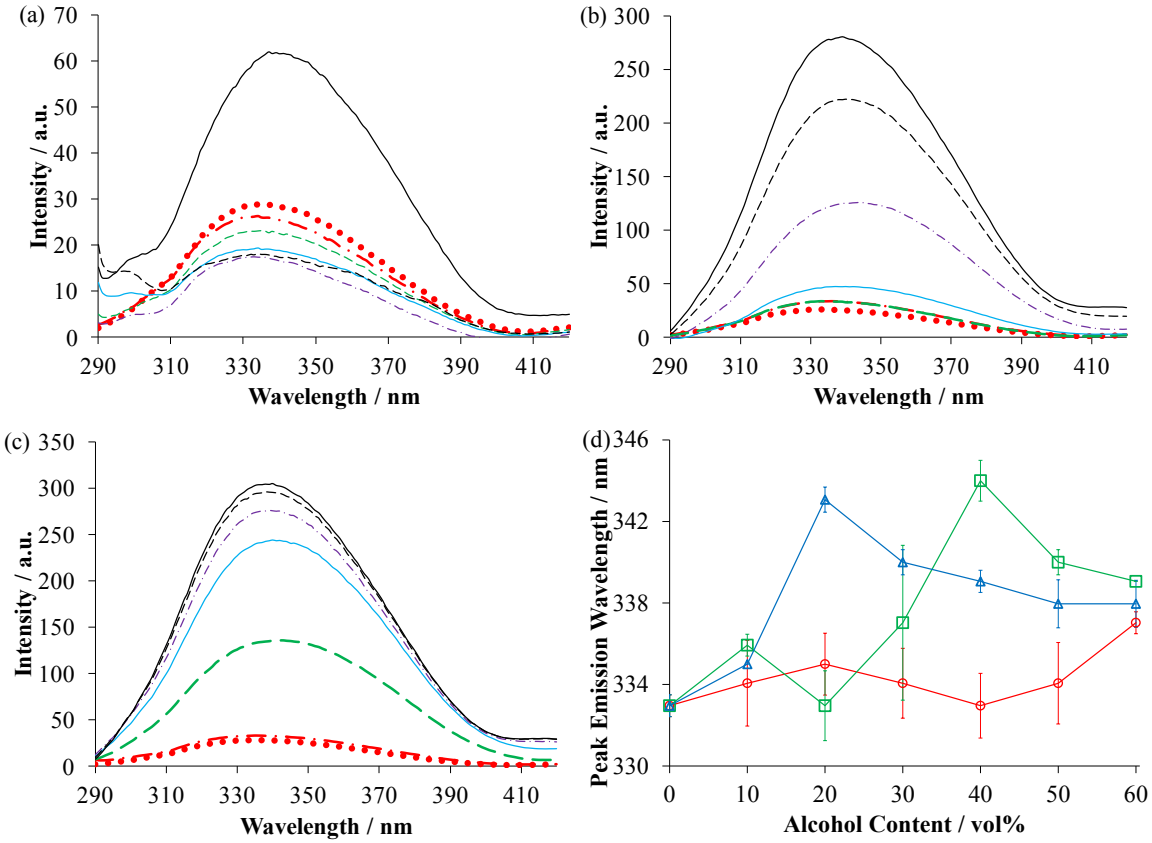

Figure 6.13 Fluorescence spectra of 0.2 g L^{-1} in 0.1 M PB with 0% (dotted red curve), 10% (dot-dashed red curve), 20% (dashed green curve), 30% (blue solid curve), 40% (purple dot-dashed curve), 50% (dashed black curve), or 60% (solid black curve) of MeOH (a), EtOH (b), or 1-PrOH (c). The peak emission wavelength was plotted as a function of alcohol content (d) for MeOH (red circles), EtOH (green squares), and 1-PrOH (blue triangles) with one standard deviation from three replicates.

Red-shifted Trp emission peaks for BHb were seen at high (60%) MeOH concentrations, but were in evidence at lower EtOH and 1-PrOH concentrations. The red-shifted fluorescence peak is likely due to increased exposure of the Trp residues to the electrolyte. Although a decrease in fluorescence intensity is typically expected as the Trp emission peak red-shifts due to increased solvent exposure, the resonance energy transfer mechanism must be overcoming this effect, resulting in increased Trp emission intensity shown in Figure 6.13a-c. As the alcohol content continues to increase beyond the most red-shifted Trp emission peak (> 40% EtOH or > 20% 1-PrOH), the Trp

emission peak blue-shifts and continued to increase in intensity. At these alcohol concentrations, the blue-shift and intensity increase was likely due to a change in the polarity of the solvent that the Trp residues were exposed to since increasing the alcohol content decreases the polarity of the electrolyte.

Additionally, a second smaller emission peak at 300 nm was observed in BHb-containing electrolyte with 30%, 50%, or 60% MeOH (Figure 6.13a). The Tyr residue was assigned to this weaker peak due to its shorter peak wavelength and smaller quantum yield than Trp.[32] The Tyr peak was not used to elucidate protein structure because the peak did not appear in every spectra at different alcohol concentrations, likely due significant overlap from the fluorescing Trp residues.[32]

The fluorescence data here suggest that MeOH-induced changes to BHb are different from the changes induced by either EtOH or 1-PrOH. Lower Trp emission intensities for electrolytes containing < 50% MeOH were observed but having either 60% MeOH, 10-60% EtOH, or 10-60% 1-PrOH in the electrolyte resulted in higher fluorescence intensity (Figure 6.13a-c). These data suggest that for electrolytes containing < 50% MeOH, the Trp environments changed differently from those induced by either EtOH or 1-PrOH, implying that the exact mechanism behind the MeOH-induced changes were different from those of EtOH and 1-PrOH. This interpretation agrees with the previous UV/Vis data, where an increase in heme Fe-histidine interactions were observed for EtOH and 1-PrOH but there was no similar observation for any concentration of MeOH tested.

Overall, the use of fluorescence suggests that the addition of an alcohol changes the Trp polar environment in BHb. The results suggest that the Trp-heme distance

increased and the polarity of the environment near the Trp residues in BHb changed with the addition of more EtOH or 1-PrOH, but these changes in MeOH were not obvious until 60% MeOH was present, meaning that similar alcohol-induced changes occurred for EtOH and 1-PrOH but differently for MeOH. This interpretation is consistent with the UV/Vis absorption data, which also suggested that MeOH-induced changes for MeOH less than 60% were different from those of EtOH and 1-PrOH. 1-PrOH was shown to be more effective than either MeOH or EtOH in denaturing BHb since less of this alcohol was required to induce structural changes in BHb, agreeing with the previous UV/Vis results. The possible consequences of these results on the increased electrochemical reduction of BHb seen previously in Chapter 5 will be discussed next.

6.4.3 Consideration of Structural Changes in BHb and its Electrochemistry

Unfolding of BHb is known to increase its electrochemical activity.[29] UV/Vis data (Section 6.4.1) provided evidence for denaturation, where the Fe-histidine distance and steric hindrance changed within the heme. UV/Vis data also suggested that the Tyr residues experienced changing polarities in their environments and were likely exposed to the electrolyte when sufficient alcohol was added to the electrolyte. The use of fluorescence spectroscopy (Section 6.4.2) suggested that the protein structure, likely including the heme cavities, is opening with the addition of alcohol to the BHb-containing electrolyte, where the Trp-heme distance increased and the Trp residues were more exposed to the electrolyte. Together with the results from Section 5.4, the BHb-reduction increased with more alcohol in the electrolyte as the BHb structure changed, indicated by these spectroscopic results. Reedy *et al.* suggested that a solvent-exposed

heme would result in a negative heme reduction potential shift,[207] which is likely true based on the DPV data seen in Section 5.4 and the increased solvent exposure of the Tyr and Trp residues interpreted from the UV/Vis and fluorescence data in Sections 6.4.1 and 6.4.2.

Subtle structural changes in the heme groups of BHb may be related to the increased electrochemistry shown in Chapter 5. From the UV/Vis results (Section 6.4.1), the Fe-histidine interaction was suggested to be weaker with the addition of sufficient alcohol to the electrolyte. Adding less polar alcohols, such as 1-PrOH, required smaller volumes than a more polar alcohol like MeOH to weaken the Fe-histidine interaction. Weakening this interaction would loosen the Fe in the heme from the unraveling globin structure with increased steric hindrance near the heme (Section 6.4.1), which is possible as the globin unravels with increasing solvent exposure in the protein; thus increasing accessibility to the redox-active hemes to increase BHb-reduction. Additionally, increases in the Trp-heme distance from fluorescence data were suggested for electrolytes containing 60% MeOH, and all concentrations of EtOH and 1-PrOH studied here, further confirming that BHb is unfolding. Low MeOH concentrations resulted in little protein denaturation (up to 30% MeOH), resulting in small increases in BHb electroactivity, but for 40-50% MeOH, BHb continued to denature through other means, since the polar environments of the Trp and Tyr residues continued to change. Together with the electrochemical results in Chapter 5, the BHb electroactivity is increasing as the BHb structure unfolds. These interpretations are consistent with the UV/Vis (Section 6.4.1), fluorescence (Section 6.4.2) and DPV data (Chapter 5).

In terms of BHb electrochemistry, adding 60% MeOH to the electrolyte loosened the BHb structure (indicated by increased Trp-heme distance, increasing solvent exposure near the Tyr and Trp residues, and loosening of the heme Fe-histidine), leading to better access to the heme groups and increased BHb electroactivity. Additionally, EtOH and 1-PrOH induced another change not observed in any concentration of MeOH, which was the tightening of the Fe-histidine interaction. This additional specific change did not appear to have a direct significant effect on the BHb electroactivity, but does appear to be a result of protein denaturation. Therefore, unravelling of the BHb structure appears to be an important factor involved in increasing BHb electroactivity.

All of the UV/Vis absorption and fluorescence data show that the BHb structure is changing, but cannot be used alone to reliably predict the BHb electroactivity. Both the carbon surface oxides on the glassy carbon electrode and the film thickness also influence the BHb electroactivity, which will be considered in the next section.

6.5 Dominant Mechanisms Affecting the Electrochemical Activity of BHb in Aqueous-alcohol Electrolyte

Multiple possible factors affect the electrochemical reduction of BHb; the mechanisms identified and studied in this thesis include: changing the carbon-oxygen surface groups, incorporation of BHb into a film, and structural changes in BHb, likely resulting in greater access to the electrochemically active heme groups. For different types and concentrations of alcohol, different mechanisms appear to dominate. This section examines which mechanisms are likely dominant for each alcohol at particular concentrations with the ultimate goal of improving the electrochemical activity of BHb.

As a reminder, Section 6.2 showed increased Hb electroactivity with decreases in C=O carbonyl or C-O ether groups, Sections 6.3.1 and 6.3.3.2 showed that alcohols affect the adsorption of BHb into an electroactive film, and Section 6.4 showed the alcohol-induced denaturation of BHb. Protein denaturation was indicated by a combination of changing the polarity of the environments around the Tyr and Trp residues, increased solvent exposure, increased Trp-heme distance, and changes in the heme Fe-histidine environment.

Figure 6.14a shows the electrochemical response (charge) as a function of MeOH concentration in the BHb-containing electrolyte. MeOH contents up to 30% resulted in little increased BHb-reduction, but higher concentrations resulted in significant BHb electroactivity, with 60% MeOH exhibiting the largest BHb-reduction across all three alcohols and concentrations used in this research. The expected decrease in BHb electroactivity due to increased C-O surface groups is offset by the expected increase in BHb electroactivity due to decreased C=O surface groups for electrolytes containing up to 30% MeOH (Section 6.2); this together with a small increase in film thickness (Figure 6.9, Section 6.3.3.2) and signs of little protein denaturation (Section 6.4) may explain the small increase in BHb-reduction for electrolytes containing up to 30% MeOH (Figure 6.14a). The large increase in BHb-reduction as MeOH increased above 30% was most likely in part due to significant decreases in C-O and C=O surface groups. Additionally, signs of greater protein denaturation were obvious as the MeOH content was increased up to 60%, all of which likely further increased BHb-reduction. The increase in film thickness for 30 to 60% MeOH was similar to that for 0 to 30% MeOH where there was very little increase in BHb electroactivity, suggesting that the film contributed negligibly

to the increase in BHb electroactivity for > 40% MeOH. Therefore, the increases in BHb electroactivity for > 40% MeOH must be mainly from decreases in C-O and C=O surface groups and denaturation of BHb, yielding the highest electroactivity.

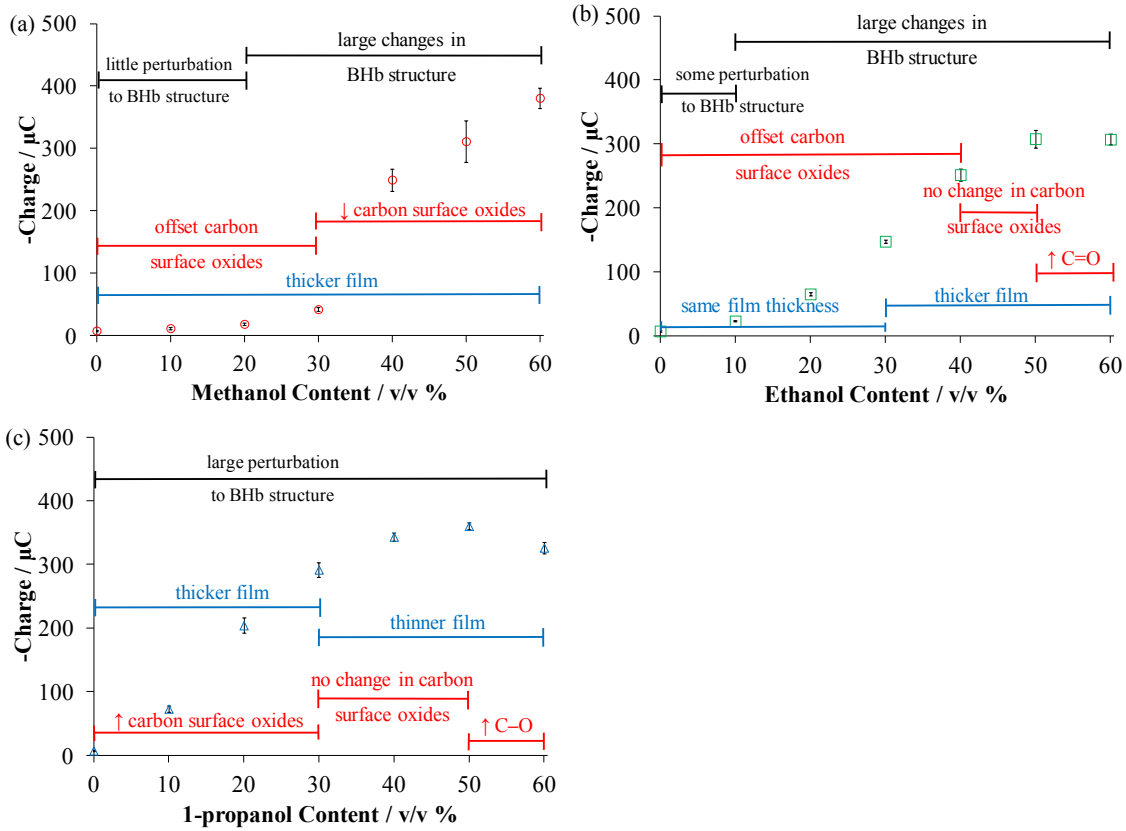

Figure 6.14 Background-subtracted BHb charge for different concentrations of MeOH (a), EtOH (b), or 1-PrOH (c) with 0.2 g L^{-1} BHb in PB with different mechanisms likely contributing to BHb-reduction. The BHb charge data were reproduced from Figure 5.3d in Section 5.4 and the mechanisms likely contributing to BHb-reduction were interpreted from the data shown in this chapter. The error bars indicate one standard deviation from three replicate trials.

In the case of EtOH, the mechanisms that contributed to the increased BHb-reduction seen for MeOH also apply, but at different concentrations of the alcohol (Figure 6.14a and b). BHb exposed to 30% EtOH resulted in higher BHb electroactivity, but no change in the film thickness versus BHb not exposed to any alcohol, suggesting that the film thickness at that concentration was not a good indicator of BHb

electroactivity. A decrease in C=O and increase in C-O surface groups offset each other's change in BHb activity (30% EtOH, Section 6.2); thus, unraveling of the protein structure through large changes in the polar environments of the Trp and Tyr residues with increased Trp-heme distance (up to 40% EtOH) likely contributed the majority of the increased BHb electroactivity. As BHb continued to unravel due to more solvent exposure (up to 60% EtOH), a looser heme structure was also evident (50-60% EtOH, Figure 6.14b) with continued increase in Trp-heme distance. As the EtOH content approached 60%, a small increase in film thickness was observed, but likely insufficient to cause a significant change in BHb-reduction since its film thickness was similar to the carbon sample incubated in 30% MeOH, which had little influence on BHb-reduction. A large increase in BHb electroactivity was expected for 60% EtOH but a significant increase in inhibiting C=O carbonyl surface groups was observed upon exposure to 60% EtOH, which was likely responsible for the observed plateaued BHb-reduction for that concentration of EtOH. BHb denaturation and changes in carbon surface oxides are competing mechanisms, which is contrary to the results seen with MeOH where the carbon surface oxides and BHb denaturation worked together to further increase BHb electroactivity. These interpretations suggest that for < 60% EtOH, denaturation of the protein structure is the overall dominant mechanism in increasing BHb-reduction, but was inhibited by the increase in C=O surface groups, as seen in electrolytes with 60% EtOH.

Of the three alcohols tested in this research, 1-PrOH denatured BHb the most and produced the thickest film on the carbon electrode surface. Some decrease in BHb-reduction was expected due to the increase in C-O and C=O surface groups for 30%

1-PrOH content, but an increase in BHb-reduction was still observed, suggesting that the denaturation of BHb was the dominant mechanism leading to enhanced BHb-reduction. The thicker film formation may have also partly contributed to the increased BHb-reduction and cannot be ruled out. Protein denaturation was most significant for 1-PrOH concentrations up to 40% and the biggest increases in BHb electroactivity were observed at those concentrations. However, increasing 1-PrOH concentrations beyond 40% resulted in a plateau (50% 1-PrOH) and a decrease (60% 1-PrOH) in BHb electroactivity that may have been caused, in part, by the formation of a thinner film (60% 1-PrOH, Section 6.3.3.2) and by more inhibiting C-O surface groups (50% to 60% 1-PrOH, Section 6.2), suggesting that the film thickness and carbon surface oxides may also be an important factor in BHb-reduction for these high 1-PrOH concentrations. These results and interpretations suggest that the enhanced BHb-reduction due to 1-PrOH was likely overall dominated by the denaturation of BHb, but forming a thinner film and increasing carbon surface oxides may have inhibited the BHb electroactivity in electrolytes containing high 1-PrOH concentrations.

The combined interpretation of the data suggests that the denaturation of BHb was usually the dominant mechanism governing the increased BHb-reduction. The data more specifically suggest that the decreased carbon-oxygen (C-O and C=O) surface groups and denaturation of BHb mainly contributed to the enhanced BHb-reduction due to MeOH and <60% EtOH exposure. Protein film thickness contributed negligibly to BHb electroactivity in electrolytes containing either MeOH or EtOH, but cannot be ruled out for 1-PrOH. In the case of adding either 30% 1-PrOH or 40-50% EtOH, increases in the C=O or C-O surface oxides was expected to decrease BHb electroactivity, but an increase

was observed, implying that the denaturation of BHb was a more important mechanism than changes in the carbon surface oxides for these alcohols. However, sufficiently high amounts of C=O and C-O surface oxides formed from exposure to high concentrations of either EtOH or 1-PrOH resulted in a plateaued or decreased BHb electroactivity.

6.6 Conclusions

Multiple factors were seen to be involved in the increased BHb electroactivity upon exposure to a water-miscible primary alcohol. The mechanisms explored in this chapter were: changes to the carbon-oxygen surface groups on glassy carbon, formation of a BHb film, and structural changes in BHb. Changes in carbon surface oxides were examined by the use of XPS, while evidence of a film formation was examined using electrochemistry and spectroscopic ellipsometry. Structural changes in BHb were examined using both UV/Vis absorption spectroscopy and fluorescence. Information gathered from all of these techniques were combined together with the electrochemical results to determine which mechanism was more influential in increasing BHb electroactivity.

Denaturation of BHb was usually the dominant mechanism in increasing BHb electroactivity when adding any one of MeOH, EtOH, or 1-PrOH to the electrolyte. Although clear evidence was presented for many subtle changes in the BHb structure upon exposure to 1-PrOH, EtOH, and high concentrations of MeOH, those changes alone were not sufficient to explain the increases in BHb-reduction in aqueous-alcohol electrolyte. Changes to the carbon-oxygen surface groups on glassy carbon also affected BHb electroactivity. For example, the addition of MeOH led to increased BHb

electroactivity (decreased C-O and C=O surface groups), but high concentrations of 1-PrOH and EtOH led to a decrease (increased C-O and C=O surface groups). Electrolytes containing 60% MeOH had the best BHb electroactivity of all the alcohols and concentrations tested because of both the denaturation of BHb and a decrease in the inhibiting carbon surface oxides favoring BHb electroactivity. An increase in the electrochemically inhibiting carbonyl and ether surface groups appeared to have a lesser effect on the BHb-reduction as seen in the presence of lower 1-PrOH concentrations in the electrolyte, suggesting that the denaturation of BHb was a more important factor than changing the carbon surface oxides.

There was also clear evidence for an electrochemically active BHb film adsorbed onto glassy carbon when incubated in BHb with or without alcohol. The incubation solutions containing 1-PrOH created thicker and more electroactive films than either EtOH or MeOH. Increasing the film thickness may increase with BHb-reduction, but it appeared to have less impact than the other mechanisms on increasing BHb-reduction. For example, 30% EtOH did not result in a thicker film, yet the BHb-reduction increased due to changes in the BHb structure, again suggesting that change in the protein structure of BHb was more important. The different mechanisms governing BHb-reduction in aqueous-alcohol electrolytes cannot and should not be considered in isolation since all of the mechanisms discussed in this chapter affected BHb-reduction for different types and concentrations of water-miscible primary alcohols.

Chapter 7 Conclusions and Future Work

7.1 Conclusions

The research presented in this thesis focused on developing a fundamental understanding of what enhances and inhibits BHb electroactivity on carbon electrode materials. As shown in this thesis, different carbon-oxygen surface groups affected the electrochemical reduction of BHb with fundamental implications because different carbon electrode materials have differing carbon surface oxides, explaining why BHb is active on some carbon materials and inactive on others. In Chapter 4 of this work, carbon-oxygen surface groups were identified using ATR-FTIR, TPD, and C_{1s} XPS. Separately, CVs and DPVs were used to track BHb electroactivity. Surface ethers, quinones, and carbonyls were found to inhibit BHb-reduction. Carbon surface modifications by the use of ultrasonication and electroreduction were employed to confirm the inhibitory effects of surface ethers and carbonyls. Modification by the use of ultrasonication converted a powdered carbon electrode material that was previously electrochemically inactive with BHb into a BHb-active material by decreasing surface ethers. Further modification by the use of electroreduction removed surface carbonyl groups, further enhancing BHb electroactivity. These carbon electrode modifications, presented in Chapter 4, were relatively easy to implement and are recommended for carbon materials employed for the electrochemical detection of BHb. Knowing which carbon surface functional groups inhibit BHb activity allows for more insightful modification of carbon electrode materials to improve BHb detection. This knowledge

may also allow a wider range of carbon materials to be used, including more affordable carbon materials since inactive carbons may be more easily modified to become active.

Previous literature reports debated whether carbon surface oxides increased or decreased Hb electroactivity. Experimental evidence is presented in this thesis provides showing that an increase in surface ethers, carbonyls, and quinones on a carbon electrode material decrease BHb electroactivity in aqueous electrolyte. This can then be used to resolve the apparent contradictory conclusions drawn in some literature reports since it is not the overall degree of carbon oxidation that is significant, rather the specific carbon surface oxide groups that are key. The apparent contradictions likely arise from research groups using electrodes with different types of carbon surface oxides.

In examining the literature related to the apparent contradictory reactivity between Hb and a carbon electrode, it was noted that some results could be separated based on whether or not an alcohol-containing binder was used. One common route of alcohol exposure is in preparation of thin films involving a binder, such as Nafion, to hold BHb onto the electrode surface. In this thesis, exposing a glassy carbon electrode and BHb to a water-miscible primary alcohol was observed to increase the electrochemical reduction of BHb. 1-PrOH present in a Nafion suspension used to immobilize BHb on a carbon electrode resulted in almost an order of magnitude larger BHb-reduction current versus Nafion without any alcohol. An increase in BHb electroactivity was observed when any one of the three alcohols (MeOH, EtOH, 1-PrOH) was added to the electrolyte. The addition of 60% MeOH to the BHb-containing electrolyte resulted in the largest BHb-reduction increase. For the purposes of sensing BHb in an aqueous-alcohol electrolyte with no binder, 60% MeOH should be present to maximize the

electrochemical reduction of BHb. If a binder must be used to immobilize BHb, it should ideally not contain any alcohol to prevent changes to the BHb structure and carbon surface, which may be misattributed to increases in the BHb electrochemical signal to other components of the biosensor. However, 10% MeOH resulted in the least change in the BHb protein structure and the smallest increase in BHb-reduction of all the alcohols tested. Electrochemical Hb biosensors prepared with a binder containing an alcohol should be used with care where a low MeOH content is preferred to minimize alcohol-induced changes to the carbon electrode and to BHb; the use of 1-PrOH, EtOH, or high MeOH content in a binder should be avoided.

Multiple factors were considered in an attempt to understand the mechanisms by which alcohol exposure affects the BHb-reduction. The factors explored in this thesis were changes in carbon-oxygen surface groups before and after exposure to aqueous-alcohol electrolyte, the creation of a BHb film on carbon, and denaturation of BHb in the aqueous-alcohol electrolytes. C_{1s} XPS was used to monitor the carbon-oxygen surface groups, spectroscopic ellipsometry to estimate film thicknesses, and UV/Vis absorption and fluorescence to monitor BHb denaturation. These three factors played varying roles in BHb-reduction for different alcohol types and concentrations. The thickness of the BHb film formed on the carbon electrode surface contributed little to BHb electroactivity, except when incubated in 1-PrOH. Incubating glassy carbon in BHb with a less polar alcohol such as 1-PrOH resulted in a thicker and more electrochemically active film than either MeOH or EtOH. Overall, the denaturation of BHb was generally most important for electrolytes containing MeOH, EtOH, or 1-PrOH, where unfolding of the protein appeared to allow easier access to the heme groups. A change in carbon-oxygen surface

groups was also an important factor where C=O and C-O surface groups were decreasing for high MeOH concentrations, resulting in increased BHb-reduction, but increasing C=O or C-O surface groups for high EtOH or 1-PrOH concentrations respectively inhibited BHb electroactivity. 1-PrOH exposure was shown to change BHb protein structure more than either EtOH or MeOH, which was correlated to the large increases in BHb-reduction. EtOH and 1-PrOH likely changed the BHb protein structure in a similar way, different from MeOH. Even though change to BHb structure was important, all three of these factors (carbon surface oxides, film formation, BHb denaturation) likely contributed together favorably in 60% MeOH-containing electrolyte, resulting in the largest BHb-reduction seen.

Based on the work presented in this thesis, different parameters involved in the voltammetric detection of BHb in a buffered electrolyte can be optimized. The carbon electrode material should have the lowest possible surface ether, carbonyl, and quinone content. To help achieve this, a powdered carbon electrode material can be ultrasonicated in water to lower the surface ether content, followed by the use of an electroreduction procedure to decrease the surface carbonyl content. Ideally, the electrolyte will contain 60% MeOH to sufficiently denature BHb and decrease C-O and C=O surface groups, while the remainder of the electrolyte is composed of BHb in an aqueous buffer. A DPV should be recorded to clearly observe the BHb reduction peak. Following these recommended steps should optimize the voltammetric response of BHb.

7.2 Future Work

Two different directions may be taken to continue the research presented in this thesis. One direction would be to examine how alcohols interact with the carbon surface, resulting in a change in the carbon-oxygen surface groups. In particular, how does MeOH react with the carbon surface, resulting in decreased carbonyl surface groups and increased BHb electroactivity? A possibility may simply be dissolving impurities on the carbon surface and/or the surface carbonyl groups. Another possibility may be that MeOH reduces the surface carbonyls, resulting in a C-O surface group or free carbon site, or conversely oxidizes the surface carbonyls into CO_2 that will then leave the carbon surface. However, more questions arise because 1-PrOH exposure resulted in a more oxidized carbon surface. The length of the alcohol's alkyl chain clearly changes the reaction, but it is currently unclear how. Infrared spectroscopy and mass spectrometry may be able to elucidate possible products or impurities dissolved in the alcohol solvent after being exposed to the polished glassy carbon. Understanding the mechanism behind how the carbon surface oxides are removed may be exploited to further optimize the removal of the carbon surface oxides to further improve BHb electroactivity.

Further investigation of carbon surface oxides on BHb electroactivity may proceed using a gold electrode surface. Modification of the gold surface using thiol groups to build and control the presence of different specific carbon-oxygen surface groups may allow a more thorough systematic investigation of these surface groups on BHb electroactivity. This method may also allow further investigation into how the water-miscible alcohols affect particular types of carbon surface oxides to enhance BHb electrochemistry.

A second direction that may be taken is to examine the adsorbed BHb film. Determining the composition of the film and orientation of the hemes within the film on the carbon electrode would be an interesting future endeavor. Greater BHb electroactivity is expected if the heme groups in the film are arranged closer to the carbon electrode surface or if there are simply more BHb and, therefore, heme groups in the film. Radiolabeling and XPS may be used to quantify the BHb surface concentrations on the carbon surface. Identifying where and how BHb is oriented in the film may be aided by the use of radiolabeling. Additionally, angle-resolved XPS studies of BHb films on glassy carbon scanning for C_{1s}, N_{1s} and Fe_{2p} at different angles may elucidate how the heme groups are oriented in the film. This technique would yield information regarding whether there are more redox-active Fe from the hemes concentrated towards the top of the film, the middle, or the interface between the glassy carbon and the film. The procedure may also be repeated on BHb adsorbed onto carbon surfaces with more C=O and C-O surface groups resulting in inhibited BHb electroactivity to determine how these surface groups may be changing the orientation of the heme groups in the film relative to a carbon surface with fewer C=O and C-O surface groups. The carbon surface oxides themselves may also be changing upon BHb adsorption, which could indicate how BHb binds to the carbon surface.

To complement the estimated protein film thickness measurements obtained from spectroscopic ellipsometry data, other techniques such as X-ray reflectivity or angle-resolved XPS could be used. The obvious disadvantage of using X-ray techniques is that radiation damage may be introduced to the adsorbed BHb film. An additional disadvantage of these techniques is that the sample is placed in a high vacuum, which

will likely decrease the adsorbed film thickness and may not be completely representative of the sample used for electrochemical studies.

Further questions may arise regarding what happens to the adsorbed BHb on the carbon surface after it is electrochemically reduced. A combined technique, such as the combination of electrochemistry and XPS,[241] would be ideal to examine and learn the fate of the BHb. For instance, it is unknown whether BHb remains attached to the carbon surface, or if the iron from the heme groups remains within the film after reduction. Other unknowns, such as whether the attached heme iron remains reduced on the carbon, will be of fundamental importance. The amount of potential knowledge and information gained would be unsurpassed.

References

(1) Nakamura, H.; Karube, I. *Anal. Bioanal. Chem.* **2003**, *377*, 446–468.

(2) Amine, A.; Mohammadi, H.; Bourais, I.; Palleschi, G. *Biosens. Bioelectron.* **2006**, *21*, 1405–1423.

(3) Rogers, K. *Anal. Chim. Acta* **2006**, *568*, 222–231.

(4) Grieshaber, D.; MacKenzie, R.; Vörös, J.; Reimhult, E. *Sensors* **2008**, *8*, 1400–1458.

(5) Wang, J. *Biosens. Bioelectron.* **2006**, *21*, 1887–1892.

(6) Zhang, S.; Wright, G.; Yang, Y. *Biosens. Bioelectron.* **2000**, *15*, 273–282.

(7) Nagel, R. *Hemoglobin Disorders: Molecular Methods and Protocols*; Humana Press: Totowa, N.J., USA, 2003; pp 2, 27, 46, 49, 51-53, 60-62, 101-102, 108, 133, 140, 146.

(8) Umbreit, J. *Am. J. Hematol.* **2007**, *82*, 134–144.

(9) Alayash, A. I.; Patel, R. P.; Cashon, R. E. *Antioxid. Redox Signal.* **2001**, *3*, 313–327.

(10) Mansouri, A.; Lurie, A. *Am. J. Hematol.* **1993**, *42*, 7–12.

(11) Scheller, F.; Bistolas, N.; Liu, S.; Jänchen, M.; Katterle, M.; Wollenberger, U. *Adv. Colloid Interface Sci.* **2005**, *116*, 111–120.

(12) Toh, R. J.; Peng, W. K.; Han, J.; Pumera, M. *RSC Adv.* **2014**, *4*, 8050–8054.

(13) Pei, S.; Qu, S.; Zhang, Y. *Sensors* **2010**, *10*, 1279–1290.

(14) Cai, C.; Chen, J. *Anal. Biochem.* **2004**, *325*, 285–292.

(15) Chen, J.; Stöcklein, W.; Scheller, F.; Wollenberger, U. *Anal. Lett.* **2003**, *36*, 2049–2059.

(16) Hanrahan, K.-L.; MacDonald, S.; Roscoe, S. *Electrochim. Acta* **1996**, *41*, 2469–2479.

(17) Shen, L.; Hu, N. *Biochim. Biophys. Acta - Bioenerg.* **2004**, *1608*, 23–33.

(18) Zhao, L.; Liu, H.; Hu, N. *J. Colloid Interface Sci.* **2006**, *296*, 204–211.

(19) Chen, X.; Ruan, C.; Kong, J.; Yang, R.; Deng, J. *Electroanalysis* **1998**, *10*, 695–699.

(20) Zhao, Y.-D.; Bi, Y.-H.; Zhang, W.-D.; Luo, Q.-M. *Talanta* **2005**, *65*, 489–494.

(21) Cao, D.; Hu, N. *Biophys. Chem.* **2006**, *121*, 209–217.

(22) Ma, G.; Lu, T.; Xia, Y. *Bioelectrochemistry* **2007**, *71*, 180–185.

(23) Kumar, A.; Gayathri, P.; Barathi, P.; Vijayaraghavan, R. *J. Phys. Chem. C* **2012**, *116*, 23692–23703.

(24) Kou, H.; Jia, L.; Wang, C.; Ye, W. *Electroanalysis* **2012**, *24*, 1799–1803.

(25) George, S.; Lee, H. *J. Phys. Chem. B* **2009**, *113*, 15445–15454.

(26) Toh, R. J.; Peng, W. K.; Han, J.; Pumera, M. *Sci. Rep.* **2014**, *4*, 1–6.

(27) Zijlstra, W. G.; Buursma, A.; Meeuwsen-van der Roest, W. P. *Clin. Chem.* **1991**, *37*, 1633–1638.

(28) Sunderman, F. W. *Hemoglobin, its precursors and metabolites*; Lippincott: Philadelphia, USA, 1964; pp 14-15.

(29) Li, X.; Zheng, W.; Zhang, L.; Yu, P.; Lin, Y.; Su, L.; Mao, L. *Anal. Chem.* **2009**, *81*, 8557–8563.

(30) Weissbluth, M. *Hemoglobin Cooperativity and Electronic Properties*; Springer-Verlag: Berlin, 1974; pp 18, 21, 138.

(31) Perutz, M. F.; Heidner, E. J.; Ladner, J. E.; Beetlestone, J. G.; Ho, C.; Slade, E. F. *Biochemistry* **1974**, *13*, 2187–2200.

(32) Ghisaidoobe, A.; Chung, S. *Int. J. Mol. Sci.* **2014**, *15*, 22518–22538.

(33) Alpert, B.; Jameson, D.; Weber, G. *Photochem. Photobiol.* **1980**, *31*, 1–4.

(34) Perutz, M.; Fermi, G.; Poyart, C.; Pagnier, J.; Kister, J. *J. Mol. Biol.* **1993**, *233*, 536–545.

(35) Pettersen, E.; Goddard, T.; Huang, C.; Couch, G.; Greenblatt, D.; Meng, E.; Ferrin, T. *J. Comput. Chem.* **2004**, *25*, 1605–1612.

(36) Sun, Y.; Liu, X.; Fan, C.; Zhang, W.; Li, G. *Bioelectrochemistry* **2004**, *64*, 23–27.

(37) Hill, R. J.; Konigsberg, G. G.; Lyman, C. C. *J. Biol. Chem.* **1962**, *237*, 1549–1554.

(38) Wittenberg, J.; Wittenberg, B.; Peisach, J.; Blumberg, W. *Proc. Natl. Acad. Sci.* **1970**, *67*, 1846–1853.

(39) Schmalzel, J.; Steinke, J.; Randal, V.; Shepherd, A. *Am J Physiol.* **1989**, *257*, 1306–1311.

(40) Frasca, D.; Dahyot-Fizelier, C.; Catherine, K.; Levrat, Q.; Debaene, B.; Mimoz, O. *Crit. Care Med.* **2011**, *39*, 2277–2282.

(41) von Schenck, H.; Falkensson, M.; Lundberg, B. *Clin. Chem.* **1986**, *32*, 526–529.

(42) Gehring, H.; Hornberger, C.; Dibbelt, L.; Roth-Isgkeit, A.; Gerlach, K.; Schumacher, J.; Schmucker, P. *Acta Anaesthesiol. Scand.* **2002**, *46*, 980–986.

(43) Sinex, J. E. *Am. J. Emerg. Med.* **1999**, *17*, 59–67.

(44) Gulaboski, R.; Mirčeski, V.; Bogeski, I.; Hoth, M. *J. Solid State Electrochem.* **2012**, *16*, 2315–2328.

(45) Green, M.; Lias, R. Electrochemical assay for haemoglobin. Patent US4876205 A, 1989.

(46) Hideki, K.; Sugawara, K.; Kawasaki, M.; Hasebe, K.; Nakamura, H.; Tanaka, S. *Anal. Sci.* **2014**, *15*, 589–592.

(47) Brett, C.; Inzelt, G.; Kertesz, V. *Anal. Chim. Acta* **1999**, *385*, 119–123.

(48) Ye, J.; Baldwin, R. *Anal. Chem.* **1988**, *60*, 2263–2268.

(49) Pakapongpan, S.; Palangsuntikul, R.; Surareungchai, W. *Electrochim. Acta* **2011**, *56*, 6831–6836.

(50) Wu, Y.; Hu, S. *Microchim Acta* **2007**, *159*, 1–17.

(51) Sun, W.; Gao, R.; Jiao, K. *J. Phys. Chem. B* **2007**, *111*, 4560–4567.

(52) Ma, G.-X.; Wang, Y.-G.; Wang, C.-X.; Lu, T.-H.; Xia, Y.-Y. *Electrochim. Acta* **2008**, *53*, 4748–4753.

(53) Xu, H.; Dai, H.; Chen, G. *Talanta* **2010**, *81*, 334–338.

(54) Shan, D.; Han, E.; Xue, H.; Cosnier, S. *Biomacromolecules* **2007**, *8*, 3041–3046.

(55) Yao, H.; Li, N.; Xu, J.-Z.; Zhu, J.-J. *Talanta* **2007**, *71*, 550–554.

(56) Lu, Q.; Hu, S. *Chem. Phys. Lett.* **2006**, *424*, 167–171.

(57) Liu, H.; Hu, N. *Anal. Chim. Acta* **2003**, *481*, 91–99.

(58) Liu, P.; Zhang, X.; Feng, L.; Xiong, H.; Wang, S. *Am. J. Biomed. Sci.* **2011**, *3*, 70–77.

(59) Liu, H.-H.; Wan, Y.-Q.; Zou, G.-L. *Anal. Bioanal. Chem.* **2006**, *385*, 1470–1476.

(60) Topoglidis, E.; Lutz, T.; Willis, R.; Barnett, C.; Cass, A.; Durrant, J. *Faraday Discuss.* **2000**, 35–46.

(61) Topoglidis, E.; Campbell, C.; Cass, A.; Durrant, J. *Langmuir* **2001**, *17*, 7899–7906.

(62) Topoglidis, E.; Astuti, Y.; Duriaux, F.; Grätzel, M.; Durrant, J. *Langmuir* **2003**, *19*, 6894–6900.

(63) Salimi, A.; Sharifi, E.; Noorbakhsh, A.; Soltanian, S. *Electrochem. Commun.* **2006**, *8*, 1499–1508.

(64) Salimi, A.; Hallaj, R.; Soltanian, S. *Biophys. Chem.* **2007**, *130*, 122–131.

(65) He, Y.; Sheng, Q.; Zheng, J.; Wang, M.; Liu, B. *Electrochim. Acta* **2011**, *56*, 2471–2476.

(66) Krajewska, A.; Radecki, J.; Radecka, H. *Sensors* **2008**, *8*, 5832–5844.

(67) Lu, Q.; Hu, S.; Pang, D.; He, Z. *Chem. Commun.* **2005**, *20*, 2584–2585.

(68) Liu, M.; Shi, G.; Zhang, L.; Cheng, Y.; Jin, L. *Electrochem. Commun.* **2006**, *8*, 305–310.

(69) Xu, M.-Q.; Wu, J.-F.; Zhao, G.-C. *Sensors.* **2013**, *13*, 7492–7504.

(70) Hong, J.; Zhao, Y.-X.; Xiao, B.-L.; Moosavi-Movahedi, A. A.; Ghourchian, H.; Sheibani, N. *Sensors* **2013**, *13*, 8595–8611.

(71) Zhao, X.; Mai, Z.; Dai, Z.; Zou, X. *Talanta* **2011**, *84*, 148–154.

(72) Lei, C.; Wollenberger, U.; Bistolas, N.; Guiseppi-Elie, A.; Scheller, F. *Anal. Bioanal. Chem.* **2002**, *372*, 235–239.

(73) Zhou, Y.; Li, Z.; Hu, N.; Zeng, Y.; Rusling, J. *Langmuir* **2002**, *18*, 8573–8579.

(74) Zhou, Y.; Hu, N.; Zeng, Y.; Rusling, J. *Langmuir* **2002**, *18*, 211–219.

(75) Bajpai, A.; Sachdeva, R. *J. Appl. Polym. Sci.* **2002**, *85*, 1607–1618.

(76) Guo, Z.; Chen, J.; Liu, H.; Cha, C. *Anal. Chim. Acta* **2008**, *607*, 30–36.

(77) Wei, S.; Dandan, W.; Ruifang, G.; Kui, J. *Electrochem. Commun.* **2007**, *9*, 1159–1164.

(78) Lu, Q.; Li, C. *Biosens. Bioelectron.* **2008**, *24*, 767–772.

(79) Xu, Y.; Hu, C.; Hu, S. *Bioelectrochemistry* **2009**, *74*, 254–259.

(80) Zhao, X.; Mai, Z.; Dai, Z.; Zou, X. *Electroanalysis* **2010**, *22*, 2277–2283.

(81) Fan, C.; Wagner, G.; Li, G. *Bioelectrochemistry* **2001**, *54*, 49–51.

(82) Liu, C.; Bo, A.; Cheng, G.; Lin, X.; Dong, S. *Biochim. Biophys. Acta* **1998**, *1385*, 53–60.

(83) Zhang, W.; Zhou, H.; Li, G.; Scheer, H. *Biophys. Chem.* **2004**, *111*, 229–233.

(84) Katterle, M.; Wollenberger, U.; Scheller, F. *Electroanalysis* **1997**, *9*, 1393–1396.

(85) Li, G.; Liao, X.; Fang, H.; Chen, H. *J. Electroanal. Chem.* **1994**, *369*, 267–269.

(86) Ye, B.; Zhou, X. *Electroanalysis* **1996**, *8*, 1165–1168.

(87) Fan, C.; Li, G.; Zhuang, Y.; Zhu, J.; Zhu, D. *Electroanalysis* **2000**, *12*, 205–208.

(88) Wildgoose, G.; Abiman, P.; Compton, R. *J. Mater. Chem.* **2009**, *19*, 4875–4886.

(89) McCreery, R. *Chem. Rev.* **2008**, *108*, 2646–2687.

(90) Wissler, M. *J. Power Sources* **2006**, *156*, 142–150.

(91) Frysz, C. A.; Chung, D. D. L. *Carbon* **1997**, *35*, 1111–1127.

(92) Serp, P.; Figueiredo, J. *Carbon Materials for Catalysis*; John Wiley & Sons: Hoboken, N.J., USA, 2009; pp 48.

(93) Figueiredo, J.; Pereira, M.; Freitas, M.; Órfão, J. *Carbon* **1999**, *37*, 1379–1389.

(94) Bockris, J.; Reddy, A.; Gamboa-Aldeco, M. *Modern Electrochemistry 2A Fundamentals of Electrodics*; Second Edition; Kluwer Academic Publishers: New York, Boston, Dordrecht, London, Moscow, 2000; pp 775-778, 871-876.

(95) Wang, J. *Analytical Electrochemistry*; Second Edition; John Wiley & Sons Inc., 2001; pp 2, 18-21, 68, 69.

(96) Winter, M.; Brodd, R. J. *Chem. Rev.* **2004**, *104*, 4245–4270.

(97) Boehm, H. *Carbon* **1994**, *32*, 759–769.

(98) Valdes, H.; Sanchez-Polo, M.; Rivera-Utrilla, J.; Zaror, C. A. *Langmuir* **2002**, *18*, 2111–2116.

(99) Kim, C.-H.; Pyun, S.-I.; Shin, H.-C. *J. Electrochem. Soc.* **2002**, *149*, A93–A98.

(100) Salame, I. I.; Bagreev, A.; Bandosz, T. J. *J. Phys. Chem. B* **1999**, *103*, 3877–3884.

(101) Salame, I. I.; Bandosz, T. J. *J. Colloid Interface Sci.* **2001**, *240*, 252–258.

(102) Biniak, S.; Szymański, G.; Siedlewski, J.; Świątkowski, A. *Carbon* **1997**, *35*, 1799–1810.

(103) Seredych, M.; Bandosz, T. *Energy & Fuels* **2008**, *22*, 850–859.

(104) Boehm, H. . *Carbon* **2002**, *40*, 145–149.

(105) Kazmierczak, J.; Biniak, S.; Swiatkowski, A.; Radeke, K.-H. *J. Chem. Soc. Faraday Trans.* **1991**, *87*, 3557–3561.

(106) Swiatkowski, A.; Pakula, M.; Biniak, S.; Walczyk, M. *Carbon* **2004**, *42*, 3057–3069.

(107) Bandosz, T.; Jagiello, J.; Schwarz, J. *Anal. Chem.* **1992**, *64*, 891–895.

(108) Ishizaki, C.; Martí, I. *Carbon* **1981**, *19*, 409–412.

(109) Hsieh, C. T.; Teng, H. *Carbon* **2002**, *40*, 667–674.

(110) Zhuang, Q.; Kyotani, T.; Tomita, A. *Energy & Fuels* **1994**, *8*, 714–718.

(111) Mattson, J.; Mark, H.; Weber, W. *Anal. Chem.* **1969**, *41*, 355–358.

(112) Rockley, M.; Ratcliffe, A.; Davis, D.; Woodard, M. *Appl. Spectrosc.* **1984**, *38*, 553–556.

(113) Zhao, Q. L.; Zhang, Z. L.; Bao, L.; Pang, D. W. *Electrochem. Commun.* **2008**, *10*, 181–185.

(114) Lowde, D.; Williams, J.; Attwood, P.; Bird, R.; McNicol, B.; Short, R. *J. Chem. Soc. Faraday Trans. 1 Phys. Chem. Condens. Phases* **1979**, *75*, 2312–2324.

(115) Kozlowski, C.; Sherwood, P. *J. Chem. Soc. Faraday Trans. 1 Phys. Chem. Condens. Phases* **1985**, *81*, 2745–2756.

(116) Papirer, E.; Lacroix, R.; Donnet, J.; Nanse, G.; Fioux, P. *Carbon* **1994**, *32*, 1341–1358.

(117) Okpalugo, T.; Papakonstantinou, P.; Murphy, H.; McLaughlin, J.; Brown, N. *Carbon* **2005**, *43*, 153–161.

(118) Kangasniemi, K.; Condit, D.; Jarvi, T. *J. Electrochem. Soc.* **2004**, *151*, E125–E132.

(119) Kamau, G.; Willis, W.; Rusling, J. *Anal. Chem.* **1985**, *57*, 545–551.

(120) Nkrumah-Amoako, K.; Roberts, E.; Brown, N.; Holmes, S. *Electrochim. Acta* **2014**, *135*, 568–577.

(121) Ren, L.; Yang, F.; Li, Y.; Liu, T.; Zhang, L.; Ning, G.; Liu, Z.; Gao, J.; Xu, C. *RSC Adv.* **2014**, *4*, 63048–63054.

(122) Ganguly, A.; Sharma, S.; Papakonstantinou, P.; Hamilton, J. *J. Phys. Chem. C* **2011**, *115*, 17009–17019.

(123) Kundu, S.; Wang, Y.; Xia, W.; Muhler, M. *J. Phys. Chem. C* **2008**, *112*, 16869–16878.

(124) Velo-Gala, I.; López-Peñalver, J.; Sánchez-Polo, M.; Rivera-Utrilla, J. *Carbon* **2014**, *67*, 236–249.

(125) Goertzen, S.; Thériault, K.; Oickle, A.; Tarasuk, A.; Andreas, H. *Carbon* **2010**, *48*, 1252–1261.

(126) Oickle, A.; Goertzen, S.; Hopper, K.; Abdalla, Y.; Andreas, H. *Carbon* **2010**, *48*, 3313–3322.

(127) Haydar, S.; Moreno-Castilla, C.; Ferro-García, M. a.; Carrasco-Marín, F.; Rivera-Utrilla, J.; Perrard, A.; Joly, J. P. *Carbon* **2000**, *38*, 1297–1308.

(128) Socrates, G. *Infrared Characteristic Group Frequencies*; Second Edition; John Wiley & Sons Ltd.: New York, N.Y., USA,, 1994; pp 59, 62-72, 80-103.

(129) Tolstoy, V.; Chernyshova, I.; Skryshevsky, V. *Handbook of Infrared Spectroscopy of Ultrathin Films*; John Wiley & Sons, Inc.: Hoboken, N.J., USA, 2003; pp 1, 28.

(130) Harrick, N. J.; Riederman, N. H. *Spectrochim. Acta* **1965**, *21*, 2135–2139.

(131) Mattson, J.; Mark, H. *J. Colloid Interface Sci.* **1969**, *31*, 131–144.

(132) Lide, D. *CRC Handbook of Chemistry and Physics, Internet Version*; 2005; pp. 8–120 & 12–134 & 12–136.

(133) Watts, J.; Wolstenholme, J. *An Introduction to Surface Analysis by XPS and AES*; John Wiley & Sons Ltd.: New York, N.Y., USA, 2003; pp 2, 5-7, 13, 17-23, 28, 30, 42, 56, 64-66, 75-76, 111.

(134) Arwin, H. *Thin Solid Films* **2000**, *377–378*, 48–56.

(135) Mora, M.; Wehmeyer, J.; Synowicki, R.; Garcia, C. *Biological Interactions on Materials Surfaces*; Springer US: New York, N.Y., USA, 2009; pp. 19, 22–24, 33.

(136) Tompkins, H.; Irene, E. *Handbook of Ellipsometry*; William Andrew Publishing: Norwich, N.Y., USA, 2005; pp 71-74, 77, 84, 86-89, 94, 246, 279, 282, 683, 734.

(137) Jellison, G. *Thin Solid Films* **1996**, *290–291*, 40–45.

(138) J. A. Woollam Co. Inc. *CompleteEASE™ Data Analysis Manual*, 2008; pp 18, 20–22, 70, 74, 79, 99, 121, 140.

(139) Lucarini, V.; Saarinen, J.; Peiponen, K.; Vartiainen, E. *Optical Sciences Kramers-Kronig Relations in Optical Materials Research*; Springer: Berlin, Germany, 2005; pp 35.

(140) Butt, H.-J.; Cappella, B.; Kappl, M. *Surf. Sci. Rep.* **2005**, *59*, 1–152.

(141) Giessibl, F. *Rev. Mod. Phys.* **2003**, *75*, 949–983.

(142) Vahdat, V.; Carpick, R. *ACS Nano* **2013**, *7*, 9836–9850.

(143) Wang, C.-M.; Brinigar, W. *Biochemistry* **1979**, *18*, 4960–4977.

(144) Harris, D. *Quantitative Chemical Analysis*; Seventh Edition; W. H. Freeman and Company: New York, USA, 2007; pp 390, 392, 394, 425.

(145) Teale, F. W.; Weber, G. *Biochem. J.* **1957**, *65*, 476–482.

(146) Weber, G.; Teale, F. *Discuss. Faraday Soc.* **1959**, 134–141.

(147) Fontaine, M.; Jameson, D.; Alpert, B. *FEBS Lett.* **1980**, *116*, 310–314.

(148) Sebban, P.; Coppey, M.; Alpert, B.; Lindqvist, L.; Jameson, M. *Photochem. Photobiol.* **1980**, *32*, 727–731.

(149) Majidi, M. R.; Saadatirad, A.; Alipour, E. *Electroanalysis* **2011**, *23*, 1984–1990.

(150) Perutz, M.; Shih, D.; Williamson, D. *J. Mol. Biol.* **1994**, *239*, 555–560.

(151) Mai, Z.; Zhao, X.; Dai, Z.; Zou, X. *Anal. Biochem.* **2010**, *399*, 23–29.

(152) Portet, C.; Chmiola, J.; Gogotsi, Y.; Park, S.; Lian, K. *Electrochim. Acta* **2008**, *53*, 7675–7680.

(153) Cachet-Vivier, C.; Keddam, M.; Vivier, V.; Yu, L. T. *J. Electroanal. Chem.* **2013**, *688*, 12–19.

(154) Cha, C. S.; Chen, J.; Liu, P. F. *Biosens. Bioelectron.* **1998**, *13*, 87–94.

(155) Lin, R.; Taberna, P. L.; Chmiola, J.; Guay, D.; Gogotsi, Y.; Simon, P. *J. Electrochem. Soc.* **2009**, *156*, A7-A12.

(156) Cachet-Vivier, C.; Vivier, V.; Cha, C. S.; Nedelec, J.-Y.; Yu, L. T. *Electrochim. Acta* **2001**, *47*, 181–189.

(157) Satpati, A. K.; Bard, A. J. *Anal. Chem.* **2012**, *84*, 9498–9504.

(158) MacDougall, D.; Rainsbury, J.; Brown, J.; Bance, M.; Adamson, R. *J. Biomed. Opt.* **2015**, *20*, 056008-1 to 056008-8.

(159) Oickle, A.; Tom, J.; Andreas, H. *Carbon* **2016**, *110*, 232–242.

(160) Guo, H.; Wang, X.; Qian, Q.; Wang, F.; Xia, X. *ACS Nano* **2009**, *3*, 2653–2659.

(161) DuPont; *Product Information*, Nafion Polymer Dispersions. 2004, pp 1–2.

(162) Chisaka, M.; Iijima, T.; Tomita, A.; Yaguchi, T.; Sakurai, Y. *J. Electrochem. Soc.* **2010**, *157*, B1701–B1706.

(163) Sevilla, M.; Valle-Vigón, P.; Tartaj, P.; Fuertes, A. *Carbon* **2009**, *47*, 2519–2527.

(164) Rosenthal, D.; Ruta, M.; Schlögl, R.; Kiwi-Minsker, L. *Carbon* **2010**, *48*, 1835–1843.

(165) Brender, P.; Gadiou, R.; Rietsch, J.-C.; Fioux, P.; Dentzer, J.; Ponche, A.; Vix-Guterl, C. *Anal. Chem.* **2012**, *84*, 2147–2153.

(166) Lakowicz, J. *Principles of Fluorescence Spectroscopy*; Second Edition; Springer Science + Business Media: New York, USA, 1999; pp 53.

(167) Panchompoo, J.; Aldous, L.; Compton, R. *New J. Chem.* **2010**, *34*, 2643–2653.

(168) Ranganathan, S.; McCreery, R. *Anal. Chem.* **2001**, *73*, 893–900.

(169) Cain, S.; Cantu, A.; Brunnelle, R.; Lyter, A. *J Forensic Sci* **1978**, *23*, 643–661.

(170) Fan, C.; Hu, X.; Li, G.; Zhu, J.; Zhu, D. *Anal. Sci.* **2000**, *16*, 463–465.

(171) MacDonald, S. M.; Roscoe, S. G. *Electrochim. Acta* **1997**, *42*, 1189–1200.

(172) Hibbert, D. B.; Weitzner, K.; Carter, P. *J. Electrochem. Soc.* **2001**, *148*, E1-E7.

(173) Black, J. The role of charge redistribution in the self-discharge of electrochemical capacitor electrodes, 2010; PhD thesis, Dalhousie University; pp 55, 62, 76, 78, 79.

(174) Gambou-Bosca, A.; Bélanger, D. *J. Electrochem. Soc.* **2015**, *162*, A5115–A5123.

(175) Soboleva, T.; Zhao, X.; Malek, K.; Xie, Z.; Navessin, T.; Holdcroft, S. *ACS Appl. Mater. Interfaces* **2010**, *2*, 375–384.

(176) Papadopoulos, S.; Jürgens, K. D.; Gros, G. *Biophys. J.* **2000**, *79*, 2084–2094.

(177) Wang, Y.; Alsmeyer, D. C.; Mccreery, R. L. *Chem. Mater.* **1990**, 557–563.

(178) Ferrari, A.; Robertson, J. *Phys. Rev. B* **2001**, *64*, 075414-1 to 075414-13.

(179) Antunes, E. F.; Lobo, A. O.; Corat, E. J.; Trava-Airoldi, V. J.; Martin, A. A.; Veríssimo, C. *Carbon* **2006**, *44*, 2202–2211.

(180) Cuesta, A.; Dhamelincourt, P.; Laureyns, J.; Martinez-Alonso, A.; Tascon, J. M. D. *Carbon* **1994**, *32*, 1523–1532.

(181) Chu, P. K.; Li, L. *Mater. Chem. Phys.* **2006**, *96*, 253–277.

(182) Nathan, M.; Smith, J.; Tu, K. *J. Appl. Phys.* **1974**, *45*, 2370.

(183) Otake, Y.; Jenkins, R. G. *Carbon* **1993**, *31*, 109–121.

(184) Marchon, B.; Carrazza, J.; Heinemann, H.; Somorjai, G. a. *Carbon* **1988**, *26*, 507–514.

(185) Bleda-Martínez, M. J.; Lozano-Castelló, D.; Morallón, E.; Cazorla-Amorós, D.; Linares-Solano, A. *Carbon* **2006**, *44*, 2642–2651.

(186) Zielke, U.; Hüttinger, K.; Hoffman, W. *Carbon* **1996**, *34*, 983–998.

(187) Givan, A.; Loewenschuss, A.; Nielsen, C. J. *J. Mol. Struct.* **2002**, *604*, 147–157.

(188) Fanning, P. E.; Vannice, M. A. *Carbon* **1993**, *31*, 721–730.

(189) Krishnankutty, N.; Vannice, M. A. *Chem. Mater.* **1995**, *7*, 754–763.

(190) Davis, L.; MacDonald, N.; Palmberg, P.; Riach, G.; Weber, R. *Handbook of Auger Electron Spectroscopy*; Second Edition; Physical Electronics Division, Perkin-Elmer Corporation: Eden Prairie, Minnesota, USA, 1976; pp 16, Addendum.

(191) Morabito, J. *Anal. Chem.* **1974**, *46*, 189–196.

(192) Wagner, C.; Zatko, D.; Raymond, R. *Anal. Chem.* **1980**, *52*, 1445–1451.

(193) Zhang, H.; Coury, L. *Anal. Chem.* **1993**, *65*, 1552–1558.

(194) Guittonneau, F.; Abdelouas, A.; Grambow, B.; Huclier, S. *Ultrason. Sonochem.* **2010**, *17*, 391–398.

(195) Godet, C.; David, D.; Sabbah, H.; Ababou-Girard, S.; Solal, F. *Appl. Surf. Sci.* **2009**, *255*, 6598–6606.

(196) Dintinger, J.; Klein, S.; Ebbesen, T. *Adv. Mater.* **2006**, *18*, 1267–1270.

(197) Yoshida, T.; Asano, H.; Santos, J. H.; Qi, Z. M.; Takatsu, A.; Kato, K.; Matsuda, N. *Electron. Commun. Japan, Part II* **2003**, *86*, 61–66.

(198) Manning, L.; Jenkins, W.; Hess, J.; Vandegriff, K.; Winslow, R.; Manning, J. *Protein Sci.* **1996**, *5*, 775–781.

(199) Shaeffer, J.; McDonald, M.; Turci, S.; Dinda, D.; Bunn, H. *J. Biol. Chem.* **1984**, *259*, 14544–14547.

(200) Manning, J.; Dumoulin, A.; Li, X.; Manning, L. *J. Biol. Chem.* **1998**, *273*, 19359–19362.

(201) Wang, S.; Xie, F.; Liu, G. *Talanta* **2009**, *77*, 1343–1350.

(202) Faulkner, K.; Bonaventura, C.; Crumbliss, A. *J. Biol. Chem.* **1995**, *270*, 13604–13612.

(203) Li, P.; Ding, Y.; Lu, Z.; Li, Y.; Zhu, X.; Zhou, Y.; Tang, Y.; Chen, Y.; Cai, C.; Lu, T. *Talanta* **2013**, *115*, 228–234.

(204) Herskovits, T.; Gadegbeku, B.; Jaillet, H. *J. Biol. Chem.* **1970**, *245*, 2588–2598.

(205) Jun, C.; Xue, Y.; Liu, R.; Wang, M. *Spectrochim. Acta. A. Mol. Biomol. Spectrosc.* **2011**, *79*, 1406–1410.

(206) Tom, J.; Andreas, H. A. *Carbon* **2017**, *112*, 230–237.

(207) Reedy, C.; Elvekrog, M.; Gibney, B. *Nucleic Acids Res.* **2008**, *36*, D307–D313.

(208) Muhoberac, B.; Brill, A. *Biochemistry* **1980**, *19*, 5157–5167.

(209) Brill, A.; Castleman, B.; McKnight, M. *Biochemistry* **1976**, *15*, 2309–2316.

(210) Asakura, T.; Adachi, K.; Schwartz, E. *J. Biol. Chem.* **1978**, *253*, 6423–6425.

(211) Yang, H.-H.; McCreery, R. L. *J. Electrochem. Soc.* **2000**, *147*, 3420–3428.

(212) Kutsche, I.; Gildehaus, G.; Schuller, D.; Schumpe, A. *J. Chem. Eng. Data* **1984**, *29*, 286–287.

(213) Kretschmer, C.; Nowakowska, J.; Wiebe, R. *J. Ind. Eng. Chem.* **1946**, *38*, 506–509.

(214) Tokunaga, J. *J. Chem. Eng. Data* **1975**, *20*, 41–46.

(215) Ranganathan, S.; Kuo, T.; McCreery, R. *Anal. Chem.* **1999**, *71*, 3574–3580.

(216) Moyer, D.; Wightman, J. *Surf. Interface Anal.* **1989**, *14*, 496–504.

(217) Lousinian, S.; Logothetidis, S. *Microelectron. Eng.* **2007**, *84*, 479–485.

(218) Logothetidis, S.; Gioti, M.; Lousinian, S.; Fotiadou, S. *Thin Solid Films* **2005**, *482*, 126–132.

(219) Jellison, G.; Modine, F. *Appl. Phys. Lett* **1996**, *69*, 371–373.

(220) Weber, J.; Hansen, T.; van de Sanden, M.; Engeln, R. *J. Appl. Phys.* **2009**, *106*, 123503-1 to 123503-9.

(221) Kodera, S.; Okajima, T.; Iwabuki, H.; Kitaguchi, D.; Kuroda, S.; Yoshinobu, T.; Tanizawa, K.; Futai, M.; Iwasaki, H. *Anal. Biochem.* **2003**, *321*, 65–70.

(222) Bolotov, V.; Davletkil'deev, N.; Korotenko, A.; Mosur, E.; Proskurina, O.; Sten'kin, Y. *Tech. Phys.* **2011**, *56*, 1053–1055.

(223) Arwin, H. *Appl. Spectrosc.* **1986**, *40*, 313–318.

(224) Fisk, A. *Proc. Natl. Acad. Sci. U. S. A.* **1950**, *36*, 518–523.

(225) Burstein, E.; Vedenkina, N.; Ivkova, M. *Photochem. Photobiol.* **1973**, *18*, 263–279.

(226) Puiu, A.; Fiorani, L.; Menicucci, I.; Pistilli, M.; Lai, A. *Sensors.* **2015**, *15*, 14415–14434.

(227) Williams, M. W.; Arakawa, E. T. *J. Appl. Phys.* **1972**, *43*, 3460–3463.

(228) Pocard, N.; Alsmeyer, D.; McCreery, R.; Neenan, T.; Callstrom, M. *J. Mater. Chem.* **1992**, *2*, 771–784.

(229) Katritzky, A.; Sild, S.; Karelson, M. *J. Chem. Inf. Comput. Sci.* **1998**, *38*, 1171–1176.

(230) Richter, A.; Kuzmenko, I. *Langmuir* **2013**, *29*, 5167–5180.

(231) Vallee, A.; Humblot, V.; Pradier, C.-M. *Acc. Chem. Res.* **2010**, *43*, 1297–1306.

(232) Häkkinen, H. *Nat. Chem.* **2012**, *4*, 443–455.

(233) Van Dyke, B.; Saltman, P.; Armstrong, F. *J. Am. Chem. Soc.* **1996**, *118*, 3490–3492.

(234) Muhoberac, B.; Shelnutt, J.; Ondrias, M. *FEBS Lett.* **1988**, *228*, 310–316.

(235) Kelly, S.; Jess, T.; Price, N. *Biochim. Biophys. Acta* **2005**, *1751*, 119–139.

(236) Bailey, J.; Beaven, G.; Chignell, D.; Gratzer, W. *Eur. J. Biochem.* **1968**, *7*, 5–14.

(237) Protein Databank; Identifier 1HDA. 2017.

(238) Alpert, B.; Jameson, D.; Weber, G. *Photochem. Photobiol.* **1978**, *31*, 1–4.

(239) Chen, Y.; Liu, B.; Yu, H.; Barkley, M. *J. Am. Chem. Soc.* **1996**, *118*, 9271–9278.

(240) Chen, Y.; Barkley, M. D. *Biochemistry* **1998**, *37*, 9976–9982.

(241) Foelske-Schmitz, A.; Weingarth, D.; Kötz, R. *Electrochim. Acta* **2011**, *56*, 10321–10331.

Appendix A Copyright Agreement for Reproducing Figure 4.1b

RightsLink Printable License

JOHN WILEY AND SONS LICENSE
TERMS AND CONDITIONS

Aug 16, 2017

This Agreement between Justin Tom ("You") and John Wiley and Sons ("John Wiley and Sons") consists of your license details and the terms and conditions provided by John Wiley and Sons and Copyright Clearance Center.

License Number	4170830696811
License date	Aug 16, 2017
Licensed Content Publisher	John Wiley and Sons
Licensed Content Publication	Electroanalysis
Licensed Content Title	Voltammetric Determination of Hemoglobin Using a Pencil Lead Electrode
Licensed Content Author	Mir Reza Majidi,Afsaneh Saadatirad,Esmaeel Alipour
Licensed Content Date	Jul 5, 2011
Licensed Content Pages	7
Type of use	Dissertation/Thesis
Requestor type	University/Academic
Format	Electronic
Portion	Figure/table
Number of figures/tables	1
Original Wiley figure/table number(s)	Figure 1
Will you be translating?	No
Title of your thesis / dissertation	The Influence of Carbon-oxygen Surface Groups and a Water-miscible Primary Alcohol on the Voltammetric Detection of Bovine Hemoglobin in Aqueous Electrolyte using Carbon Electrodes
Expected completion date	Dec 2017
Expected size (number of pages)	200
Requestor Location	Justin Tom Department of Chemistry Dalhousie University Halifax, NS B3H 4R2 Canada Attn: Justin Tom
Publisher Tax ID	EU826007151
Billing Type	Invoice
Billing Address	Justin Tom Department of Chemistry Dalhousie University Halifax, NS B3H 4R2

Canada
Attn: Justin Tom

Total 0.00 USD

Terms and Conditions

TERMS AND CONDITIONS

This copyrighted material is owned by or exclusively licensed to John Wiley & Sons, Inc. or one of its group companies (each a"Wiley Company") or handled on behalf of a society with which a Wiley Company has exclusive publishing rights in relation to a particular work (collectively "WILEY"). By clicking "accept" in connection with completing this licensing transaction, you agree that the following terms and conditions apply to this transaction (along with the billing and payment terms and conditions established by the Copyright Clearance Center Inc., ("CCC's Billing and Payment terms and conditions"), at the time that you opened your RightsLink account (these are available at any time at http://myaccount.copyright.com).

Terms and Conditions

- The materials you have requested permission to reproduce or reuse (the "Wiley Materials") are protected by copyright.

- You are hereby granted a personal, non-exclusive, non-sub licensable (on a stand-alone basis), non-transferable, worldwide, limited license to reproduce the Wiley Materials for the purpose specified in the licensing process. This license, **and any CONTENT (PDF or image file) purchased as part of your order,** is for a one-time use only and limited to any maximum distribution number specified in the
- license. The first instance of republication or reuse granted by this license must be completed within two years of the date of the grant of this license (although copies prepared before the end date may be distributed thereafter). The Wiley Materials shall not be used in any other manner or for any other purpose, beyond what is granted in the license. Permission is granted subject to an appropriate acknowledgement given to the author, title of the material/book/journal and the publisher. You shall also duplicate the copyright notice that appears in the Wiley publication in your use of the Wiley Material. Permission is also granted on the understanding that nowhere in the text is a previously published source acknowledged for all or part of this Wiley Material. Any third party content is expressly excluded from this permission.

With respect to the Wiley Materials, all rights are reserved. Except as expressly granted by the terms of the license, no part of the Wiley Materials may be copied, modified, adapted (except for minor reformatting required by the new Publication), translated, reproduced, transferred or distributed, in any form or by any means, and no derivative works may be made based on the Wiley Materials without the prior permission of the respective copyright owner.**For STM Signatory Publishers clearing permission under the terms of the STM Permissions Guidelines only, the terms of the license are extended to include subsequent editions and for editions in other languages, provided such editions are for the work as a whole in situ and does not involve the separate exploitation of the permitted figures or extracts,** You may not alter, remove or suppress in any manner any copyright, trademark or

other notices displayed by the Wiley Materials. You may not license, rent, sell, loan, lease, pledge, offer as security, transfer or assign the Wiley Materials on a stand-alone basis, or any of the rights granted to you hereunder to any other person.

- The Wiley Materials and all of the intellectual property rights therein shall at all times remain the exclusive property of John Wiley & Sons Inc, the Wiley Companies, or their respective licensors, and your interest therein is only that of having possession of and the right to reproduce the Wiley Materials pursuant to Section 2 herein during the continuance of this Agreement. You agree that you own no right, title or interest in or to the Wiley Materials or any of the intellectual property rights therein. You shall have no rights hereunder other than the license as provided for above in Section 2. No right, license or interest to any trademark, trade name, service mark or other branding ("Marks") of WILEY or its licensors is granted hereunder, and you agree that you shall not assert any such right, license or interest with respect thereto

- NEITHER WILEY NOR ITS LICENSORS MAKES ANY WARRANTY OR REPRESENTATION OF ANY KIND TO YOU OR ANY THIRD PARTY, EXPRESS, IMPLIED OR STATUTORY, WITH RESPECT TO THE MATERIALS OR THE ACCURACY OF ANY INFORMATION CONTAINED IN THE MATERIALS, INCLUDING, WITHOUT LIMITATION, ANY IMPLIED WARRANTY OF MERCHANTABILITY, ACCURACY, SATISFACTORY
- QUALITY, FITNESS FOR A PARTICULAR PURPOSE, USABILITY, INTEGRATION OR NON-INFRINGEMENT AND ALL SUCH WARRANTIES ARE HEREBY EXCLUDED BY WILEY AND ITS LICENSORS AND WAIVED BY YOU.

- WILEY shall have the right to terminate this Agreement immediately upon breach of this Agreement by you.

- You shall indemnify, defend and hold harmless WILEY, its Licensors and their respective directors, officers, agents and employees, from and against any actual or threatened claims, demands, causes of action or proceedings arising from any breach of this Agreement by you.

IN NO EVENT SHALL WILEY OR ITS LICENSORS BE LIABLE TO YOU OR ANY OTHER PARTY OR ANY OTHER PERSON OR ENTITY FOR ANY SPECIAL, CONSEQUENTIAL, INCIDENTAL, INDIRECT, EXEMPLARY OR PUNITIVE DAMAGES, HOWEVER CAUSED, ARISING OUT OF OR IN CONNECTION WITH THE DOWNLOADING, PROVISIONING, VIEWING OR USE OF THE MATERIALS REGARDLESS OF THE FORM OF ACTION, WHETHER FOR BREACH OF CONTRACT, BREACH OF WARRANTY, TORT, NEGLIGENCE, INFRINGEMENT OR OTHERWISE (INCLUDING, WITHOUT LIMITATION, DAMAGES BASED ON LOSS OF PROFITS, DATA, FILES, USE, BUSINESS OPPORTUNITY OR CLAIMS OF THIRD PARTIES), AND WHETHER OR NOT THE PARTY HAS BEEN ADVISED OF THE POSSIBILITY OF SUCH DAMAGES. THIS LIMITATION SHALL APPLY NOTWITHSTANDING ANY FAILURE OF ESSENTIAL PURPOSE OF ANY LIMITED REMEDY PROVIDED

HEREIN.

- Should any provision of this Agreement be held by a court of competent jurisdiction to be illegal, invalid, or unenforceable, that provision shall be deemed amended to achieve as nearly as possible the same economic effect as the original provision, and the legality, validity and enforceability of the remaining provisions of this Agreement shall not be affected or impaired thereby.

- The failure of either party to enforce any term or condition of this Agreement shall not constitute a waiver of either party's right to enforce each and every term and condition of this Agreement. No breach under this agreement shall be deemed waived or excused by either party unless such waiver or consent is in writing signed by the party granting such waiver or consent. The waiver by or consent of a party to a breach of any provision of this Agreement shall not operate or be construed as a waiver of or consent to any other or subsequent breach by such other party.

- This Agreement may not be assigned (including by operation of law or otherwise) by you without WILEY's prior written consent.

- Any fee required for this permission shall be non-refundable after thirty (30) days from receipt by the CCC.

- These terms and conditions together with CCC's Billing and Payment terms and conditions (which are incorporated herein) form the entire agreement between you and WILEY concerning this licensing transaction and (in the absence of fraud) supersedes all prior agreements and representations of the parties, oral or written. This Agreement may not be amended except in writing signed by both parties. This Agreement shall be binding upon and inure to the benefit of the parties' successors, legal representatives, and authorized assigns.

- In the event of any conflict between your obligations established by these terms and conditions and those established by CCC's Billing and Payment terms and conditions, these terms and conditions shall prevail.

- WILEY expressly reserves all rights not specifically granted in the combination of (i) the license details provided by you and accepted in the course of this licensing transaction, (ii) these terms and conditions and (iii) CCC's Billing and Payment terms and conditions.

- This Agreement will be void if the Type of Use, Format, Circulation, or Requestor Type was misrepresented during the licensing process.

- This Agreement shall be governed by and construed in accordance with the laws of the State of New York, USA, without regards to such state's conflict of law rules. Any legal action, suit or proceeding arising out of or relating to these Terms and Conditions or the breach thereof shall be instituted in a court of competent jurisdiction in New York County in the State of New York in the United States of America and each party

hereby consents and submits to the personal jurisdiction of such court, waives any objection to venue in such court and consents to service of process by registered or certified mail, return receipt requested, at the last known address of such party.

WILEY OPEN ACCESS TERMS AND CONDITIONS

Wiley Publishes Open Access Articles in fully Open Access Journals and in Subscription journals offering Online Open. Although most of the fully Open Access journals publish open access articles under the terms of the Creative Commons Attribution (CC BY) License only, the subscription journals and a few of the Open Access Journals offer a choice of Creative Commons Licenses. The license type is clearly identified on the article.

The Creative Commons Attribution License

The Creative Commons Attribution License (CC-BY) allows users to copy, distribute and transmit an article, adapt the article and make commercial use of the article. The CC-BY license permits commercial and non-

Creative Commons Attribution Non-Commercial License

The Creative Commons Attribution Non-Commercial (CC-BY-NC)License permits use, distribution and reproduction in any medium, provided the original work is properly cited and is not used for commercial purposes.(see below)

Creative Commons Attribution-Non-Commercial-NoDerivs License

The Creative Commons Attribution Non-Commercial-NoDerivs License (CC-BY-NC-ND) permits use, distribution and reproduction in any medium, provided the original work is properly cited, is not used for commercial purposes and no modifications or adaptations are made. (see below)

Use by commercial "for-profit" organizations

Use of Wiley Open Access articles for commercial, promotional, or marketing purposes requires further explicit permission from Wiley and will be subject to a fee.

Further details can be found on Wiley Online Library
http://olabout.wiley.com/WileyCDA /Section/id-410895.html

Other Terms and Conditions:

v1.10 Last updated September 2015

Questions? customercare@copyright.com or +1-855-239-3415 (toll free in the US) or +1-978-646-2777.

Appendix B Copyright Agreements for Chapter 4

RightsLink Printable License

ELSEVIER LICENSE
TERMS AND CONDITIONS

Aug 16, 2017

This Agreement between Justin Tom ("You") and Elsevier ("Elsevier") consists of your license details and the terms and conditions provided by Elsevier and Copyright Clearance Center.

License Number	4170831378648
License date	Aug 16, 2017
Licensed Content Publisher	Elsevier
Licensed Content Publication	Carbon
Licensed Content Title	The influence of carbon-oxygen surface functional groups of carbon electrodes on the electrochemical reduction of hemoglobin
Licensed Content Author	Justin Tom,Heather A. Andreas
Licensed Content Date	Feb 1, 2017
Licensed Content Volume	112
Licensed Content Issue	n/a
Licensed Content Pages	8
Start Page	230
End Page	237
Type of Use	reuse in a thesis/dissertation
Intended publisher of new work	other
Portion	full article
Format	electronic
Are you the author of this Elsevier article?	Yes
Will you be translating?	No
Title of your thesis/dissertation	The Influence of Carbon-oxygen Surface Groups and a Water-miscible Primary Alcohol on the Voltammetric Detection of Bovine Hemoglobin in Aqueous Electrolyte using Carbon Electrodes
Expected completion date	Dec 2017
Estimated size (number of pages)	200
Requestor Location	Justin Tom Department of Chemistry Dalhousie University Halifax, NS B3H 4R2 Canada Attn: Justin Tom
Total	0.00 USD
Terms and Conditions	

INTRODUCTION

1. The publisher for this copyrighted material is Elsevier. By clicking "accept" in connection with completing this licensing transaction, you agree that the following terms and conditions apply to this transaction (along with the Billing and Payment terms and conditions established by Copyright Clearance Center, Inc. ("CCC"), at the time that you opened your Rightslink account and that are available at any time at http://myaccount.copyright.com).

GENERAL TERMS

2. Elsevier hereby grants you permission to reproduce the aforementioned material subject to the terms and conditions indicated.

3. Acknowledgement: If any part of the material to be used (for example, figures) has appeared in our publication with credit or acknowledgement to another source, permission must also be sought from that source. If such permission is not obtained then that material may not be included in your publication/copies. Suitable acknowledgement to the source must be made, either as a footnote or in a reference list at the end of your publication, as follows:

"Reprinted from Publication title, Vol /edition number, Author(s), Title of article / title of chapter, Pages No., Copyright (Year), with permission from Elsevier [OR APPLICABLE SOCIETY COPYRIGHT OWNER]." Also Lancet special credit - "Reprinted from The Lancet, Vol. number, Author(s), Title of article, Pages No., Copyright (Year), with permission from Elsevier."

4. Reproduction of this material is confined to the purpose and/or media for which permission is hereby given.

5. Altering/Modifying Material: Not Permitted. However figures and illustrations may be altered/adapted minimally to serve your work. Any other abbreviations, additions, deletions and/or any other alterations shall be made only with prior written authorization of Elsevier Ltd. (Please contact Elsevier at permissions@elsevier.com). No modifications can be made to any Lancet figures/tables and they must be reproduced in full.

6. If the permission fee for the requested use of our material is waived in this instance, please be advised that your future requests for Elsevier materials may attract a fee.

7. Reservation of Rights: Publisher reserves all rights not specifically granted in the combination of (i) the license details provided by you and accepted in the course of this licensing transaction, (ii) these terms and conditions and (iii) CCC's Billing and Payment terms and conditions.

8. License Contingent Upon Payment: While you may exercise the rights licensed immediately upon issuance of the license at the end of the licensing process for the transaction, provided that you have disclosed complete and accurate details of your proposed use, no license is finally effective unless and until full payment is received from you (either by publisher or by CCC) as provided in CCC's Billing and Payment terms and conditions. If full payment is not received on a timely basis, then any license preliminarily granted shall be deemed automatically revoked and shall be void as if never granted. Further, in the event that you breach any of these terms and conditions or any of CCC's Billing and Payment terms and conditions, the license is automatically revoked and shall be void as if never granted. Use of materials as described in a revoked license, as well as any use of the materials beyond the scope of an unrevoked license, may constitute copyright infringement and publisher reserves the right to take any and all action to protect its copyright in the materials.

9. Warranties: Publisher makes no representations or warranties with respect to the licensed material.

10. Indemnity: You hereby indemnify and agree to hold harmless publisher and CCC, and their respective officers, directors, employees and agents, from and against any and all claims arising out of your use of the licensed material other than as specifically authorized pursuant to this license.

11. No Transfer of License: This license is personal to you and may not be sublicensed, assigned, or transferred by you to any other person without publisher's written permission.

12. No Amendment Except in Writing: This license may not be amended except in a writing signed by both parties (or, in the case of publisher, by CCC on publisher's behalf).

13. Objection to Contrary Terms: Publisher hereby objects to any terms contained in any purchase order, acknowledgment, check endorsement or other writing prepared by you, which terms are inconsistent with these terms and conditions or CCC's Billing and Payment terms and conditions. These terms and conditions, together with CCC's Billing and Payment terms and conditions (which are incorporated herein), comprise the entire agreement between you and publisher (and CCC) concerning this licensing transaction. In the event of any conflict between your obligations established by these terms and conditions and those established by CCC's Billing and Payment terms and conditions, these terms and conditions shall control.

14. Revocation: Elsevier or Copyright Clearance Center may deny the permissions described in this License at their sole discretion, for any reason or no reason, with a full refund payable to you. Notice of such denial will be made using the contact information provided by you.

Failure to receive such notice will not alter or invalidate the denial. In no event will Elsevier or Copyright Clearance Center be responsible or liable for any costs, expenses or damage incurred by you as a result of a denial of your permission request, other than a refund of the amount(s) paid by you to Elsevier and/or Copyright Clearance Center for denied permissions.

LIMITED LICENSE

The following terms and conditions apply only to specific license types:

15. **Translation**: This permission is granted for non-exclusive world **English** rights only unless your license was granted for translation rights. If you licensed translation rights you may only translate this content into the languages you requested. A professional translator must perform all translations and reproduce the content word for word preserving the integrity of the article.

16. **Posting licensed content on any Website**: The following terms and conditions apply as follows: Licensing material from an Elsevier journal: All content posted to the web site must maintain the copyright information line on the bottom of each image; A hyper-text must be included to the Homepage of the journal from which you are licensing at http://www.sciencedirect.com/science/journal/xxxxx or the Elsevier homepage for books at http://www.elsevier.com; Central Storage: This license does not include permission for a scanned version of the material to be stored in a central repository such as that provided by Heron/XanEdu.

Licensing material from an Elsevier book: A hyper-text link must be included to the Elsevier homepage at http://www.elsevier.com . All content posted to the web site must maintain the copyright information line on the bottom of each image.

Posting licensed content on Electronic reserve: In addition to the above the following

clauses are applicable: The web site must be password-protected and made available only to bona fide students registered on a relevant course. This permission is granted for 1 year only. You may obtain a new license for future website posting.

17. **For journal authors:** the following clauses are applicable in addition to the above:

Preprints:

A preprint is an author's own write-up of research results and analysis, it has not been peer-reviewed, nor has it had any other value added to it by a publisher (such as formatting, copyright, technical enhancement etc.).

Authors can share their preprints anywhere at any time. Preprints should not be added to or enhanced in any way in order to appear more like, or to substitute for, the final versions of articles however authors can update their preprints on arXiv or RePEc with their Accepted Author Manuscript (see below).

If accepted for publication, we encourage authors to link from the preprint to their formal publication via its DOI. Millions of researchers have access to the formal publications on ScienceDirect, and so links will help users to find, access, cite and use the best available version. Please note that Cell Press, The Lancet and some society-owned have different preprint policies. Information on these policies is available on the journal homepage.

Accepted Author Manuscripts: An accepted author manuscript is the manuscript of an article that has been accepted for publication and which typically includes author-incorporated changes suggested during submission, peer review and editor-author communications.

Authors can share their accepted author manuscript:

- immediately
  - via their non-commercial person homepage or blog
  - by updating a preprint in arXiv or RePEc with the accepted manuscript
  - via their research institute or institutional repository for internal institutional uses or as part of an invitation-only research collaboration work-group
  - directly by providing copies to their students or to research collaborators for their personal use
  - for private scholarly sharing as part of an invitation-only work group on commercial sites with which Elsevier has an agreement
- After the embargo period
  - via non-commercial hosting platforms such as their institutional repository
  - via commercial sites with which Elsevier has an agreement

In all cases accepted manuscripts should:

- link to the formal publication via its DOI
- bear a CC-BY-NC-ND license - this is easy to do
- if aggregated with other manuscripts, for example in a repository or other site, be shared in alignment with our hosting policy not be added to or enhanced in any way to appear more like, or to substitute for, the published journal article.

Published journal article (JPA): A published journal article (PJA) is the definitive final record of published research that appears or will appear in the journal and embodies all value-adding publishing activities including peer review co-ordination, copy-editing, formatting, (if relevant) pagination and online enrichment.

Policies for sharing publishing journal articles differ for subscription and gold open access articles:

Subscription Articles: If you are an author, please share a link to your article rather than the full-text. Millions of researchers have access to the formal publications on ScienceDirect, and so links will help your users to find, access, cite, and use the best available version. Theses and dissertations which contain embedded PJAs as part of the formal submission can be posted publicly by the awarding institution with DOI links back to the formal publications on ScienceDirect.

If you are affiliated with a library that subscribes to ScienceDirect you have additional private sharing rights for others' research accessed under that agreement. This includes use for classroom teaching and internal training at the institution (including use in course packs and courseware programs), and inclusion of the article for grant funding purposes.

Gold Open Access Articles: May be shared according to the author-selected end-user license and should contain a CrossMark logo, the end user license, and a DOI link to the formal publication on ScienceDirect.
Please refer to Elsevier's posting policy for further information.

18. **For book authors** the following clauses are applicable in addition to the above: Authors are permitted to place a brief summary of their work online only. You are not allowed to download and post the published electronic version of your chapter, nor may you scan the printed edition to create an electronic version. **Posting to a repository:** Authors are permitted to post a summary of their chapter only in their institution's repository.

19. **Thesis/Dissertation**: If your license is for use in a thesis/dissertation your thesis may be submitted to your institution in either print or electronic form. Should your thesis be published commercially, please reapply for permission. These requirements include permission for the Library and Archives of Canada to supply single copies, on demand, of the complete thesis and include permission for Proquest/UMI to supply single copies, on demand, of the complete thesis. Should your thesis be published commercially, please reapply for permission. Theses and dissertations which contain embedded PJAs as part of the formal submission can be posted publicly by the awarding institution with DOI links back to the formal publications on ScienceDirect.

Elsevier Open Access Terms and Conditions

You can publish open access with Elsevier in hundreds of open access journals or in nearly 2000 established subscription journals that support open access publishing. Permitted third party re-use of these open access articles is defined by the author's choice of Creative Commons user license. See our open access license policy for more information.

Terms & Conditions applicable to all Open Access articles published with Elsevier:

Any reuse of the article must not represent the author as endorsing the adaptation of the article nor should the article be modified in such a way as to damage the author's honour or reputation. If any changes have been made, such changes must be clearly indicated.

The author(s) must be appropriately credited and we ask that you include the end user license and a DOI link to the formal publication on ScienceDirect.

If any part of the material to be used (for example, figures) has appeared in our publication with credit or acknowledgement to another source it is the responsibility of the user to ensure their reuse complies with the terms and conditions determined by the rights holder.

Additional Terms & Conditions applicable to each Creative Commons user license:

CC BY: The CC-BY license allows users to copy, to create extracts, abstracts and new

works from the Article, to alter and revise the Article and to make commercial use of the Article (including reuse and/or resale of the Article by commercial entities), provided the user gives appropriate credit (with a link to the formal publication through the relevant DOI), provides a link to the license, indicates if changes were made and the licensor is not represented as endorsing the use made of the work. The full details of the license are available at http://creativecommons.org/licenses/by/4.0.

CC BY NC SA: The CC BY-NC-SA license allows users to copy, to create extracts, abstracts and new works from the Article, to alter and revise the Article, provided this is not done for commercial purposes, and that the user gives appropriate credit (with a link to the formal publication through the relevant DOI), provides a link to the license, indicates if changes were made and the licensor is not represented as endorsing the use made of the work. Further, any new works must be made available on the same conditions. The full details of the license are available at http://creativecommons.org/licenses/by-nc-sa/4.0.

CC BY NC ND: The CC BY-NC-ND license allows users to copy and distribute the Article, provided this is not done for commercial purposes and further does not permit distribution of the Article if it is changed or edited in any way, and provided the user gives appropriate credit (with a link to the formal publication through the relevant DOI), provides a link to the license, and that the licensor is not represented as endorsing the use made of the work. The full details of the license are available at http://creativecommons.org/licenses/by-nc-nd/4.0. Any commercial reuse of Open Access articles published with a CC BY NC SA or CC BY NC ND license requires permission from Elsevier and will be subject to a fee. Commercial reuse includes:

- Associating advertising with the full text of the Article
- Charging fees for document delivery or access
- Article aggregation
- Systematic distribution via e-mail lists or share buttons

Posting or linking by commercial companies for use by customers of those companies.

20. **Other Conditions**:

v1.9

ELSEVIER LICENSE
TERMS AND CONDITIONS

Aug 16, 2017

This Agreement between Justin Tom ("You") and Elsevier ("Elsevier") consists of your license details and the terms and conditions provided by Elsevier and Copyright Clearance Center.

License Number	4170831056291
License date	Aug 16, 2017
Licensed Content Publisher	Elsevier
Licensed Content Publication	Carbon
Licensed Content Title	Carbon oxidation and its influence on self-discharge in aqueous electrochemical capacitors
Licensed Content Author	Alicia M. Oickle,Justin Tom,Heather A. Andreas
Licensed Content Date	Dec 1, 2016
Licensed Content Volume	110
Licensed Content Issue	n/a
Licensed Content Pages	11
Start Page	232
End Page	242
Type of Use	reuse in a thesis/dissertation
Intended publisher of new work	other
Portion	figures/tables/illustrations
Number of figures/tables /illustrations	4
Format	electronic
Are you the author of this Elsevier article?	Yes
Will you be translating?	No
Original figure numbers	Figure 5 and three figures from the Supplementary Data (Figures SI1, SI2, SI3)
Title of your thesis/dissertation	The Influence of Carbon-oxygen Surface Groups and a Water-miscible Primary Alcohol on the Voltammetric Detection of Bovine Hemoglobin in Aqueous Electrolyte using Carbon Electrodes
Expected completion date	Dec 2017
Estimated size (number of pages)	200
Requestor Location	Justin Tom Department of Chemistry Dalhousie University Halifax, NS B3H 4R2

Canada
Attn: Justin Tom

Total 0.00 USD

Terms and Conditions

INTRODUCTION

1. The publisher for this copyrighted material is Elsevier. By clicking "accept" in connection with completing this licensing transaction, you agree that the following terms and conditions apply to this transaction (along with the Billing and Payment terms and conditions established by Copyright Clearance Center, Inc. ("CCC"), at the time that you opened your Rightslink account and that are available at any time at http://myaccount.copyright.com).

GENERAL TERMS

2. Elsevier hereby grants you permission to reproduce the aforementioned material subject to the terms and conditions indicated.

3. Acknowledgement: If any part of the material to be used (for example, figures) has appeared in our publication with credit or acknowledgement to another source, permission must also be sought from that source. If such permission is not obtained then that material may not be included in your publication/copies. Suitable acknowledgement to the source must be made, either as a footnote or in a reference list at the end of your publication, as follows:

"Reprinted from Publication title, Vol /edition number, Author(s), Title of article / title of chapter, Pages No., Copyright (Year), with permission from Elsevier [OR APPLICABLE SOCIETY COPYRIGHT OWNER]." Also Lancet special credit - "Reprinted from The Lancet, Vol. number, Author(s), Title of article, Pages No., Copyright (Year), with permission from Elsevier."

4. Reproduction of this material is confined to the purpose and/or media for which permission is hereby given.

5. Altering/Modifying Material: Not Permitted. However figures and illustrations may be altered/adapted minimally to serve your work. Any other abbreviations, additions, deletions and/or any other alterations shall be made only with prior written authorization of Elsevier Ltd. (Please contact Elsevier at permissions@elsevier.com). No modifications can be made to any Lancet figures/tables and they must be reproduced in full.

6. If the permission fee for the requested use of our material is waived in this instance, please be advised that your future requests for Elsevier materials may attract a fee.

7. Reservation of Rights: Publisher reserves all rights not specifically granted in the combination of (i) the license details provided by you and accepted in the course of this licensing transaction, (ii) these terms and conditions and (iii) CCC's Billing and Payment terms and conditions.

8. License Contingent Upon Payment: While you may exercise the rights licensed immediately upon issuance of the license at the end of the licensing process for the transaction, provided that you have disclosed complete and accurate details of your proposed use, no license is finally effective unless and until full payment is received from you (either by publisher or by CCC) as provided in CCC's Billing and Payment terms and conditions. If full payment is not received on a timely basis, then any license preliminarily granted shall be deemed automatically revoked and shall be void as if never granted. Further, in the event that you breach any of these terms and conditions or any of CCC's Billing and Payment terms and conditions, the license is automatically revoked and shall be void as if never

granted. Use of materials as described in a revoked license, as well as any use of the materials beyond the scope of an unrevoked license, may constitute copyright infringement and publisher reserves the right to take any and all action to protect its copyright in the materials.

9. Warranties: Publisher makes no representations or warranties with respect to the licensed material.

10. Indemnity: You hereby indemnify and agree to hold harmless publisher and CCC, and their respective officers, directors, employees and agents, from and against any and all claims arising out of your use of the licensed material other than as specifically authorized pursuant to this license.

11. No Transfer of License: This license is personal to you and may not be sublicensed, assigned, or transferred by you to any other person without publisher's written permission.

12. No Amendment Except in Writing: This license may not be amended except in a writing signed by both parties (or, in the case of publisher, by CCC on publisher's behalf).

13. Objection to Contrary Terms: Publisher hereby objects to any terms contained in any purchase order, acknowledgment, check endorsement or other writing prepared by you, which terms are inconsistent with these terms and conditions or CCC's Billing and Payment terms and conditions. These terms and conditions, together with CCC's Billing and Payment terms and conditions (which are incorporated herein), comprise the entire agreement between you and publisher (and CCC) concerning this licensing transaction. In the event of any conflict between your obligations established by these terms and conditions and those established by CCC's Billing and Payment terms and conditions, these terms and conditions shall control.

14. Revocation: Elsevier or Copyright Clearance Center may deny the permissions described in this License at their sole discretion, for any reason or no reason, with a full refund payable to you. Notice of such denial will be made using the contact information provided by you.

Failure to receive such notice will not alter or invalidate the denial. In no event will Elsevier or Copyright Clearance Center be responsible or liable for any costs, expenses or damage

incurred by you as a result of a denial of your permission request, other than a refund of the amount(s) paid by you to Elsevier and/or Copyright Clearance Center for denied permissions.

LIMITED LICENSE

The following terms and conditions apply only to specific license types:

15. **Translation**: This permission is granted for non-exclusive world **English** rights only unless your license was granted for translation rights. If you licensed translation rights you may only translate this content into the languages you requested. A professional translator must perform all translations and reproduce the content word for word preserving the integrity of the article.

16. **Posting licensed content on any Website**: The following terms and conditions apply as follows: Licensing material from an Elsevier journal: All content posted to the web site must maintain the copyright information line on the bottom of each image; A hyper-text must be included to the Homepage of the journal from which you are licensing at http://www.sciencedirect.com/science/journal/xxxxx or the Elsevier homepage for books at http://www.elsevier.com; Central Storage: This license does not include permission for a scanned version of the material to be stored in a central repository such as that provided by Heron/XanEdu.

Licensing material from an Elsevier book: A hyper-text link must be included to the Elsevier

homepage at http://www.elsevier.com . All content posted to the web site must maintain the copyright information line on the bottom of each image.

Posting licensed content on Electronic reserve: In addition to the above the following clauses are applicable: The web site must be password-protected and made available only to bona fide students registered on a relevant course. This permission is granted for 1 year only. You may obtain a new license for future website posting.

17. **For journal authors:** the following clauses are applicable in addition to the above:

Preprints:

A preprint is an author's own write-up of research results and analysis, it has not been peer-reviewed, nor has it had any other value added to it by a publisher (such as formatting, copyright, technical enhancement etc.).

Authors can share their preprints anywhere at any time. Preprints should not be added to or enhanced in any way in order to appear more like, or to substitute for, the final versions of articles however authors can update their preprints on arXiv or RePEc with their Accepted Author Manuscript (see below).

If accepted for publication, we encourage authors to link from the preprint to their formal publication via its DOI. Millions of researchers have access to the formal publications on ScienceDirect, and so links will help users to find, access, cite and use the best available version. Please note that Cell Press, The Lancet and some society-owned have different preprint policies. Information on these policies is available on the journal homepage.

Accepted Author Manuscripts: An accepted author manuscript is the manuscript of an article that has been accepted for publication and which typically includes author-incorporated changes suggested during submission, peer review and editor-author communications.

Authors can share their accepted author manuscript:

- immediately
  - via their non-commercial person homepage or blog
  - by updating a preprint in arXiv or RePEc with the accepted manuscript
  - via their research institute or institutional repository for internal institutional uses or as part of an invitation-only research collaboration work-group
  - directly by providing copies to their students or to research collaborators for their personal use
  - for private scholarly sharing as part of an invitation-only work group on commercial sites with which Elsevier has an agreement
- After the embargo period
  - via non-commercial hosting platforms such as their institutional repository
  - via commercial sites with which Elsevier has an agreement

In all cases accepted manuscripts should:

- link to the formal publication via its DOI
- bear a CC-BY-NC-ND license - this is easy to do
- if aggregated with other manuscripts, for example in a repository or other site, be shared in alignment with our hosting policy not be added to or enhanced in any way to appear more like, or to substitute for, the published journal article.

Published journal article (JPA): A published journal article (PJA) is the definitive final record of published research that appears or will appear in the journal and embodies all value-adding publishing activities including peer review co-ordination, copy-editing, formatting, (if relevant) pagination and online enrichment.

Policies for sharing publishing journal articles differ for subscription and gold open access articles:

Subscription Articles: If you are an author, please share a link to your article rather than the full-text. Millions of researchers have access to the formal publications on ScienceDirect, and so links will help your users to find, access, cite, and use the best available version. Theses and dissertations which contain embedded PJAs as part of the formal submission can be posted publicly by the awarding institution with DOI links back to the formal publications on ScienceDirect.

If you are affiliated with a library that subscribes to ScienceDirect you have additional private sharing rights for others' research accessed under that agreement. This includes use for classroom teaching and internal training at the institution (including use in course packs and courseware programs), and inclusion of the article for grant funding purposes.

Gold Open Access Articles: May be shared according to the author-selected end-user license and should contain a CrossMark logo, the end user license, and a DOI link to the formal publication on ScienceDirect.
Please refer to Elsevier's posting policy for further information.

18. **For book authors** the following clauses are applicable in addition to the above: Authors are permitted to place a brief summary of their work online only. You are not allowed to download and post the published electronic version of your chapter, nor may you scan the printed edition to create an electronic version. **Posting to a repository:** Authors are permitted to post a summary of their chapter only in their institution's repository.

19. **Thesis/Dissertation**: If your license is for use in a thesis/dissertation your thesis may be submitted to your institution in either print or electronic form. Should your thesis be published commercially, please reapply for permission. These requirements include permission for the Library and Archives of Canada to supply single copies, on demand, of the complete thesis and include permission for Proquest/UMI to supply single copies, on demand, of the complete thesis. Should your thesis be published commercially, please reapply for permission. Theses and dissertations which contain embedded PJAs as part of the formal submission can be posted publicly by the awarding institution with DOI links back to the formal publications on ScienceDirect.

Elsevier Open Access Terms and Conditions

You can publish open access with Elsevier in hundreds of open access journals or in nearly 2000 established subscription journals that support open access publishing. Permitted third party re-use of these open access articles is defined by the author's choice of Creative Commons user license. See our open access license policy for more information.

Terms & Conditions applicable to all Open Access articles published with Elsevier:

Any reuse of the article must not represent the author as endorsing the adaptation of the article nor should the article be modified in such a way as to damage the author's honour or reputation. If any changes have been made, such changes must be clearly indicated.

The author(s) must be appropriately credited and we ask that you include the end user license and a DOI link to the formal publication on ScienceDirect.
If any part of the material to be used (for example, figures) has appeared in our publication

with credit or acknowledgement to another source it is the responsibility of the user to ensure their reuse complies with the terms and conditions determined by the rights holder.

Additional Terms & Conditions applicable to each Creative Commons user license:

CC BY: The CC-BY license allows users to copy, to create extracts, abstracts and new works from the Article, to alter and revise the Article and to make commercial use of the Article (including reuse and/or resale of the Article by commercial entities), provided the user gives appropriate credit (with a link to the formal publication through the relevant DOI), provides a link to the license, indicates if changes were made and the licensor is not represented as endorsing the use made of the work. The full details of the license are available at http://creativecommons.org/licenses/by/4.0.

CC BY NC SA: The CC BY-NC-SA license allows users to copy, to create extracts, abstracts and new works from the Article, to alter and revise the Article, provided this is not done for commercial purposes, and that the user gives appropriate credit (with a link to the formal publication through the relevant DOI), provides a link to the license, indicates if changes were made and the licensor is not represented as endorsing the use made of the work. Further, any new works must be made available on the same conditions. The full details of the license are available at http://creativecommons.org/licenses/by-nc-sa/4.0.

CC BY NC ND: The CC BY-NC-ND license allows users to copy and distribute the Article, provided this is not done for commercial purposes and further does not permit distribution of the Article if it is changed or edited in any way, and provided the user gives appropriate credit (with a link to the formal publication through the relevant DOI), provides a link to the license, and that the licensor is not represented as endorsing the use made of the work. The full details of the license are available at http://creativecommons.org/licenses/by-nc-nd/4.0. Any commercial reuse of Open Access articles published with a CC BY NC SA or CC BY NC ND license requires permission from Elsevier and will be subject to a fee. Commercial reuse includes:

- Associating advertising with the full text of the Article
- Charging fees for document delivery or access
- Article aggregation
- Systematic distribution via e-mail lists or share buttons

Posting or linking by commercial companies for use by customers of those companies.

20. **Other Conditions**:

v1.9